FOREWORD

This report documents a Federal Highway Administration (FHWA) research study that was performed to assist the highway community in validating Superpave tests and specifications being used to grade asphalt binders according to their relative rutting resistances. Superpave and other asphalt mixture tests for rutting were also evaluated.

To accomplish the objective, twelve full-scale pavements were constructed at the FHWA Pavement Testing Facility in 1993. This facility is located at the Turner-Fairbank Highway Research Center in McLean, VA. The pavements were tested for rutting resistance by an Accelerated Loading Facility, which applies one-half of a rear truck axle load. The asphalt binder and mixture tests were validated using the results from these pavement tests.

This document will be of interest to people involved with Superpave and the evaluation of hot-mix asphalts for rutting performance. Recommendations are given concerning a wide range of tests. Asphalt binder and mixture tests used to measure fatigue cracking resistance were also evaluated in this project. The results will be presented in a future report

This report is being distributed on a limited basis. Copies of this report are available from the National Technical Information Service (NTIS), 5285 Port Royal Road, Springfield, Virginia 22161.

T. Paul Teng

T. Paul Teng, P.E.
Director, Office of Infrastructure
Research and Development

NOTICE

Technical Report Documentation Page

1. Report No.	2. Government Accession No.	3. Recipient's Catalog No.
FHWA-RD-99-204		

4. Title and Subtitle	5. Report Date
VALIDATION OF ASPHALT BINDER AND MIXTURE TESTS THAT MEASURE RUTTING SUSCEPTIBILITY USING THE ACCELERATED LOADING FACILITY	6. Performing Organization Code
7. Author(s) Kevin D. Stuart, Walaa S. Mogawer, and Pedro Romero	8. Performing Organization Report No.
9. Performing Organization Name and Address Office of Infrastructure R&D Federal Highway Administration 6300 Georgetown Pike McLean, VA 22101-2296	10. Work Unit No. (TRAIS) 11. Contract or Grant No. In-House Report
12. Sponsoring Agency Name and Address Office of Infrastructure R&D Federal Highway Administration 6300 Georgetown Pike McLean, VA 22101-2296	13. Type of Report and Period Covered Interim Report October 1993 - October 1999 14. Sponsoring Agency Code

15. Supplementary Notes

For additional information on this study, contact Kevin D. Stuart, HRDI-11, Federal Highway Administration, 6300 Georgetown Pike, McLean, VA 22101-2296

16. Abstract

The Accelerated Loading Facility (ALF) was used to validate the Superpave asphalt binder parameter for rutting, namely, G*/sin(delta), and several laboratory mixture tests that have been developed to predict or compare rutting performance. The ALF is a full-scale, pavement testing machine that applies one half of a single rear truck axle load.

The asphalt binders used in this study were AC-5, AC-10, AC-20, Novophalt, and Styrelf I-D, having Superpave high-temperature continuous Performance Grades (PG's) of 59, 65, 70, 77, and 88, respectively. This is the temperature at 2.20 kPa after rolling thin-film oven aging. A dynamic shear rheometer was used to obtain these data. All five binders were used with an aggregate gradation having a nominal maximum aggregate size of 19.0 mm. The PG 59 and 70 binders were also used with a gradation having a nominal maximum aggregate size of 37.5 mm. Pavements with these materials were tested by the ALF.

The relationship between G*/sin(delta) and ALF pavement rutting performance at temperatures ranging from 46 to 76 C was poor. However, the trend was correct for the unmodified binders, and the 2.20-kPa criterion used by the Superpave binder specification appeared to be valid. The main discrepancy was provided by the two modified binders, which were both highly resistant to rutting. The G*/sin(delta) for Styrelf was higher than for Novophalt, but the pavement with Novophalt was more resistant to rutting. This discrepancy was not resolved, although tests performed on mastics indicated that the relative rutting performances of the modified binders may have to be based on mastic properties.

The ALF, French Pavement Rutting Tester, Hamburg Wheel-Tracking Device, Georgia Loaded-Wheel Tester, an unconfined repeated load compression test, and six Superpave Shear Tester measurements ranked the five 19.0-mm mixtures the same as ALF based on the average test data. The rankings based on statistics were generally different, but they were similar to ALF. Therefore, any of these tests can be used to estimate the effects of various asphalt binders on rutting.

Four mixtures, consisting of the two gradations with the PG 59 and PG 70 binders, were used to determine the effect of increased nominal maximum aggregate size and the associated 0.85-percent decrease in optimum binder content on rutting performance. None of the laboratory mixture tests matched the ALF pavement rutting performances of the four mixtures. The tests listed above were sensitive to binder grade but not to aggregate gradation. The PURWheel was sensitive to gradation but did not distinguish the PG 59 binder from the PG 70 binder. The sensitivities of these tests to other key mixture variables need to be determined in future studies.

17. Key Words	18. Distribution Statement
APT, ALF, rutting susceptibility, Superpave, wheel-tracking devices, GTM, AAMAS, repeated load tests, SST, simple shear test, STOA, short-term oven aging, wheel track testers, DSR, large stone mixtures	No restrictions. This document is available to the public through the National Technical Information Service, Springfield, Virginia 22161.

19. Security Classif. (of this report)	20. Security Classif. (of this page)	21. No. of Pages	22. Price
Unclassified	Unclassified	348	

Form DOT F 1700.7 (8-72) Reproduction of completed page authorized

PROJECT PERSONNEL

The Turner-Fairbank Highway Research Center's Bituminous Mixtures Laboratory personnel who worked on this study were:

Mr. Kevin D. Stuart, Federal Highway Administration (FHWA)
Dr. Pedro Romero, SaLUT Inc., Beltsville, MD
Mr. Frank G. Davis, Jr., SaLUT
Mr. Scott M. Parobeck, SaLUT
Mr. Brian D. Newman, SaLUT
Dr. Walaa S. Mogawer, UMASS Dartmouth, North Dartmouth, MA
Mr. Richard P. Izzo, Texas Department of Transportation, Austin, TX

The Turner-Fairbank Highway Research Center's Pavement Binders and Analytical Chemistry Laboratory personnel who worked on this study were:

Dr. Brian H. Chollar, FHWA
Dr. Naga Shashidhar, SaLUT
Ms. Susan Needham, SaLUT
Dr. Mohammed Memon, SaLUT

Personnel in charge of operating the FHWA Accelerated Loading Facility (ALF) and collecting pavement data were:

Mr. James A. Sherwood, FHWA
Mr. Eugene Genova, Halifax (Halifax Corporation, Alexandria, VA)
Dr. Xicheng Qi, Halifax (Currently with SaLUT)
Mr. Mario Tinio, Halifax (Currently with SaLUT)
Mr. Dennis Lim, Halifax (Currently with SaLUT)

Dr. Ramon F. Bonaquist, formerly with the FHWA and currently the president of Advanced Asphalt Technologies, Sterling, VA, was in charge of the experimental design for the pavements and pavement construction. Dr. Bonaquist also directed the operation of the ALF at the time of pavement construction. The experimental design was developed in cooperation with the Strategic Highway Research Program (SHRP). The SHRP staff were Dr. Edward T. Harrigan and Dr. Rita B. Leahy, along with Professor Carl L. Monismith, University of California at Berkeley, and Mr. James S. Moulthrop, Sr. Dr. Harrigan is currently a senior staff member with the National Cooperative Highway Research Program, Washington, D.C.; Dr. Leahy is with Furgo-BRE, Austin TX, and Mr. Moulthrop is with Koch Materials, Austin, TX. The FHWA Eastern Federal Lands Highway Division, Sterling, VA, administered the construction contract. Frank Fee, formerly with Koch Materials and currently with CITGO Asphalt Refining Company, Moylan, PA, assisted the FHWA in obtaining the asphalt binders. Dr. Ernest Bastian, FHWA, Dr. Chris Williams, FHWA, and Dr. John S. Youtcheff, Jr., SaLUT, provided technical support during the course of the study. Dr. Williams is currently with Michigan Tech University, Houghton, MI. PURWheel tests were performed at Purdue University by Mr. Changlin Pan and Mr. James Stiady under the direction of Dr. Thomas D. White. Dr. White is currently with Mississippi State University, MS.

TABLE OF CONTENTS

LIST OF FIGURES

LIST OF TABLES

CHAPTER 1: BACKGROUND

1. Introduction

This report documents a Federal Highway Administration (FHWA) study that was performed to assist the highway community in validating Superpave binder tests and specifications, Superpave mixture tests and performance models, and other laboratory tests that have been developed to predict the performances of asphalt mixtures. Twelve pavements were constructed in 1993 at the FHWA Pavement Testing Facility, located at the Turner-Fairbank Highway Research Center, McLean, VA, to assist in validating binder and mixture tests for rutting and fatigue cracking. Each pavement had a length of 44 m, a width of 4 m, and was divided into four test sites. Therefore, 48 sites were available for testing. The pavements were tested by the FHWA Accelerated Loading Facility (ALF), which is a full-scale, pavement testing machine that applies one-half of a single rear truck axle load. The pavements were tested under conditions that promoted either rutting or the formation of fatigue cracks. The variables used to control these conditions were pavement temperature, amount of lateral wheel wander, and load. At the time of this study, the FHWA owned two ALF's, which meant two sites could be tested at the same time. Figure 1 shows a layout of the pavements, designated as lanes 1 through 12.

2. Objectives

The objectives of the rutting study were to:

- Validate the Superpave binder parameter for rutting, $G^*/\sin\delta$, using ALF pavement performance.
- Validate laboratory mixture tests for rutting when operated according to standardized or customary procedures using ALF pavement performance.
- Compare rankings based on the Superpave binder parameter $G^*/\sin\delta$ to rankings provided by the laboratory mixture tests for rutting.
- Determine the effects of nominal maximum aggregate size on rutting susceptibility.
- Determine if the influence of binder high-temperature performance grade on rutting susceptibility decreases with an increase in nominal maximum aggregate size and the associated decrease in optimum binder content.

The objectives of the fatigue-cracking study were to:

- Validate the Superpave binder parameter for fatigue cracking, $G^*\sin\delta$, using ALF pavement performance.
- Validate the hypothesis stating that, when the tensile strain at the bottom of an asphalt pavement layer is high, a binder with a low stiffness will provide more resistance to fatigue cracking than a

binder with a high stiffness, and when the tensile strain is low, a binder with a high stiffness will provide more resistance to fatigue cracking than a binder with a low stiffness.

- Validate laboratory mixture tests for fatigue cracking using ALF pavement performance.

This chapter includes the experimental designs and background information for both the rutting and fatigue-cracking studies. The remaining chapters of this report detail the findings from the rutting studies. The findings from the fatigue-cracking studies will be presented in a separate report.

3. Structural Cross-Sections of the Pavements

The asphalt pavement layer in each of the 12 pavements consisted of a single asphalt mixture. It was placed on top of an unbound crushed aggregate base, so that rutting or fatigue-cracking performance would be a function of a single mixture. Table 1 shows that the asphalt pavement layer had a nominal thickness of 200 mm, except for lanes 1 and 2, which had a thickness of 100 mm. Lanes 1 and 2 were constructed for the fatigue-cracking studies; they were not used in the rutting studies. The thickness of the unbound crushed aggregate base layer was 460 mm, except for lanes 1 and 2 where the thickness was increased to 560 mm to account for the thinner asphalt pavement layer. The prepared subgrade had a thickness of 610 mm; its classification was A-4, based on American Association of State Highway Transportation Officials (AASHTO) Designation M 145-91.[1]

4. Materials

Table 1 shows that the asphalt mixtures consisted of five binders and two gradations. The two gradations consisted of a Virginia Department of Transportation (VDOT) surface mixture gradation designated SM-3 and a VDOT base mixture gradation designated BM-3.[2] The SM-3 and BM-3 gradations had nominal maximum aggregate sizes of 19.0 and 37.5 mm, respectively. The surface mixtures in lanes 1 and 2 were placed in two 50-mm lifts. The surface mixtures in lanes 3 through 10 were placed in four 50-mm lifts. The base mixtures in lanes 11 and 12 were placed in two 100-mm lifts.

For each gradation, the binder content was held constant so that the effects of binder properties on performance could be studied without the confounding effect of changes in binder content. No reclaimed asphalt pavement materials were included in the mixtures. Samples of the binders, aggregates, and hydrated lime were stockpiled at the Pavement Testing Facility during construction so that they could be used in laboratory experiments. Hydrated lime was used as an antistripping agent.

At the time when the materials for this project were chosen and the mixtures designed, the Superpave method of mixture design had not been finalized, nor had the operating specifications for the Superpave Gyratory Compactor (SGC). Therefore, the 75-blow Marshall method was used to design

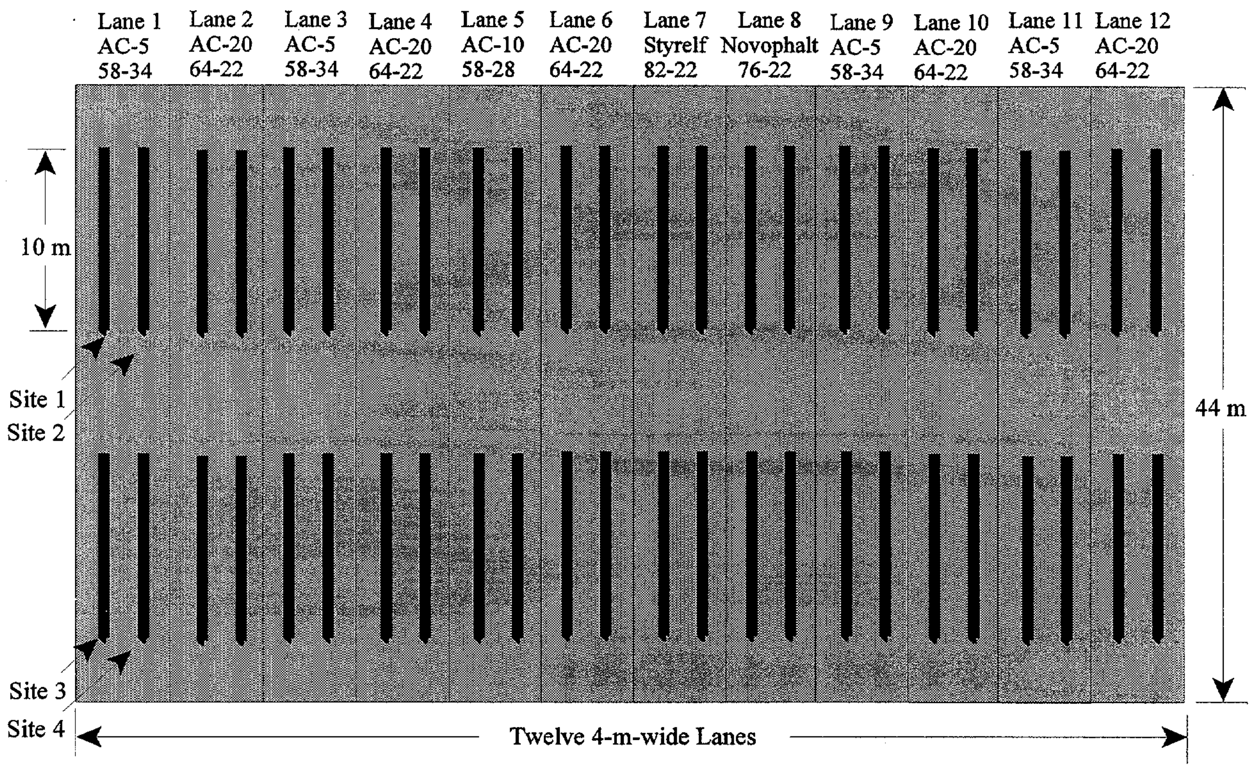

Figure 1. Layout of the test lanes at the FHWA Pavement Testing Facility.

Table 1. Pavement lanes for the Superpave validation study.

Lane Number	Characteristics of the Hot-Mix Asphalt Pavement Layer						Thickness of VDOT 21-A Unbound Crushed Aggregate Base Layer, mm	Thickness of AASHTO A-4 Uniform Subgrade, mm
	Layer Thickness, mm	VDOT Aggregate Gradation	Asphalt Binder Designation Prior to Superpave	Superpave Performance Grade (PG)	High-Temperature Continuous Grade After RTFO Aging	Intermediate Temperature Continuous Grade After RTFO & PAV		
1	100	SM-3	AC-5	58-34	59	9	560	610
2	100	SM-3	AC-20	64-22	70	17	560	610
3	200	SM-3	AC-5	58-34	59	9	460	610
4	200	SM-3	AC-20	64-22	70	17	460	610
5	200	SM-3	AC-10	58-28	65	15	460	610
6	200	SM-3	AC-20	64-22	70	17	460	610
7	200	SM-3	Styrelf™ I-D	82-22	88	18	460	610
8	200	SM-3	Novophalt™	76-22	77	20	460	610
9	200	SM-3	AC-5	58-34	59	9	460	610
10	200	SM-3	AC-20	64-22	70	17	460	610
11	200	BM-3	AC-5	58-34	59	9	460	610
12	200	BM-3	AC-20	64-22	70	17	460	610

the mixtures. However, the asphalt binders and aggregates were chosen based on the Superpave specifications at the time of construction.

a. Binders

The designations of the five binders prior to the Superpave Performance Grade system were AC-5, AC-10, AC-20, Novophalt™, and Styrelf™I-D. The AC-5, AC-10, and AC-20 were from Venezuela's Lagoven base stock. The Novophalt binder was formulated by blending the Lagoven AC-10 asphalt with 6.5-percent low-density polyethylene by mass. A high shear mill was used for blending. Blending was performed by Advanced Asphalt Technologies, Sterling, Virginia, at the paving contractor's hot-mix plant in Leesburg, Virginia. The Styrelf I-D binder was formulated by reacting the Lagoven AC-20 asphalt with 4-percent styrene-butadiene by volume. Styrelf is a product of the Koch Materials Company and is shipped in bulk form. Styrelf binders are currently called Styflex™ in the United States.

Table 2 shows that the Superpave Performance Grades (PG's) of the binders were 58-34, 58-28, 64-22, 76-22, and 82-22. These PG's were determined in accordance with 1993 and 1994 AASHTO provisional standards that were assembled and published in 1995.[3] The two modified binders were chosen to provide different high-temperature PG's, not to directly compete against each other.

The continuous PG is defined as the temperature at the specified test criterion, for example, the temperature at a $G^*/\sin\delta$ of 2.20 kPa after aging in a rolling thin-film oven (RTFO). Table 2 shows that the high-temperature continuous PG's for rutting performance, based on testing RTFO residues, were 59, 65, 70, 77, and 88. The intermediate-temperature continuous PG's for fatigue-cracking performance, based on testing rolling thin-film oven/pressure aging vessel (RFTO/PAV) residues, were 9, 15, 17, 20, and 18. The interval between PG's is 6 °C for high-temperature performance and 3 °C for intermediate-temperature performance.

The physical binder properties based on the viscosity grading system are shown in table 3. These properties were determined using AASHTO test methods.[4] The penetration and viscosity tests ranked the binders the same as the high-temperature PG's in table 2. The absolute viscosities of the Styrelf binder at 60 °C could be in error. These viscosities were difficult to obtain because they were very high. The PG system circumvents testing problems associated with using a constant temperature by specifying a required physical property that is related to performance. The temperature needed to obtain this property is then determined. Thus, binders are not tested at widely different rheological states as in the viscosity test.

Although viscosity is a fundamental measurement, it does not describe both elastic (recoverable) and viscous (permanent) deformations, whereas both deformations occur in pavements. The Dynamic Shear Rheometer (DSR) does provide a measure of both deformations. The viscosity test at 60 °C also does not provide intermediate- and low-temperature properties that are needed to rate or rank binders in terms of fatigue and thermal cracking. The

Table 2. Superpave PG's for the five binders.

Pre-Superpave Designation:	AC-5	AC-10	AC-20	Novo-phalt	Styrelf
Superpave PG:	58-34	58-28	64-22	76-22	82-22
Original Binder					
Temperature at G*/sinδ of 1.00 kPa and 10 rad/s, °C	59.4	61.9	67.9	77.3	87.2
RTFO Residue					
Temperature at G*/sinδ of 2.20 kPa and 10 rad/s, °C	59.3	65.0	70.2	76.6	88.0
RTFO/PAV Residue					
Temperature at G*sinδ of 5000 kPa and 10 rad/s, °C	9.1	14.7	16.7	20.0	17.7
Temperature at Creep Stiffness (S) of 300 MPa and 60 s, °C	-26.9	-22.1	-19.8	-19.7	-20.9
Temperature at an m-value of 0.30 and 60 s, °C	-25.3	-20.3	-17.1	-13.6	-17.4
Continuous PG's Using Samples Taken During Construction[1]					
PG at Start of Construction, Lab A	58-36	61-31	68-34	76-25	89-30
PG at Middle of Construction, Lab A	58-36	62-33	68-28	83-22	87-29
PG at End of Construction, Lab A	63-34	62-31	67-33	77-24	87-28
PG at End of Construction, Lab B	59-35	62-30	68-27	76-23	87-27

[1]The low-temperature PG is the temperature provided by the Superpave bending beam test plus 10 °C.

Table 3. Pre-Superpave physical properties of the binders.

Virgin Binder	AC-5	AC-10	AC-20	Novo-phalt	Styrelf
Penetration, 25 °C, 0.1 mm	172	113	73	54	47
Absolute Viscosity, 60 °C, dPa·s	665	1 195	2 644	13 814	60 308
Kinematic Viscosity, 135 °C, mm^2/s	256	322	476	2 184	2 484
Specific Gravity, 25/25 °C	1.007	1.024	1.022	1.022	1.020
Solubility in Trichloroethylene, %	100.00	100.00	100.00	95.92	100.00
Flash Point, COC, °C	304	304	304	326	312
Thin-Film Oven Residue					
Mass Loss, %	0.01	0.33	0.13	0.34	0.12
Penetration, 25 °C, 0.1 mm	102	66	47	40	35
Absolute Viscosity, 60 °C, dPa·s	1 758	3 223	7 183	29 844	208 185
Kinematic Viscosity, 135 °C, mm^2/s	372	509	684	3 686	4 197

susceptibility to cracking is assumed to increase as the viscosity at 60 °C increases, or the viscosity and penetration of a binder are used together to try to control cracking. The penetration test is performed at intermediate temperatures, generally 25 °C, but, like the viscosity test, it does not describe both elastic and viscous deformations. It is an empirical test that often cannot be related to the various pavement distress modes.

b. Designations for the Binders and Mixtures Used in This Study

During the course of this study, it was decided to describe the five binders using the viscosity grading system and the modifier trade names because of discrepancies that arose between the PG's and the pavement performances of the two mixtures with the modified binders. These descriptions are termed "Pre-Superpave." Discrepancies provided by modified binders are unique to the particular type of modification that is used, and the inability of the binder tests to properly characterize them. A discrepancy does not mean that the PG system is in error for most binders, or that the temperature increment between the PG's is incorrect. Therefore, trade names should be used to describe modified binders that do not fit the current PG system.

In the text of this report, the pre-Superpave designations for the five binders are given for each unmodified binder followed by the PG when general information about the binder is given. The high-temperature continuous PG at 10 rad/s and 2.20 kPa after RTFO aging is used in discussions specific to the rutting study. Only the trade names are given for the two modified binders. The pre-Superpave designation is always used in tables; in some cases, the PG is also included.

c. Aggregates

(1) Nominal Maximum Aggregate Size

All five binders were used with a VDOT SM-3 surface mixture gradation that had a nominal maximum aggregate size of 19.0 mm.[2] Nominal maximum aggregate size was based on the Superpave definition, which states that the nominal maximum aggregate size is one sieve size larger than the first sieve to retain more than 10 percent aggregate by mass.[5] A nominal maximum aggregate size of 12.5 mm is more commonly used in surface mixtures, but the larger size was chosen based on the assumption that the high temperatures and loads to be used in the pavement rutting tests would be too severe for typical VDOT surface mixtures having a nominal maximum aggregate size of 12.5 mm.

The AC-5 and AC-20 (PG 58-34 and 64-22) binders were also used with a VDOT BM-3 base mixture gradation that had a nominal maximum aggregate size of 37.5 mm. Table 1 shows that these two mixtures were placed in lanes 11 and 12. The surface and base mixtures with AC-20 (PG 64-22) are used in Northern Virginia highways subjected to heavy traffic levels, and they are highly resistant to rutting when properly designed and constructed. The aggregates were also used in pavements tested by the FHWA ALF in previous FHWA studies, but the gradations were different.

(2) Aggregate Gradations and Types of Aggregates

The aggregate gradations met 1991 VDOT specifications.[2] The gradation for the surface mixture also met VDOT specifications for an intermediate mixture, designated as IM. Tables 4 and 5 show the "target" gradations for mixtures prepared in the laboratory. These were based on the average gradations of the mixtures in the pavements. The "lab blend" gradations were the actual gradations used in laboratory mixtures. Aggregates in the laboratory were sieved down to the 1.18-mm sieve size. The aggregates were then blended to meet the target gradations as closely as possible. The target gradations are also shown in figures 2 and 3 along with the Superpave control limits.

Different sources of diabase were used in the two gradations, a fact that was not known until the time of construction. The diabase used in the surface mixtures was from Virginia Trap Rock, Leesburg, Virginia, while the diabase used in the base mixtures was from Luck Stone, Leesburg, Virginia. Both were 100-crushed, quarried aggregates from the same geologic vein. Neither aggregate source contained particles with rounded surfaces or clays. Prior to this study, the paving contractor used diabase from the Virginia Trap Rock quarry because this quarry was located next to the hot-mix plant. The paving contractor had stockpiles of this aggregate at the plant at the time of construction. However, neither the paving contractor nor Virginia Trap Rock had the No. 357 stone needed for the base mixture. Therefore, the paving contractor obtained the diabase aggregates for the base mixtures from Luck Stone.

A natural sand from the Solite Corporation, Fredericksburg, Virginia, was used in both mixtures. This sand is predominantly quartz and quartzite. One-percent hydrated lime, purchased from Chemston, Strasburg, Virginia, was used in all mixtures to prevent the occurrence of moisture damage during the duration of this study.

(3) Flat, Elongated Particles

The aggregates were tested for flat and elongated particles using ASTM D 4791.[6] At the time of construction, Superpave specified that a maximum of 10 percent particles by mass could pass a 5 to 1, length-to-thickness, ratio.[5] It was found that less than 1 percent of the diabase aggregates had a length to thickness greater than this ratio. The aggregates easily passed the Superpave specification.

A length-to-thickness ratio of 3 to 1 was also used to evaluate the aggregates. A maximum value of 20 percent using a 3-to-1 ratio has been used by some highway agencies in the past, although a firm criterion does not exist. The No. 68 diabase aggregate in the surface mixtures had an average percent passing of 21. The No. 357 and No. 8 diabase aggregates in the base mixtures had average percent passing of 19 and 12, respectively. The No. 68 and No. 357 diabase aggregates had a moderate number of flat and elongated particles based on a 3-to-1 ratio.

Table 4. Aggregate properties for the SM-3 surface mixtures.

Aggregate Gradations, Percent Passing:

Sieve Size (mm)	61% No. 68 Diabase	30% No. 10 Diabase	8% Natural Sand	1% Hydrated Lime	Target	Lab Blend
25.0	100.0				100.0	100.0
19.0	97.9				98.7	98.7
12.5	60.7				76.0	76.0
9.5	37.7	100.0	100.0		62.0	62.0
4.75	9.2	99.2	95.8		44.0	44.0
2.36	2.2	75.6	88.2		32.5	32.1
1.18	1.7	52.5	74.8		23.5	23.8
0.600	1.4	37.8	46.0		17.5	16.9
0.300	1.3	27.9	14.1		11.5	11.3
0.150	1.1	19.6	4.8		8.0	7.9
0.075	0.9	12.5	2.9	100.0	5.1	5.5

The diabase aggregates were from Virginia Trap Rock.

Specific Gravities and Percent Absorption:

Bulk Dry	2.943	2.914	2.565			2.892
Bulk SSD	2.962	2.945	2.601			2.916
Apparent	2.999	3.007	2.659	2.262		2.961
% Abs	0.6	1.1	1.4			0.8

Flat and Elongated Particles at a 3-to-1 Length-to-Thickness Ratio, Percent by Mass:

	21	NT	NT

Los Angeles Abrasion, Percent Loss by Mass:

	14	NT	NT

Bulk Dry = Bulk-Dry Specific Gravity
Bulk SSD = Bulk-Saturated-Surface-Dry Specific Gravity
Apparent = Apparent Specific Gravity
% Abs = Percent Water Absorption
NT = Not Tested

Table 5. Aggregate properties for BM-3 base mixtures.

Aggregate Gradations, Percent Passing:

Sieve Size (mm)	41% No. 357 Diabase	15% No. 8 Diabase	38% No. 10 Diabase	5% Natural Sand	1% Hydrated Lime	Target	Lab Blend
37.5	100.0					100.0	100.0
25.0	64.9					85.6	85.6
19.0	36.3					73.9	73.9
12.5	14.9	100.0				65.1	65.1
9.5	5.5	85.0	100.0	100.0		59.0	59.0
4.75	3.0	25.3	96.8	95.8		47.6	47.6
2.36	1.8	2.7	68.0	88.2		32.5	32.4
1.18	1.6	2.0	47.5	74.8		24.0	23.7
0.600	1.4	1.5	34.3	46.0		17.4	17.1
0.300	1.2	1.2	24.9	14.1		12.3	11.8
0.150	1.1	0.9	17.3	4.8		8.0	8.4
0.075	0.8	0.8	11.5	2.9	100.0	5.7	6.0

The diabase aggregates were from Luck Stone Corporation.

Specific Gravities and Percent Absorption:

	41% No. 357 Diabase	15% No. 8 Diabase	38% No. 10 Diabase	5% Natural Sand	1% Hydrated Lime	Target	Lab Blend
Bulk Dry	2.971	2.956	2.894	2.565			2.907
Bulk SSD	2.984	2.981	2.935	2.601			2.934
Apparent	3.013	3.030	3.017	2.659	2.262		2.987
% Abs	0.5	0.8	1.4	1.4			0.9

Flat and Elongated Particles at a 3-to-1 Length-to-Thickness Ratio, Percent by Mass:

	41% No. 357 Diabase	15% No. 8 Diabase	38% No. 10 Diabase	5% Natural Sand
	19	12	NT	NT

Los Angeles Abrasion, Percent Loss by Mass:

	41% No. 357 Diabase	15% No. 8 Diabase	38% No. 10 Diabase	5% Natural Sand
	20	21	NT	NT

Bulk Dry = Bulk-Dry Specific Gravity.
Bulk SSD = Bulk-Saturated-Surface-Dry Specific Gravity.
Apparent = Apparent Specific Gravity.
% Abs = Percent Water Absorption.

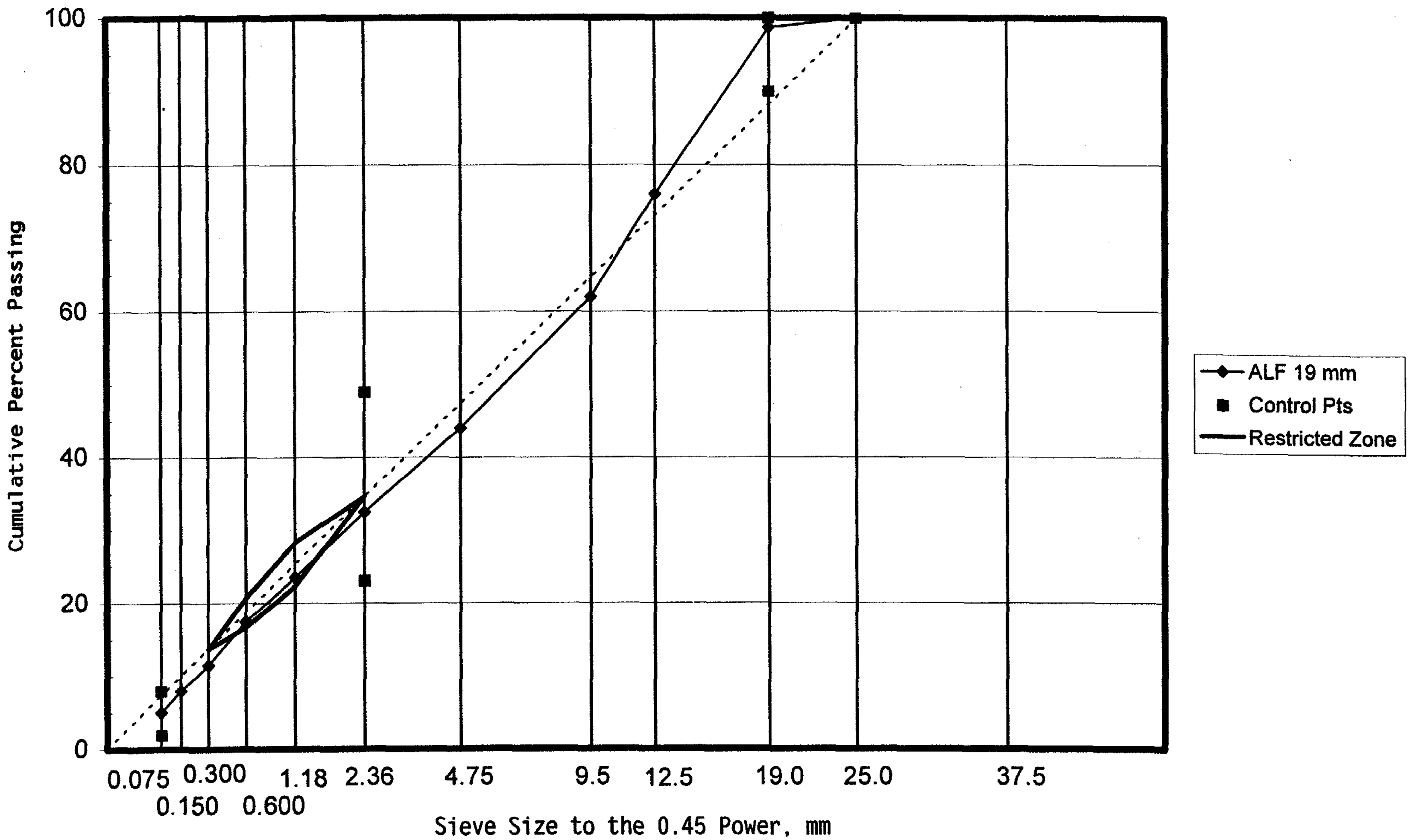

Figure 2. SM-3 aggregate gradation for the surface mixtures.

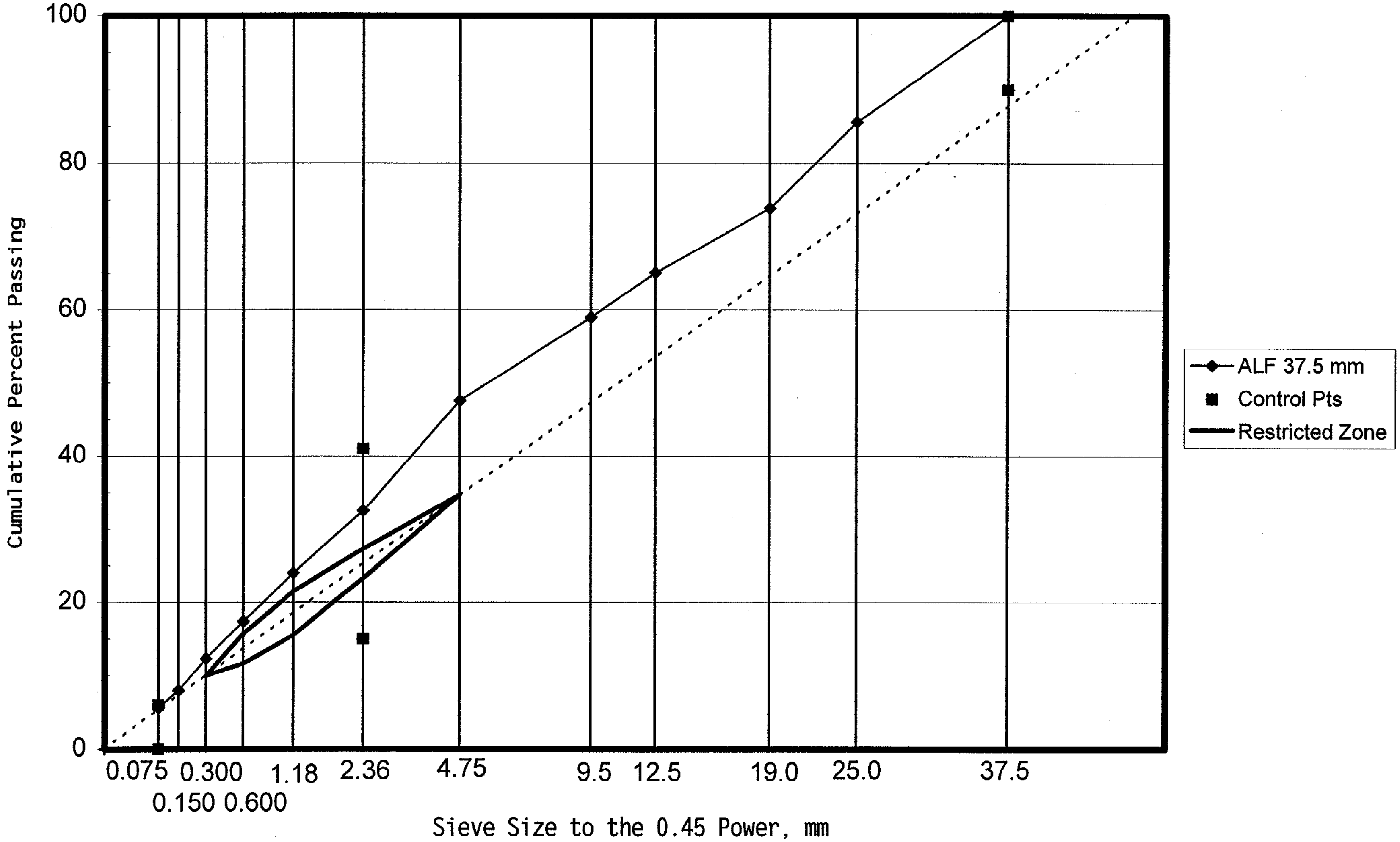

Figure 3. BM-3 aggregate gradation for the base mixtures.

(4) Los Angeles Abrasion

The No. 68 diabase aggregate in the surface mixtures had an average Los Angeles abrasion of 14 when tested in accordance with AASHTO T 96.[4] The No. 357 and No. 8 diabase aggregates in the base mixtures had average Los Angeles abrasions of 20 and 21, respectively. These values indicated that the diabase aggregates were highly resistant to abrasion. Maximum allowable losses are typically in the range of 35 to 40.[5]

(5) Fine Aggregate Angularity

Fine aggregate angularities were measured using the National Aggregate Association's Method A, which was the predecessor of AASHTO TP33-93.[3,7] This method evaluates shape and texture in terms of the percentage of voids in a dry, uncompacted sample. A high void level usually indicates high angularity and a rough texture. A low void level usually indicates the material is rounded and smooth. The 2.36- to 0.150-mm fraction of each fine aggregate was tested.

The No. 10 diabase from Virginia Trap Rock, No. 10 diabase from Luck Stone, and the natural sand from Solite had fine aggregate angularities of 49, 48, and 45 percent, respectively. Superpave required a minimum value of 45 percent for the combined fine aggregate used in surface mixtures that will have traffic levels equal to and greater than 3 million equivalent single axle loads (ESAL's).[5] All three materials individually passed this specification, indicating they had moderate to high angularities and roughnesses. The two diabase aggregates had statistically higher fine aggregate angularities than the natural sand, indicating some slight difference in the materials. Microscopic analyses indicated that particles in the larger size fractions of the natural sand were slightly more cubic in shape than the particles in the diabase aggregates. The diabase aggregates had more elongated particles.

5. Experimental Design for Testing the Pavements

a. Rutting Study

The ALF pavement tests for rutting, including the year that each test was performed, are shown in table 6. Each surface mixture was tested for rutting susceptibility at three pavement temperatures to determine the relationship between rut depth and temperature. The overall temperature range was 46 to 76 °C. The only pavement temperature that could be used for all seven mixtures was 58 °C. The large differences in rutting performance from mixture to mixture, coupled with large changes in rutting performance with a change in temperature, prohibited testing all seven mixtures at another single temperature. The pavements would either rut too quickly or not rut at all, using another single temperature. All seven mixtures were tested at 58 °C in 1994. Tests at 58 °C were repeated in 1995 on the pavements with the

Table 6. Year when each pavement was tested for rutting susceptibility.

Mixture	Pavement Test Temperature and Year of Test							
	46 °C	52 °C	58 °C	58 °C	58 °C	64 °C	70 °C	76 °C
AC-5	1997	1997	1994	1995	1998			
AC-10	1997	1996	1994					
AC-20		1996	1994	1995	1998	1997		
Styrelf			1994				1995	1997
Novophalt			1994				1995	1997
AC-5 Base			1994	1995	1998			
AC-20 Base			1994					

Table 7. Winter when each pavement was tested for fatigue-cracking susceptibility.

Lane	Mixture	Layer Thickness	Pavement Test Temperature and Year of Test		
			28 °C	19 °C	10 °C
1	AC-5	100 mm	1994 to 1995	1997 to 1998	1997 to 1998
2	AC-20	100 mm	1994 to 1995	1997 to 1998	1997 to 1998
3	AC-5	200 mm	1995 to 1996	1996 to 1997	1999 to 2000
4	AC-20	200 mm	1995 to 1996	1996 to 1997	2000 to 2001
5	AC-10	200 mm			1999 to 2000
6	AC-20	200 mm			2000 to 2001
7	Styrelf	200 mm			2000 to 2001
8	Novophalt	200 mm			2000 to 2001

AC-5 and AC-20 (PG 59 and 70) surface mixtures and the AC-5 (PG 59) base mixture to determine the repeatability of the ALF data. These pavements were tested again in 1998 to evaluate age hardening.

Lanes 9, 10, 11, and 12 were dedicated to the rutting study with the objective of determining the effect of nominal maximum aggregate size on rutting susceptibility. Table 1 shows that lanes 9 and 11 contained the AC-5 (PG 59) binder, while lanes 10 and 12 contained the AC-20 (PG 70) binder. The hypothesis to be evaluated was that an increase in nominal maximum aggregate size would decrease the optimum binder content and increase the resistance to rutting.

Another objective was to determine whether the influence of binder grade on rutting susceptibility decreases with an increase in nominal maximum aggregate size. This was to be accomplished by determining the difference in rutting susceptibility provided by the two binders at each nominal maximum aggregate size. The effects for each nominal maximum aggregate size could then be compared with each other. It was hypothesized that binder grade would have less effect on rutting susceptibility when using the larger nominal maximum aggregate size and lower binder content.

Lane 6 with the AC-20 (PG 70) surface mixture was an extra lane. It was constructed in case it was perceived that a pavement should be tested at the same time as a control pavement. The AC-20 (PG 70) surface mixture was considered the control mixture. Fluctuating pavement temperatures or changes in the properties of the underlying materials might lead to a decision that a pavement and a control pavement needed to be tested at the same time using both ALF's. The additional lane provided four additional test sites.

b. Fatigue-cracking Study

The ALF pavement tests for fatigue cracking, including the year that each test was performed, are shown in table 7. Lanes 1, 2, 3, and 4 were dedicated to the fatigue-cracking study with the objective of evaluating possible interactions between asphalt pavement layer thickness, binder grade, and temperature. The primary hypothesis to be evaluated was that softer binders perform better when the asphalt pavement layer is subjected to relatively high tensile strains, while stiffer binders perform better when the asphalt pavement layer is subjected to relatively low tensile strains.

Table 7 shows that temperatures of 28, 19, and 10 °C were used to determine the relationship between fatigue cracking and temperature for the study involving asphalt pavement layer thickness. For these experiments, the pavements were tested in pairs using both ALF's to minimize the effect that changes in the properties of the underlying materials with time might provide. Lane 1 was tested at the same time as lane 2, and lane 3 was tested at the same time as lane 4.

6. Construction Report

Details on the construction of the asphalt pavement layers are documented in a separate report.[8] All binder, aggregate, and mixture tests were performed according to AASHTO test methods.[4] The construction report includes the following:

- Binder test data collected to ensure that the properties of the binders did not change while they were being used. Binder samples were obtained during the mixture designs, from the terminal immediately before shipping, from the hot-mix plant after they arrived from the terminal, and daily during construction. The properties measured were viscosity at 135 °C using a Brookfield viscometer, $G^*/\sin\delta$ at 20 °C and 10 rad/s using the DSR, and infrared analysis, which was used to monitor the functional groups (chemistry) of the binders.

- Marshall mixture design data.

- Comparisons between design and as-constructed properties of the mixes, including aggregate gradations, natural sand contents, binder contents, air voids, and the maximum specific gravities of the mixtures.

- Quality control testing conducted by the paving contractor (binder content, aggregate gradation, nuclear density, maximum specific gravity, and pavement thickness), and quality assurance testing by the FHWA to make sure the specifications of the project were met.

As an example of the data collected during construction, and because of the importance of binder properties to this study, Superpave continuous PG's for samples taken at the start, middle, and end of construction are included in table 2. The high-temperature continuous PG's in table 2 are the temperatures at a $G^*/\sin\delta$ of 1.00 kPa using original, unaged binders. The low-temperature continuous PG's are the temperatures at an m-value of 0.300 plus 10 °C using RTFO/PAV residues. The full suite of Superpave binder tests was not performed on these samples.

The properties of the binders were generally consistent. The low-temperature continuous PG for the AC-20 (PG 64-22) binder provided the greatest amount of variability, ranging from -27 to -34 °C. This spans more than one PG. For low-temperature performance, the interval between PG's is 6 °C. Additional tests on this binder showed the low-temperature continuous PG to be approximately -28 °C.

7. Marshall Mixture Design Properties

a. Pre-Construction Marshall Mixture Designs

The 75-blow Marshall method was used to design the five SM-3 surface mixtures prior to construction.[2,4,9] The following VDOT mixture design criteria were used:

- 75 blows per side using a 4.536-kg hammer.
- Specimen diameter of 101.6 mm and thickness of 63.5 mm.
- Optimum binder content at 4-percent total air voids.
- Minimum stability of 8006 N.
- Flow between 8 and 14, except for the Novophalt and Styrelf mixtures. where only a minimum flow of 8 was required.
- Minimum Voids in the Mineral Aggregate (VMA) of 14.0.
- Voids Filled With Asphalt (VFA) between 65 and 80 percent.

A 112-blow Marshall method was used to design the two BM-3 base mixtures.[10] The stabilities in this method were divided by 2.25, while the flows were divided by 1.5. Theoretically, this conversion accounts for the larger sized specimen used in the 112-blow method compared with the 75-blow method. After converting the data, the data from the two procedures can be compared against each other, and the pass-fail criteria for the 75-blow method can be applied to data from the 112-blow method. Mixture design criteria were as follows:

- 112 blows per side using a 10.21-kg hammer.
- Specimen diameter of 152.4 mm and thickness of 95.3 mm.
- Optimum binder content at 4-percent air voids.
- Minimum stability of 8006 N based on a specimen diameter of 101.6 mm and thickness of 63.5 mm.
- Flow between 8 and 14 based on a specimen diameter of 101.6 mm and thickness of 63.5 mm.
- Minimum VMA of 12.0.
- VFA between 65 and 80 percent.

The average optimum binder contents for the surface and base mixtures were 4.9 and 4.0 percent by mass, respectively. These binder contents provided air-void levels in the range of 4 ±1 percent. All mixtures had Marshall stabilities above 11 000 N. A minimum level of 8006 N is required for pavement mixtures that will have heavy traffic levels. All mixture design criteria were met.

The dust-to-binder ratio by mass was specified by Superpave to be in the range of 0.6 to 1.2[5], although at the time of this report, AASHTO was to vote on raising the upper limit to 1.5 or 1.6. Dust is defined as the percent aggregate by mass passing the 0.075-mm sieve. Binder is defined as the effective binder content by mass (non-absorbed binder). The total binder content by mass was used prior to Superpave when calculating the ratio. Superpave changed the definition for binder, but did not change the definition for dust or the criteria. The total binder content was used when designing the mixtures for this study, although no data existed showing the applicability of the criteria to the mixtures being evaluated. The surface and base mixtures had average ratios of 1.0 and 1.2, respectively, using total binder content, and average ratios of 1.2 and 1.3 using the effective binder content. Additional details for the designs are documented in the construction report.[8]

b. Marshall and Volumetric Properties Measured During and After Pavement Construction

Marshall and volumetric properties for loose mixtures sampled and compacted during construction are given in table 8. Included in table 8 are the properties for mixtures prepared using the stockpiled materials. Binder contents of 4.85 and 4.00 were used in the latter mixtures. These were the overall average binder contents for the two types of mixtures. They were based on the results of extractions performed on samples of loose mixtures taken from the trucks during construction and on pavement cores.[8] Average gradations, shown in tables 4 and 5, were used in these mixtures.

The data in table 8, along with the gradations collected during construction, indicated that the plant-produced mixtures and laboratory-produced mixtures were essentially the same. For example, the air voids ranged from 2.5 to 4.1 percent for the plant-produced mixtures and from 2.9 to 4.3 percent for the laboratory-produced mixtures. The differences between the sets of data are most likely related to small differences in the compositions of the mixtures and to differences in short-term aging. The plant-produced loose mixtures were not oven-aged in the laboratory, while the laboratory-produced loose mixtures were oven-aged at 135 °C for 2 h before compaction. The development of the 2-h oven-aging period is discussed in chapter 2.

The data in table 8 show that the air voids for the AC-5, AC-10, and AC-20 (PG 58-34, 58-22, and 64-22) surface mixtures tended to be low, while their Marshall flows tended to be high. The air voids should be close to 4.0 percent. The maximum Marshall flow was specified to be 14 for these three mixtures. However, the paving contractor was not required to use Marshall or volumetric properties for process control in this project, and at the time of construction, this type of process control was not required by VDOT.

The Marshall stabilities and flows were examined statistically.[11] There were no statistically significant differences between most of the stabilities. The differences among the average stabilities were relatively small compared with the variability of the replicate measurements. Only the mixtures with the highest and lowest stabilities had significantly different stabilities.

In summary, all mixtures had stabilities significantly above the 8006-N minimum specification level, and there was no clear statistical ranking for the mixtures based on stability that could be compared with rankings provided by other mixture tests performed in this study. The same conclusion was found for the Marshall flows.

Table 8. Marshall mixture properties.

Mixture Type	Binder Type	Optimum Binder Content (%)	MSG	Stability (N)	Flow (0.25 mm)	Air Voids (%)	VMA (%)	VFA (%)
Properties of Plant-Produced Mixtures:								
Surface	AC-5	4.80	2.683	12 422	15.0	2.8	14.1	80.2
Surface	AC-10	4.80	2.691	13 046	15.8	2.7	13.8	80.4
Surface	AC-20	4.90	2.688	15 248	16.5	2.5	13.8	81.7
Surface	Novophalt	4.70	2.686	16 573	20.8	4.1	15.1	72.8
Surface	Styrelf	4.90	2.684	19 794	16.4	3.4	14.7	76.9
Base	AC-5	4.00	2.746	13 678	13.5	2.5	11.6	78.4
Base	AC-20	4.10	2.755	16 442	13.3	3.4	12.2	72.1
Properties of Laboratory-Prepared Mixtures:								
Surface	AC-5	4.85	2.699	11 565	14.5	3.0	13.9	78.4
Surface	AC-10	4.85	2.707	12 047	14.6	3.6	14.1	74.5
Surface	AC-20	4.85	2.706	11 232	17.6	2.9	13.5	78.5
Surface	Novophalt	4.85	2.699	16 125	16.8	4.2	14.9	71.8
Surface	Styrelf	4.85	2.701	18 536	22.8	4.0	14.7	72.8
Base	AC-5	4.00	2.750	13 295	12.8	4.3	13.1	67.2
Base	AC-20	4.00	2.750	14 168	12.4	4.2	13.0	67.7

Compaction Temperatures:

AC-5 = 121 °C
AC-10 = 127 °C
AC-20 = 135 °C
Novophalt = 141 °C
Styrelf = 141 °C

Marshall Blows Per Side:

Surface = 75
Base = 112

MSG = Maximum Specific Gravity of the Mixture.
VMA = Voids in the Mineral Aggregate.
VFA = Voids Filled With Asphalt.

8. Moisture Sensitivity

a. Pre-Construction Tests

Moisture sensitivity of the mixtures was evaluated prior to construction in accordance with ASTM Test Method D 4867.[6] In this test, the indirect (splitting) tensile strengths of conditioned and unconditioned specimens are measured. A tensile strength ratio (TSR), defined as the conditioned strength divided by the unconditioned strength, is computed in terms of a percentage. All tests were performed at an air-void level of 7 ±1 percent. The specimens were compacted by a Marshall hammer and had a diameter of 101.6 mm and thickness of 63.5 mm. Short-term oven-aging was not used because it was not part of ASTM D 4867 at the time these tests were performed.

The conditioning procedure consisted of saturating the compacted specimens so that 55 to 80 percent of their air voids were filled with water, soaking the specimens in a water bath at 60 °C for 24 h, and testing them for tensile strength at 25 °C along with the unconditioned specimens. The ASTM D 4867 optional freeze-thaw cycle was not included because it was not used by VDOT or paving contractors doing VDOT work. Mixtures with and without 1-percent hydrated lime were tested.

All mixtures with hydrated lime passed the test based on a minimum TSR of 80 percent. The TSR's of mixtures without hydrated lime ranged from 0.74 to 0.80. Even though these TSR's indicated only a slight susceptibility to moisture damage, the 1-percent hydrated lime requirement was maintained. At the time of construction, VDOT specified a TSR of 0.75.[2]

b. Tests After Construction

Tests on the five surface mixtures were repeated after construction using the stockpiled materials. A diametral modulus test, which provides a diametral modulus ratio (M_dR), was included in the evaluation along with a visual estimate of stripping. ASTM D 4867 was again used, except that the optional freezing cycle of -17.8 °C for 15 h was included to provide the most severe conditioning. The two base mixtures were not evaluated even though they were tested during the mixture design phase of the study. Theoretically, the BM-3 aggregate is too large for a specimen size of 101.6 by 63.5 mm.

The test results are shown in table 9. Pass/fail criteria of 80 percent for TSR, 70 percent for M_dR, and 10 percent for visual stripping have been recommended for conventional, dense-graded hot-mix asphalt.[5,12] Based on these criteria, the mixture with AC-5 (PG 58-34) failed the tests and the mixture with AC-10 (PG 58-28) was marginal. The other three mixtures passed the test, perhaps because they contained stiffer binders. Aggregate particles in the size range of 1.18 to 4.75 mm primarily stripped in the mixtures with the AC-5 and AC-10 (PG 58-34 and 58-28) binders, while aggregate particles greater than 12.5 mm stripped in the mixtures with the Novophalt and Styrelf binders. Visual stripping in the latter two mixtures was low. They were estimated to be 2 and 6 percent. No stripping was found in the pavements over the course of this study.

9. Superpave Volumetric Properties

Superpave was not used to design the mixtures because the methodology had not been finalized by the time of pavement construction. Mixtures produced from the stockpiled raw materials were compacted in the Troxler Model 4140 SGC after the Superpave test procedures and specifications were published in 1995.[3] The compaction temperatures were the same as those used in the Marshall mixture designs, which are shown in table 8.

All specimens were compacted to a single N-max of 174 revolutions. This N-max corresponded to an N-design of 109, which was specified by Superpave for a traffic level of 10 to 30 million ESAL's.[3] This N-design was chosen because it corresponded to a moderate to heavy level of traffic. However, it was not known how the number of ALF wheel passes at a controlled pavement temperature related to Superpave ESAL's.

Table 10 provides the optimum binder contents based on a 4.0-percent air-void level using four levels of N-design. The lower part of table 10 shows the air voids for the surface and base mixtures based on a 4.85- and 4.00-percent binder content, respectively. Both sets of data were taken from the same SGC compaction curves. The maximum specific gravity of the mixture and the bulk specific gravities of the specimens at N-max were used to determine the air voids in accordance with the 1995 Superpave specification.[3]

Superpave required a minimum VMA of 13.0 for a nominal maximum aggregate size of 19 mm, and 11.0 for a nominal maximum aggregate size of 37.5 mm. The data in table 10 show that the mixtures met these requirements at an N-design of 109. VFA was required to be between 65 and 75 percent for traffic levels equal to and greater than 3 million ESAL's. Table 10 shows that all seven mixtures had VFA above 75 percent. This upper limit is used to prevent rutting and bleeding. The Superpave requirements for VMA and VFA are based on a 4-percent air-void level. All mixtures at an N-design of 109 had air voids below 4.0 percent. These findings indicated that the gradations would have to be altered to meet the upper VFA criterion and, even with these alterations, the binder contents would probably have to be reduced. However, the VDOT mixtures used in this study did not have a history of rutting or bleeding, and the 75-blow SM-3 surface mixture had a tendency to ravel.

The low estimated N-designs at 4.0-percent air voids in table 10 indicated that the mixtures, according to Superpave, should only be used in low-volume pavements. This finding is not reasonable based on the field rutting performances of the two mixtures with AC-20 (PG 64-22) in Northern Virginia. Both mixtures are highly resistant to rutting when properly designed and constructed. Also, at the time of construction in 1993, VDOT generally used 4.5-percent binder by mass in BM-3 base mixtures, whereas only 4.0 percent was used in this study.

Table 9. Results from the ASTM D 4867 test method for moisture sensitivity performed on the five surface mixtures.

Pre-Superpave: Superpave PG:	AC-5 58-34	AC-10 58-28	AC-20 64-22	Novophalt 76-22	Styrelf 82-22
Average Indirect Tensile Strengths (TS) and Diametral Moduli (M_d) at 25 °C					
Wet TS, kPa	217	373	560	626	725
Dry TS, kPa	316	466	616	707	859
Wet M_d, MPa	455	960	1583	2526	1911
Dry M_d, MPa	713	1390	1571	3056	2445
Retained Ratios, Visual Stripping, Saturation, and Air Voids					
TS Retained Ratio, %	69	80	91	89	84
M_d Retained Ratio, %	64	69	101	83	78
Visual Stripping, %	17	10	0	2	6
Final Saturation, %	72	71	65	71	71
Air Voids, %	7.8	8.3	7.2	8.3	8.1

Table 10. Superpave Gyratory Compactor results.

Binder Type	Mixture Type	Binder Contents at 4-Percent Air Voids and Four Levels of N-design: 68	86	109	142
AC-5	Surface	4.85	4.50	4.25	4.00
AC-10	Surface	5.10	4.75	4.45	4.15
AC-20	Surface	5.10	4.80	4.50	4.25
Novophalt	Surface	5.00	4.50	4.15	3.95
Styrelf	Surface	4.55	4.20	3.95	3.80
AC-5	Base	3.90	3.65	3.50	3.35
AC-20	Base	3.90	3.65	3.45	3.25

Binder Type	Mixture Type	Air Voids at Binder Contents of 4.85 Percent for the Surface Mixtures and 4.00 Percent for the Base Mixtures, %: Marshall Impact Hammer	SGC N-design of 68	86	109	142	VMA, % at 109	VFA, % at 109	N-design, at 4.0 % Air Voids
AC-5	Surface	3.0	4.0	3.2	2.4	1.7	13.4	81.8	68
AC-10	Surface	3.6	4.6	3.8	3.1	2.3	13.6	77.9	82
AC-20	Surface	2.9	4.6	3.8	3.2	2.4	13.7	77.4	82
Novophalt	Surface	4.2	4.1	3.6	2.8	2.1	13.7	79.4	72
Styrelf	Surface	4.0	3.4	2.7	2.2	1.5	13.0	83.9	56
AC-5	Base	4.3	3.7	3.1	2.5	1.8	11.5	77.6	61
AC-20	Base	4.2	3.7	3.0	2.3	1.7	11.2	80.4	62

The Superpave volumetric requirements were based on relationships between mixture volumetric properties and the pavement performances of dense-graded mixtures. However, the majority of these mixtures were designed using the Marshall hammer and not a gyratory compactor. Adjustments to the N-designs given in the 1995 and 1998 Superpave specifications may be needed for some mixtures.[3] (Authors' note: AASHTO was reviewing new proposed N-designs when this report was being published in 1999.)

10. SGC Revolutions Needed to Obtain Air Voids That Matched the Final Air Voids of the Pavements

The air voids in and out of the wheelpaths were measured and evaluated during this study. The air-void data shown in table 11 were collected from 1994 to 1997. Analyses of the data are given in chapters 2 and 3. The information concerning the SGC is included in this chapter because it complements the preceding information on this compactor.

After each ALF pavement test was completed, the number of SGC revolutions needed to match the final air-void level of the pavement was determined. Table 11 shows the required number of revolutions based on the air voids in the top and bottom halves of the pavements. The average is also given.

The revolutions in table 11 can only be considered estimates for N-design, because the 1995 Superpave methodology for calculating the specimen air-void level as a function of SGC revolutions often led to air voids that were high at low revolutions relative to AASHTO T 166-93.[4] The air voids provided by the 1995 procedure included the air voids in contact with the cylindrical surface of the mold. These air voids would not be part of the specimen if the specimen were to be removed from the mold and tested using AASHTO T 166. AASHTO T 166, which is the standardized procedure for determining density, uses the saturated surface-dry condition to determine the volume of a specimen. This volume does not include the volume of any surface air voids. Therefore, AASHTO T 166 can provide a lower volume and a higher density compared with the SGC procedure. If this occurs, the revolutions provided by the SGC are too high. (Authors' note: This procedure was changed in 1999 so that the air voids would be directly measured using specimens removed from the molds at the desired N-design.) A second reason why the revolutions in table 11 can only be considered estimates is that it was assumed that the ultimate density of each pavement was reached before the pavement test was terminated. However, the change in pavement density was not monitored during the ALF tests, and the tests were not stopped at the same rut depth.

The data show that most of the gyratory revolutions were low relative to an N-design of 109. The revolutions ranged from 18 for the bottom half of the pavement with the Novophalt surface mixture tested at 58 °C to 128 for the bottom half of the pavement with the AC-5 (PG 59) base mixture tested at 58 °C. The revolutions were very low for the Novophalt and Styrelf mixtures, which generally had high air-void levels before and after testing. The data indicated that adjustments to the N-designs given in the 1995 and 1998 Superpave specifications may be needed for some mixtures.[3]

Table 11. Number of Superpave gyratory revolutions needed to obtain the final pavement air-void levels.

Superpave PG:	58-34	58-28	58-34	58-28	64-22
Conventional:	AC-5	AC-10	AC-5	AC-10	AC-20
Lane Number:	03	05	09	05	06
Final Rut Depth[1]	20	21	24	21	21
Test Temp, °C:	46	46	52	52	52
Top 100 mm of Pavement					
Initial Air Voids, %	7.4	6.4	5.6	8.3	8.6
Densification, %	3.6	2.0	1.8	1.5	3.1
Final Air Voids, %	3.8	4.4	3.8	6.8	5.5
Revolutions	71	70	71	36	53
Bottom 100 mm of Pavement					
Initial Air Voids, %	7.8	5.9	5.0	8.1	8.1
Densification, %	2.6	2.1	2.2	4.9	3.5
Final Air Voids, %	5.2	3.8	2.8	3.2	4.6
Revolutions	48	84	96	102	69
Entire Pavement					
Initial Air Voids, %	7.6	6.1	5.3	8.2	8.4
Densification, %	3.1	2.0	2.0	3.2	3.3
Final Air Voids, %	4.5	4.1	3.3	5.0	5.1
Revolutions	59	76	82	58	59
Applied ALF Wheel Passes (ESAL's)	250,000	125,000	3,500	25,000	215,000

[1]In the 200-mm thick asphalt pavement layer.

Table 11. Number of Superpave gyratory revolutions needed to obtain the final pavement air-void levels (continued).

	Surface Mixture					Base Mixture	
Superpave PG:	58-34	58-28	64-22	76-22	82-22	58-34	64-22
Conventional:	AC-5	AC-10	AC-20	Novphlt[2]	Styrelf	AC-5	AC-20
Lane Number:	09	05	10	08	07	11	12
Final Rut Depth[1]	26	27	31	9	22	24	24
Test Temp, °C:	58	58	58	58	58	58	58
Top 100 mm of Pavement							
Initial Air Voids, %	7.8	8.5	9.1	11.9	11.9	6.7	7.4
Densification, %	4.4	2.9	5.4	3.4	4.3	3.6	2.4
Final Air Voids, %	3.4	5.6	3.7	8.5	7.6	3.1	5.0
Revolutions	80	50	90	21	28	90	41
Bottom 100 mm of Pavement							
Initial Air Voids, %	7.0	8.4	8.3	10.8	12.8	6.0	7.4
Densification, %	4.2	5.1	4.9	1.8	4.6	3.8	2.3
Final Air Voids, %	2.8	3.3	3.4	9.0	8.2	2.2	5.1
Revolutions	97	99	99	18	24	128	39
Entire Pavement							
Initial Air Voids, %	7.4	8.4	8.7	11.4	12.3	6.3	7.4
Densification, %	4.3	4.0	5.2	2.6	4.4	3.7	2.4
Final Air Voids, %	3.1	4.4	3.5	8.8	7.9	2.6	5.0
Revolutions	88	70	93	19	26	109	41
Applied ALF Wheel Passes (ESAL's)	2,000	4,000	10,000	208,805	200,000	20,000	200,000

[1]In the 200-mm thick asphalt pavement layer.
[2]Novophalt.

Table 11. Number of Superpave gyratory revolutions needed to obtain the final pavement air-void levels (continued).

Superpave PG:	64-22	76-22	82-22	76-22	82-22
Conventional:	AC-20	Novophalt	Styrelf	Novophalt	Styrelf
Lane Number:	06	08	07	08	07
Final Rut Depth[1]	21	17	21	17	21
Test Temp, °C:	64	70	70	76	76
Top 100 mm of Pavement					
Initial Air Voids, %	8.4	11.0	12.3	9.1	10.4
Densification, %	2.9	3.2	5.5	2.3	5.7
Final Air Voids, %	5.5	7.8	6.8	6.8	4.7
Revolutions	53	25	27	32	47
Bottom 100 mm of Pavement					
Initial Air Voids, %	9.0	10.1	12.1	10.4	9.9
Densification, %	5.3	3.6	5.5	4.2	4.4
Final Air Voids, %	3.7	6.5	6.6	6.2	5.5
Revolutions	90	35	29	38	38
Entire Pavement					
Initial Air Voids, %	8.7	10.6	12.2	9.7	10.2
Densification, %	4.1	3.4	5.5	3.2	5.1
Final Air Voids, %	4.6	7.2	6.7	6.5	5.1
Revolutions	69	29	28	35	42
Applied ALF Wheel Passes (ESAL's)	8,000	125,000	125,000	700,000	225,000

[1]In the 200-mm thick asphalt pavement layer.

11. Confounding Factors in This Study

This section of the report lists factors that could have affected the results of this study or the interpretation of the data. Most studies on asphalt mixtures and pavements have variables that cannot be controlled and often confound the results that are obtained. Even so, the numerous variables that affect pavement performance were controlled in this study to a higher degree than studies using in-service pavements.

Aggregates with high qualities, in terms of angularity, gradation, and hardness, were chosen for this study based on the expectation that the modified binders would be used in pavements containing high-quality aggregates that are subjected to heavy traffic levels. To justify the higher costs associated with most modified binders, these binders must provide benefits that match or exceed their cost regardless of the quality of the aggregate. The VDOT SM-3 surface mixture with the AC-20 (PG 64-22) binder has been used in Northern Virginia highways subjected to heavy traffic levels. This mixture is highly resistant to rutting when properly designed and constructed, although at the time of construction in 1993, VDOT also used an AC-30 asphalt binder with the SM-3 gradation in some pavements to further increase its resistance to rutting. The maximum allowable thickness is 50 mm. The SM-3 surface mixture used in this study also met the requirements for a VDOT IM-1A intermediate mixture.[2] The maximum allowable thickness for this application is 75 mm. Based on the experiences of many highway agencies, some mixtures are more resistant to rutting when used in thin lifts compared with thick lifts because the maximum aggregate size is approached as the thickness of the lift is decreased. Maximum layer thicknesses have been developed over time based on a variety of pavement experiences. Thus, even though the SM-3 surface mixture with the AC-20 (PG 64-22) binder is highly resistant to rutting when properly designed and constructed, its performance using a thickness of 200 mm is not known.

Although some mixtures rut less if used in thin lifts compared with thick lifts, thin lifts placed on Portland cement concrete may rut more than thick lifts when rutting is calculated as a percentage of the thickness of the lift. Complexities related to layer thickness and the properties of underlying layers were not evaluated in this study.

The BM-3 base mixture with AC-20 (PG 64-22) is used in Northern Virginia highways subjected to heavy traffic levels. This mixture is highly resistant to rutting when properly designed and constructed. However, a BM-3 mixture is always overlaid with intermediate and surface courses, whereas the two base mixtures constructed for this study were not overlaid. Therefore, for an equal amount of loading, the stresses from the load should be higher in the ALF pavements compared with in-service pavements. Even so, it was expected that the base mixture in lane 12 with the AC-20 (PG 64-22) binder would be highly resistant to rutting.

Even though the pavements in this study were heated to control the test temperature (discussed in chapter 2 of this report), a precisely controlled environment was not obtainable because the FHWA pavement test facility is an outdoor facility. When the pavement test temperature during a rutting test deviated by more than 6 °C from the target temperature due to a cold rain, the pavement test was suspended until the target temperature could be reestablished. A value of 3 °C was used for the fatigue-cracking tests. The effect of stopping the ALF, if any, on the pavement performance data was unknown and could not be taken into account.

One objective of this study was to validate several predictive laboratory mixture tests using ALF. However, the conventional test temperatures and applied stresses used by most of the laboratory mixture tests did not match the temperatures and stresses in the ALF pavement tests. Test temperatures and stresses in many laboratory mixture tests, such as wheel-tracking tests, have been chosen based on empirical relationships between the test data and the performances of in-service pavements that are subjected to some range in traffic level, vehicle speed, and temperature. These empirical relationships include the effects of having boundaries in the laboratory test, such as steel holders or platens, that are not the same as for in-service pavements.

Other possible confounding factors were (1) differences in material and volumetric properties from pavement to pavement, including the fact that the SM-3 surface mixtures contained 8-percent natural sand, while the BM-3 base mixtures contained 5-percent natural sand, and (2) binder properties can have seasonal variations that are a function of whether the pavement temperature has been increasing or decreasing over a period of several months. Seasonal variations are not considered in most studies.

CHAPTER 2: VALIDATION OF THE SUPERPAVE BINDER PARAMETER FOR RUTTING BASED ON ALF PAVEMENT TESTS AT 58 °C

1. Superpave Binder Parameter for Rutting

a. Derivation of $G^*/\sin\delta$

The Superpave binder specification uses the parameter $G^*/\sin\delta$ to specify binders according to rutting susceptibility at high pavement temperatures. This parameter is measured using a dynamic shear rheometer (DSR), which subjects a sample of binder between two parallel plates to oscillatory shear. Tests in this study were performed on RTFO residues. The high-temperature continuous PG of each binder is the temperature that provides a $G^*/\sin\delta$ of 2.20 kPa.

The binder specification also requires unaged binders to be tested by the DSR at high temperatures to control tenderness. To accomplish this, the temperature that provides a $G^*/\sin\delta$ of 1.00 kPa is determined. These temperatures were obtained, but they were not used in this study. Table 2 in chapter 1 shows that the two sets of high-temperature grades were close.

The binder parameter $G^*/\sin\delta$ is based on dissipated energy. With each cycle of loading, the work done in deforming an asphalt or an asphalt pavement at high temperatures is partially recovered by the elastic component of the strain and partially dissipated by the viscous flow component of the strain and any associated generation of heat. The energy dissipated by the viscous flow component per cycle of loading can be calculated using:

$$\Delta U = \int \tau \, d\gamma \tag{1}$$

The following relationship is obtained for a sine wave loading upon integrating equation (1) from 0 to 2π:[13]

$$\Delta U = \pi \, \tau_{max} \, \gamma_{max} \, \sin\delta \tag{2}$$

where:
ΔU = Energy loss per cycle, or dissipated energy
π = 3.14159,
τ = Shear stress,
γ = Shear strain,
τ_{max} = Maximum shear stress,
γ_{max} = Maximum shear strain, and
δ = Phase angle.

Superpave uses a stress-controlled type of pavement loading where each binder will be subjected to the same maximum stress or set of stresses. Therefore, the maximum shear stress is a constant along with π, and equation (2) becomes:

$$\Delta U \propto \gamma_{max} \sin\delta \qquad (3)$$

Since $|G^*| = \tau_{max}/\gamma_{max}$ and $\gamma_{max} = \tau_{max}/|G^*|$, equation (2) can also be written as follows:

$$\Delta U = (\pi\ \tau_{max}^2 \sin\delta)/|G^*| \qquad (4)$$

where: $|G^*|$ = the absolute value of the complex shear modulus.

For a stress-controlled type of pavement loading, the maximum shear stress is a constant along with π, and thus equation (4) becomes:

$$\Delta U \propto \sin\delta/|G^*| \qquad (5)$$

Superpave uses this equation because $|G^*|$ is a constant in the linear viscoelastic range. Therefore, all asphalt binders do not have to be tested using the same maximum shear stress. Furthermore, a stress- or strain-controlled DSR can be used to obtain the individual parameters G* and sinδ. These parameters can then be used to calculate $\sin\delta/|G^*|$, which is only valid for a stress-controlled mode of loading applied in the form of a sine wave in the linear viscoelastic range.

As $\sin\delta/|G^*|$ decreases, rutting susceptibility should decrease. This can be accomplished by decreasing sinδ or increasing $|G^*|$. $|G^*|$ is a measure of the total resistance of the binder to strain. Sinδ, which is equal to the loss modulus G″ divided by G*, is a relative measure of the viscous flow component of the strain. Equations (3) and (5) are equivalent, but the meaning of ΔU is more readily apparent using equation (3). In equation (3), dissipated energy is proportional to the permanent shear strain, which is the maximum shear strain times sinδ. Thus, if the response to a stress is purely elastic, then:

$$\delta = 0,\ \sin\delta = 0,\ \text{and}\ \Delta U = 0 \qquad (6)$$

If the response to a stress is purely viscous, then γ_{max} consists entirely of permanent strain, and:

$$\delta = 90,\ \sin\delta = 1,\ \text{and}\ \Delta U \propto \gamma_{max} \qquad (7)$$

Two changes to equation (5) were made when developing the binder specification. First, the absolute value symbols for G* were dropped. G* is the complex shear modulus that is a vector containing an imaginary element, while $|G^*|$ is the dynamic shear modulus that is a scalar containing no imaginary element. Normally, when the absolute value symbols are dropped, $|G^*|$ is described simply as G, which is called the dynamic shear modulus. In Superpave only the absolute value symbols were dropped for simplification purposes. Technically, the term should be described as $|G^*|$.

Second, because most asphalt paving technologists have some understanding of the term "modulus," the parameter $\sin\delta/G^*$ was inverted to $G^*/\sin\delta$ for convenience. Based on dissipated energy, $G^*/\sin\delta$ is inversely proportional to the energy dissipated by the viscous flow component of the strain; therefore, as $G^*/\sin\delta$ increases, rutting susceptibility should decrease.

b. G*/sinδ's of the Binders Corresponding to the ALF Pavement Tests

Samples of the five binders were aged using the RTFO and tested by the DSR to determine $G^*/\sin\delta$ as a function of temperature and angular frequency.[14] All tests were performed in the linear viscoelastic range. For DSR tests at 40 °C and higher, a 1-mm gap and 25-mm diameter plates were used. For tests below 40 °C, a 2-mm gap and 8-mm diameter plates were used. As expected, $G^*/\sin\delta$ decreased with an increase in temperature and with a decrease in angular frequency.

The $G^*/\sin\delta$'s of the five binders at the pavement test temperature of 58 °C and an angular frequency of 2.25 rad/s were obtained. These $G^*/\sin\delta$'s were compared with the ALF pavement test results. A DSR angular frequency of 2.25 rad/s was chosen based upon a vehicle speed of 80 km/h being equivalent to the standard DSR angular frequency of 10.0 rad/s. Therefore, the speed of the ALF, which was 18 km/h, was divided by 8.0 km/h per rad/s to obtain a DSR angular frequency of 2.25 rad/s. This frequency, which accounts for the relatively slow speed of the ALF, is called the "ALF angular frequency" in this report. The $G^*/\sin\delta$'s of the binders at the standard angular frequency of 10.0 rad/s and at 2.25 rad/s are given in table 12 and figures 4 and 5. (Authors' note: Superpave currently equates a vehicle speed of 100 km/h to 10.0 rad/s, whereas, 80 km/h was equated to 10.0 rad/s by Superpave when this study started. This change was made without the addition of new data and is inconsequential. The relationship between vehicle speed and DSR angular frequency is inherent in the test method.)

A frequency of 10.0 Hz, which is equivalent to a total loading time of 0.1 s/cycle, is used in most repeated load mixture tests for fatigue cracking and rutting. The peak load occurs at 0.05 s. This loading time has been in use for more than 30 years. It was based on a vehicle speed of 80 ±10 km/h (22 ±3 m/s) and an average pavement deflection basin length of 2.2 m:

$$\text{time} = \text{distance}/\text{speed} = 2.2\ \text{m}/22\ \text{m/s} = 0.1\ \text{s}$$

Because the loading time of 0.1 s is based on an average deflection basin due to pavement bending, it is reasonable to assume this loading time can be used in repeated load tests for fatigue cracking. (The applicability of using 2.2 m vs. some other length is a separate issue.) Whether the entire deflection basin should be used to establish the loading time for rutting tests can be questioned, but 0.1 s is the loading time most commonly used for repeated load compression and shear tests for rutting. Based on physics and a loading time of 0.1 s, the angular frequency for the DSR should be:

$$\omega = 2\pi f = 2\pi/t = (6.28\ \text{rad/cycle})/(0.1\ \text{s/cycle}) = 62.8\ \text{rad/s}$$

where: ω = angular frequency, rad/s
2π = conversion, rad/cycle
f = frequency = $1/t$, Hz, or cycles/s
t = time period of one cycle, s/cycle

Superpave should use a standard frequency of 62.8 rad/s. The use of 10.0 rad/s in lieu of 62.8 rad/s means that Superpave equates 10.0 rad/s to 10.0 Hz to 80 km/h (or 100 km/h). No justification for this discrepancy is known. It was decided to use an angular frequency of 2.25 rad/s, which was based on a vehicle speed of 80 km/h being equivalent to the standard DSR angular frequency of 10.0 rad/s.

When comparing the $G^*/\sin\delta$'s given in table 12 with each other, it should be kept in mind, that as the test temperature decreases, at some temperature the rheological properties of the binders will change such that the parameter $G^*/\sin\delta$ is no longer a valid measure of rutting susceptibility. This temperature is unknown and should vary from binder to binder. Because no rest period is used in the DSR test, the time dependent recoverable strain (delayed elastic strain) that would be recovered if a rest period were to be included, is measured as permanent strain by the DSR. The amount of time dependent recoverable strain should decrease with an increase in temperature, and should be negligible for unmodified binders at the test temperatures used to grade these binders. This warning also applies to figures 4 and 5. The data in table 2 of chapter 1 should be used to compare the moderate and low temperature properties of the binders.

2. Background for the ALF Pavement Tests

The ALF consists of a structural frame, 29 m in length, containing a moving wheel assembly. The wheel assembly models one-half of a single rear truck axle and can apply loads ranging from 44.5 to 100.1 kN. Approximately 8,600 wheel passes can be applied per day if no distress surveys are needed; 50,000 wheel passes can be applied per week, which includes time for maintenance. To simulate highway traffic, the ALF loads the pavement in one direction. The loads can also be distributed from side to side to simulate traffic wander. The ALF is computer controlled, permitting a 24-h operation. The ALF is shown in figures 6 and 7. Additional information on the ALF is given in appendix A.

The ALF in the rutting study was operated according to the following characteristics:

- Super single tire with a tire pressure of 690 kPa.
- Load of 43 kN.
- No lateral wheel wander.
- Speed of 18.5 km/h.
- Total wheelpath length of 13.7 m (the distress surveys are performed on a 10-m section).
- An infrared heating system and thermocouples in the pavements provided the required pavement temperature at the required pavement depth.

Table 12. G*/sinδ after RTFO vs. temperature and angular frequency.

Temp. (°C)	AC-5	AC-10	AC-20	Novophalt	Styrelf
G*/sinδ at 10.0 rad/s, Standard Angular Frequency for the DSR, Pa:					
10	5 172 000	11 990 000	17 880 000	26 390 000	22 550 000
20	862 000	2 001 000	3 074 000	5 603 000	5 106 000
30	173 100	386 600	666 300	1 154 000	1 053 000
40	38 640	82 800	159 900	263 600	270 900
50	7 528	15 880	30 660	60 150	75 960
58	2 600	5 285	10 010	21 090	35 170
60	2 096	4 202	7 897	16 580	28 504
70	653	1 238	2 226	4 965	11 380
G*/sinδ at 2.25 rad/s, Angular Frequency for the ALF, Pa:					
10	2 240 000	5 364 000	8 335 000	12 560 000	11 074 118
20	351 800	833 500	1 383 000	2 279 000	2 294 000
30	62 220	143 900	267 700	425 400	466 900
40	11 910	26 350	54 470	92 470	117 700
50	2 057	4 446	9 002	19 140	31 790
58	664	1 384	2 702	6 826	13 710
60	526	1 084	2 100	4 914	11 570
70	155	299	549	1 306	4 435

Table 13. High-temperature continuous PG at the standard DSR angular frequency of 10 rad/s and the ALF angular frequency of 2.25 rad/s.

Conventional Designation:	AC-5	AC-10	AC-20	Novo-phalt	Styrelf
At G*/sinδ = 2.20 kPa, 10.0 rad/s, °C	59	65	70	77	88
At G*/sinδ = 2.20 kPa, 2.25 rad/s, °C	50	56	59	66	77
Temperature Difference, °C	9	9	11	11	11
Average Temperature Difference = 10 °C					

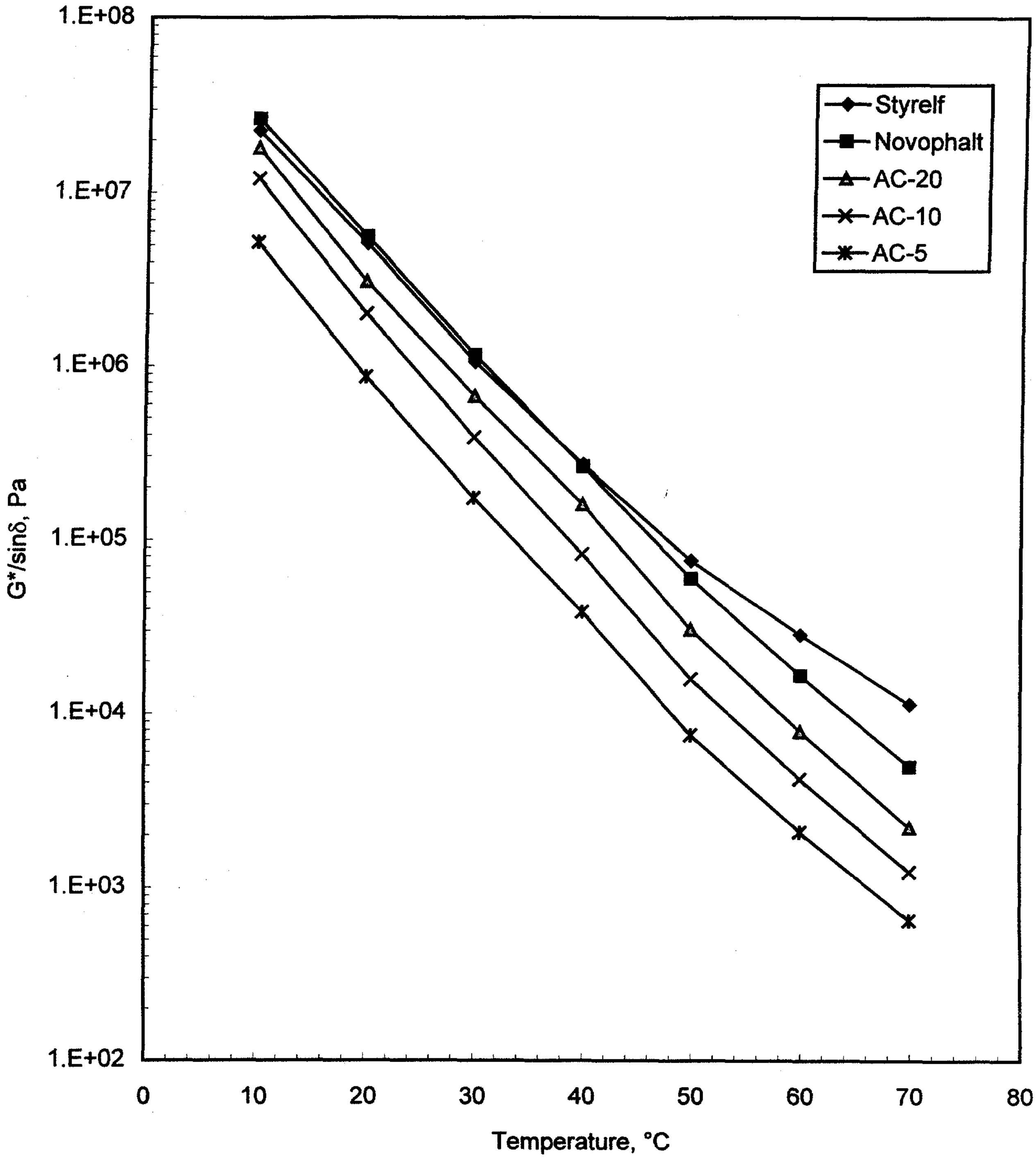

Figure 4. G*/sinδ vs. temperature at a DSR frequency of 10.0 rad/s.

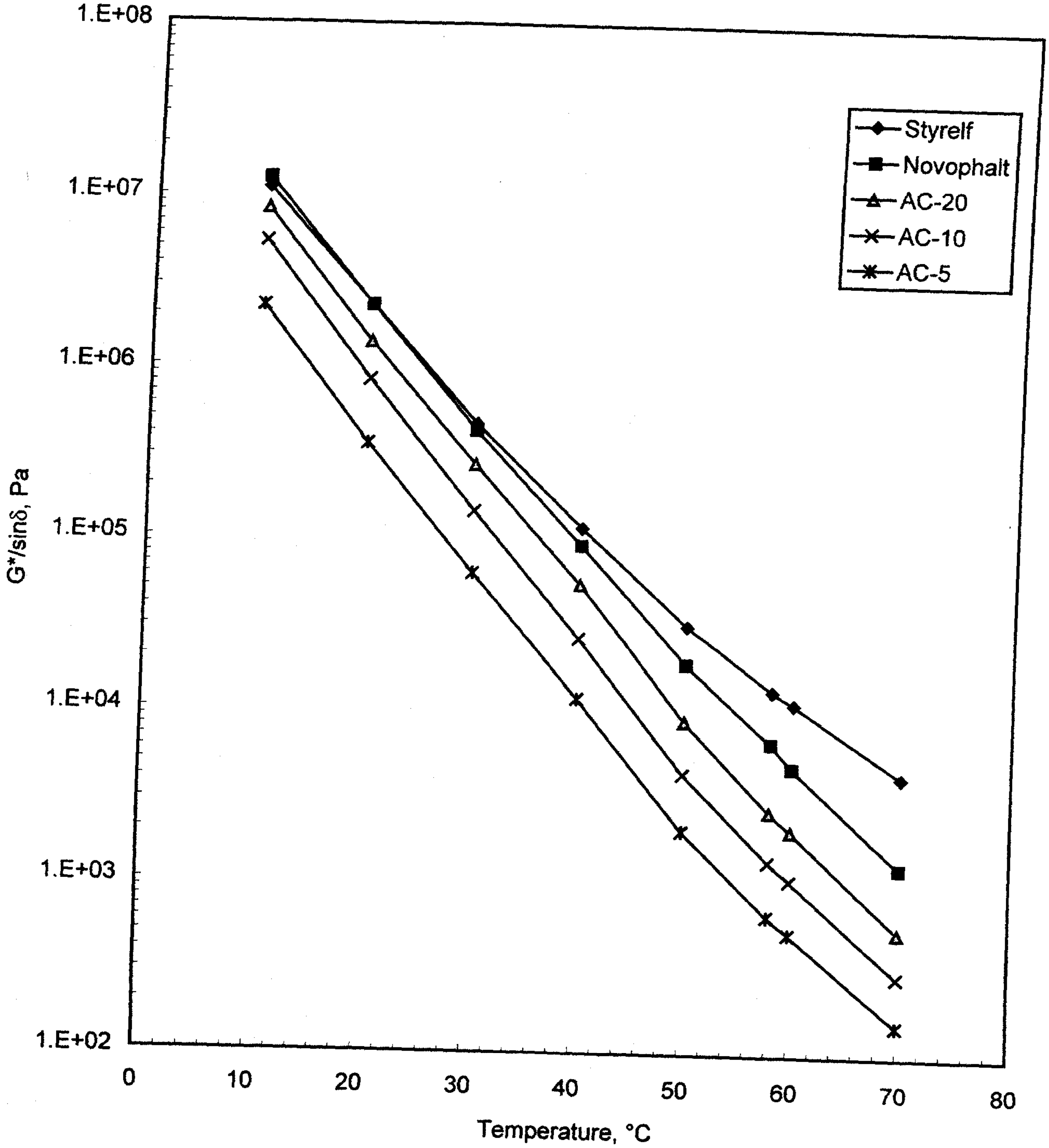

Figure 5. G*/sinδ vs. temperature at a DSR frequency of 2.25 rad/s.

Figure 6. The FHWA Accelerated Loading Facility and typical ruts in the pavements.

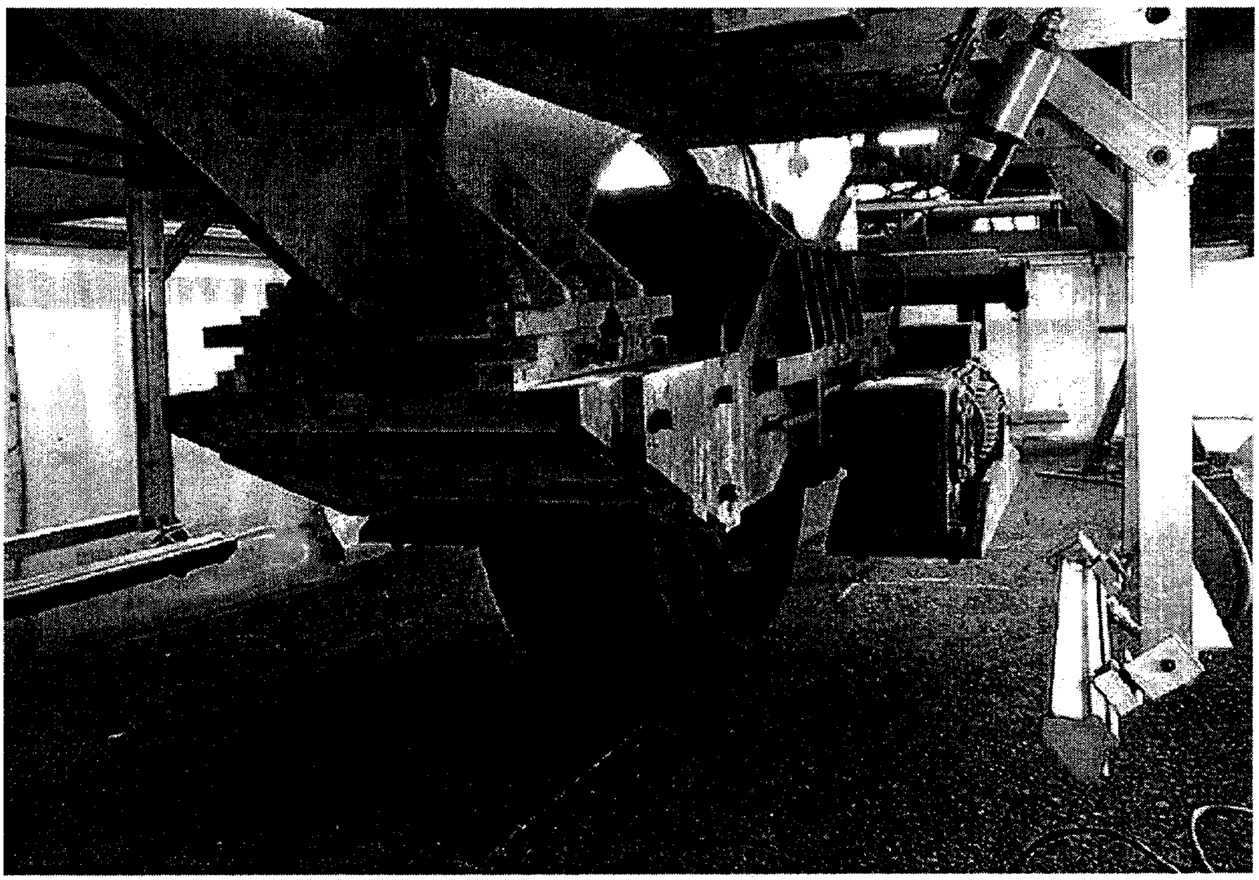

Figure 7. Close-up of the ALF super single tire
and heat lamps on the right and left sides of the tire.

A super single tire and no wander were chosen in lieu of a dual wheel tire and wander so that the data collected in this study could be used to develop or refine performance prediction models in future studies. This type of loading is the easiest to model. The following data were collected:

- Temperature of the asphalt pavement layer versus depth.
- Transverse and longitudinal surface profiles.
- Crack mapping.
- Deformations in underlying layers.
- Core properties in and out of the wheelpath.
- Profiles after trenching.

Pavement temperature was controlled during trafficking using infrared lamps attached to the bottom of the ALF frame. Temperatures at pavement depths of 0, 20, 102, and 197 mm were recorded by thermocouples at two locations outside, but close to, the wheelpath. A target temperature of 70 °C at a depth of 20 mm was initially chosen so that the pavement tests would be performed at a temperature near the middle of the high-temperature PG's of the five binders. However, the Superpave binder specification is based on traffic speeds of 80 to 100 km/h while the ALF travels at 18 km/h. Therefore, the slow speed of the ALF would make the pavement tests too severe at 70 °C. Table 13 provides the temperatures of the five binders at a $G^*/\sin\delta$ of 2.20 kPa and frequencies of 10.0 and 2.25 rad/s. According to the temperatures in table 13, a test performed at 2.25 rad/s and a selected temperature is equivalent to a test performed at 10 rad/s and a 10 °C higher temperature. Assuming this relationship is applicable to the ALF, an ALF pavement test at 58 °C and 18 km/h is equivalent to an ALF pavement test at 68 °C if the speed could be increased to 80 to 100 km/h. Because of this, the target temperature was reduced approximately two grades to 58 °C. This is equivalent to the shift in high-temperature PG for "standing" traffic loadings, defined as less than 20 km/h in the 1998 AASHTO provisional standard MP2.[(3)] The temperature at a depth of 20 mm was controlled in this study because Superpave recommended that the temperature at this depth be used to represent the temperature of a pavement.[(15)] The locations for the thermocouples are shown in figure 8.

All seven mixtures were tested at 58 °C in 1994. Tests at 58 °C were repeated in 1995 on the pavements with the AC-5 and AC-20 (PG 59 and 70) surface mixtures and the AC-5 (PG 59) base mixture to determine the repeatability of the ALF data. These three pavements were chosen because after the seven pavements were tested, the ALF rutting performances of the poorest performing pavements, which included these three pavements, were close to each other. The ALF rutting performances of the best performing pavements were distinctly different.

A minimum of seven distress surveys was performed on each pavement during trafficking using Long-Term Pavement Performance distress survey methods.[(16)] The surveys included transverse profiles, longitudinal profiles, and the number and severity of cracks. A rut depth of 20 mm in the asphalt pavement layer was defined as the failure point for the rutting studies. This rut depth is equivalent to 10 percent strain, and it was measured based on the initial pavement surface elevation. The measurement did not include any upward heaving outside the wheelpath.

After pavement failure, three 152.4-mm diameter cores were taken from the wheelpath and eight 152.4-mm cores were taken outside the wheelpath to determine air voids and densification, and to verify asphalt pavement layer thickness, rut depth, binder content, aggregate gradation, and maximum specific gravity. The thicknesses of the lifts in and out of the wheelpath were measured to estimate how much permanent deformation occurred in each lift. The surface mixtures were placed in four lifts while the base mixtures were placed in two lifts. The locations for the cores are shown in figure 8.

The rut depth in the asphalt pavement layer alone was measured during each distress survey using a survey rod and level. After the crushed aggregate base layer was compacted during construction, aluminum plates were attached to its surface using nails at three locations in the wheelpath. Before each pavement site was tested by the ALF, holes were drilled through the asphalt pavement layer to each plate. A short reference rod was then screwed into each plate. During each distress survey, a metal rod connected to the bottom of a survey rod was put into each hole and placed on top of the reference rod. A survey level was then used to determine the distance the plate had moved downward. This provided the amount of rutting in the underlying layers, which was subtracted from the total rut depth to determine the amount of rutting in the asphalt pavement layer alone. The amount of rutting in the underlying layers was desired to be negligible. The locations for the reference rods and plates are shown in figure 8. A sketch of the device is shown in figure 9.

3. ALF Pavement Tests Results at 58 °C

The only pavement test temperature that was used for all seven mixtures was 58 °C. The large differences in performance from mixture to mixture coupled with large changes in performance with a change in temperature prohibited testing all seven mixtures at another, single temperature.

a. Temperature and Material Properties

The average pavement temperatures during trafficking for each lane and at each depth are given in table 14. The average temperatures based on the data from all lanes at depths of 0, 20, 102, and 197 mm were 60, 58, 56, and 51 °C, respectively. Rankings for $G^*/\sin\delta$ at these temperatures and the ALF angular frequency of 2.25 rad/s are given in table 15. These rankings were determined using Fisher's Least Significant Difference (LSD) statistical procedure. Fisher's LSD determines which averages are not significantly different from other averages. Averages that are not significantly different are grouped together. The groups are then ranked from highest to lowest and coded with a letter. Binders that fall into more than one group will have more than one letter assigned to it. Fisher's LSD is performed in conjunction with an analysis of variance at a 95-percent confidence level. The letter "A" indicates the highest $G^*/\sin\delta$. The $G^*/\sin\delta$'s of the five binders were significantly different at all four temperatures.

Even though the target temperature of 58 °C was met based on the overall average temperature, table 14 shows that the range in average temperature at a depth of 20 mm from lane to lane was 55 to 60 °C. How these differences in temperature affected the rut depths was not quantitatively known, and thus could not be taken into account. The temperatures from all lanes at a depth of 20 mm provided 95-percent confidence limits of 58 ±4 °C based on two times the sample standard deviation, $\pm 2\sigma_{(n-1)}$, where "n" is the number of samples.

The average air voids are given in table 14. The as-constructed air voids of the pavements, based on cores taken from out of the wheelpath, differed by as much as 6 percent from lane to lane. Construction specifications were developed to provide low lane-to-lane variability in material composition. This included air voids, aggregate gradation, and binder content. The intent of this specification was not achieved in terms of air voids.

Table 14 includes the decrease in air voids, or densification, due to trafficking. By comparing the densification in the top half of each asphalt pavement to that of the bottom half, it was found that they were virtually the same for five out of seven mixtures. More densification occurred in the top half (3.4 percent) of the Novophalt surface mixture than in its bottom half (1.8 percent). Unexpectedly, less densification occurred in the top half (2.9 percent) of the AC-10 (PG 65) surface mixture than in its bottom half (5.1 percent). The average densification based on the data from all lanes was 3.8 percent in both the top and bottom halves. Regression analyses using the data from all mixtures or from the surface mixtures only showed that $G^*/\sin\delta$ and amount of densification did not correlate ($r^2 = 0$). Aggregate gradation also appeared to have little to no effect on densification.

The average decrease in air voids due to trafficking ranged from 2.4 percent for lane 12 to 5.2 percent for lane 10. Multiplying these values by the asphalt pavement layer thickness of 200 mm gives a range in rut depth from 4.8 to 10.4 mm. Dividing these values by the average rut depth of 24 mm for all lanes at termination suggests that 20 to 44 percent of the 24-mm rut depth was densification. As the percent rut depth from densification increases, the percent rut depth from viscous flow decreases, and vice versa. However, the results from these calculations could be in error. The air voids in the wheelpaths were only determined after the pavements had failed, and the pavement tests were not terminated solely on some scientific basis, such as some fixed amount of rutting in the asphalt pavement layer. In fact, some of the final rut depths differed by more than 10 mm. Because of this, the differences in densification from lane to lane was a confounding factor that could not be adequately taken into account.

The aggregate gradations, binders contents, and maximum specific gravities of samples acquired during construction and from pavement cores taken after pavement failure are given in appendix B.

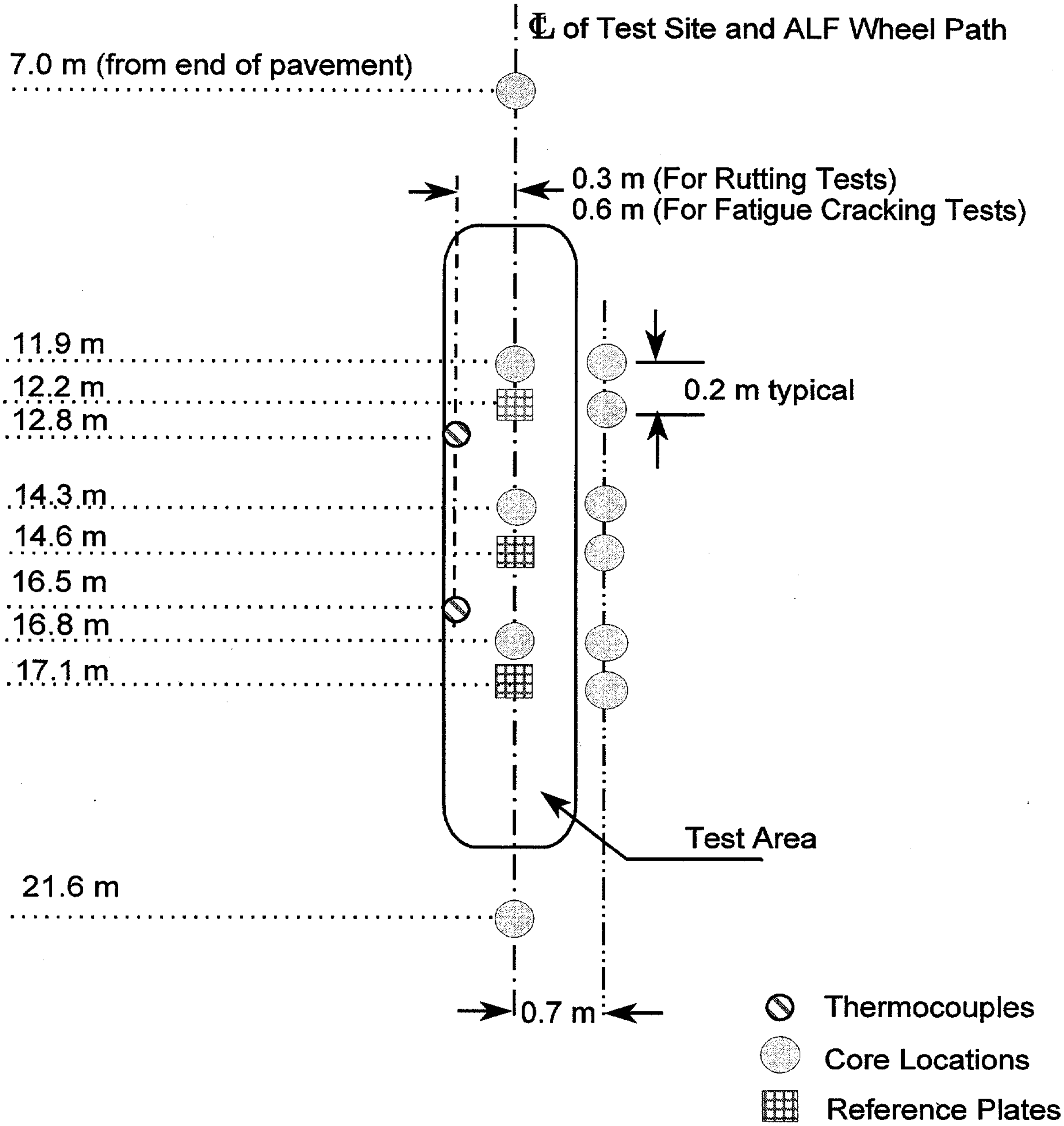

Figure 8. Thermocouple, core, and reference plate locations for each site.

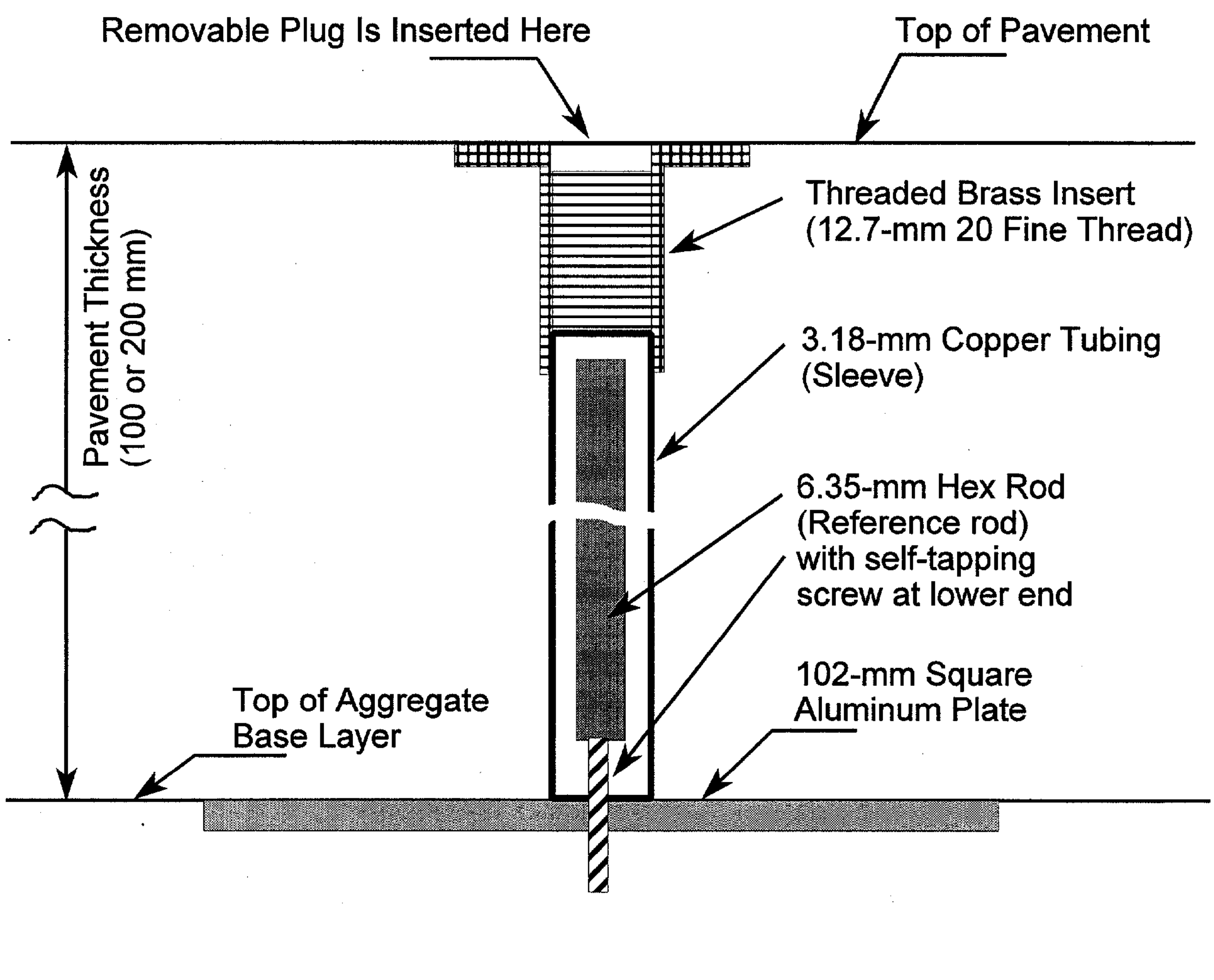

Figure 9. Drawing of the reference rod used to measure the amount of rutting in the layers below the asphalt pavement layer.

Table 14. Pavement temperatures and air voids.

	Surface Mixture					Base Mixture	
Pre-Superpave:	AC-5	AC-10	AC-20	Novophalt	Styrelf	AC-5	AC-20
Superpave PG:	59	65	70	77	88	59	70
Lane Number:	9	5	10	8	7	11	12
Pavement Depth	**Pavement Temperature, °C**						
0 mm	62	62	60	56	61	60	59
20 mm	58	60	58	55	59	58	57
102 mm	55	55	55	54	59	56	56
197 mm	51	49	51	48	56	51	51
Difference from 0 mm to 197 mm:	11	13	9	8	5	9	8
	Air Voids, Top 100 mm of Pavement, Percent						
Out of Wheelpath	7.8	8.5	9.1	11.9	11.9	6.7	7.4
In Wheelpath	3.4	5.6	3.7	8.5	7.6	3.1	5.0
Decrease	4.4	2.9	5.4	3.4	4.3	3.6	2.4
	Air Voids, Bottom 100 mm of Pavement, Percent						
Out of Wheelpath	7.0	8.4	8.3	10.8	12.8	6.0	7.4
In Wheelpath	2.8	3.3	3.4	9.0	8.2	2.2	5.1
Decrease	4.2	5.1	4.9	1.8	4.6	3.8	2.3
Average Decrease for Entire Layer	4.3	4.0	5.2	2.6	4.4	3.7	2.4

G*/sinδ for the Novophalt and Styrelf Surface Mixtures at 2.25 rad/s, Pa

Pavement Depth, mm	Novophalt Temp, °C	Novophalt G*/sinδ	Styrelf Temp, °C	Styrelf G*/sinδ	Comparison of G*/sinδ (by *t*-test)
0	56	8 300	61	10 550	Novophalt < Styrelf
20	55	9 680	59	12 590	Novophalt < Styrelf
102	54	11 140	59	12 590	Novophalt ≈ Styrelf
197	48	26 510	56	18 070	Novophalt > Styrelf

Table 15. G*/sinδ after RTFO corresponding to the ALF pavements tests.[1]

Pre-Superpave Designation:	AC-5	AC-10	AC-20	Novo-phalt	Styrelf
Superpave PG:	59	65	70	77	88
G*/sinδ at 60 °C, and 2.25 rad/s (18 km/h), Pa	526 E	1 084 D	2 100 C	4 914 B	11 570 A
G*/sinδ at 58 °C, and 2.25 rad/s (18 km/h), Pa	664 E	1 384 D	2 702 C	6 826 B	13 710 A
G*/sinδ at 56 °C, and 2.25 rad/s (18 km/h), Pa	872 E	1 833 D	3 632 C	8 296 B	17 620 A
G*/sinδ at 51°C, and 2.25 rad/s (18 km/h), Pa	1 813 E	3 892 D	7 918 C	17 560 B	29 030 A

[1]The letters "A" through "E" are the statistical ranking, with "A" denoting the highest G*/sinδ.

b. Rut Depths

(1) Rut Depth vs. ALF Wheel Pass Relationships Using the Raw Data and a Rut Depth Model

The rut depths in the asphalt pavement layer and the total rut depths were fitted according to the following rut depth model using the Gauss-Newton statistical method:

$$RD = aN^b$$

where:

- RD = rutting depth in asphalt pavement layer or all layers, mm;
- N = ALF wheel passes;
- a = intercept, and
- b = slope.

The rut depths up to 10,000 ALF wheel passes are shown in figures 10 through 13. As stated previously, these rut depths are based on the original elevation of the pavement surface before testing. Figure 10 shows the measured rut depths in the asphalt pavement layer while figure 11 shows the rut depths in the asphalt pavement layer using the above rut depth model. Figures 12 and 13 show the same relationships using the total rut depth, which is the rut depth in all pavement layers. The rut depth model was used to provide a smooth relationship between rut depth and wheel passes.

Table 16 shows the wheel passes at rut depths of 15 and 20 mm based on the raw data and the rut depth model. The large differences in wheel passes provided by these two methods for the pavement with Styrelf was the result of having to obtain the wheel passes where the slope was low. When the slope in terms of rut depth per wheel pass is low, the error in wheel passes at a given rut depth is high, and the ability of the method to accurately define the relationship between rut depth and wheel passes becomes extremely important. Extrapolations include, and can magnify, the error. Subsequent analyses performed in this study are based on the relationships from the rut depth model.

Table 16 also shows that fewer than 3,000 ALF wheel passes were required to obtain a rut depth of 20 mm for the three surface mixtures with the unmodified binders. This shows that the change in target pavement test temperature from 70 to 58 °C, which was done to account for the slow speed of the ALF, was necessary. Tests at 70 °C would be too severe for these three pavements.

(2) Comparison of the Rut Depth in the Asphalt Pavement Layer to the Total Rut Depth

The ALF wheel passes at rut depths of 10, 15, and 20 mm are given in table 17. As expected, the wheel passes based on the rut depth in the asphalt pavement layer alone were higher than those based on the total rut depth. These differences were attributed to rutting in the crushed aggregate base. The differences were very high for the two mixtures with modified binders. For example, 23,200 wheel passes were needed to obtain a total rut depth of 20 mm in lane 7 with Styrelf, whereas approximately 220,000 wheel passes would be needed to obtain this same rut depth in the asphalt pavement layer alone. Based on a maximum allowable total rut depth of 20 mm, the data indicate that lanes 7 and 8 with the modified binders failed before a significant amount of rutting occurred in the asphalt pavement layer. These pavements also exhibited no upward heaving outside the wheelpath. The pavements with the unmodified binders did heave. This shows that even though the two modified binders drastically increase pavement life on the basis of the rut depths in the asphalt pavement layer, a significantly longer pavement life on the basis of total rut depth would have been obtained if the asphalt pavement layer was thicker than the 200-mm layer that was placed. A more stable crushed aggregate base layer should also increase pavement life based on total rut depth. Table 17 includes the percent rut depth in the asphalt pavement layer. The pavements with the modified binders had the lowest percentages.

(3) Statistical Rankings for the Pavements

The rut depths in the asphalt pavement layer were used to rank the mixtures. To statistically rank the mixtures according to rutting susceptibility, the average variability in rut depth provided by lanes 9, 10, and 11 had to be applied to the other four lanes. Only these three lanes were tested in both 1994 and 1995. The data in tables 14 and 17 for these lanes are the average data. The replicate data are given in table 18.

The replicate data from lanes 9, 10, and 11 provided two relationships for each lane: the average rut depth (RD_{avg}) vs. wheel pass and two standard deviations of the rut depth ($2\sigma_{(n-1)}$) vs. wheel pass. The latter relationship provided 95-percent confidence bands for the rut depths in the form of $RD_{avg} \pm 2\sigma_{(n-1)}$. A relationship between $2\sigma_{(n-1)}$ and RD_{avg} using the data from all three replicated pavement tests was computed. This relationship is shown in figure 14. The variability in rut depth, expressed as $\pm 2\sigma_{(n-1)}$, increased with an increase in RD_{avg} and was nearly linear:

$$2\sigma_{(n-1)} = 0.221416(RD)^{1.04465} \qquad r^2 = 0.72$$

where:

$2\sigma_{(n-1)}$ = two times the standard deviation of the rut depths, where the sample variance was used, and

Rd_{avg} = average rut depth in the asphalt pavement layer.

Each ALF pavement test provided a relationship between rut depth and ALF wheel passes. To rank the seven mixtures, 95-percent confidence bands were determined for each mixture by substituting the rut depths for RD_{avg} in the above equation and calculating $2\sigma_{(n-1)}$. The confidence bands were computed using the rut depth $\pm 2\sigma_{(n-1)}$. For each of the three lanes that were tested twice, the rut depths at each wheel pass were first averaged. The confidence bands were then applied to these averages. When the confidence bands of the mixtures overlapped at the higher numbers of wheel passes, it was concluded that the rut depths were not significantly different. The rankings based on the $\pm 2\sigma_{(n-1)}$ confidence bands are given in table 19. The rut depth data from the beginning to the end of each test are given in appendix C. For the five surface mixtures, table 19 shows that only the AC-10 and AC-20 (PG 65 and 70) mixtures were not significantly different. However, this ranking cannot be considered exact and undisputable because of the poor r^2 of 0.72 for the relationship shown in figure 14. Rankings based on $\pm 1\sigma_{(n-1)}$ are included in table 19 as supplementary information.

A second method for statistically ranking the mixtures, based on an average coefficient of variation, was also used. This method consisted of calculating an average coefficient of variation in terms of wheel passes at a rut depth of 20 mm using the three pairs of replicate rut depths. This coefficient of variation was found to be 0.22. Replicate ALF wheel passes at a rut depth of 20 mm for all seven mixtures were then calculated using this coefficient.

As shown by table 20, the sample standard deviation was calculated by multiplying the average wheel pass times 0.22. The sample standard deviation and the average wheel pass were then used to calculate two replicate wheel passes. A normal distribution was assumed. The mixtures were then ranked using analyses of variance and Fisher's LSD. Log wheel passes were ranked because the sample standard deviation increased with an increase in wheel passes. Table 20 shows that the ranking for the five surface mixtures at a rut depth of 20 mm was identical to the ranking provided by the $\pm 1\sigma_{(n-1)}$ and $\pm 2\sigma_{(n-1)}$ confidence bands in table 19. Only the AC-10 and AC-20 (PG 65 and 70) mixtures were not significantly different. Tables 19 and 20 show that the rankings provided by the two methods using all seven mixtures were different. Rankings at rut depths of 10 and 15 mm are included in table 20. A slightly different ranking for the five surface mixtures was obtained at a rut depth of 10 mm.

Like the first method for ranking the mixtures, the second ranking method cannot be considered exact and undisputable. The coefficients of variation provided by the three replicated pavement tests at a 20-mm rut depth were 0.31, 0.00, and 0.35. This provided the average coefficient of 0.22. If a coefficient of variation of 0.33 were to be used instead of 0.22, the wheel passes for the mixtures with the AC-5 and AC-10 (PG 59 and 65) binders would not be significantly different.

(4) Comparisons of the Rut Depths at Various Wheel Passes

Comparing the rut depths at various ALF wheel passes was found to be problematic because the pavements failed at widely different wheel passes. The wheel passes at a rut depth of 20 mm in the asphalt pavement layer ranged from 670 to more than 200,000. Either excessive extrapolations leading to very high rut depths would have to be applied to the data from pavements that failed quickly, or the pavements would have to be compared at very low numbers of wheel passes. At low wheel passes, the poorest performing pavements control how a set of mixtures will rank, and the rut depths for the best performing mixtures tend to be the same regardless of test temperature. Comparisons based on the rut depths at a specific number of wheel passes were used in this study when appropriate. Comparisons at 2,000 wheel passes for pavement tests at 58 and 70 °C have been previously reported.[17,18]

c. Pavement Cracks

Cracks were only observed in the lane with the Novophalt (PG 76-22) mixture. Thin longitudinal cracks were observed on the pavement surface on both sides of the wheelpath at the point where the pavement was bending the greatest. All cracks initiated at the surface of the pavement.

4. Validation of G*/sinδ Based on the ALF Pavement Data From the Five Surface Mixtures

The two rankings in table 21 show a reversed order for Novophalt and Styrelf. The G*/sinδ of Styrelf was higher than the G*/sinδ of Novophalt, but the Novophalt mixture was least susceptible to rutting. Table 14 shows that the temperatures of the pavement with Novophalt were lower than those for Styrelf. The corresponding G*/sinδ's are included at the bottom of table 14. Statistical analyses of the G*/sinδ's showed that, at depths of 0 and 20 mm, the G*/sinδ's of the Novophalt binder were still significantly lower than those for Styrelf. However, the G*/sinδ's were not significantly different at 102 mm, while the G*/sinδ of the Novophalt binder was significantly higher than for Styrelf at 197 mm. This confounded the experiment but did not clearly explain the reversal.

The data are shown graphically in figure 15. The r^2 between log ALF wheel passes and G*/sinδ for the five surface mixtures was 0.34. Therefore, the degree of correlation was very poor. The r^2 for the seven mixtures was 0.32.

5. Validation of G*/Sinδ Based on the Data From the AC-5 and AC-20 (PG 59 and 70) Surface and Base Mixtures

a. Effect of Nominal Maximum Aggregate Size on Rutting Susceptibility

The wheel passes needed to produce a 20-mm rut depth in the AC-5 and AC-20 (PG 59 and 70) surface and base mixtures were examined. These data are included in table 17. The AC-5 (PG 59) base mixture required 11,990 wheel passes compared with 670 wheel passes for the AC-5 (PG 59) surface mixture. The base mixture increased the required wheel passes by 1,700 percent. The AC-20 (PG 70) base mixture required 57,520 wheel passes compared with 2,730 wheel passes for the AC-20 (PG 70) surface mixture. This base mixture increased the required wheel passes by 2,000 percent. Decreases in rutting susceptibility due to the increase in nominal maximum aggregate size also occurred at rut depths of 10 and 15 mm. Increased nominal maximum aggregate size and the associated 0.85-percent decrease in optimum binder content significantly decreased rutting susceptibility for both binder grades.

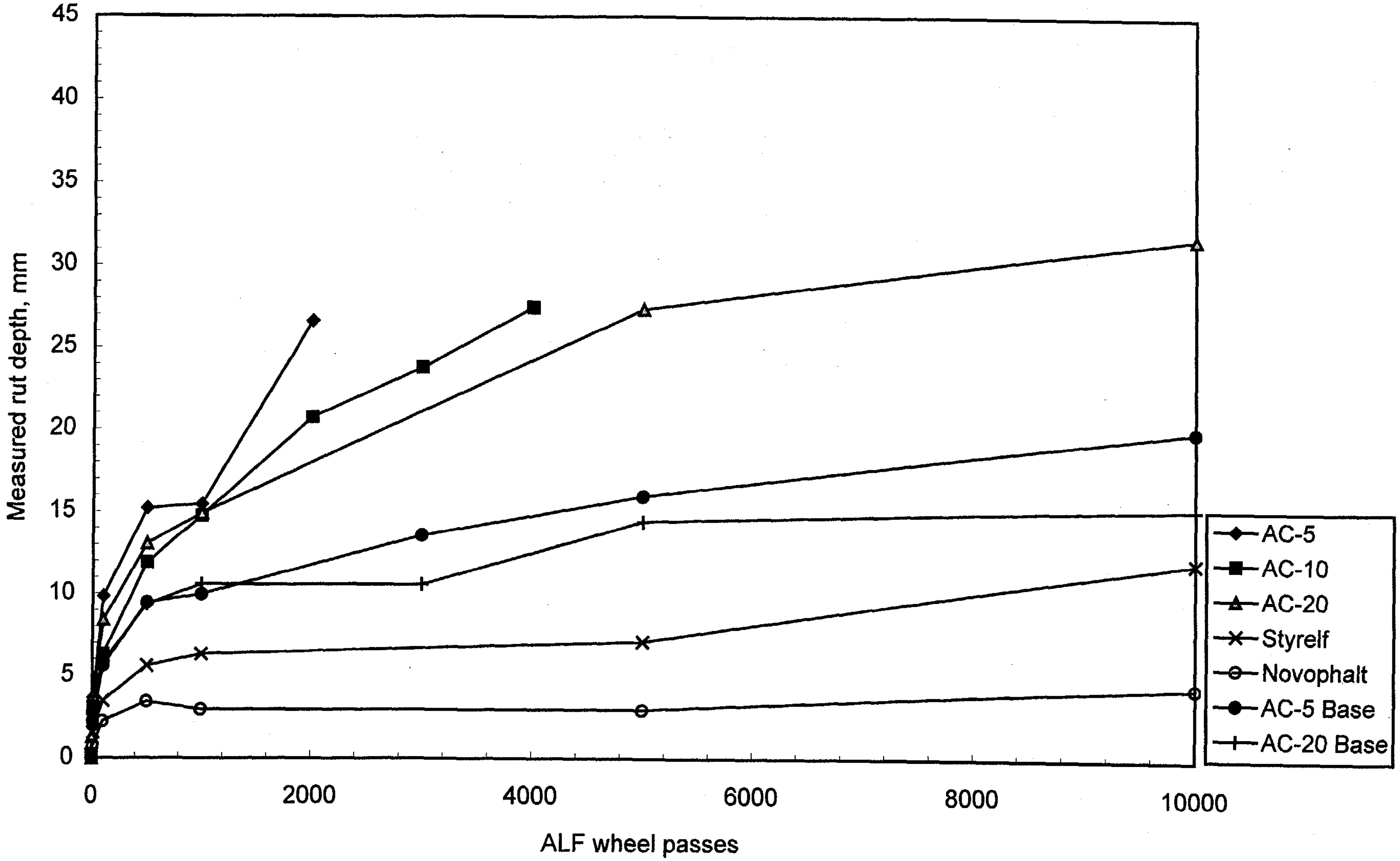

Figure 10. Measured rut depth in the asphalt pavement layer vs. ALF wheel passes.

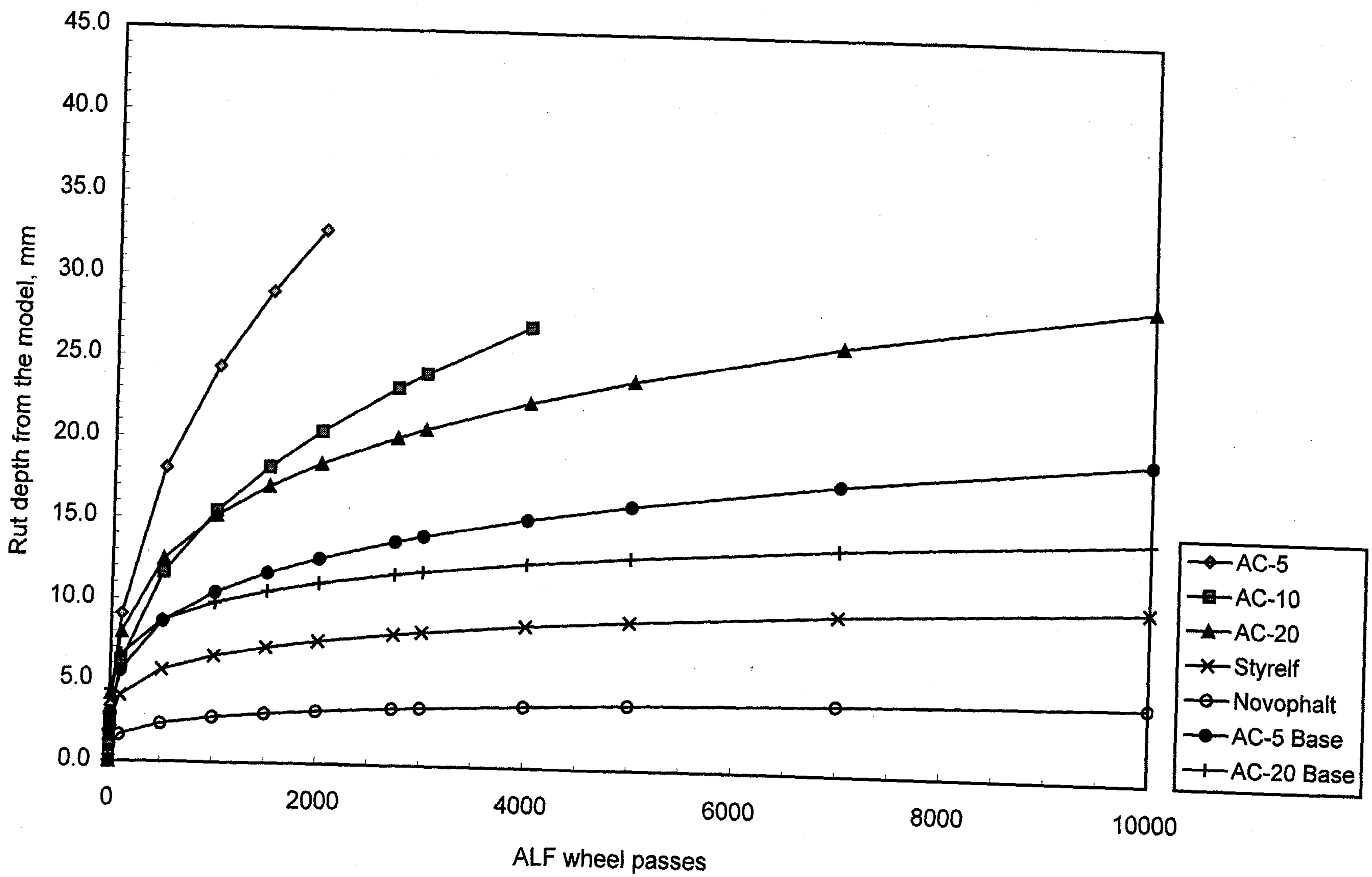

Figure 11. Rut depth in the asphalt pavement layer from the model vs. ALF wheel passes.

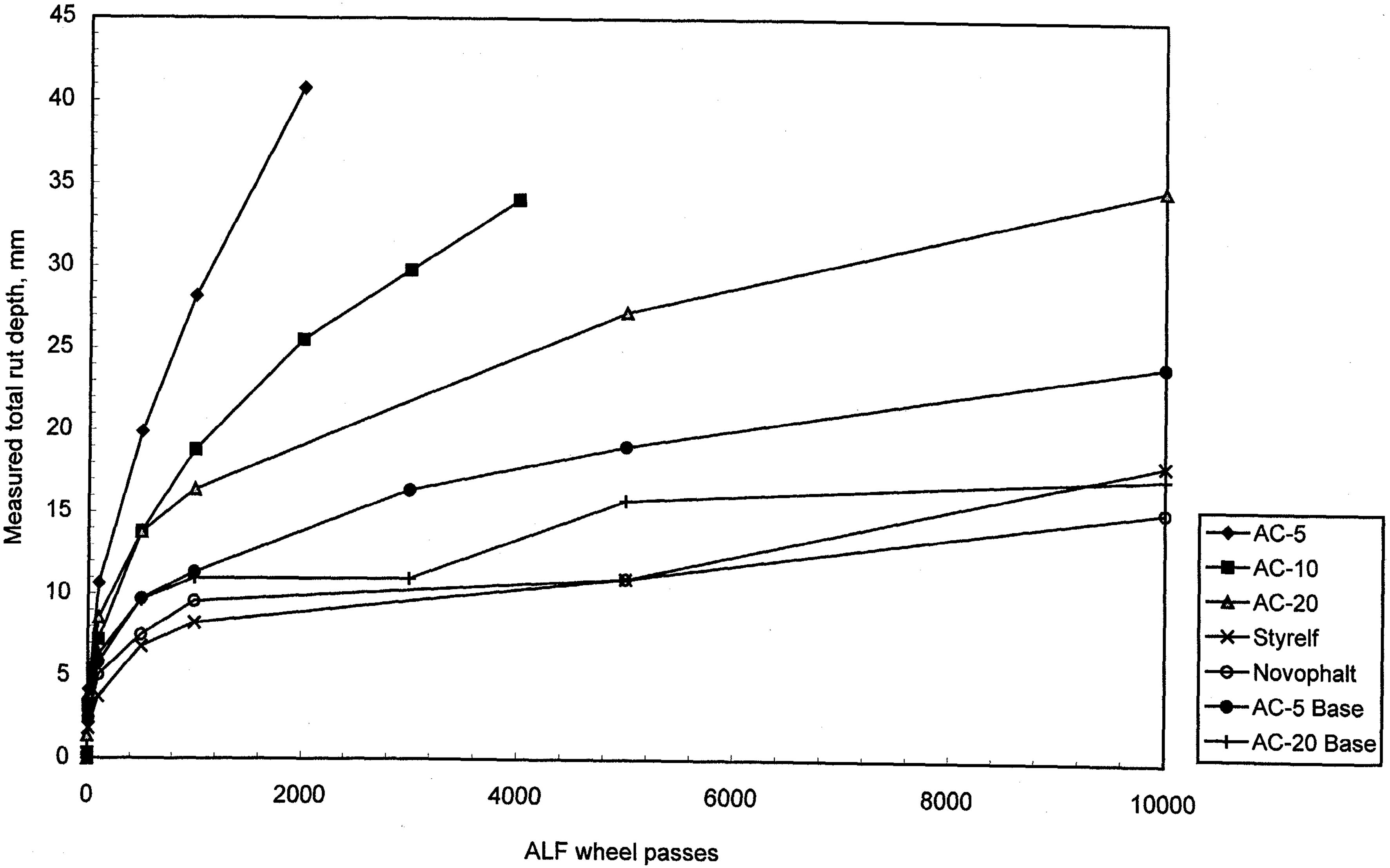

Figure 12. Measured total rut depth vs. ALF wheel passes.

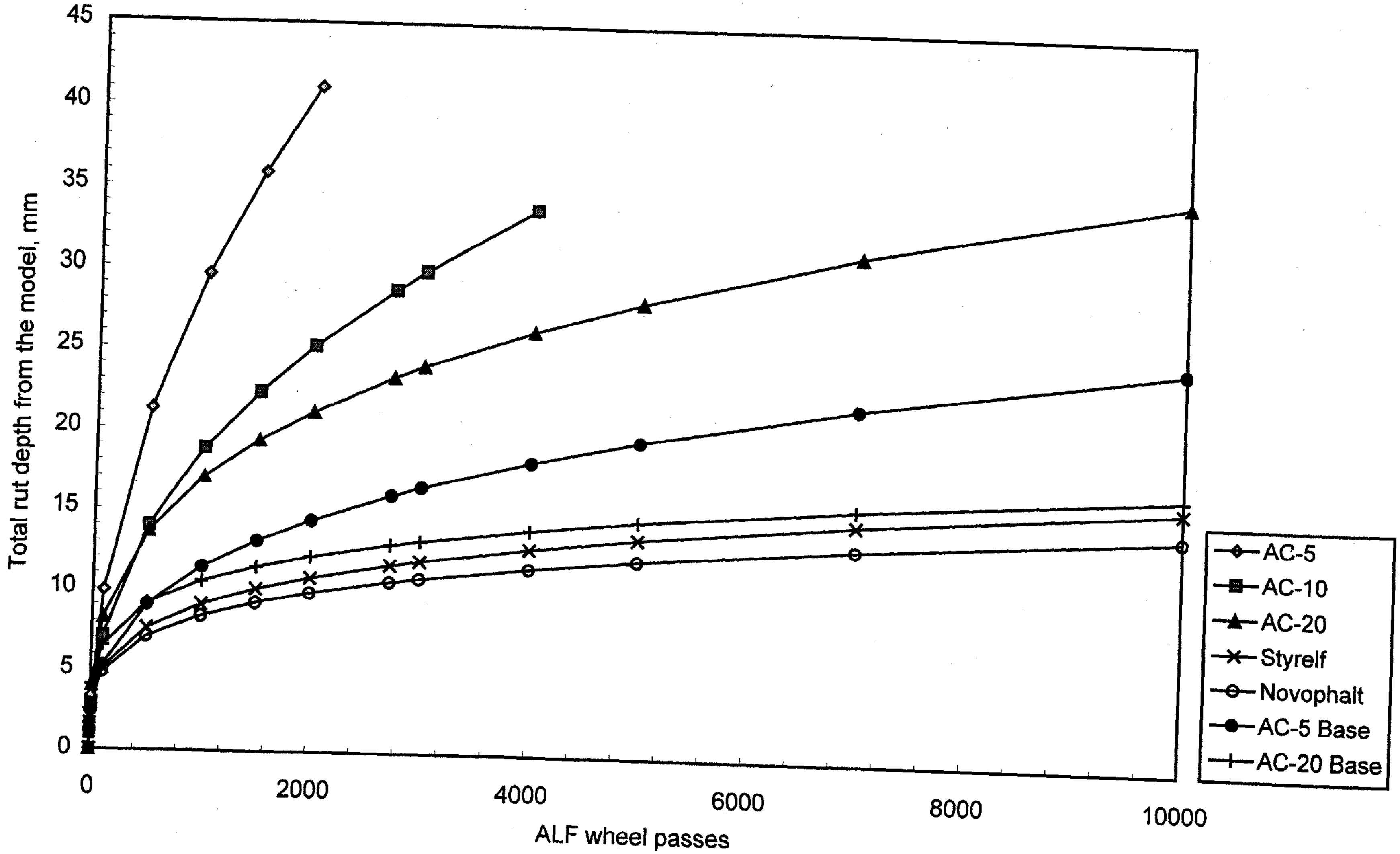

Figure 13. Total rut depth from the model vs. ALF wheel passes.

Table 16. Pavement rankings based on the average ALF wheel passes needed to obtain rut depths of 15 and 20 mm using the raw data and the rut depth model.

		ALF Wheel Passes at a 15-mm Rut Depth in the Asphalt Pavement Layer		ALF Wheel Passes at a 20-mm Rut Depth in the Asphalt Pavement Layer	
Mixture	Temp °C	Raw Data	Rut Depth Model	Raw Data	Rut Depth Model
Novophalt	58	ND[1]	1,750,000[2]	ND[1]	6,000,000[2]
Styrelf	58	32,610	55,540	400,000[3]	220,000[3]
AC-20 Base	58	8,750	11,220	43,780	57,520
AC-5 Base	58	4,170	4,240	10,000	11,990
AC-20	58	1,030	980	2,640	2,730
AC-10	58	1,050	940	1,880	1,900
AC-5	58	480	340	1,410	670

[1]No data; the test was terminated at a rut depth of 9 mm because the mixture stopped rutting.

[2]Determined by extrapolation. The test was terminated at a rut depth of 9 mm (208,805 wheel passes).

[3]Determined by extrapolation. The test was terminated at a rut depth of 18 mm (200,000 wheel passes).

Table 17. Average ALF pavement data.

ALF Wheel Passes Required to Obtain Rut Depths of 10, 15, and 20 mm in the Asphalt Pavement Layer

Mixture	Wheel Passes at a Rut Depth of 10 mm	Wheel Passes at a Rut Depth of 15 mm	Wheel Passes at a Rut Depth of 20 mm
Novophalt	293,000[1]	1,750,000[1]	6,000,000[1]
Styrelf	7,910	55,540	220,000[1]
AC-20 Base	1,120	11,220	57,520
AC-5 Base	990	4,240	11,990
AC-20	230[2]	980	2,730
AC-10	340[2]	940	1,900
AC-5	130	340	670

ALF Wheel Passes Required to Obtain Rut Depths of 10, 15, and 20 mm in All Pavement Layers

Mixture	Wheel Passes at a Rut Depth of 10 mm	Wheel Passes at a Rut Depth of 15 mm	Wheel Passes at a Rut Depth of 20 mm
Novophalt	2,130	11,760	39,600
Styrelf	1,480	7,400	23,200
AC-20 Base	790	5,540	22,100
AC-5 Base	690	2,310	5,450
AC-20	200[2]	710	1,790
AC-10	230[2]	590	1,160
AC-5	110	260	480

Percent Rut Depth in the Asphalt Pavement Layer When the Total Rut Depth is 10, 15, 20, or 30 mm

Mixture	10 mm	15 mm	20 mm	30 mm
Novophalt	33	32	32	31
Styrelf	71	66	63	58
AC-20 Base	94	88	85	79
AC-5 Base	93	86	81	75
AC-20	95	92	89	85
AC-10	84	83	82	81
AC-5	93	90	87	84

[1]Determined by extrapolation.
[2]Reversed ranking compared with the data at 15 and 20 mm.

Table 18. ALF replicate pavement data.

	Surface Mixture AC-5 (PG 59) Lane 9			Surface Mixture AC-20 (PG 70) Lane 10			Base Mixture AC-5 (PG 59) Lane 11		
	Site 2	Site 1	Avg	Site 2	Site 1	Avg	Site 2	Site 1	Avg
Pavement Depth	**Pavement Temperature, °C**								
0 mm	62	61	62	61	59	60	62	58	60
20 mm	59	57	58	59	57	58	60	56	58
102 mm	55	55	55	55	55	55	58	55	56
197 mm	51	52	51	51	51	51	52	50	51
Difference from 0 mm to 197 mm:	11	9	11	10	8	9	10	8	9
	Air Voids, Top 100 mm of Pavement, Percent								
Out of Wheelpath	7.7	7.8	7.8	9.3	8.8	9.1	6.0	7.3	6.7
In Wheelpath	3.6	3.2	3.4	3.4	3.9	3.7	2.2	4.0	3.1
Densification	4.1	4.6	4.4	5.9	4.9	5.4	3.8	3.3	3.6
	Air Voids, Bottom 100 mm of Pavement, Percent								
Out of Wheelpath	7.9	6.1	7.0	9.5	7.2	8.3	6.0	6.1	6.0
In Wheelpath	3.1	2.5	2.8	3.7	3.2	3.4	1.9	2.6	2.2
Densification	4.8	3.6	4.2	5.8	4.0	4.9	4.1	3.5	3.8
Average Decrease for Entire Layer	4.4	4.1	4.3	5.8	4.4	5.2	4.0	3.4	3.7
Rut Depth in Asphalt Layer	**Number of ALF Wheel Passes**								
10 mm	115	143	129	262	206	234	612	1363	988
15 mm	279	395	337	1031	937	984	2946	5544	4245
20 mm	521	814	667	2724	2741	2733	8984	15000	11992
Total Rut Depth	**Number of ALF Wheel Passes**								
10 mm	85	140	112	226	169	197	707	676	692
15 mm	212	310	261	739	687	713	2224	2399	2312
20 mm	407	546	476	1713	1859	1786	5012	5895	5454

Note: Site 2 is listed first because it was tested before site 1.

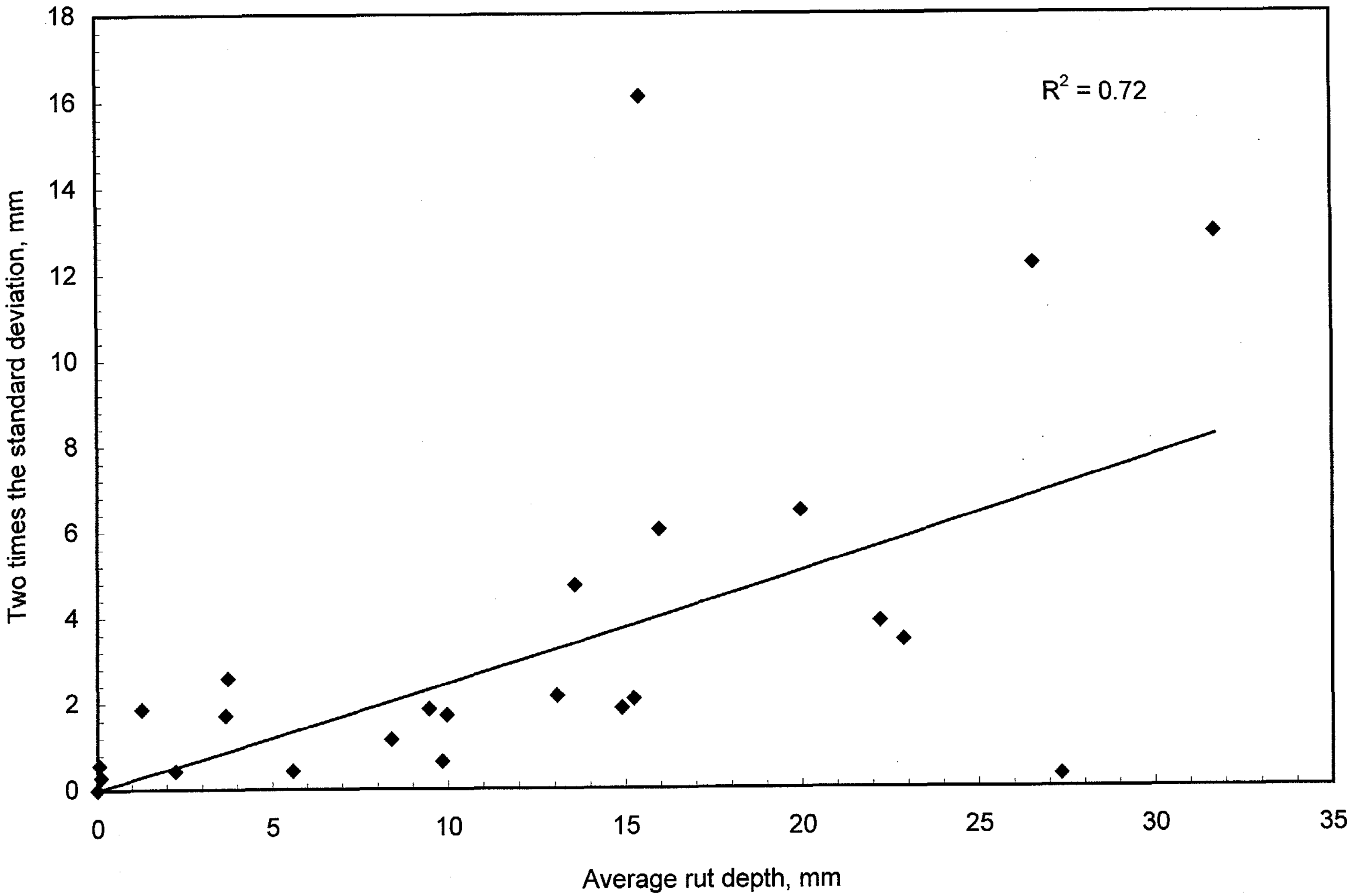

Figure 14. Relationship between two times the standard deviation of the rut depth and the average rut depth.

Table 19. Rankings for the pavements tested at 58 °C based on confidence bands for the rut depth vs. ALF wheel pass relationships.[1]

	Average ALF Wheel Pass at a Rut Depth of 20 mm		Statistical Ranking[2] Based on $\mu \pm 1\sigma_{(n-1)}$		Statistical Ranking[2] Based on $\mu \pm 2\sigma_{(n-1)}$	
	All Mixtures		All Mixtures	Surface Mixtures	All Mixtures	Surface Mixtures
Novophalt	A	6,000,000	A	A	A	A
Styrelf	B	220,000	B	B	B	B
AC-20 Base	C	57,520	B		BC	
AC-5 Base	D	11,990	C		CD	
AC-20	E	2,730	D	C	DE	C
AC-10	F	1,900	D	C	E	C
AC-5	G	670	E	D	F	D

[1]The letters are the statistical ranking, with "A" denoting the mixture with the lowest susceptibility to rutting.

[2]μ = average wheel pass and $\sigma_{(n-1)}$ = sample standard deviation

Table 20. Rankings for the pavements tested at 58 °C based on the coefficient of variation (CV).[1]

	Statistical Ranking Based on Log ALF Wheel Passes at a Rut Depth of 20 mm and a coefficient of variation (CV) of 0.22					
	Average Wheel Pass	Sample Standard Deviation $\sigma_{(n-1)}$	Calculated Replicate Number 1	Calculated Replicate Number 2	Ranking, All Mixtures	Ranking, Surface Mixtures
Novophalt	6,000,000	1,320,000	5,067,000	6,933,000	A	A
Styrelf	220,000	48,400	186,600	255,400	B	B
AC-20 Base	57,520	12,654	48,600	66,400	C	
AC-5 Base	11,990	2,638	10,130	13,860	D	
AC-20	2,730	601	2,310	3,160	E	C
AC-10	1,900	418	1,600	2,200	E	C
AC-5	670	147	560	770	F	D

	Statistical Ranking Based on Log Wheel Passes at a Rut Depth of 10 mm and a CV of 0.29		Statistical Ranking Based on Log Wheel Passes at a Rut Depth of 15 mm and a CV of 0.25	
	All Mixtures	Surface Mixtures	All Mixtures	Surface Mixtures
Novophalt	A	A	A	A
Styrelf	B	B	B	B
AC-20 Base	C		C	
AC-5 Base	C		D	
AC-20	D	C	E	C
AC-10	DE	CD	E	C
AC-5	E	D	F	D

[1]The letters are the statistical ranking, with "A" denoting the mixture with the lowest susceptibility to rutting.

Table 21. Rankings for the five surface mixtures at 58 °C based on $G^*/\sin\delta$ at 2.25 rad/s and ALF pavement performance.

Binder, $G^*/\sin\delta$ at 2.25 rad/s	ALF Pavement Performance
(A) Styrelf	(A) Novophalt
(B) Novophalt	(B) Styrelf
(C) AC-20	(C) AC-20
(D) AC-10	(C) AC-10
(E) AC-5	(D) AC-5

Note: "A" denotes the binder with the highest $G^*/\sin\delta$ or pavement with the lowest susceptibility to rutting.

The rut depths at 2,730 ALF wheel passes were also compared. The AC-20 (PG 70) surface mixture was considered the control mixture in this analysis, and a rut depth of 20 mm was considered the failure level. The rut depths in the AC-20 (PG 70) surface and base mixtures at 2,730 ALF wheel passes were 20 and 12 mm, respectively. The rut depths in the AC-5 (PG 59) surface and base mixtures at 2,730 ALF wheel passes were 35 and 14 mm, respectively. Increased nominal maximum aggregate size and the associated 0.85-percent decrease in optimum binder content significantly decreased rutting susceptibility for both binder grades.

Both analyses showed that the increase in nominal maximum aggregate size from 19.0 to 37.5 mm, and the associated 0.85-percent decrease in optimum binder content, significantly decreased rutting susceptibility based on ALF pavement performance. This was expected. No binder parameter can provide the effects that mixture composition and aggregate properties have on pavement performance. Binder specifications should provide some minimal level of performance.

b. Interaction Between Nominal Maximum Aggregate Size and Grade of Binder

The data in table 17 show that the AC-20 (PG 70) surface mixture required 2,730 wheel passes compared with 670 wheel passes for the AC-5 (PG 59) surface mixture to obtain a rut depth of 20 mm. The wheel passes for the AC-20 (PG 70) surface mixture is 310 percent higher than for the AC-5 (PG 59) surface mixture. The AC-20 (PG 70) base mixture required 57,520 wheel passes compared to 11,990 wheel passes for the AC-5 (PG 59) base mixture. The wheel passes for the AC-20 (PG 70) base mixture is 380 percent higher than for the AC-5 (PG 59) base mixture. At a rut depth of 15 mm, the percent increase in wheel passes obtained by changing from the AC-5 (PG 59) binder to the AC-20 (PG 70) binder was 190 percent for the surface mixtures, and 165 percent for the base mixtures. At a rut depth of 10 mm, the percent increase in wheel passes obtained by changing from the AC-5 (PG 59) binder to the AC-20 (PG 70) binder was 80 percent for the surface mixtures, and 130 percent for the base mixtures. Overall, the percentages for the base mixtures are not significantly lower than the percentages for the surface mixtures. Therefore, the increase in nominal maximum aggregate size and associated 0.85-percent decrease in optimum binder content did not decrease the effect of high-temperature PG on rutting susceptibility on a percentage basis.

6. Evaluation of Other Binder Parameters

a. DSR Parameters From Sine Wave Tests

The following binder parameters were evaluated to determine if they could explain the discrepancy for the Novophalt and Styrelf binders: G^*, δ, $\sin\delta$, $\tan\delta$, δ for RTFO/PAV residues, and $G^*/\sin\delta$ at an angular frequency of 63.1 rad/s. The binder parameters G^*, δ, $\sin\delta$, and $\tan\delta$ were evaluated because of the finding that the Styrelf binder had a lower δ compared with the other binders. Table 22 shows the data for the five binders at frequencies of 10.0 and 2.51 rad/s. An angular frequency of 2.51 rad/s was used in lieu of the ALF angular frequency of 2.25 rad/s because 2.51 rad/s was the angular frequency closest to 2.25 rad/s at which the DSR automatically recorded data. The data at an angular frequency of 2.25 rad/s would have to be found through interpolation, which was not necessary for this analysis. All data were recorded at a test temperature of 60 °C. Three replicate tests were performed on each binder.

Table 22 shows that all parameters provided the same ranking. All averages for a given parameter were found to be significantly different at a 95-percent confidence level. The ranking for the binders was not dependent on angular frequency.

The phase angles after RTFO/PAV aging were evaluated to determine the effect of increased aging. The data are given in table 23. The phase angles decreased with increased aging, but the binders ranked the same.

$G^*/\sin\delta$ at an angular frequency of 63.1 rad/s was also evaluated. Table 23 shows that the binders ranked the same at all three angular frequencies. The angular frequency of 63.1 rad/s was based on the equation $\omega = 2\pi/t = 62.8$ rad/s using a loading time of 0.1 s. An angular frequency of 63.1 rad/s was used in lieu of 62.8 rad/s because 63.1 rad/s was the angular frequency closest to 62.8 rad/s at which the DSR automatically recorded data.

b. Zero Shear Viscosity

Zero shear viscosity, or low shear rate limiting viscosity, was also measured at 60 °C using the DSR. In this test, the viscosity of a binder is measured at progressively lower shear rates until a constant viscosity is obtained. This viscosity does not include the time dependent recoverable strain when this type of strain exists. Time-dependent recoverable strains are not measured in the Superpave DSR test because it does not include a rest period after each loading cycle. This strain is erroneously included in the permanent strain.

The zero shear viscosities are shown at the bottom of table 22. The ranking provided by this parameter was the same as that provided by the other parameters, and the averages were found to be significantly different at a 95-percent confidence level.

c. Cumulative Permanent Strain After Four Cycles of Repeated Loading

When evaluating asphalt mixtures for rutting susceptibility using repeated load tests, a rest period is generally added after each cycle of loading to simulate how pavements are loaded. At temperatures used in these tests, generally from 0 to 60 °C, the strain vs. time relationships after unloading provide three types of strain: (1) an elastic strain that is instantaneously recovered, (2) a delayed elastic strain that is recovered over time, and (3) a permanent strain that is not recovered. The amount of delayed elastic strain that is recovered increases with an increase in the rest period until

Table 22. Binder parameters at 60 °C after RTFO.

Binder Parameter	AC-5	AC-10	AC-20	Novophalt	Styrelf
G*/sinδ, Pa, 10.0 rad/s	2 096	4 202	7 897	16 580	28 500
G*/sinδ, Pa, 2.51 rad/s	526	1 084	2 100	4 914	11 570
G*, Pa, 10.0 rad/s	2 070	4 133	7 707	15 700	23 600
G*, Pa, 2.51 rad/s	523	1 076	2 075	4 740	9 535
Phase Angle, δ, 10.0 rad/s	81.0	79.6	77.4	71.2	55.9
Phase Angle, δ, 2.51 rad/s	84.2	83.0	81.2	74.7	55.5
sinδ, 10.0 rad/s	0.988	0.984	0.976	0.947	0.828
sinδ, 2.51 rad/s	0.995	0.993	0.988	0.965	0.824
tanδ, 10.0 rad/s	6.31	5.45	4.47	2.94	1.48
tanδ, 2.51 rad/s	9.84	8.14	6.46	3.66	1.46
Zero Shear Viscosity, Pa·s	241	514	1 050	2 960	13 200

Table 23. Additional tests on the five ALF binders at 60 °C.

	RTFO Residue		RTFO/PAV Residue	
	Phase Angle Angular Frequency, rad/s		Phase angle Angular Frequency, rad/s	
Binder	2.51	10.0	2.51	10.0
Novophalt	74.7	71.2	64.7	61.7
Styrelf	55.5	55.9	50.0	50.8
AC-20	81.2	77.4	70.9	67.2
AC-10	83.0	79.6	73.5	69.4
AC-5	84.2	81.0	75.3	70.8

Binder Parameter	AC-5	AC-10	AC-20	Novophalt	Styrelf
G*/sinδ, Pa, 63.1 rad/s	10 455	20 364	36 410	73 155	86 787
G*/sinδ, Pa, 10.0 rad/s	2 096	4 202	7 897	16 580	28 500
G*/sinδ, Pa, 2.51 rad/s	526	1 084	2 100	4 914	11 570

all of this strain is recovered. Virtually no delayed elastic strain is recovered when there is no rest period, as in the DSR test. Thus, if a binder being tested by the DSR has a delayed elastic strain, this strain will be included in the permanent strain. This may lead to a G*/sinδ that is too low compared with the G*/sinδ's of binders that have no delayed elastic strain. It may also be low based on comparisons with pavement performance or the results of repeated load mixture tests that use rest periods. Unmodified asphalt binders generally do not have a significant amount of delayed elastic strain at temperatures used to determine their high-temperature PG.

The five ALF binders were tested using a stress-controlled DSR to determine whether they had measurable delayed elastic strains and, if they did, whether this strain varied from binder to binder and could account for the discrepancy concerning Novophalt and Styrelf. A 500-Pa stress was applied to each binder in the form of a square wave with a load duration of 1.0 s, followed by a rest period. Four cycles of loading and unloading were applied. Rest periods of 1.0 and 9.0 s and test temperatures of 52, 64, and 70 °C were employed. The strain was continuously recorded during the test. Typical stress vs. time and strain vs. time relationships are shown in figure 16.

One method used to evaluate asphalt mixtures for rutting susceptibility consists of measuring the amount of permanent strain that accumulates due to some specified number of loading cycles. The five ALF binders were evaluated in this manner, but only four cycles of loading were used because this was the maximum number of cycles that the DSR could apply. Table 24 shows the cumulative permanent strains after the four cycles of loading. Cumulative permanent strain increased with temperature as expected. The data show that the five binders ranked the same at both rest periods and at all three temperatures. This ranking matched the previous rankings shown in table 22. The data indicated that Styrelf should be least susceptible to rutting.

The percent decrease in cumulative permanent strain due to the use of the longer rest period is included in table 24. Binders that recover more delayed elastic strain during the rest period relative to the total strain will have a greater percent decrease in cumulative permanent strain. Table 24 shows that Styrelf had the highest percent decrease at each temperature, followed by Novophalt. The percent decrease was small for each of the three unmodified binders at all three temperatures. If time dependent recoverable strains were to be taken into account in the binder specification, Styrelf would be the best binder in terms of rutting resistance, and the G*/sinδ's for the Styrelf and Novophalt binders would be further apart compared with the values provided by the current testing protocols.

Analyses of the percent permanent strain provided by individual cycles of loading also showed the effect of rest period. The data for the fourth loading cycle are given in table 25. Binders that recovered more delayed elastic strain during the longer rest period have greater decreases in the percent permanent strain per cycle. Equation (3) in this chapter showed that dissipated energy is proportional to permanent strain. Table 25 shows that the decrease in permanent strain due to the increase in rest period was low to none for Novophalt and the three unmodified binders at all three temperatures. Therefore, the dissipated energies and PG's for these binders would not be expected to change significantly with the addition of a rest period. The permanent strain at 52 °C for the Styrelf binder using a 9-s rest period was less than half of the permanent strain using a 1-s rest period. In Superpave, each time dissipated energy is halved, the PG increases one grade, or 6 °C. Therefore, it is possible that the use of a 9-s rest period would increase the PG of the Styrelf binder by one grade. The effect of the rest period should decrease with an increase in temperature; therefore, it was hypothesized that the effect of the rest period on the Styrelf binder would be low if it were to be tested at its high-temperature grade of 88 °C. However, the data show that when testing binders at the same temperature, there can be an error in $G^*/\sin\delta$ if a rest period is needed but not used. Even so, the use of a rest period in this study would make the $G^*/\sin\delta$'s for Styrelf and Novophalt be further apart. Thus, the discrepancy was not related to the absence of a rest period.

The percent permanent strains per loading cycle are relatively high in table 25 compared with the percent permanent strains from repeated load mixture and pavement tests. For example, the percent permanent strain per ALF wheel pass at 58 °C was estimated to range from 0.6 percent for the Novophalt surface mixture to 2.9 percent for the AC-5 (PG 59) surface mixture. Table 25 shows that the percent permanent strain per loading cycle in the DSR test would be above 80 percent at 58 °C for all binders except Styrelf. Aggregate interlock is a major factor affecting the results of mixture and pavement tests. Because of these large differences in strain, any interaction between the effects of the binders and the aggregate may lead to discrepancies in the rankings provided by binder and mixture tests. The Superpave binder specification does not consider interactions. Appendix D provides additional data.

7. Properties of Binders Recovered From Pavement Cores

Binders were extracted and recovered from cores and tested by the DSR after the ALF pavement tests were completed. Whether the Novophalt binder could be recovered without the properties of the binder being altered by the heat and solvent used in the process was questionable. Advanced Asphalt Technologies, which supplied the binder, performed tests that indicated it could be recovered using a rotary evaporator. An additional test was performed by the Federal Highway Administration (FHWA) to confirm Advanced Asphalt Technologies' finding. Samples of the Novophalt binder were aged using the RTFO and then tested by the DSR before and after recovery. The binder samples were soaked in solvent before recovery for the length of time the binder would be in solvent if it were to be extracted from aggregates. The binder samples were not mixed with aggregates, and it was assumed that no polyethylene would get caught in the filter during an actual extraction. The recovery process did not affect the average high-temperature continuous PG, being 75.5 °C before recovery and 76.0 °C after recovery. However, none of the recovered binder properties should be assumed to exactly represent in-place binder properties, especially for the two modified binders where the

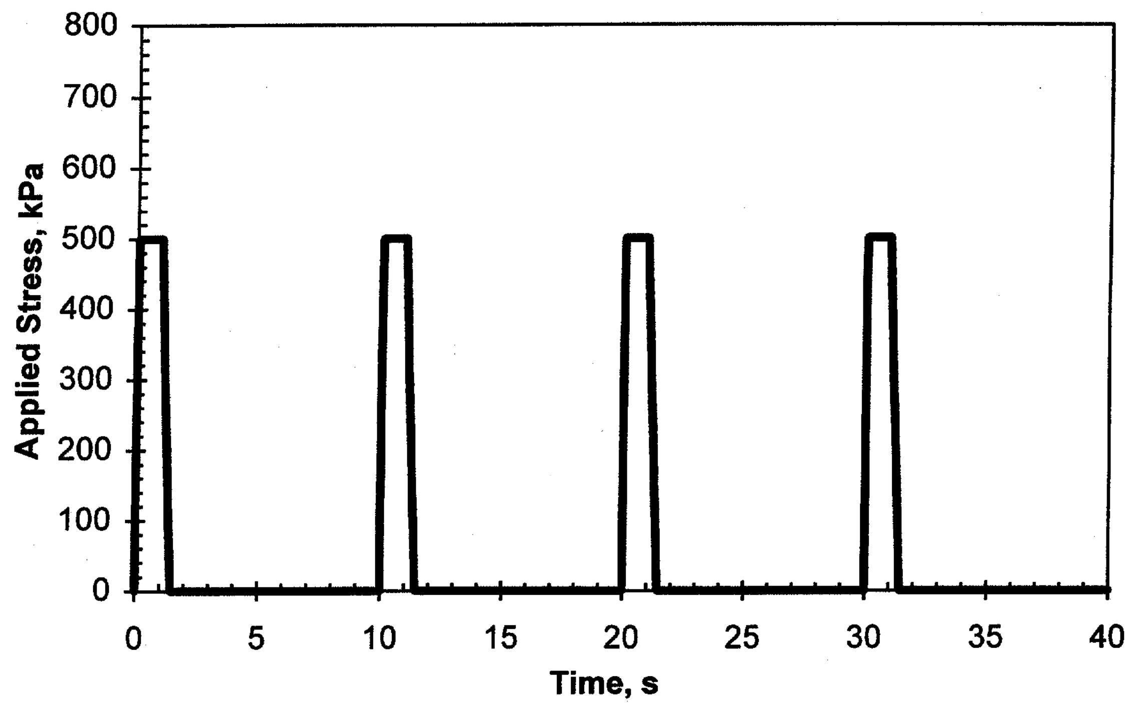

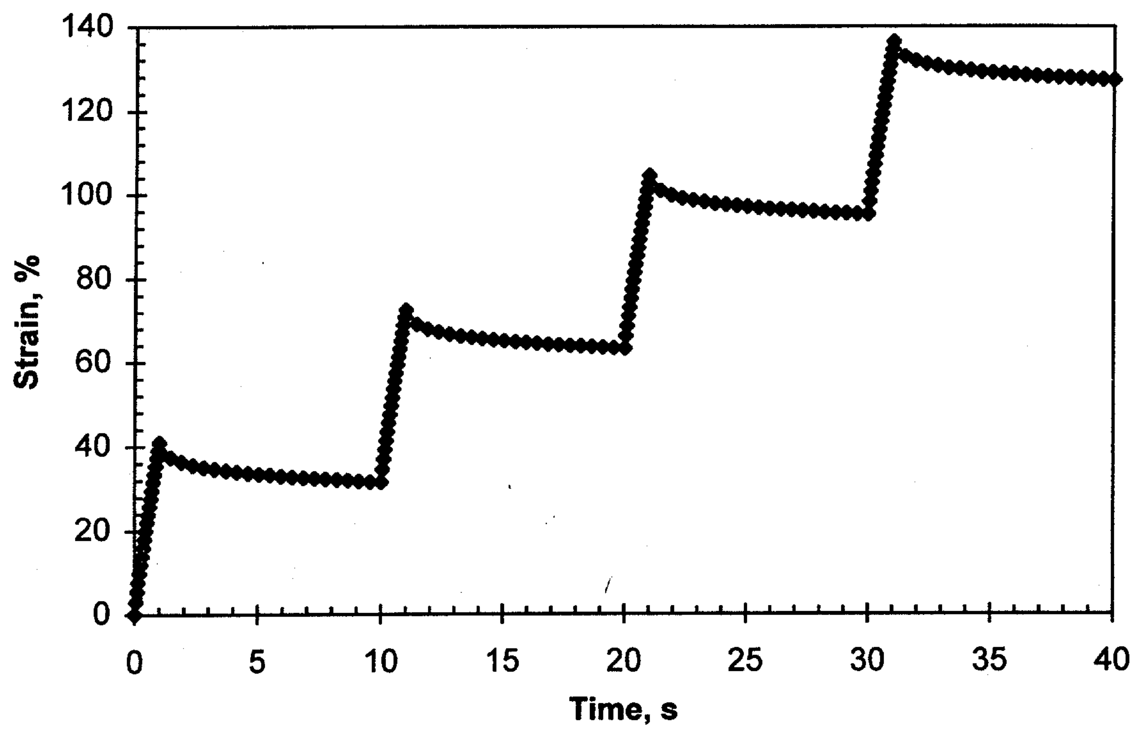

Figure 16. Typical plot of applied DSR stress and resultant shear strain vs. time for the test consisting of a 1.0-s load duration followed by a 9.0-s rest period.

Table 24. Cumulative permanent strain after four cycles of repeated loading using RTFO residues.

Binder	Temperature = 52 °C Rest Period 1 s	9 s	Decrease	Percent Decrease	Temperature = 64 °C Rest Period 1 s	9 s	Decrease	Percent Decrease
Styrelf	0.07	0.02	0.05	250	0.32	0.15	0.17	88
Novophalt	0.14	0.11	0.03	27	0.84	0.70	0.14	20
AC-20	0.39	0.36	0.03	8	2.91	2.77	0.14	5
AC-10	1.34	1.25	0.09	7	9.73	9.46	0.27	3
AC-5	1.80	1.75	0.05	3	11.40	11.00	0.40	4

Binder	Temperature = 70 °C Rest Period 1 s	9 s	Decrease	Percent Decrease
Styrelf	0.63	0.33	0.30	91
Novophalt	1.78	1.49	0.29	19
AC-20	7.03	6.81	0.22	3
AC-10	19.20	18.90	0.30	2
AC-5	24.70	24.30	0.40	2

Table 25. Percent permanent strain for the 4th cycle of loading (Permanent Strain x 100 ÷ Total Strain).

Binder	Temperature = 52 °C Rest Period 1 s	9 s	Decrease	Temperature = 64 °C Rest Period 1 s	9 s	Decrease	Temperature = 70 °C Rest Period 1 s	9 s	Decrease
Styrelf	72	34	38	77	50	27	79	56	23
Novophalt	89	80	9	94	87	7	95	89	6
AC-20	94	91	3	98	96	2	99	98	1
AC-10	96	92	4	99	99	0	100	100	0
AC-5	97	95	2	99	99	0	100	100	0

Table 26. Properties of binders recovered from cores taken from the wheelpath after performing the ALF pavement test for rutting.

Mixture Type	High-temperature continuous PG based on a G*/sinδ of 2.20 kPa and an angular frequency of 10.0 rad/s			G*/sinδ at 10.0 rad/s and the pavement test temperature of 58 °C	
	RTFO Residue	Recovered Binder, 1994 Test	Recovered Binder, 1995 Test	Recovered Binder, 1994 Test	Recovered Binder, 1995 Test
AC-5 Surface and Base Mixtures					
AC-5 Surf	59	63	68	4.3	7.9
AC-5 Base	59	67	72	6.9	12.7
AC-20 Surface and Base Mixtures					
AC-20 Surf	70	72	78	12.4	25.0
AC-20 Base	70	78	NT	29.0	NT
Other Surface Mixtures					
AC-10	65	67	NT	7.2	NT
Novophalt	77	81	NT	29.1	NT
Styrelf	88	86	NT	37.3	NT

NT = Not tested.

structure of the two-phase system may depend on time and aggregate surface properties.

The high-temperature continuous PG's of the binders are shown in table 26. The binders recovered from the 1994 pavement cores were stiffer than the RTFO residues, except for the Styrelf binder. The greatest difference in temperature for the five surface mixtures was 4 °C, which was provided by the Novophalt binder (81 versus 77). This difference was relatively small compared with the difference of 8 °C provided by the two base mixtures: 67 versus 59 for the AC-5 (PG 59) base mixture, and 78 versus 70 for the AC-20 (PG 70) base mixture. Most likely, the 0.85-percent lower binder content for the base mixtures allowed more aging to occur during construction and early pavement life.

The 1994 core data in table 26 show that the AC-5 (PG 59) base mixture was 4 °C higher in grade than the AC-5 (PG 59) surface mixture (67 versus 63). The AC-20 base mixture was 6 °C higher in grade than the AC-20 (PG 70) surface mixture (78 versus 72). These differences may be an additional reason why each base mixture performed significantly better than its associated surface mixture when tested by the ALF. The $G^*/\sin\delta$'s at 10.0 rad/s and 58 °C also show the differences in binder properties.

Although the three pavements tested in 1995 were considered replicate pavement tests, the 1994 and 1995 PG's suggest that the pavements had aged between 1994 and 1995. Table 18 shows that the numbers of ALF wheel passes needed to obtain rut depths of 10, 15, and 20 mm in the asphalt pavement layer were higher in 1995 (site 1) compared with 1994 (site 2) for the AC-5 (PG 59) surface and base mixtures. These increases in wheel passes could be due to age hardening. The 1995 and 1994 wheel passes (sites 1 and 2) for the AC-20 (PG 70) surface mixture were virtually equal, thus age hardening appeared to have little to no effect on the pavement performances of this mixture. If age hardening was a factor in this study, its effect was that it increased the standard deviation used to rank the mixtures in tables 19 and 20, thus making it more difficult for the ALF pavement performances of the mixtures to be significantly different.

The 1994 core data did not explain the reversal in performance for the Novophalt and Styrelf binders. The PG's for the recovered binders show that the Styrelf binder had a higher grade than the Novophalt binder, although the difference in PG was only 5 °C (86 versus 81) compared with 11 °C (88 versus 77) for the RTFO residues.

8. Conclusions

- In general, binders with higher $G^*/\sin\delta$'s after RTFO aging provided mixtures with lower pavement rutting susceptibilities for a given nominal maximum aggregate size.

- The main discrepancy between $G^*/\sin\delta$ at 58 °C after RTFO aging and the ALF pavement performances of the five surface mixtures at 58 °C was that the Novophalt binder had a $G^*/\sin\delta$ of 6.83 kPa compared with 13.7 kPa for the Styrelf binder, but the asphalt pavement layer with Novophalt had a significantly lower susceptibility to rutting. The

ALF produced a rut depth of 20 mm in the asphalt pavement layer with Styrelf at 220,000 wheel passes. The rut depth in the asphalt pavement layer with Novophalt was only 9.4 mm at 220,000 wheel passes.

- The following binder parameters did not explain the discrepancy provided by the Novophalt and Styrelf binders: G^*, δ, $\sin\delta$, $\tan\delta$, zero shear viscosity, δ using RTFO/PAV residues, $G^*/\sin\delta$ after RTFO at angular frequencies ranging from 2.51 to 63.1 rad/s, cumulative permanent strain after four cycles of repeated loading, and $G^*/\sin\delta$ of binders recovered from pavement cores. All binder properties ranked Styrelf higher than Novophalt.

- The increase in nominal maximum aggregate size from 19.0 to 37.5 mm, and the associated 0.85-percent decrease in optimum binder content, decreased rutting susceptibility based on ALF pavement performance. To obtain a rut depth of 20 mm in the asphalt pavement layer, the AC-5 (PG 59) base mixture required 11,990 wheel passes compared with 670 wheel passes for the AC-5 (PG 59) surface mixture. The AC-20 (PG 70) base mixture required 57,520 wheel passes compared with 2,730 wheel passes for the AC-20 (PG 70) surface mixture. The effect was statistically significant for both binder grades.

- Part of the decrease in pavement rutting susceptibility provided by the increase in nominal maximum aggregate size could have been due to differences in age hardening. The high-temperature continuous PG of the binder recovered from the AC-5 (PG 59) base mixture was higher than the high-temperature continuous PG of the binder recovered from the AC-5 (PG 59) surface mixture. The same result was found for the two mixtures containing the AC-20 (PG 70) binder. Most likely, the 0.85-percent lower binder content for the base mixtures allowed more aging to occur during construction and early pavement life.

- Although the increase in nominal maximum aggregate size decreased rutting susceptibility, it did not reduce the influence of binder grade on rutting performance on a percentage basis. The increase in ALF wheel passes resulting from an increase in the high-temperature continuous PG from 59 to 70 was 310 percent for the surface mixtures and 380 percent for the base mixtures.

9. Comment on Binder Specifications

- No binder parameter can provide the effects that mixture composition and aggregate properties have on pavement performance, including the effect of nominal maximum aggregate size and changes in binder content. Binder specifications should provide some minimal level of performance.

CHAPTER 3: VALIDATION OF THE SUPERPAVE BINDER PARAMETER FOR RUTTING BASED ON ALF PAVEMENT PERFORMANCE AT ALL TEST TEMPERATURES

1. Background

This validation effort consisted of comparing the $G^*/\sin\delta$'s of the five binders to the pavement rutting performances of the five surface mixtures. The $G^*/\sin\delta$'s to be used in the comparisons were measured by the DSR using the pavement test temperatures at a 20-mm depth and a frequency of 2.25 rad/s. The target pavement temperatures were 46, 52, 58, 64, 70, and 76 °C. These temperatures were chosen because they are used by the Superpave asphalt binder specification. The $G^*/\sin\delta$'s of the binders are presented in table 27 along with statistical rankings provided by Fisher's LSD. The binders had significantly different $G^*/\sin\delta$'s at each temperature. All DSR tests were performed in the linear viscoelastic range using a 1-mm gap and 25-mm diameter plates. All surface mixtures were tested by the ALF at 58 °C and two of the other temperatures listed above. The two temperatures were chosen based on the pavement performances of the mixtures at 58 °C.

2. ALF Pavement Tests Results

The order in which the pavements were tested and the site tested are shown in table 28. The average data for each ALF pavement test are given in table 29.

a. Pavement Temperatures

The average pavement temperature for each test site as a function of depth is given in table 29. The temperatures from multiple sites having the same target temperature were averaged. These temperatures are shown in table 30. Included in table 30 are 95-percent confidence limits based on two times the standard deviation (2σ). These limits were computed by pooling the standard deviations from multiple test sites having the same target temperature. The average temperature at a depth of 20 mm and confidence limits based on 2σ, were 46 ±4, 51 ±6, 58 ±4, 64 ±5, 70 ±5, and 75 ±8 °C. Only the temperatures recorded during pavement testing were used in the calculations. The temperatures recorded during downtime were not used. Note that the temperatures overlap. Even so, it was found that rutting performance varied significantly from one average temperature to another. A typical plot for the pavement temperatures at the four depths is shown in figure 17.

b. Pavement Air Voids and Densification

The average air voids are given in table 29. The as-constructed air voids of the pavements, based on cores taken from out of the wheelpath, differed by as much as 4 percent from lane to lane. The ramifications of this on the validation effort were not apparent. The pavements with Styrelf and Novophalt had the highest initial air-void levels.

Table 29 includes the percent decrease in air voids due to trafficking, which is also called densification. The average densification based on the data from all test sites at all temperatures was 3.7 percent with a $2\sigma_{(n-1)}$ of 2.2 percent. By comparing the average densification in the top half of each asphalt pavement layer with that of the bottom half, it was found that the difference in air voids was less than or equal to 1.1 percent, or $1\sigma_{(n-1)}$, in 9 out of 15 pavement tests. Unexpectedly, the average densification was greater in the bottom half in four out of the six remaining pavement tests. None of the air voids in the top and bottom halves of the cores were significantly different at a 95-percent confidence level, or $2\sigma_{(n-1)}$. The data also show that densification was not higher in the pavements with Styrelf and Novophalt, which had the highest initial air-void levels.

Table 31 provides densifications in the top and bottom halves of the asphalt pavement layer that were calculated using the same initial air-void level. For a given test site, the average air-void level provided by the top halves of the cores taken from outside the wheelpath was used as the initial air-void level. By comparing the densifications shown in table 31, it was found that the difference in air voids between the top and the bottom halves was less than or equal to 1.1 percent in 11 out of 15 pavement tests. Densification was greater in the bottom half in three out of the four remaining pavement tests. The data indicated that when the average densification was higher in the bottom half, it was not because the bottom half had an initial air-void level that was higher than for the top half. It was concluded that it may be possible for the average densification to be greater in the bottom half of a 200-mm-thick pavement when tested by the ALF. However, none of the air voids in the top and bottom halves of the cores were significantly different at a 95-percent confidence level.

The average densification for all sites ranged from 2.0 to 5.5 percent. Multiplying these values by the asphalt pavement layer thickness of 200 mm gives a range in rut depth from 4 to 11 mm. Dividing these two values by the failure level of 20 mm suggests that 20 to 55 percent of the 20-mm maximum allowable rut depth was densification. Test sites with lower percentages of densification would have higher percentages of rut depth due to viscous flow. However, as enumerated in chapter 2, these percentages can only be considered approximate.

c. Aggregate Gradation, Binder Contents, and Maximum Specific Gravity

The aggregate gradations, binder contents, and maximum specific gravities of samples acquired during construction and from pavement cores taken after pavement failure are given in appendix B. The data did not provide an explanation for any of the discrepancies found in this study.

Table 27. G*/sinδ after RTFO corresponding to the ALF pavements tests.[1]

Pre-Superpave Designation:	AC-5	AC-10	AC-20	Novo-phalt	Styrelf
High-temperature Continuous PG:	59	65	70	77	88
ALF Pavement Tests, G*/sinδ at 2.25 rad/s (18 km/h) and 46 °C, Pa	4 061 E	8 865 D	18 280 C	35 710 B	52 910 A
ALF Pavement Tests, G*/sinδ at 2.25 rad/s (18 km/h) and 52 °C, Pa	1 557 E	3 329 D	6 744 C	14 880 B	25 910 A
ALF Pavement Tests, G*/sinδ at 2.25 rad/s (18 km/h) and 58 °C, Pa	664 E	1 384 D	2 702 C	6 826 B	13 710 A
ALF Pavement Tests, G*/sinδ at 2.25 rad/s (18 km/h) and 64 °C, Pa	314 E	637 D	1 175 C	2 849 B	7 841 A
ALF Pavement Tests, G*/sinδ at 2.25 rad/s (18 km/h) and 70 °C, Pa	155 E	229 D	549 C	1 304 B	4 435 A
ALF Pavement Tests, G*/sinδ at 2.25 rad/s (18 km/h) and 76 °C, Pa	97 E	185 D	285 C	642 B	2 381 A

[1]The letters "A" through "E" are the statistical ranking, with "A" denoting the highest G*/sinδ.

Table 28. Order in which the pavements were tested.

Lane Number:			1	2	3	4	5	6	7	8	9	10	11	12
Conventional AC Designation:			5	20	5	20	10	20	S	N	5	20	5	20
Surface or Base Mixture:			S	S	S	S	S	S	S	S	S	S	B	B
Distress	**Year**	**Temperature**	**Order of Testing**											
Rutting	1994	58 °C	-	-	-	-	5	-	6	1	2	4	3	7
Rutting	1995	58 °C	-	-	-	-	-	-	-	-	8	9	10	-
Rutting	1995	70 °C	-	-	-	-	-	-	11	12	-	-	-	-
Rutting	1996	52 °C	-	-	-	-	14	13	-	-	-	-	-	-
Rutting	1997	64 °C	-	-	-	-	-	15	-	-	-	-	-	-
Rutting	1997	52 °C	-	-	-	-	-	-	-	-	16	-	-	-
Rutting	1997	46 °C	-	-	18	-	17	-	-	-	-	-	-	-
Rutting	1997	76 °C	-	-	-	-	-	-	20	19	-	-	-	-
Distress	**Year**	**Temperature**	**Site Tested: 1, 2, 3, or 4**											
Rutting	1994	58 °C	-	-	-	-	2	-	2	2	2	2	2	1
Rutting	1995	58 °C	-	-	-	-	-	-	-	-	1	1	1	-
Rutting	1995	70 °C	-	-	-	-	-	-	1	1	-	-	-	-
Rutting	1996	52 °C	-	-	-	-	1	1	-	-	-	-	-	-
Rutting	1997	64 °C	-	-	-	-	-	2	-	-	-	-	-	-
Rutting	1997	52 °C	-	-	-	-	-	-	-	-	3	-	-	-
Rutting	1997	46 °C	-	-	3	-	4	-	-	-	-	-	-	-
Rutting	1997	76 °C	-	-	-	-	-	-	3	3	-	-	-	-

Notes:

5 = AC-5 (PG 59).
10 = AC-10 (PG 65).
20 = AC-20 (PG 70).
S = Styrelf (PG 88).
N = Novophalt (PG 77).

Table 29. ALF pavement data for the surface mixtures.

Superpave PG:	58-34	58-28	58-34	58-28	64-22
Conventional:	AC-5	AC-10	AC-5	AC-10	AC-20
Lane Number:	03	05	09	05	06
Target Temp, °C:	46	46	52	52	52
Pavement Depth	**Pavement Temperature, °C**				
0 mm	ND	ND	55	54	54
20 mm	46	44	53	50	51
102 mm	45	44	46	46	50
197 mm	44	39	43	42	42
Difference from 0 mm to 197 mm:	ND	ND	12	12	12
	Final Air Voids, Top 100 mm of Pavement, Percent				
Out of Wheelpath	7.4	6.4	5.6	8.3	8.6
In Wheelpath	3.8	4.4	3.8	6.8	5.5
Decrease	3.6	2.0	1.8	1.5	3.1
	Final Air Voids, Bottom 100 mm of Pavement, Percent				
Out of Wheelpath	7.8	5.9	5.0	8.1	8.1
In Wheelpath	5.2	3.8	2.8	3.2	4.6
Decrease	2.6	2.1	2.2	4.9	3.5
Average Decrease for Entire Layer	3.1	2.0	2.0	3.2	3.3
Rut Depth in Asphalt Layer	**Number of ALF Wheel Passes From the Rut Depth Model**				
10 mm	2,820	2,980	190	2,140	4,200
15 mm	33,330	20,840	740	8,300	35,500
20 mm	192,000	82,920	1,950	21,720	161,400
Total Rut Depth	**Number of ALF Wheel Passes From the Rut Depth Model**				
10 mm	480	1,250	180	910	1,010
15 mm	3,800	5,280	510	2,760	5,620
20 mm	16,520	14,650	1,050	6,070	19,020
Total Rut Depth	**Percentage of Rut Depth in the Asphalt Pavement Layer**				
10 mm	75	84	98	77	76
15 mm	70	75	89	72	70
20 mm	67	70	83	68	67
30 mm	63	63	75	63	62

ND = No data.

Table 29. ALF pavement data for the surface mixtures (continued).

Superpave PG:	58-34	58-28	64-22	76-22	82-22
Conventional:	AC-5	AC-10	AC-20	Novophalt	Styrelf
Lane Number:	09	05	10	08	07
Target Temp, °C:	58	58	58	58	58
Pavement Depth	**Pavement Temperature, °C**				
0 mm	62	62	60	56	61
20 mm	58	60	58	55	59
102 mm	55	55	55	54	59
197 mm	51	49	51	48	56
Difference from 0 mm to 197 mm:	11	13	9	8	5
	Final Air Voids, Top 100 mm of Pavement, Percent				
Out of Wheelpath	7.8	8.5	9.1	11.9	11.9
In Wheelpath	3.4	5.6	3.7	8.5	7.6
Decrease	4.4	2.9	5.4	3.4	4.3
	Final Air Voids, Bottom 100 mm of Pavement, Percent				
Out of Wheelpath	7.0	8.4	8.3	10.8	12.8
In Wheelpath	2.8	3.3	3.4	9.0	8.2
Decrease	4.2	5.1	4.9	1.8	4.6
Average Decrease for Entire Layer	4.3	4.0	5.2	2.6	4.4
Rut Depth in Asphalt Layer	**Number of ALF Wheel Passes From the Rut Depth Model**				
10 mm	130	340	230	293,000[1]	7,910
15 mm	340	940	980	1,750,000[1]	55,540
20 mm	670	1,900	2,730	6,000,000[1]	220,000[2]
Total Rut Depth	**Number of ALF Wheel Passes From the Rut Depth Model**				
10 mm	110	230	200	2,130	1,480
15 mm	260	590	710	11,760	7,400
20 mm	480	1,160	1,790	39,600	23,160
Total Rut Depth	**Percentage of Rut Depth in the Asphalt Pavement Layer**				
10 mm	93	84	95	33	71
15 mm	90	83	91	32	66
20 mm	87	82	89	32	63
30 mm	84	81	85	31	58

[1]From extrapolation. This ALF test was terminated at 208,800 wheel passes.
[2]From extrapolation. This ALF test was terminated at 200,000 wheel passes.

Table 29. ALF pavement data for the surface mixtures (continued).

Superpave PG:	64-22	76-22	82-22	76-22	82-22
Conventional:	AC-20	Novophalt	Styrelf	Novophalt	Styrelf
Lane Number:	06	08	07	08	07
Target Temp, °C:	64	70	70	76	76
Pavement Depth	**Pavement Temperature, °C**				
0 mm	65	74	73	80	ND
20 mm	64	70	70	75	75
102 mm	61	67	69	72	73
197 mm	58	61	62	64	70
Difference from 0 mm to 197 mm:	7	13	11	16	ND
	Final Air Voids, Top 100 mm of Pavement, Percent				
Out of Wheelpath	8.4	11.0	12.3	9.1	10.4
In Wheelpath	5.5	7.8	6.8	6.8	4.7
Decrease	2.9	3.2	5.5	2.3	5.7
	Final Air Voids, Bottom 100 mm of Pavement, Percent				
Out of Wheelpath	9.0	10.1	12.1	10.4	9.9
In Wheelpath	3.7	6.5	6.6	6.2	5.5
Decrease	5.3	3.6	5.5	4.2	4.4
Average Decrease for Entire Layer	4.1	3.4	5.5	3.2	5.0
Rut Depth in Asphalt Layer	**Number of ALF Wheel Passes From the Rut Depth Model**				
10 mm	670	5,750	1,520	31,650	3,040
15 mm	2,640	62,840	17,430	349,250	38,760
20 mm	7,000	340,000[1]	98,300	1,900,000[2]	236,000
Total Rut Depth	**Number of ALF Wheel Passes From the Rut Depth Model**				
10 mm	240	1,780	410	4,890	520
15 mm	920	9,450	2,760	20,840	3,120
20 mm	2,410	30,840	10,650	58,300	11,160
Total Rut Depth	**Percentage of Rut Depth in the Asphalt Pavement Layer**				
10 mm	74	82	81	73	75
15 mm	73	73	74	62	68
20 mm	73	67	69	55	62
30 mm	73	59	63	47	55

ND = No data.
[1]From extrapolation. The value could be from 180,000 to 340,000 wheel passes.
[2]From extrapolation.

Table 30. Average pavement temperature (μ) and confidence limits ($\pm 2\sigma$) vs. pavement depth.

Pavement Depth, mm	Rutting Tests 46 °C $\mu \pm 2\sigma$	52 °C $\mu \pm 2\sigma$	58 °C $\mu \pm 2\sigma$	64 °C $\mu \pm 2\sigma$	70 °C $\mu \pm 2\sigma$	76 °C $\mu \pm 2\sigma$
0	ND	54 ±4	60 ±5	65 ±4	74 ±7	80 ±8
20	46 ±4	51 ±6	58 ±4	64 ±5	70 ±5	75 ±8
102	45 ±4	50 ±4	56 ±3	61 ±3	68 ±3	72 ±8
197	42 ±5	42 ±5	52 ±3	58 ±5	61 ±3	66 ±8
ΔTemp	>4	12	8	7	13	14

ND = No data.

Δ Temp = Average difference in temperature from the surface of the pavement to the bottom of the pavement, °C.

Table 31. Normalized percent pavement densification.

Superpave PG:	58-34	58-28	58-34	58-28	64-22
Conventional:	AC-5	AC-10	AC-5	AC-10	AC-20
Lane Number:	03	05	09	05	06
Target Temp, °C:	46	46	52	52	52
Top Half, %	3.6	2.0	1.8	1.5	3.1
Bottom Half, %	2.2	2.6	2.8	5.1	4.0
Superpave PG:	58-34	58-28	64-22	76-22	82-22
Conventional:	AC-5	AC-10	AC-20	Novophalt	Styrelf
Lane Number:	09	05	10	08	07
Target Temp, °C:	58	58	58	58	58
Top Half, percent	4.4	2.9	5.4	3.4	4.3
Bottom Half, percent	5.0	5.2	5.7	2.9	3.7
Superpave PG:	64-22	76-22	82-22	76-22	82-22
Conventional:	AC-20	Novophalt	Styrelf	Novophalt	Styrelf
Lane Number:	06	08	07	08	07
Target Temp, °C:	64	70	70	76	76
Top Half, percent	2.9	3.2	5.5	2.3	5.7
Bottom Half, percent	4.7	4.5	5.7	2.9	4.9

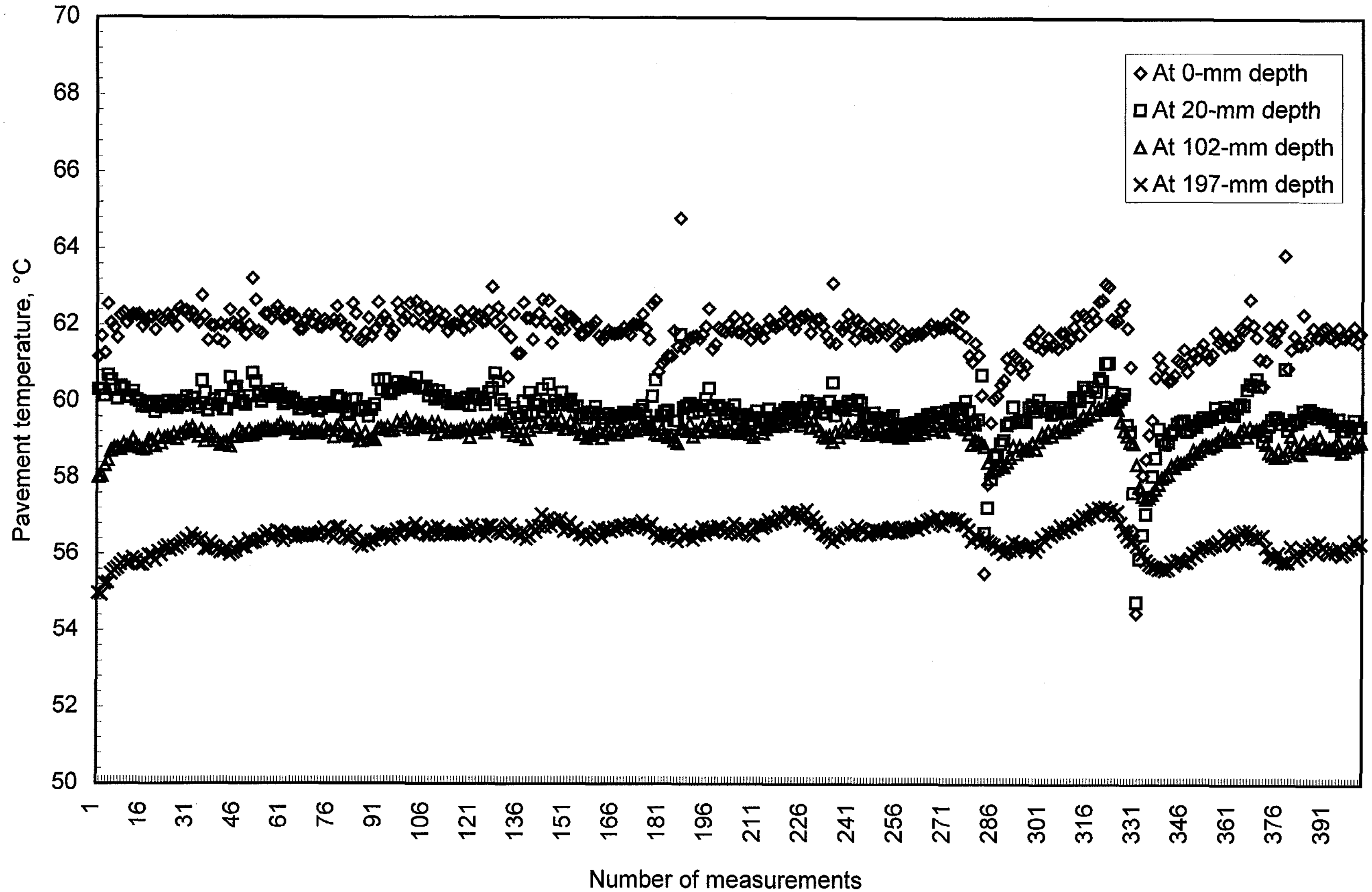

Figure 17. Example of pavement temperature vs. time (lane 7 site 2).

d. Pavement Cracks

Surface cracks less than 4 mm in width were observed on some of the pavements tested for rutting susceptibility. The bowed sidewalls of the tire, being wider than the tire imprint, started to tear the mixture on each side of the tire when the rut depths were high. These tears were at an angle of about 0.45 rad (25 degrees) relative to the forward direction of the wheel. Tears up to 7 mm in width were observed on lane 9 at a test temperature of 52 °C. This lane contained the AC-5 (PG 58-34) binder.

Thin, longitudinal, tensile cracks due to pavement bending were visible on the pavement with Novophalt when tested at 58 and 70 °C, and on the pavement with Styrelf when tested at 70 °C. These cracks occurred on both sides of the wheelpath at the point where the pavement surface was bending the greatest. All cracks initiated at the surface of the pavement. They were first observed when the total rut depth in all layers was approximately 25 mm.

Neither type of crack would be expected to occur on pavements where the wheels can wander.

e. Pavement Rutting Data

The ALF wheel passes that provided rut depths of 10, 15, and 20 mm in the asphalt pavement layer using the Gauss-Newton model are shown in tables 29 and 32. The rut depths for the pavement tests up to 10,000 wheel passes are shown in figures 18 and 19. The measured rut depths from the beginning to the end of each test, the corresponding rut depths based on the Gauss-Newton model, and additional supporting graphs are given in appendix C. (Also included in appendix C is a comparison of the downward only total rut depth and the peak-to-valley total rut depth. The latter rut depth includes any uplift of mixture outside the wheelpath.)

The tests on the Novophalt pavement at 58, 70, and 76 °C, and the test on the Styrelf pavement at 58 °C, were terminated before a 20-mm rut depth was obtained. The final rut depths in the asphalt pavement layer and in all layers are given in table 33. The Novophalt pavement tests at 58 and 76 °C were terminated because the mixture virtually stopped rutting at rut depths of 9 and 17 mm, respectively. The test at 70 °C was terminated prematurely at 125,000 wheel passes. The wheel passes for this test needed to provide a rut depth of 20 mm could be from 180,000 to 340,000, depending upon the method of extrapolation. The test on the Styrelf pavement at 58 °C was terminated because the rutting rate became very low. The wheel passes needed to provide a rut depth of 20 mm could be from 220,000 to 400,000, depending upon the method of extrapolation. The test on the Styrelf pavement at 70 °C was terminated after a 20-mm rut depth was obtained. Even so, the number of wheel passes at a rut depth of 20 mm could be from 98,300 to 145,000 because the Gauss-Newton model fit the data poorly at high numbers of wheel passes.

3. Validation of G*/Sinδ

The rut depths in the asphalt pavement layer were used to validate G*/sinδ. The data in table 32 show that the G*/sinδ's of the Novophalt and Styrelf binders did not agree with the rut depths at all three pavement test temperatures. The Styrelf binder had the higher G*/sinδ, but the pavement with Novophalt was more resistant to rutting. Other discrepancies between the data are discussed later in this chapter. Figures 20 and 21 show that the relationship between ALF wheel passes at a 20-mm rut depth and G*/sinδ was poor, although the trend was correct for the unmodified binders. The wheel passes from the Gauss-Newton model are shown in figure 20, while the measured wheel passes are shown in figure 21. The scatter in the data was the same using a failure rut depth of 10, 15, or 20 mm. For the pavement tests where the wheel passes depended on the method of extrapolation, the same level of scatter was obtained regardless of the method of extrapolation that was used. If the data from the Novophalt and Styrelf pavement tests are excluded from the analysis, a minimum allowable G*/sinδ of 3.3 to 4.4 kPa would eliminate the poorest performing mixtures.

As stated previously, approximately 20 to 55 percent of the 20-mm maximum allowable rut depth in the asphalt pavement layer was densification. Because the amount of densification was not constant from pavement to pavement, it was decided to subtract the rut depth due to densification from the total rut depth in the asphalt pavement layer to obtain and analyze the rut depth due to viscous flow. The rut depth due to densification was calculated from the reduction in air voids provided by cores taken from in and out of the wheelpath after failure. It was then assumed that the rut depth due to densification occurred prior to obtaining a 10-mm rut depth due to viscous flow and was thereafter a constant. Thus, for each pavement test, the rut depth due to densification was subtracted from the rut depths in the asphalt pavement layer to provide a relationship between the rut depth due to viscous flow and ALF wheel passes. Table 34 provides the number of ALF wheel passes at a 10-mm rut depth due to viscous flow. Figure 22 shows that the relationship using these rut depths was similar to those shown in figures 20 and 21.

As discussed in chapter 2, the problem encountered when performance was based on the rut depths at a constant number of ALF wheel passes was that either excessive extrapolations had to be performed to obtain the rut depths for pavements that failed quickly, or the pavements had to be compared at wheel passes that were low relative to the lives of longest lasting pavements. Even so, it was decided to compare the G*/sinδ's of the binders to the rut depths at 2,730 wheel passes from the Gauss-Newton model. The AC-20 (PG 70) surface mixture was considered the control mixture in this analysis. This mixture failed at 2,730 wheel passes based on a rut depth of 20 mm. The data are given in table 34. The rut depths for many of the pavements were relatively low; thus, the assumption that the rut depth due to densification could be subtracted from the total rut depth in the asphalt pavement layer was not valid and could not be used. Figure 23 shows that the relationship was poor, although all pavements with a G*/sinδ around 3.3 kPa and greater were performing well at 2,730 wheel passes. No data point was found to be an outlier.

Table 32. ALF wheel passes based on the Gauss-Newton model that were needed to obtain rut depths of 10, 15, and 20 mm in the asphalt pavement layer.

Mixture	Temp °C	Wheel Passes at a Rut Depth of 10 mm	Wheel Passes at a Rut Depth of 15 mm	Wheel Passes at a Rut Depth of 20 mm	G*/sinδ at 2.25 rad/s (Pa)
Novophalt	76	31,652	349,250	1,900,000[1]	642
Styrelf	76	3,040	38,760	236,000	2 381
Novophalt	70	5,750	62,840	340,000[1]	1 304
Styrelf	70	1,520	17,430	98,300	4 435
AC-20	64	670	2,640	7,000	1 175
Novophalt	58	293,000[1]	1,750,000[1]	6,000,000[1]	6 826
Styrelf	58	7,910	55,540	220,000[1]	13 710
AC-20	58	230	980	2,730	2 702
AC-10	58	340	940	1,900	1 384
AC-5	58	130	340	670	664
AC-20	52	4,200	35,500	161,400	6 744
AC-10	52	2,140	8,300	21,720	3 329
AC-5	52	190	740	1,950	1 557
AC-10	46	2,980	20,840	82,920	8 865
AC-5	46	2,820	33,330	192,000	4 061

[1]From extrapolation.

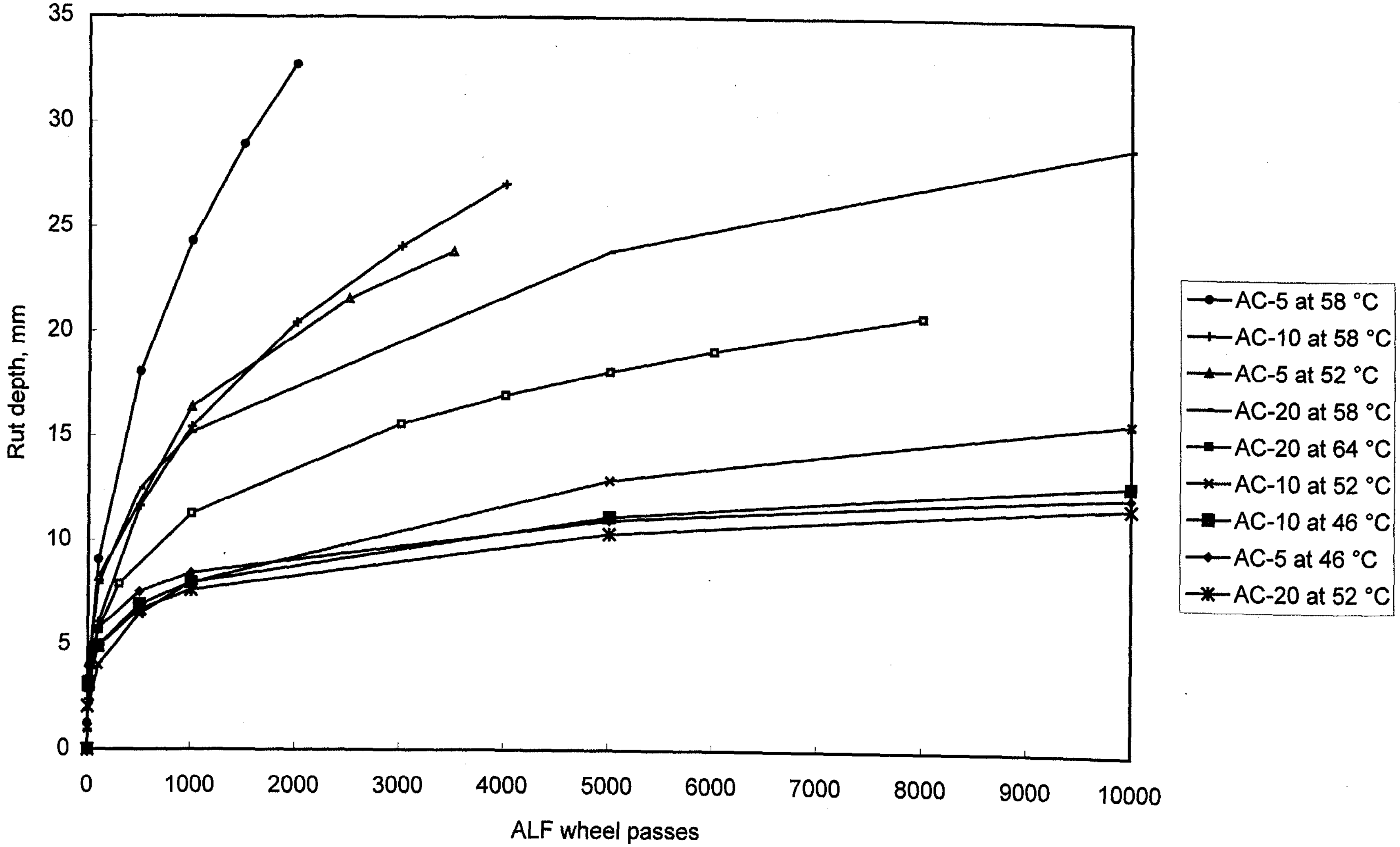

Figure 18. Rut depths in asphalt pavement layer vs. ALF wheel passes using the Gauss-Newton model.

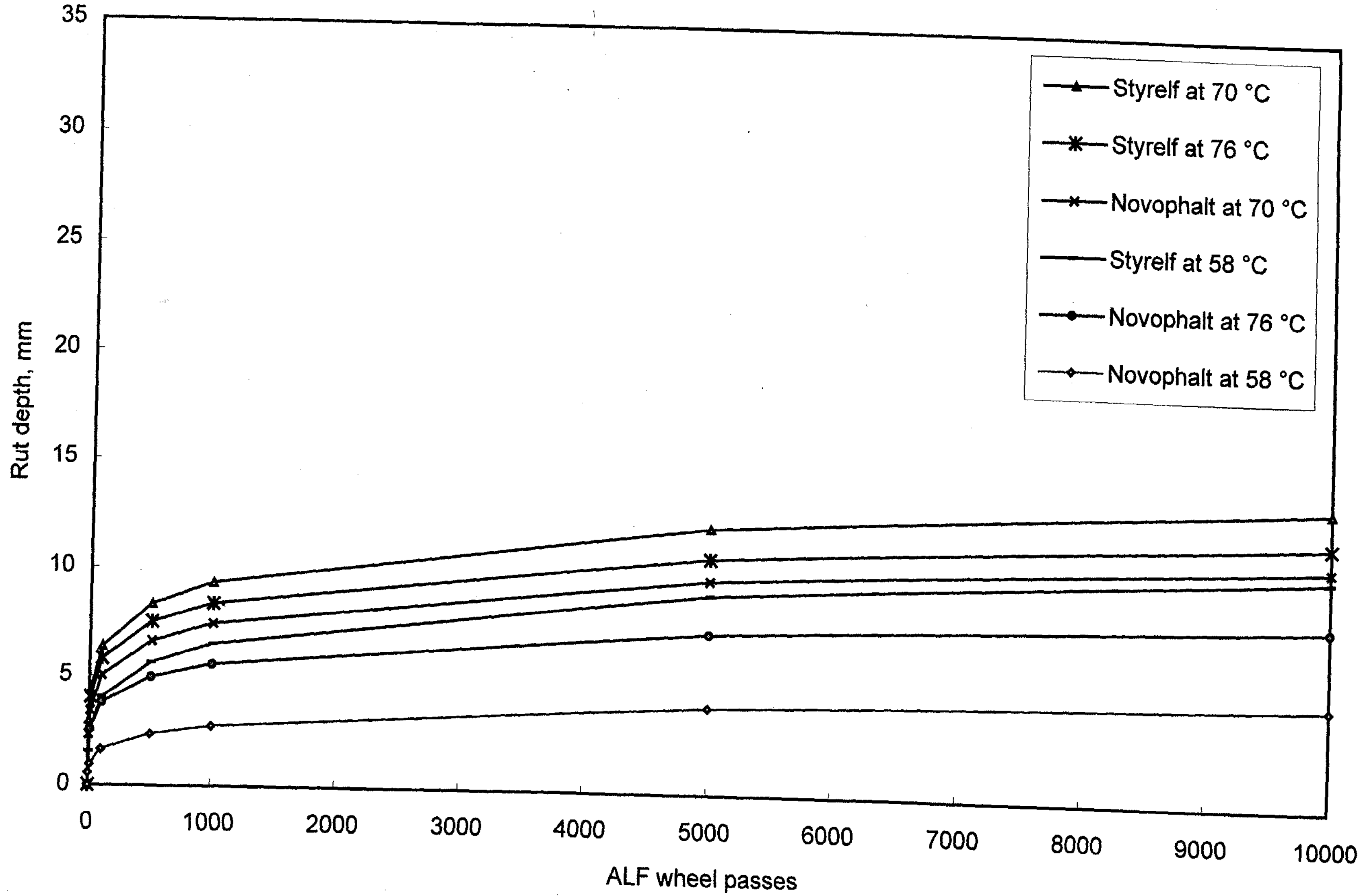

Figure 19. Rut depths in asphalt pavement layers with modified binders vs. ALF wheel passes using the Gauss-Newton model.

Table 33. Final rut depths for the pavements tested for rutting.

Lane Number:			1	2	3	4	5	6	7	8	9	10	11	12
Pre-Superpave Designation:			5	20	5	20	10	20	S	N	5	20	5	20
Surface or Base Mixture:			S	S	S	S	S	S	S	S	S	S	B	B
Distress	**Year**	**Temperature**	**Final Rut Depth in the Asphalt Pavement Layer, mm**											
Rutting	1994	58 °C	-	-	-	-	27	-	18	9	22	36	25	24
Rutting	1995	58 °C	-	-	-	-	-	-	-	-	31	27	23	-
Rutting	1995	70 °C	-	-	-	-	-	-	21	17	-	-	-	-
Rutting	1996	52 °C	-	-	-	-	21	21	-	-	-	-	-	-
Rutting	1997	64 °C	-	-	-	-	-	21	-	-	-	-	-	-
Rutting	1997	52 °C	-	-	-	-	-	-	-	-	24	-	-	-
Rutting	1997	46 °C	-	-	-	-	21	-	-	-	-	-	-	-
Rutting	1997	46 °C	-	-	20	-	-	-	-	-	-	-	-	-
Rutting	1997	76 °C	-	-	-	-	-	-	-	17	-	-	-	-
Rutting	1997	76 °C	-	-	-	-	-	-	21	-	-	-	-	-
Distress	**Year**	**Temperature**	**Final Total Rut Depth, mm**											
Rutting	1994	58 °C	-	-	-	-	34	-	32	29	40	37	36	31
Rutting	1995	58 °C	-	-	-	-	-	-	-	-	42	33	31	-
Rutting	1995	70 °C	-	-	-	-	-	-	34	28	-	-	-	-
Rutting	1996	52 °C	-	-	-	-	34	35	-	-	-	-	-	-
Rutting	1997	64 °C	-	-	-	-	-	29	-	-	-	-	-	-
Rutting	1997	52 °C	-	-	-	-	-	-	-	-	32	-	-	-
Rutting	1997	46 °C	-	-	-	-	35	-	-	-	-	-	-	-
Rutting	1997	46 °C	-	-	34	-	-	-	-	-	-	-	-	-
Rutting	1997	76 °C	-	-	-	-	-	-	-	41	-	-	-	-
Rutting	1997	76 °C	-	-	-	-	-	-	40	-	-	-	-	-

Notes:

5 = AC-5 (PG 59).
10 = AC-10 (PG 65).
20 = AC-20 (PG 70).
S = Styrelf (PG 88).
N = Novophalt (PG 77).

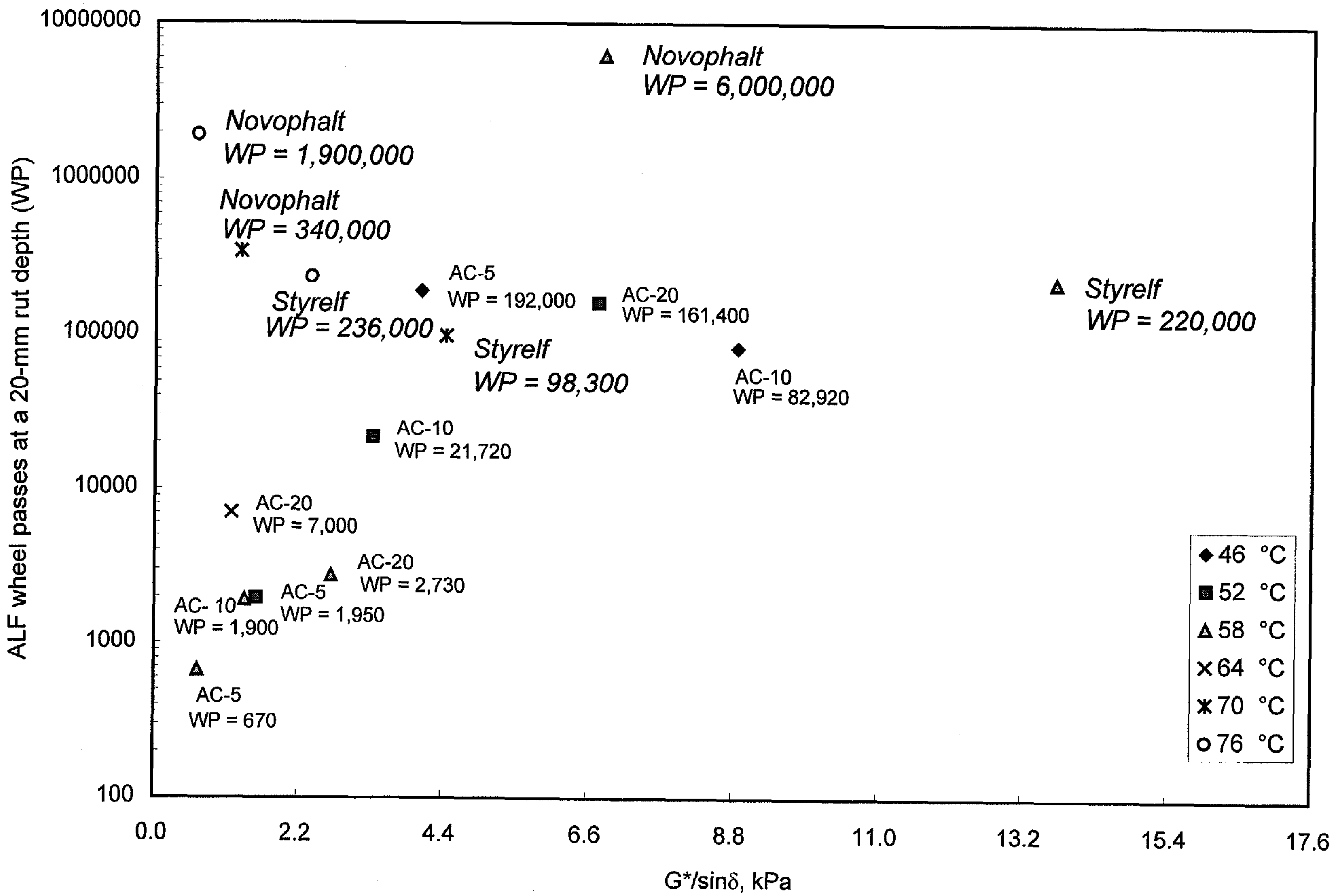

Figure 20. ALF wheel passes at a 20-mm rut depth based on the Gauss-Newton model for the five surface mixtures vs. G*/sinδ at 2.25 rad/s after RTFO.

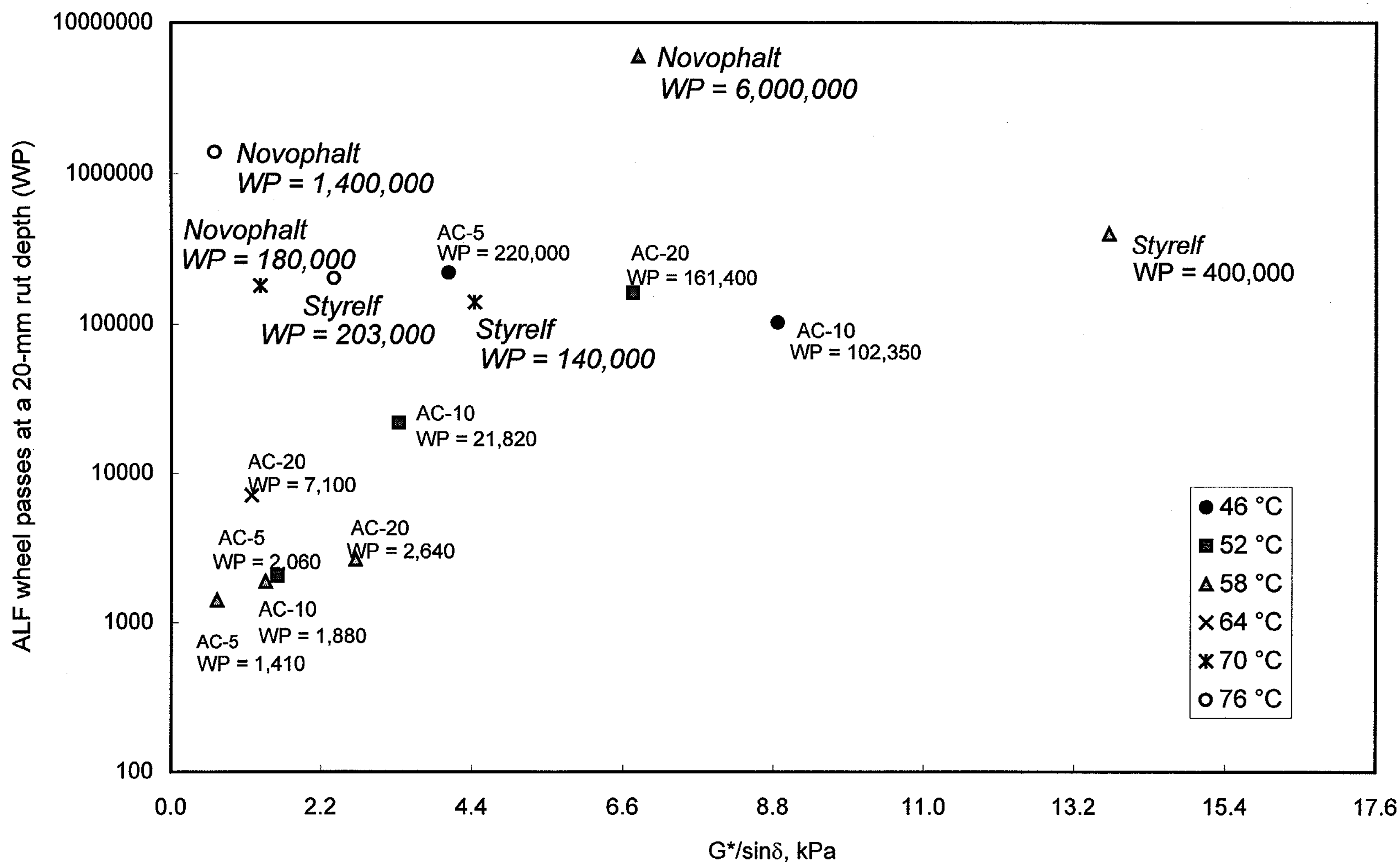

Figure 21. ALF wheel passes at a 20-mm rut depth based on the measured data for the five surface mixtures vs. G*/sinδ at 2.25 rad/s after RTFO.

Table 34. **ALF wheel passes that provided a rut depth of 10 mm due to viscous flow, and rut depths in the asphalt pavement layer at 2,730 wheel passes.**

Pavement Mixture	Temperature, °C	Wheel Passes at 10 mm of Viscous Flow	Rut Depth in the Asphalt Pavement Layer at 2,730 Wheel Passes	G*/sinδ (Pa)
Novophalt	76	600,000	6.6	642
Styrelf	76	225,000	10.8	2 381
Novophalt	70	125,000	15.0	1 304
Styrelf	70	132,000	12.2	4 435
AC-20	64	5,000	15.6	1 175
Novophalt	58	406,000[1]	3.5	6 826
Styrelf	58	161,000	8.0	13 710
AC-20	58	2,900	20.1	2 702
AC-10	58	1,500	23.2	1 384
AC-5	58	550	37.4	664
AC-20	52	61,000	9.2	6 744
AC-10	52	11,250	12.9	3 329
AC-5	52	735	22.1	1 557
AC-10	46	15,000	9.9	8 865
AC-5	46	55,000	9.8	4 061

[1]From extrapolation.

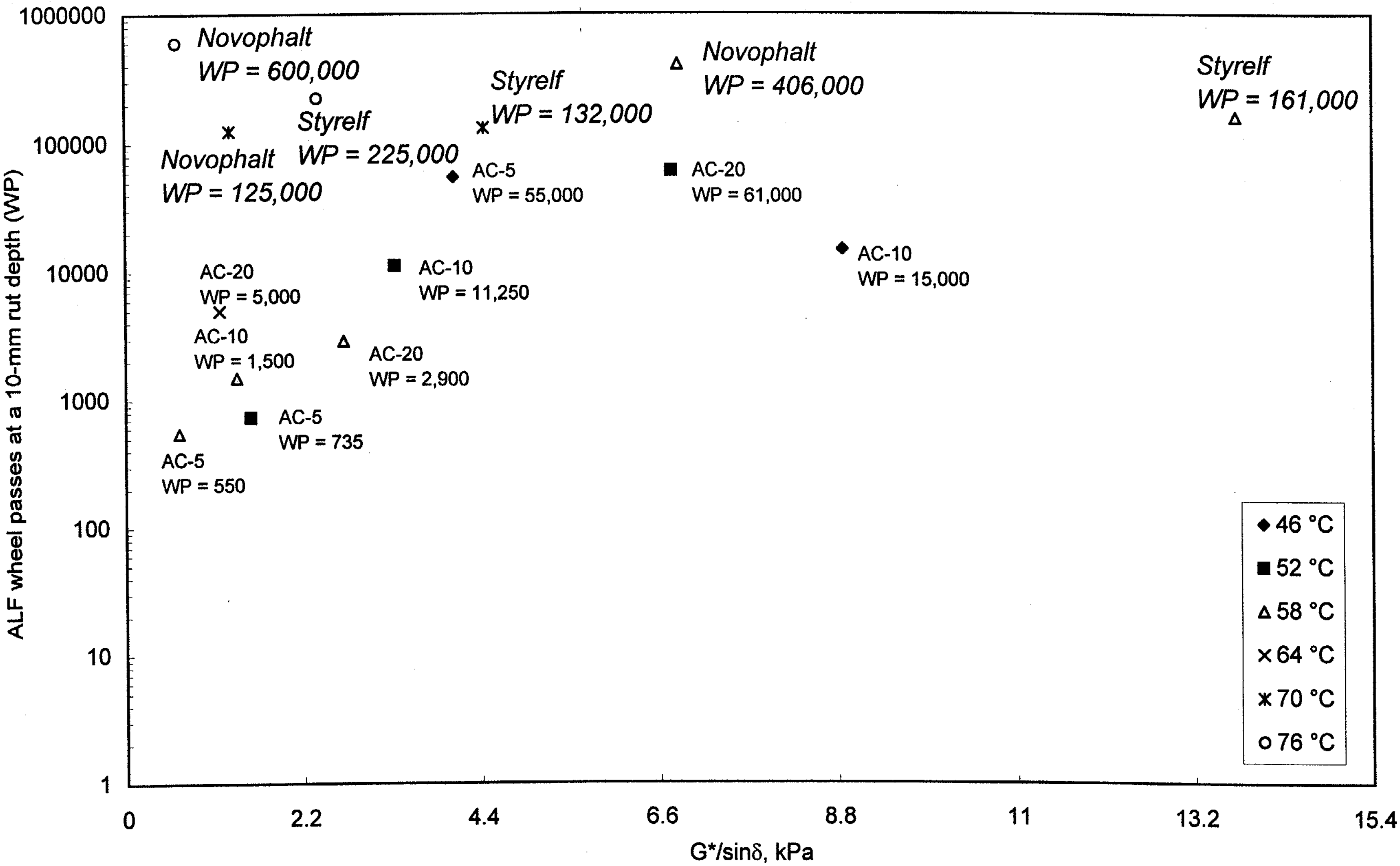

Figure 22. ALF wheel passes at a 10-mm rut depth due to viscous flow vs. G*/sinδ at 2.25 rad/s after RTFO.

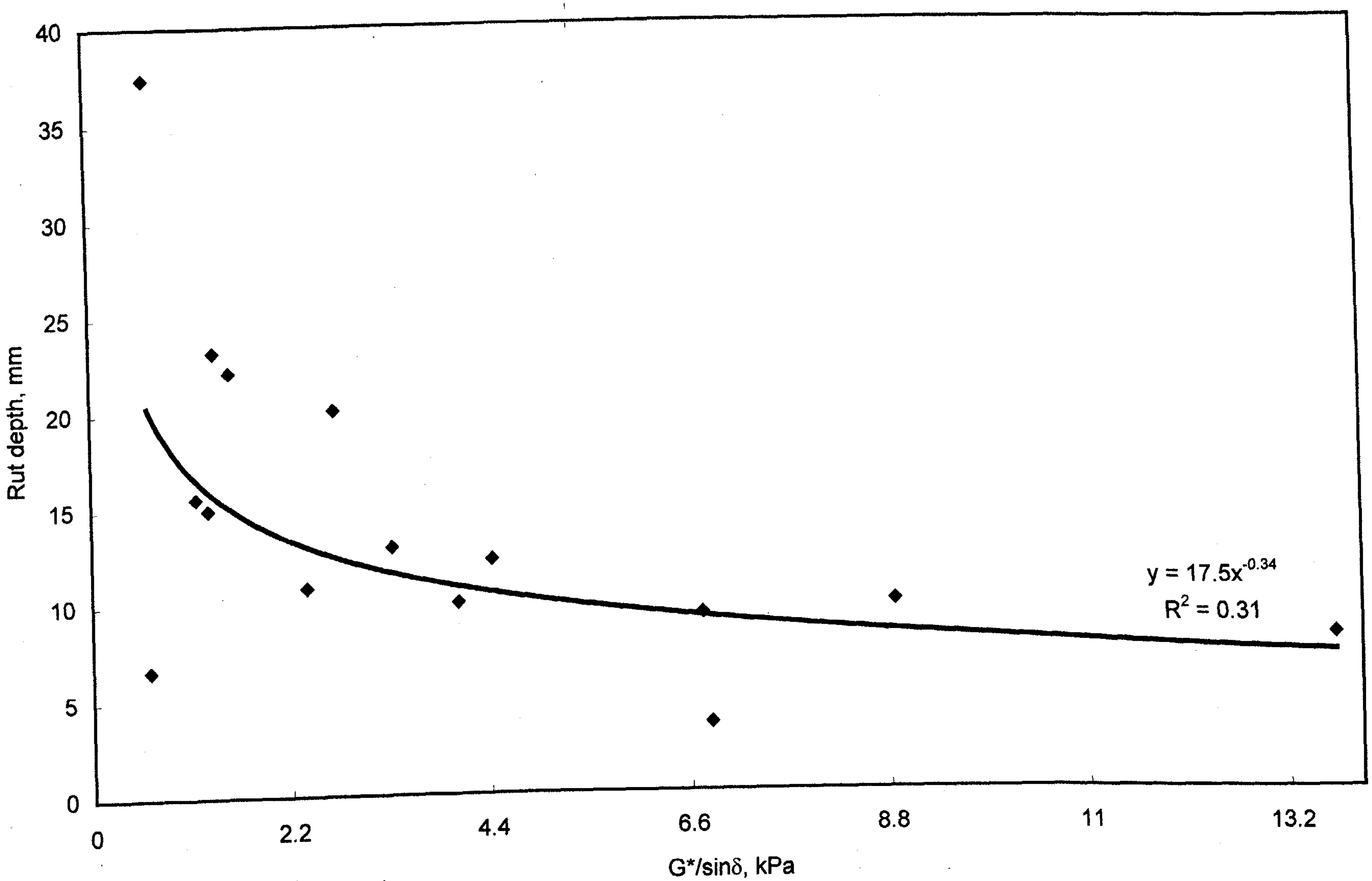

Figure 23. Rut depth at 2,730 ALF wheel passes vs. G*/sinδ at 2.25 rad/s after RTFO.

Table 35 provides the pavement data according to binder type. These data show that there were discrepancies between the ALF wheel passes and temperature for the pavements with Novophalt, Styrelf, and AC-20 (PG 70). It was hypothesized that the binders hardened over time, thus providing relatively high wheel passes for the tests performed in 1997. The mixture with the AC-5 (PG 59) binder also performed better than the mixture with the AC-10 (PG 65) binder at 46 °C, although both tests were performed in 1997. Table 36 shows how the high-temperature continuous PG's of binders recovered from the pavements varied from test to test. The binders were recovered from the top halves of the pavements, although rutting occurred throughout the asphalt pavement layer. Based on these PG's, most of the binders during pavement testing were stiffer than the laboratory binder samples tested after RTFO aging. Unfortunately, the PG's did not explain the discrepancy for the Styrelf pavement tests or the discrepancy for the AC-5 and AC-10 (PG 59 and 65) pavement tests performed in 1997 at 46 °C.

Table 37 provides the $G^*/\sin\delta$'s of the recovered binders at the pavement test temperature and 10.0 rad/s. These data did not explain the discrepancies except, possibly, for the Novophalt binder, which had a higher $G^*/\sin\delta$ at 76 °C than at 70 °C. Figure 24 presents the relationship between these $G^*/\sin\delta$'s and ALF wheel passes. The replicate ALF tests performed at 58 °C on the pavements with the AC-5 and AC-20 (PG 59 and 70) binders were treated as individual tests because table 37 showed that the $G^*/\sin\delta$'s were higher in 1995 compared with 1994. The relationship was poor, and all $G^*/\sin\delta$'s were above the Superpave specification level of 2.20 kPa. Figure 25 shows that the relationship using the ALF wheel passes at a 10-mm rut depth due to viscous flow was also poor. The use of recovered binder properties did not improve the correlation between $G^*/\sin\delta$ and ALF pavement rutting performance.

Table 38 provides the $G^*/\sin\delta$'s of the recovered binders at the pavement test temperature and 2.25 rad/s. Most $G^*/\sin\delta$'s were above the Superpave specification level of 2.20 kPa. Figures 26 and 27 show that the trend was correct for the pavements with unmodified binders, except for the low number of wheel passes for the AC-10 (PG 65) pavement test at 46 °C shown in figure 27. Figure 28 provides the relationship between the rut depths at 2,730 wheel passes and the $G^*/\sin\delta$'s of the recovered binders at 2.25 rad/s. All pavements with a $G^*/\sin\delta$ around 10.0 kPa and greater were performing well at 2,730 wheel passes. No data point was found to be an outlier.

4. Supplemental Analyses Performed on the ALF Pavement Data

a. Rut Depth in the Asphalt Pavement Layer vs. Total Rut Depth

The relationship between the ALF wheel passes that provided a total rut depth of 20 mm and the ALF wheel passes that provided a rut depth of 20 mm in the asphalt pavement layer is shown in figure 29. The wheel passes for the Novophalt pavement tests at 58 and 76 °C, which were found to be greater than 1,000,000 through extrapolation, are not included. Figure 30 shows the data for the four pavements that had the lowest number of wheel passes at failure.

The wheel passes at a 20-mm rut depth differed the most for the pavements that had the least percentage of rutting in the asphalt pavement layer. For example, the data plotted in figure 29 showed that 19,020 wheel passes were required to obtain a total rut depth of 20 mm for the AC-20 (PG 70) pavement test at 52 °C, while 161,400 wheel passes were required for a rut depth of 20 mm in the asphalt pavement layer. These wheel passes differ by 750 percent. The data plotted in figure 30 showed that 1,790 wheel passes were required to obtain a total rut depth of 20 mm for the AC-20 (PG 70) pavement test at 58 °C, while 2,730 wheel passes were required for a rut depth of 20 mm in the asphalt pavement layer. These wheel passes differ by 53 percent. A thicker asphalt pavement layer or a more stable crushed aggregate base layer would have provided significantly longer pavement lives based on total rut depth.

Table 29 includes the percentage of rut depth in the asphalt pavement layer based on the total rut depth. For each given pavement test, the percentage of rut depth in the asphalt pavement layer decreased with increasing total rut depth. As the asphalt pavement layer failed due to rutting and became thinner because of lateral shearing, the percentage of rutting in the underlying layers increased.

b. Percentage of Rut Depth in Each Asphalt Pavement Lift

Table 39 shows the percent rut depth in each pavement lift after each pavement test was completed. These percent rut depths were based on the decreases in the thicknesses of the lifts; thus, they include both the rut depth due to densification and viscous flow. The data were analyzed to determine where the highest percentage of rutting occurred in the pavements. The surface mixtures were placed in four 50-mm lifts, while the base mixtures were placed in two 100-mm lifts. Based on the number of times a lift received a ranking of one, the highest average percentage of rutting occurred most often in the lower lifts. This finding was not supported by the number of times a surface mixture lift received a ranking of two. Based on the statistical rankings, shown by the letters A through D in table 39, it could not be concluded that any lift or group of two or three lifts rutted the most. Rutting occurred in all lifts and was variable.

c. Evaluation of the Slopes and Intercepts From the Rut Depth vs. ALF Wheel Pass Relationships

(1) Introduction

The slope and the intercept obtained from a regression analysis are often used to describe the relationship between pavement rut depth and wheel passes (or ESAL's). Tables 40 and 41 show the slopes and intercepts provided by two models: the Gauss-Newton model, which is also called the linearization method, and a log-log model. The Gauss-Newton model, not performed in log-log space, was the preferred model in this study because relationships based on log rut depth vs. log wheel pass can be biased toward rut depths at low numbers of wheel passes.

Table 35. ALF wheel passes that were needed to obtain rut depths of 10, 15, and 20 mm in the asphalt pavement layer.

Mixture	Pavement Temp, °C and Year of Test		Rut Depth of 10 mm	Rut Depth of 15 mm	Rut Depth of 20 mm	G*/sinδ after RTFO Aging (Pa)
Novophalt	76	1997	31,652	349,250	1,900,000[1]	642
Novophalt	70	1995	5,750	62,840	340,000[1]	1 304
Novophalt	58	1994	293,000[1]	1,750,000[1]	6,000,000[1]	6 826
Styrelf	76	1997	3,040	38,760	236,000	2 381
Styrelf	70	1995	1,520	17,430	98,300	4 435
Styrelf	58	1994	7,910	55,540	220,000[1]	13 710
AC-20	64	1997	670	2,640	7,000	1 175
AC-20	58	1994	262	1,031	2,724	2 702
AC-20	58	1995	206	937	2,741	2 702
AC-20	52	1996	4,200	35,500	161,400	6 744
AC-10	58	1994	340	940	1,900	1 384
AC-10	52	1996	2,140	8,300	21,720	3 329
AC-10	46	1997	2,980	20,840	82,920	8 865
AC-5	58	1994	115	279	521	664
AC-5	58	1995	143	395	814	664
AC-5	52	1997	190	740	1,950	1 557
AC-5	46	1997	2,820	33,330	192,000	4 061

[1]From extrapolation.

Table 36. High-temperature continuous PG based on a $G^*/\sin\delta$ of 2.20 kPa and an angular frequency of 10.0 rad/s.

Mixture Designation	PG's of RTFO Residues	PG's of Binders Recovered From Cores Taken From the Wheelpath After Performing ALF Rutting Tests at the Following Pavement Temperatures							
		1994 58 °C	1995 58 °C	1995 70 °C	1996 52 °C	1997 52 °C	1997 64 °C	1997 46 °C	1997 76 °C
AC-5	59	63	68	--	--	68	--	67	--
AC-10	65	67	--	--	75	--	--	70	--
AC-20	70	72	78	--	78	--	82	--	--
Styrelf	88	86	--	94	--	--	--	--	88
Novophalt	77	81	--	84	--	--	--	--	93
AC-5 Base	59	67	72	--	--	--	--	--	--
AC-20 Base	70	78	--	--	--	--	--	--	–

Table 37. G*/sinδ of binders recovered from wheelpath cores at the pavement test temperature and an angular frequency of 10.0 rad/s.

Mixture Designation	Year of Pavement Test, Test Temperature, and G*/sinδ, kPa							
	1994 58 °C	1995 58 °C	1995 70 °C	1996 52 °C	1997 52 °C	1997 64 °C	1997 46 °C	1997 76 °C
AC-5	4.3	7.9	--	--	21.0	--	39.0	--
AC-10	7.2	--	--	ND	--	--	70.6	--
AC-20	12.4	25.0	--	ND	--	21.3	--	--
Styrelf	37.3	--	19.6	--	--	--	--	8.4
Novophalt	29.1	--	12.0	--	--	--	--	15.6
AC-5 Base	6.9	12.7	--	--	--	--	--	--
AC-20 Base	29.0	--	--	--	--	--	--	--

ND = No data. (These data were not obtained when the binders were originally tested. When the binders were later retested, they were found to have hardened in the containers during storage.)

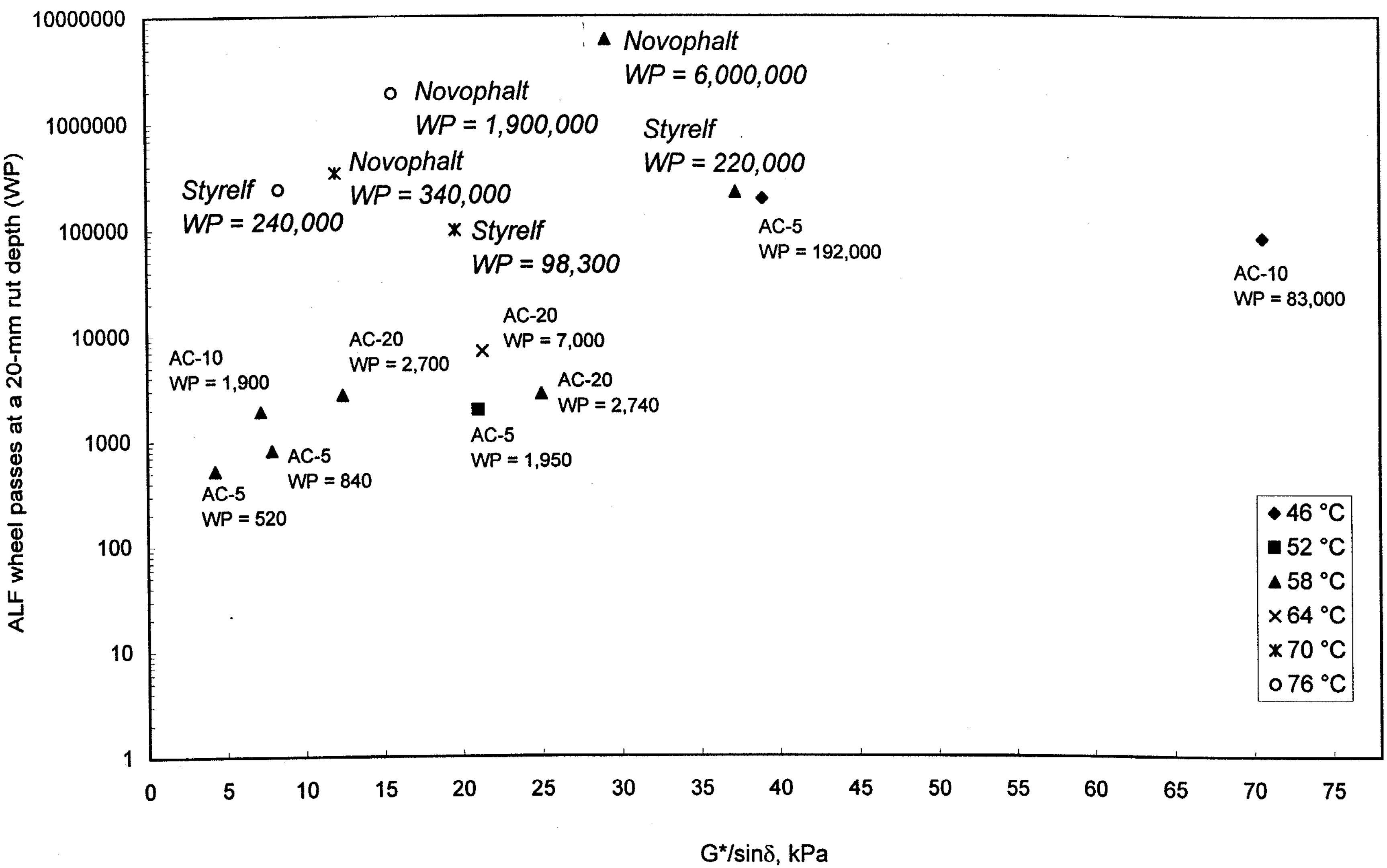

Figure 24. ALF wheel passes at a 20-mm rut depth from the Gauss-Newton model vs. G*/sinδ at the pavement test temperature and 10 rad/s using binders recovered from wheelpath cores.

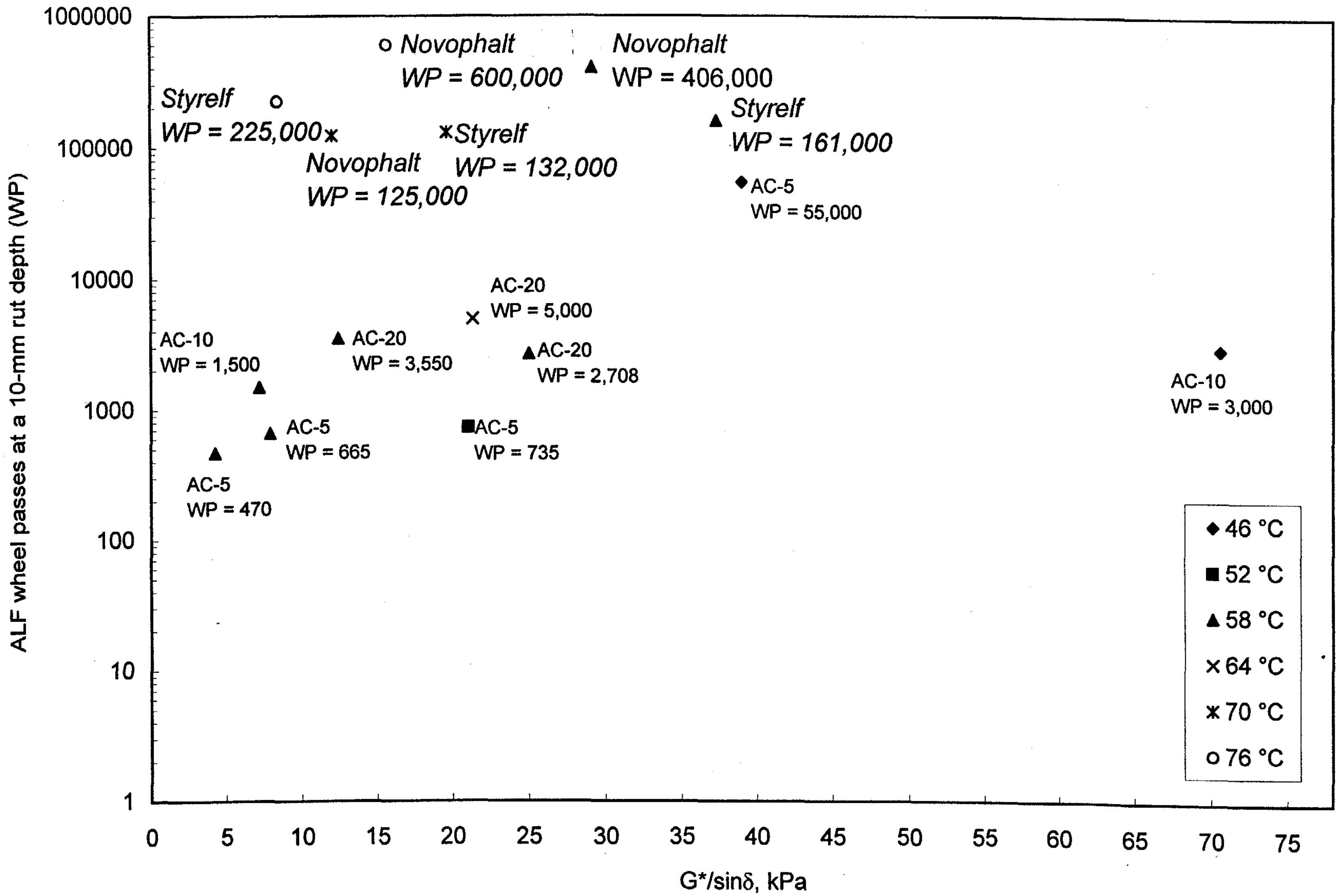

Figure 25. ALF wheel passes at a 10-mm rut depth due to viscous flow vs. G*/sinδ at the pavement test temperature and 10 rad/s using binders recovered from wheelpath cores.

Table 38. G*/sinδ of binders recovered from wheelpath cores at the pavement test temperature and an angular frequency of 2.25 rad/s.

Mixture Designation	Year of Pavement Test, Test Temperature, and G*/sinδ, kPa							
	1994 58 °C	1995 58 °C	1995 70 °C	1996 52 °C	1997 52 °C	1997 64 °C	1997 46 °C	1997 76 °C
AC-5	1.3	ND	--	--	5.6	--	11.3	--
AC-10	3.4	--	--	15.8	--	--	23.1	--
AC-20	4.3	ND	--	ND	--	7.8	--	--
Styrelf	23.3	--	13.0	--	--	--	--	3.5
Novophalt	13.7	--	4.8	--	--	--	--	4.4
AC-5 Base	1.7	5.5	--	--	--	--	--	--
AC-20 Base	11.6		--	--	--	--	--	--

ND = No data. (These data were not obtained when the binders were originally tested. When the binders were later retested, they were found to have hardened in the containers during storage.)

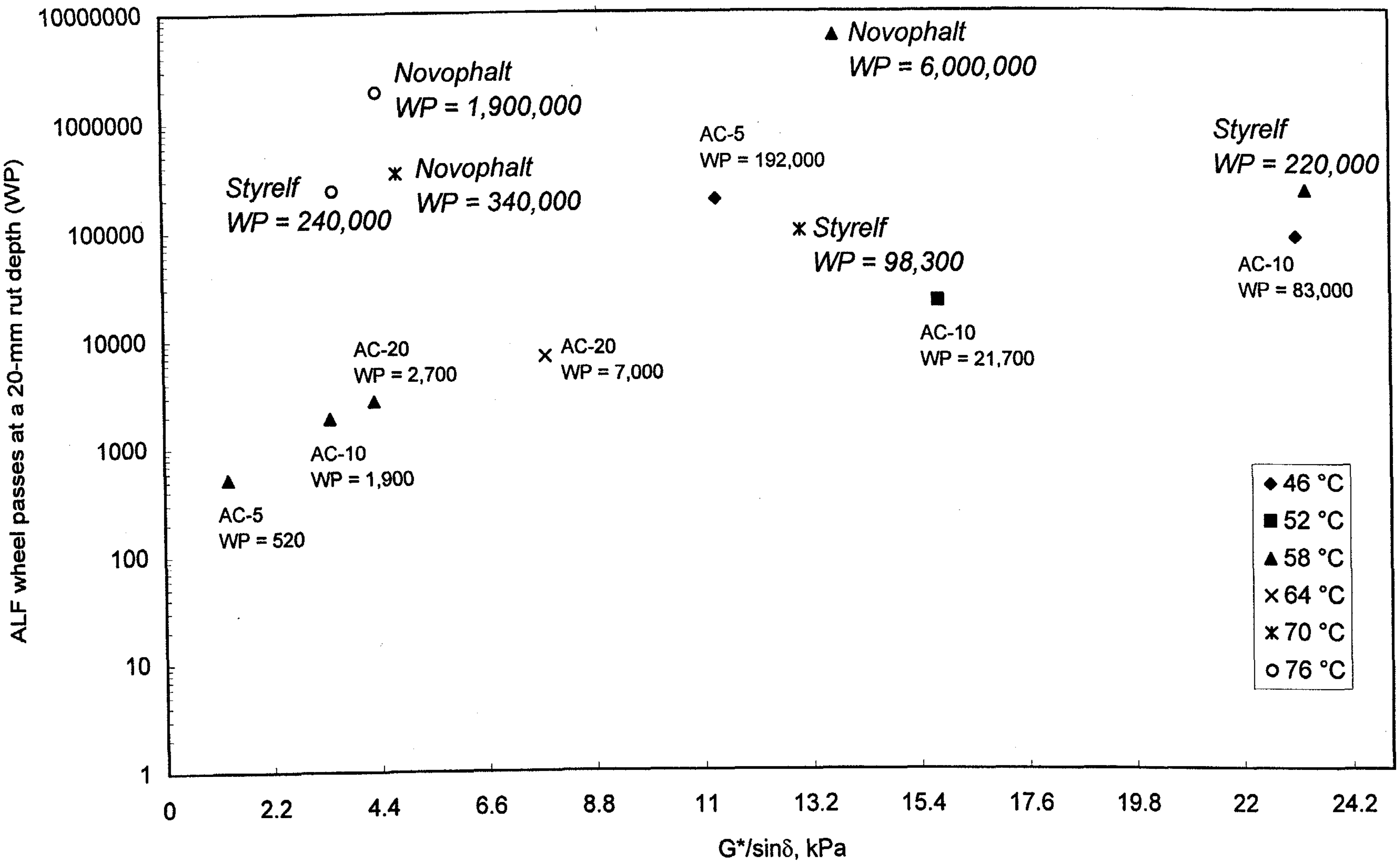

Figure 26. ALF wheel passes at a 20-mm rut depth from the Gauss-Newton model vs. G*/sinδ at the pavement test temperature and 2.25 rad/s using binders recovered from wheelpath cores.

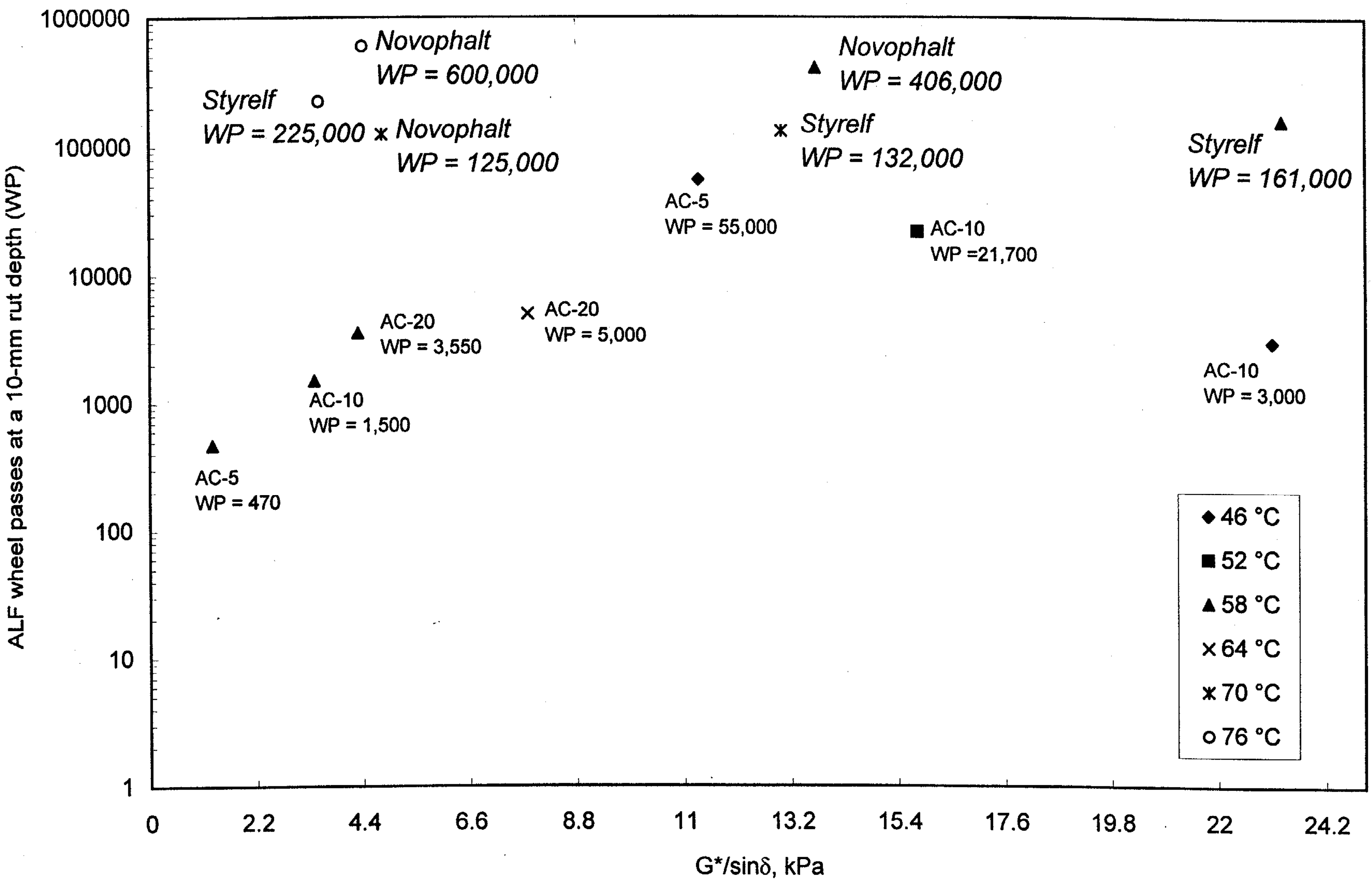

Figure 27. ALF wheel passes at a 10-mm rut depth due to viscous flow vs. G*/sinδ at the pavement test temperature and 2.25 rad/s using binders recovered from wheelpath cores.

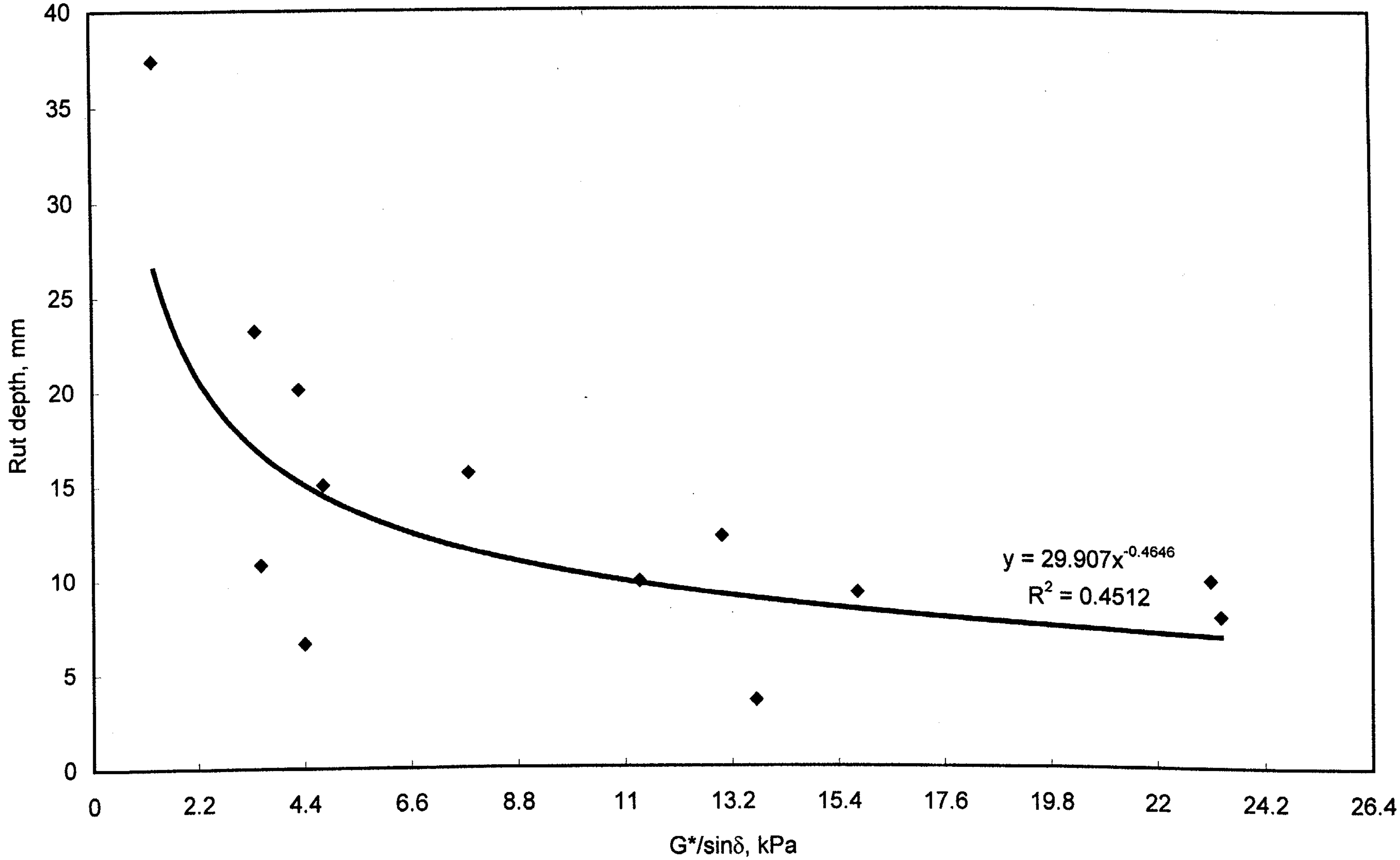

Figure 28. Rut depth at 2,730 ALF wheel passes vs. G*/sinδ at the pavement test temperature and 2.25 rad/s using binders recovered from wheelpath cores.

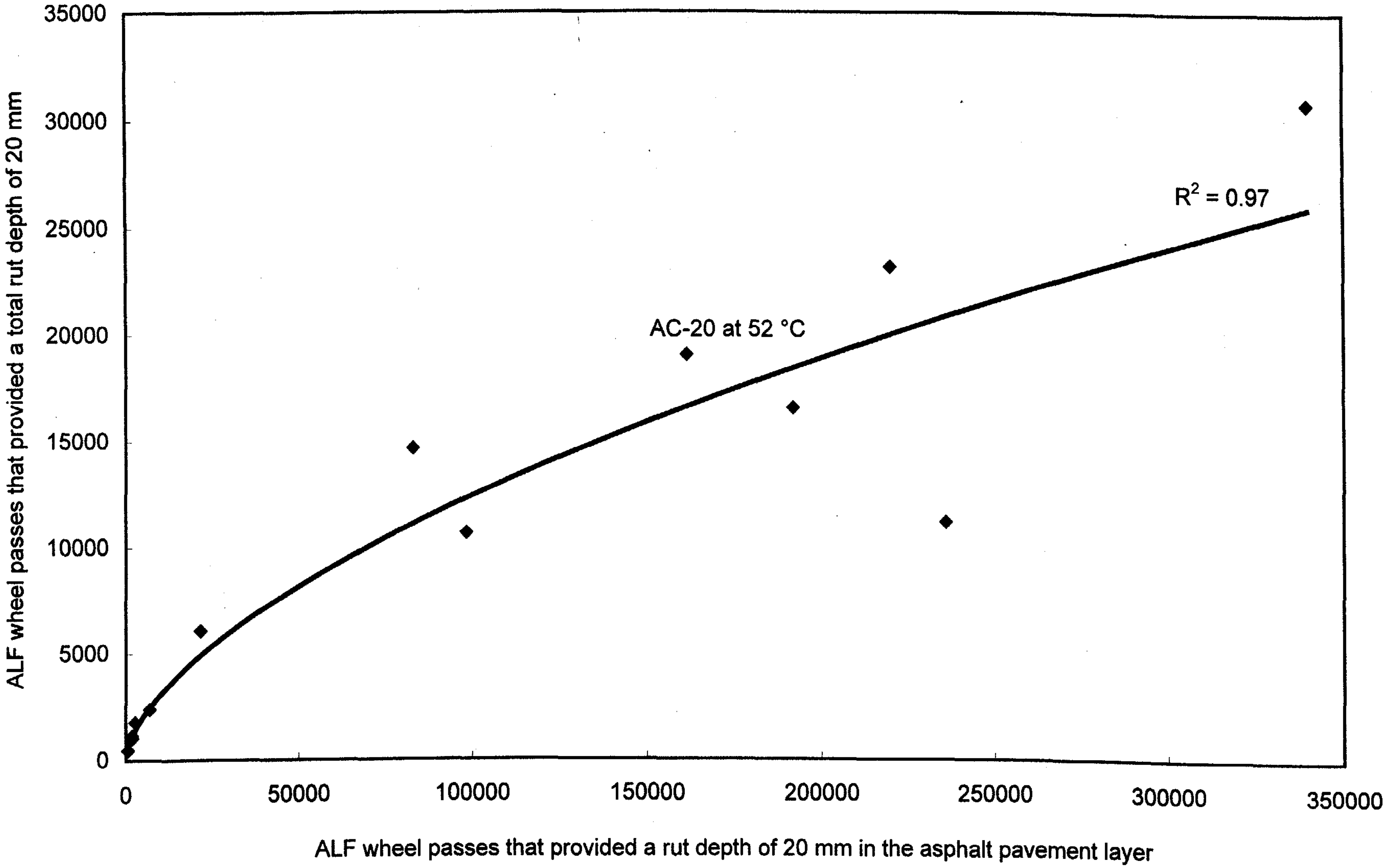

Figure 29. ALF wheel passes that provided a total rut depth of 20 mm vs. the ALF wheel passes that provided a rut depth of 20 mm in the asphalt pavement layer.

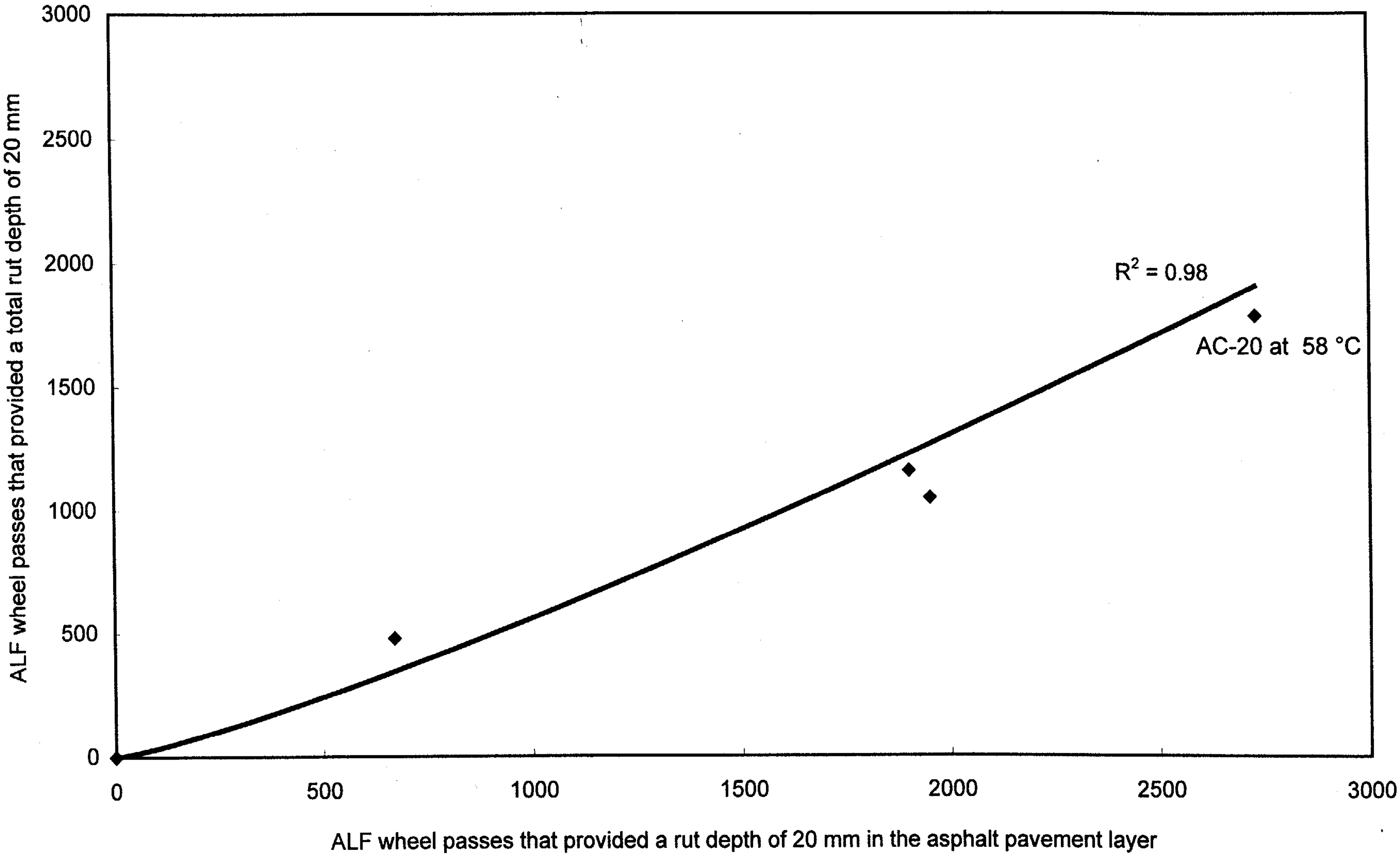

Figure 30. ALF wheel passes that provided a total rut depth of 20 mm vs. ALF wheel passes that provided a rut depth of 20 mm in the asphalt pavement layer for the poorest performing mixtures.

Table 39. Percent rut depth in each lift with numerical and statistical ranking.[1]

Superpave PG:	58-34	58-28	58-34	58-28	64-22
Conventional:	AC-5	AC-10	AC-5	AC-10	AC-20
Mixture Type:	Surface	Surface	Surface	Surface	Surface
Lane Number:	3	5	9	5	6
Test Temp, °C:	46	46	52	52	52
Lift 4 (Top)	30 2 AC	18 3 A	22 3 AB	19 4 A	No Data
Lift 3	16 3 AD	16 4 A	35 2 A	27 1 A	
Lift 2	59 1 A	21 2 A	38 1 A	27 1 A	
Lift 1	-5 4 BCD	45 1 A	5 4 B	27 1 A	

Superpave PG:	58-34	58-28	64-22	76-22	82-22
Conventional:	AC-5	AC-10	AC-20	Novophalt	Styrelf
Mixture Type:	Surface	Surface	Surface	Surface	Surface
Lane Number:	9	5	10	8	7
Test Temp, °C:	58	58	58	58	58
Lift 4 (Top)	11 3 AC	24 3 A	14 4 A	20 3 A	32 2 A
Lift 3	36 2 AB	31 2 A	29 2 A	24 2 A	34 1 A
Lift 2	44 1 A	34 1 A	38 1 A	24 2 A	16 4 A
Lift 1	9 4 BC	11 4 A	19 3 A	32 1 A	18 3 A

Superpave PG:	64-22	76-22	82-22	76-22	82-22
Conventional:	AC-20	Novophalt	Styrelf	Novophalt	Styrelf
Mixture Type:	Surface	Surface	Surface	Surface	Surface
Lane Number:	6	8	7	8	7
Test Temp, °C:	64	70	70	76	76
Lift 4 (Top)	24 3 A	25 2 A	13 4 B	42 1 A	30 2 AB
Lift 3	18 4 A	35 1 A	22 2 B	26 3 AC	50 1 A
Lift 2	27 2 A	25 2 A	22 2 B	3 4 BC	13 3 AC
Lift 1	31 1 A	15 4 A	43 1 A	29 2 AB	7 4 BC

[1]The letters are the statistical ranking, with "A" denoting the mixture(s) with the greatest percentage of rut depth. The numbers are the ranking based on the averages alone, with "1" denoting the mixture with the greatest percentage of rut depth.

Table 39. Percent rut depth in each lift with numerical and statistical ranking (continued).[1]

Superpave PG:	58-34		64-22		58-34[3]		64-22[3]		58-34[3]	
Conventional:	AC-5		AC-20		AC-5		AC-20		AC-5	
Mixture Type:	Base[2]		Base[2]		Surface		Surface		Base[2]	
Lane Number:	11		12		9		10		11	
Test Temp, °C:	58		58		58		58		58	
Lift 4 (Top)					26	2 A	41	1 A		
Lift 3					18	4 A	34	2 AB		
Lift 2	44	2 A	43	2 A	25	3 A	12	3 B	68	1 A
Lift 1	56	1 A	57	1 A	31	1 A	12	3 B	32	2 A

	Number of Times the Lift Had a Ranking of 1 or 2 (Surface Mixtures Only)	
	Ranking of 1	Ranking of 2
Lift 4 (Top)	2	5
Lift 3	4	7
Lift 2	6	5
Lift 1 (Bottom)	6	1

[1]The letters are the statistical ranking, with "A" denoting the mixture(s) with the greatest percentage of rut depth. The numbers are the ranking based on the averages alone, with "1" denoting the mixture with the greatest percentage of rut depth.

[2]The base mixtures were placed in two 100-mm lifts.

[3]Replicate pavement test.

Table 40. Slopes and intercepts for rut depths in the asphalt pavement layer provided by the Gauss-Newton and log-log models.

Ranking Based on a 20-mm Rut Depth	ALF Wheel Passes	Pavement Temp, °C	Gauss-Newton Model			Log-Log Model		
			Slope	Intercept	r^2	Slope	Intercept	r^2
Novophalt	1900000	76	0.17	1.7	0.99	0.16	2.0	0.98
Styrelf	236000	76	0.16	2.8	0.99	0.18	2.3	0.97
Novophalt	340000	70	0.17	2.3	1.00	0.17	2.5	1.00
Styrelf	98300	70	0.17	3.0	1.00	0.17	3.2	1.00
AC-20	7000	64	0.30	1.5	0.99	0.30	1.4	0.99
Novophalt	6000000	58	0.23	0.6	0.98	0.27	0.4	0.92
Styrelf	220000	58	0.21	1.6	0.97	0.31	0.5	0.91
AC-20 Base	57520	58	0.18	2.9	0.99	0.26	1.3	0.89
AC-5 Base	11990	58	0.27	1.6	0.99	0.47	0.3	0.86
AC-20	2730	58	0.28	2.2	1.00	0.34	1.5	0.99
AC-10	1900	58	0.41	0.9	1.00	0.53	0.4	0.92
AC-5	670	58	0.43	1.3	0.96	0.57	0.4	0.87
AC-20	161400	52	0.19	2.0	0.99	0.32	0.5	0.90
AC-10	21720	52	0.30	1.0	0.99	0.46	0.3	0.90
AC-5	1950	52	0.30	2.1	0.99	0.27	2.5	0.98
AC-10	82920	46	0.21	1.9	0.99	0.25	1.2	0.98
AC-5	192000	46	0.16	2.7	0.99	0.21	1.7	0.95
r^2 between log ALF wheel passes and slope or intercept at 58 °C			0.46	0.04		0.54	0.01	
r^2 between log ALF wheel passes and slope or intercept at all temperatures			0.60	0.01		0.40	0.01	

Table 41. Slopes and intercepts for total rut depth provided by the Gauss-Newton and log-log models.

Ranking Based on a 20-mm Rut Depth	ALF Wheel Passes	Pavement Temp, °C	Gauss-Newton Model			Log-Log Model		
			Slope	Intercept	r^2	Slope	Intercept	r^2
Novophalt	58300	76	0.28	0.9	0.99	0.22	1.9	0.98
Styrelf	11160	76	0.23	2.4	0.99	0.22	2.5	0.99
Novophalt	30840	70	0.24	1.6	0.98	0.23	1.9	0.98
Styrelf	10650	70	0.21	2.8	0.99	0.28	1.5	0.96
AC-20	2410	64	0.30	2.0	1.00	0.32	1.7	0.99
Novophalt	39600	58	0.24	1.6	0.99	0.31	0.8	0.92
Styrelf	23160	58	0.25	1.6	0.98	0.34	0.6	0.96
AC-20 Base	22100	58	0.21	2.5	0.99	0.27	1.3	0.93
AC-5 Base	5450	58	0.34	1.1	1.00	0.42	0.6	0.94
AC-20	1790	58	0.32	1.9	1.00	0.34	1.6	0.99
AC-10	1160	58	0.42	1.0	1.00	0.52	0.5	0.95
AC-5	480	58	0.48	1.1	1.00	0.64	0.4	0.90
AC-20	19020	52	0.24	2.0	1.00	0.34	0.6	0.93
AC-10	6070	52	0.37	0.8	1.00	0.51	0.3	0.92
AC-5	1050	52	0.39	1.3	0.99	0.33	2.1	0.97
AC-10	14650	46	0.28	1.3	0.99	0.32	0.9	0.99
AC-5	16520	46	0.20	3.0	0.99	0.23	2.0	0.97
r^2 between log ALF wheel passes and slope or intercept at 58 °C			0.86	0.17		0.67	0.04	
r^2 between log ALF wheel passes and slope or intercept at all temperatures			0.71	0.03		0.46	0.02	

at a failure level of 20 mm decreased, which meant that the slope increased with an increase in rutting susceptibility. The slopes of 0.18 (see table 40) and 0.21 (see table 41) at 58 °C for the pavement with the AC-20 (PG 70) base mixture are relatively low compared with the other slopes at 58 °C, while the intercepts of 2.9 and 2.5 are relatively high. A reason for this finding was not apparent.

Table 42 provides rankings for the average slope at 58 °C, the average slope plus and minus the standard deviation ($\pm 1\sigma_{n-1}$), and the average slope plus and minus two times the standard deviation ($\pm 2\sigma_{n-1}$). The latter two parameters provide 66- and 95-percent confidence levels. The slopes used in this evaluation were taken from the relationships between the rut depth in the asphalt pavement layer and ALF wheel pass. They are not based on total rut depth. The standard deviations were obtained using the data from the three ALF pavement tests that were replicated, as explained in chapter 2. Table 42 includes the average slopes and the upper and lower limits based on both $1\sigma_{n-1}$ and $2\sigma_{n-1}$. Pavements with overlapping confidence limits had slopes that were not significantly different; therefore, they received the same ranking. Pavements with the ranking "A" had the lowest slopes.

Although ALF rutting performance at 58 °C may be a function of the slope more than the intercept, the rankings in table 42 show that the slope alone is not sufficient for evaluating rutting performance. The intercept can significantly contribute to the rut depth. Note that in the rut depth model shown above, the intercept "a" is multiplied times N^b, thus it can have a significant effect on the rut depth.

(3) Slopes and Intercepts From the Gauss-Newton Model at Test Temperatures of 58, 70, and 76 °C

The Novophalt and Styrelf data in table 40 show that the increase in temperature from 58 to 70 °C decreased the slope and increased the intercept based on the rut depths in the asphalt pavement layer. This finding for the slope conflicts with the data at 58 °C where the mixtures that were more susceptible to rutting tended to have higher slopes. The slopes and intercepts in table 41, based on total rut depth, provided no firm conclusions.

As previously indicated, the pavements with Novophalt and Styrelf performed better at 76 °C than at 70 °C. This confounding effect could not be adequately considered in the analyses of the slopes and intercepts. The slopes for both binders at both 76 and 70 °C were either equal to or close to each other. The intercepts at 76 °C were lower than those at 70 °C.

The slopes at temperatures other than 58 °C were not statistically ranked because 58 °C was the only temperature at which all seven pavements were tested. Applying standard deviations to the data at temperatures other than 58 °C, based on the data from only three replicate tests at 58 °C, did not seem justifiable.

(4) Slopes and Intercepts From the Gauss-Newton Model at Test Temperatures of 46, 52, and 58 °C

The data show that an increase in temperature from 46 °C to 52 °C to 58 °C increased the slope based on both the rut depth in the asphalt pavement layer and total rut depth. The intercept increased or decreased with an increase in temperature, but in the majority of cases, the intercept decreased. The increase in slope with increasing temperature matches expectations, unlike the decreases in slope provided by the two modified binders when the temperature was increased from 58 °C to 70 °C.

(5) Log-Log Rut Depth Model

The log-log model provided the same conclusions as the Gauss-Newton model, and table 43 provided the same result as table 42; i.e., the slope alone is insufficient for evaluating performance.

The r^2 for each individual relationship between rut depth and ALF wheel passes are included in tables 40 and 41. The Gauss-Newton model provided higher r^2's for most pavement tests, although the r^2's from both models were high.

(6) Interdependence of Slope and Intercept

The slopes from all mixtures at all temperatures were linearly regressed against the intercepts to determine if they were related. For the slopes and intercepts provided by the Gauss-Newton method, the r^2 was 0.37 for the data based on the rut depths in the asphalt pavement layer, and 0.50 for the data based on total rut depth. For the slopes and intercepts from the log-log transformations, the r^2 was 0.55 for data based on either the rut depths in the asphalt pavement layer or total rut depth. All three r^2 indicate that the four relationships were poor.

Although none of the four regressions between the slope and intercept provided a high correlation, all four relationships were inversed. As the slope increased, the intercept decreased. This type of inverse relationship would only be expected if densification occurs early in the lives of a set of pavements and the pavements with higher susceptibilities to rutting densify the least during trafficking. This is possible because asphalt paving mixtures that are susceptible to rutting often compact to lower air-void levels during construction. However, the ALF pavement air-void data did not support this premise. The air-void data in table 29 for tests at 58 °C show that densification was not necessarily lower for the pavements that were most susceptible to rutting. Furthermore, none of the four sets of intercepts correlated with the decreases in air voids. The r^2's were zero. It was concluded that a decrease in the intercept does not mean that densification or densification and initial rutting due to viscous flow are lower, as might intuitively be expected.

Table 42. Pavement rankings at 58 °C based on the average slope from the Gauss-Newton model and on $\pm 1\sigma_{(n-1)}$ and $\pm 2\sigma_{(n-1)}$ confidence bands for the slope.[1]

Ranking Based on a 20-mm Rut Depth	Based on the Average Slope		Based on the Avg Slope $\pm 1\sigma_{(n-1)}$		Based on the Avg Slope $\pm 2\sigma_{(n-1)}$	
	All Mixtures	Surface Mixtures	All Mixtures	Surface Mixtures	All Mixtures	Surface Mixtures
Novophalt	C	B	B	A	AB	A
Styrelf	B	A	B	A	AB	A
AC-20 Base	A		A		A	
AC-5 Base	D		C		B	
AC-20	E	C	C	B	B	A
AC-10	F	D	D	C	C	B
AC-5	G	E	D	C	C	B

Mixture	Average Slope	$-1\sigma_{(n-1)}$	$+1\sigma_{(n-1)}$	$-2\sigma_{(n-1)}$	$+2\sigma_{(n-1)}$
Novophalt	0.227	0.212	0.242	0.197	0.257
Styrelf	0.208	0.195	0.221	0.182	0.234
AC-20 Base	0.176	0.166	0.186	0.157	0.195
AC-5 Base	0.274	0.254	0.294	0.233	0.315
AC-20	0.282	0.261	0.303	0.239	0.325
AC-10	0.406	0.367	0.445	0.327	0.485
AC-5	0.429	0.386	0.472	0.343	0.515

[1]The letter "A" denotes the mixture(s) with the lowest slope.

Table 43. Pavement rankings at 58 °C based on the average slope from the log-log model and on $\pm 1\sigma_{(n-1)}$ and $\pm 2\sigma_{(n-1)}$ confidence bands for the slope.[1]

Ranking Based on a 20-mm Rut Depth	Based on the Average Slope		Based on the Avg Slope $\pm 1\sigma_{(n-1)}$		Based on the Avg Slope $\pm 2\sigma_{(n-1)}$	
	All Mixtures	Surface Mixtures	All Mixtures	Surface Mixtures	All Mixtures	Surface Mixtures
Novophalt	B	A	A	A	A	A
Styrelf	C	B	AB	AB	A	A
AC-20 Base	A		A		A	
AC-5 Base	E		C		B	
AC-20	D	C	B	B	A	A
AC-10	F	D	CD	C	B	B
AC-5	G	E	D	C	B	B

Mixture	Average Slope	$-1\sigma_{(n-1)}$	$+1\sigma_{(n-1)}$	$-2\sigma_{(n-1)}$	$+2\sigma_{(n-1)}$
Novophalt	0.270	0.247	0.293	0.223	0.317
Styrelf	0.310	0.285	0.335	0.260	0.360
AC-20 Base	0.260	0.237	0.283	0.214	0.306
AC-5 Base	0.470	0.441	0.499	0.412	0.528
AC-20	0.340	0.314	0.366	0.289	0.391
AC-10	0.530	0.499	0.561	0.469	0.591
AC-5	0.570	0.539	0.601	0.507	0.633

[1]The letter "A" denotes the mixture(s) with the lowest slope.

Another reason why an inverse relationship may be obtained is that when the slope is high, there tends to be less curvature in the relationship between rut depth and wheel passes near the start of the test. This can decrease the intercept and provide an inverse relationship. A mixture that fails very rapidly could provide an equation with an intercept close to zero. It was concluded that the slope and intercept are not fundamental material properties; they are only regression coefficients.[17]

5. Conclusions

a. Validation of G*/sinδ

The following conclusions are based on comparisons between G*/sinδ and the ALF pavement rutting performances of five mixtures consisting of a single gradation and five binders: AC-5, AC-10, AC-20, Novophalt, and Styrelf 1-D. These binders had high-temperature continuous grades of 59, 65, 70, 77, and 88 after RTFO, respectively, based on a G*/sinδ of 2.20 kPa. Each mixture was tested by the ALF at three pavement temperatures.

- The overall relationship between G*/sinδ after RTFO aging and ALF pavement rutting performance was poor, although the trend was correct for the unmodified binders. The G*/sinδ of the Styrelf binder after RTFO aging was higher than the G*/sinδ of the Novophalt binder after RTFO aging at each pavement test temperature, but the pavement with Novophalt was always more resistant to rutting. This was the major discrepancy between G*/sinδ after RTFO aging and ALF pavement rutting performance that was found.

- When the data from the Novophalt and Styrelf pavement tests were excluded from the analysis, a minimum allowable G*/sinδ of 4.40 kPa eliminated the poorest performing mixtures. Even so, pavement life still varied significantly when the G*/sinδ's of the binders were above 4.40 kPa.

- There were discrepancies between ALF pavement rutting performance and pavement test temperature for the pavements with the AC-20, Novophalt, and Styrelf binders. It was hypothesized that the binders hardened over the 3.5-year period needed to perform the pavement tests. However, the G*/sinδ's of the binders recovered from the pavements after failure did not explain the discrepancies, and the use of these G*/sinδ's did not improve the relationship with ALF pavement rutting performance. Some of the mixtures failed rapidly even though the G*/sinδ's of the recovered binders were above the Superpave minimum criterion of 2.20 kPa.

b. Other Conclusions Provided by the ALF

- The reductions in air voids due to trafficking (densification) in the top and bottom halves of the 200-mm-thick asphalt pavement layer were not significantly different at a 95-percent confidence level for any pavement test. Based on the average densification in the top and bottom halves, it was found that the average densification in the bottom half could be greater than, equal to, or less than the average densification in the top half.

- The decreases in air voids due to trafficking indicated that when the rut depth in the asphalt pavement layer was 20 mm, the range in percent densification was approximately 20 to 55 percent, which is 4 to 11 mm.

- Based on the rutting data from all pavements, rutting occurred in all asphalt pavement lifts. No particular lift or group of lifts consistently rutted the most. The rut depths used in this analysis consisted of both the rut depth due to densification and viscous flow.

- By splitting the total rut depth into the percent rut depth in the asphalt pavement layer and the percent rut depth in the underlying layers, it was found that the percentage of rutting in the asphalt pavement layer decreased with increasing total rut depth. The percentage of rutting in the underlying layer increased as the asphalt pavement layer became thinner due to lateral shearing and flow.

- Pavement surface cracks due to both pavement bending and the sides of the super single tire tearing the pavement were observed during a few pavement tests when the total rut depth was greater than 20 mm. All cracks initiated at the surface of the pavement. Neither type of crack would be expected to occur on pavements where the wheels can wander.

- The ALF wheel passes at a 20-mm rut depth were generally used to represent long-term pavement performance in this study. However, the pavement rut depths at 2,730 wheel passes, and the rates of rutting at 2,000 wheel passes, were also used to represent performance. The rate of rutting is the change in rut depth with a change in wheel passes.[17] When using the latter two methods, the pavements were compared at wheel passes that were low relative to the lives of longest lasting pavements. When using these types of analyses, temperature may have no apparent effect on the performances of the longest lasting pavements.

c. Evaluation of the Slopes and Intercepts From the Rut Depth vs. ALF Wheel Pass Relationships

The slope and intercept obtained from a regression analysis are often used to describe the relationship between pavement rut depth and wheel passes, or ESAL's. In this study, the Gauss-Newton statistical method, not performed in log-log space, and a log-log transformation were used to calculate slopes and intercepts for the various ALF pavement tests. Slopes and intercepts were determined for both the rut depth in the asphalt pavement layer and total rut depth. The sets of slopes and intercepts were each regressed against the number of ALF wheel passes that provided a 20-mm rut depth to determine whether the wheel passes were primarily a function of the slope or the intercept. The analyses provided the following conclusions:

- The slopes provided r^2's ranging from 0.40 to 0.86. The intercepts provided r^2's close to zero. The slopes correlated to ALF wheel passes more than the intercepts.

- The Gauss-Newton and log-log methods can provide a different slope and intercept for the data from a given pavement, but the sets of slopes and intercepts provided by these two methods for the ALF pavement tests led to the same conclusions, described in the next two bullet points.

- Even though the slopes correlated to ALF wheel passes more than the intercepts, the data showed that the slope alone cannot be used as a rutting performance indicator. Long-term rutting performance must be based on accumulated rut depth. The rate of rutting can also be used because it accounts for both the slope and the intercept.[17] However, the rates of rutting for a set of pavements must be determined at a constant number of wheel passes and prior to the point where the rut depths from most of the pavements become linear with wheel passes.

- The slope and intercept are not fundamental material properties; they are regression coefficients. An increase in test temperature provided both increases and decreases in the slope depending upon the mixture and temperature range. If the slope increased with increasing temperature, the intercept tended to decrease, and vice versa. However, the trend was not consistent. For the pavement tests at 58 °C, the slope increased as the ALF wheel passes at a failure level of 20 mm decreased, which meant that the slope increased with an increase in rutting susceptibility. The intercepts provided no trend at 58 °C.

6. Final Discussion and Recommendations

- Reasons for the discrepancies between the $G^*/\sin\delta$'s of the modified binders and ALF pavement performance need to be determined.

- The relationship between $G^*/\sin\delta$ after RTFO aging and ALF pavement rutting performance for the unmodified binders suggested that the Superpave $G^*/\sin\delta$ criterion of 2.20 kPa is low. The data indicated that a criterion around 4.40 kPa may be needed. However, the 1997 Superpave binder specification recommended an increase of one high-temperature PG for the ALF traffic level, which was above 10 million ESAL's based on a 20-year design life.[3] An increase of one high-temperature PG is equivalent to doubling the criterion from 2.20 to 4.40 kPa. Thus, the data supported the current criterion of 2.20 kPa if the PG can be adjusted based on both traffic loading (speed) and ESAL's. A potential flaw in this analysis is that it is unknown how the number of ALF wheel passes applied to a pavement at a constant, high temperature relates to Superpave ESAL's. Furthermore, if the five asphalt binders were to be used in other mixtures, different pavement performances would be obtained for the same PG.

CHAPTER 4: VALIDATION OF LABORATORY MIXTURE TESTS FOR RUTTING SUSCEPTIBILITY

1. Mixture Tests Evaluated

ALF pavement performance was used to validate a variety of asphalt mixture tests used to predict rutting. Pavement performance was defined as the number of wheel passes required to obtain a rut depth of 20 mm in the asphalt pavement layer at 58 °C. Rut depth was defined as the downward distance from the original surface elevation of the pavement. This rut depth does not include any uplift outside of the wheelpath due to shearing. This rut depth was chosen because the laboratory wheel-tracking devices only measure the downward rut depth. The following tests were evaluated using practices and temperatures that were recommended at the time of testing:

- Marshall Stability and Flow at 60 °C.

- U.S. Corps of Engineers Gyratory Testing Machine (GTM) at 60 °C.
  - Maximum Static Shear Strength (Sg).
  - Gyratory Stability Index (GSI).
  - Gyratory Elasto-Plastic Index (GEPI).
  - Refusal Air-Void Level.

- French Pavement Rutting Tester (French PRT) at 60 °C.
  - Percent Rut Depth at 30,000 Cycles (60,000 Wheel Passes).
  - Slope of Log Rut Depth vs. Log Cycles Relationship.

- Georgia Loaded-Wheel Tester (Georgia LWT) at 40 °C.
  - Rut Depth at 8,000 Cycles (16,000 Wheel Passes).

- Hamburg Wheel-Tracking Device (Hamburg WTD) at 50 °C.
  - Rut Depth at 10,000 and 20,000 Wheel Passes.
  - Creep Slope.

- Asphalt-Aggregate Mixture Analysis System (AAMAS) at 40 °C.
  - Unconfined Compressive Strength Test.
  - Unconfined Compressive Repeated Load Test.
  - Unconfined Compressive Creep Test.

- Repeated Load Compression Test at 40 °C.
  - Dynamic Modulus at 200 Cycles.
  - Cumulative Permanent Strain at 10,000 Cycles.
  - Slope from the Linear Portion of the Log Permanent Strain vs. Log Time Relationship.

- Superpave Shear Tester (SST) at 40 and 58 °C.
  - Simple Shear at Constant Height.
  - Frequency Sweep at Constant Height.
  - Repeated Shear at Constant Height.

The testing strategy was to use recommended test procedures and laboratory-prepared mixtures whose compositions met the overall average compositions of the mixtures in the pavements. Based on the results of these tests, it would be decided whether the test procedures, the compositions of the mixtures, or the degree of aging should be changed to better match the conditions for each individual ALF pavement test.

Binder contents of 4.85 and 4.00 percent by mass were used in the surface and base mixtures, respectively. The target air-void level was 8 ±1 percent, except for the Marshall tests. Specimens were tested 3 to 5 days after fabrication so that the amount of aging was consistent from test to test.

The mixtures were ranked according to their performance in each test based on the average data and Fisher's LSD, which is performed in conjunction with an analysis of variance at a 95-percent confidence level. Mixtures assigned the letter "A" were the least susceptible to rutting. When the variances could not be pooled because of heterogeneity, the statistical ranking was based on comparing averages with confidence limits provided by two standard deviations ($\mu \pm 2\sigma_{(n-1)}$) instead of Fisher's LSD. Linear and nonlinear regressions were also performed but were not used because the number of data points was generally insufficient for making valid conclusions.

2. Short-term Oven Aging Study

At the time of construction in 1993, Superpave recommended that loose mixtures in the mixture design process be oven aged for 4 h at 135 °C prior to compaction.[19] This procedure is called short-term oven aging (STOA). It reportedly produces an amount of aging that will occur somewhere between 6 and 24 months after construction. To better simulate the degree of aging that occurred during plant production of the mixtures used in this study, an STOA study was performed.

The STOA study consisted of aging laboratory mixtures in a forced draft oven at 135 °C for 0, 1, 2, and 4 h, recovering the binders, recovering binders from ALF pavement cores, performing Superpave tests on the recovered binders, and comparing the test results to determine the appropriate aging period. Three replicate samples were tested for each aging period. The mixtures chosen for this study were the surface mixture with AC-5 (PG 59), the base mixture with AC-5 (PG 59), and the surface mixture with AC-20 (PG 70). Cores were taken from four ALF pavements constructed with these mixtures, including two pavements with the AC-20 (PG 70) surface mixture as a check on pavement-to-pavement variability.

The recovered binders were tested using the DSR at 10, 30, 50, and 70 °C, Bending Beam Rheometer at -24 °C, and the Brookfield Viscometer at 135 °C. These tests were performed to fully examine the capability of simulating hot-mix plant aging using a forced draft oven, even though the pavements were only to be tested in the range of 10 to 76 °C. All three tests should provide the same aging period if oven aging duplicates plant aging and provides the same binder chemistry. The three tests were also chosen because they should provide the effects of aging at low, intermediate, and high temperatures.

The recovered binder properties from the aged laboratory mixtures were plotted with respect to the aging period. A regression was performed to generate a second order polynomial equation. The aging periods needed to duplicate the properties of the binders in the ALF pavements were computed for each binder and test. The differences among the data for the two AC-20 (PG 70) pavements were not significant; thus, averaged data were evaluated.

The DSR data in table 44 indicated that the STOA period needed to simulate the degree of aging that occurred during hot-mix plant production and laydown should be from 0.3 to 2.5 h. The average period was 1.3 h. An evaluation of the creep stiffnesses from the Bending Beam Rheometer provided no definitive STOA period. The slopes from the Bending Beam Rheometer led to STOA periods of 3.0 to 4.0 h, but the changes in these slopes with aging period were low. The Brookfield Viscosities indicated that a STOA period of 2.3 h was needed for the AC-20 (PG 70) surface mixture. However, the AC-5 (PG 59) binders recovered from both laboratory mixtures were stiffer than the AC-5 (PG 59) binders recovered from the cores even at an STOA of 0 h.

Overall, the required oven aging period depended on the mixture type and the binder test performed. A previous National Cooperative Highway Research Program (NCHRP) study found that the absolute viscosity at 60 °C and penetration at 25 °C can also give different short-term oven-aging periods for a given mixture.[20] This indicates that oven aging may not accurately simulate hot-mix plant aging. An aging period of 2 h was chosen as a compromise. Therefore, STOA consisted of oven aging the loose mixtures at 135 °C for 2 h before compaction.

3. Marshall Stability and Flow

Table 8 in chapter 1 shows that all seven mixtures had Marshall stabilities greater than 11 000 N compared with the 8006-N minimum stability specified for heavy traffic pavements. The stabilities and flows did not discriminate the mixtures. The differences in these properties from mixture to mixture were relatively small compared with the variability of the replicate measurements.[11] Thus, the Marshall properties were eliminated from further consideration.

4. GTM

The shear susceptibilities of the mixtures were measured using the static shear strength (Sg), gyratory stability index (GSI), gyratory elasto-plastic index (GEPI), and refusal air-void levels provided by the GTM, Model 8A-6B-4C. The GTM is a combination compaction and plane strain shear testing machine that applies stresses simulating pavement conditions.

Table 44. Short-term oven aging study.

Binder/ Mixture Type	Laboratory Aging Period, h 0	1	2	4	Pavement Core Property	Required Hours of Lab Aging
Average G* from the Dynamic Shear Rheometer at 10.0 rad/s, Pa						
AC-5 Surface						
at 10 °C	2 974 000	2 682 000	4 192 000	4 422 000	3 181 000	1.3
at 30 °C	118 500	110 300	181 500	221 800	125 800	1.2
at 50 °C	7 062	6 798	10 930	14 760	7 319	1.1
at 70 °C	630	627	916	1 301	626	1.0
AC-5 Base						
at 10 °C	2 990 000	4 295 000	5 546 000	5 516 000	3 453 000	0.3
at 30 °C	97 360	152 900	211 900	246 100	144 600	0.7
at 50 °C	5 234	8 462	12 120	15 150	8 534	0.9
at 70 °C	464	726	1 038	1 284	709	0.8
AC-20 Surface						
at 10 °C	8 359 000	8 922 000	10 730 000	11 580 000	9 827 000	1.4
at 30 °C	302 800	372 900	423 600	585 300	455 800	2.4
at 50 °C	15 690	20 810	22 750	35 240	26 210	2.5
at 70 °C	1 160	1 549	1 650	2 526	1 868	2.4
Average Creep Stiffness, S, at 60 s and -24 °C Determined by the Bending Beam Rheometer, MPa						
AC-5 Surface	92	98	124	110	139	ND
AC-5 Base	139	183	218	206	165	0.6
AC-20 Surface	284	288	312	353	333	2.5
Average Slope, m, of Log Creep Stiffness vs. Log Time at 60 s and -24 °C Determined by the Bending Beam Rheometer						
AC-5 Surface	0.40	0.40	0.38	0.36	0.36	4.0
AC-5 Base	0.38	0.37	0.36	0.34	0.35	3.0
AC-20 Surface	0.33	0.31	0.31	0.29	0.30	3.0
Average Absolute Viscosity at 135 °C Determined by the Brookfield Viscometer, Pa·s						
AC-5 Surface	0.36	0.33	0.41	0.44	0.29	<0
AC-5 Base	0.34	0.49	0.65	0.64	0.31	<0
AC-20 Surface	0.45	0.51	0.52	0.63	0.55	2.3

ND = No data; a laboratory aging period could not be predicted from the data.
Note: AC-5 = PG 59 and AC-20 = PG 70

The GTM was operated in accordance with the AAMAS with one modification.[20] NCHRP AAMAS specified a 0.035-radian gyratory angle. An angle of 0.012 radian was used instead of 0.035 radian because FHWA studies on previous pavements tested by the ALF indicated that this angle provided closer agreements between the GTM refusal densities and the ultimate pavement densities. A 0.035-radian angle provided densities that were too high. The diameter and height of each specimen were 152.4 mm. A vertical pressure of 0.83 MPa and the GTM oil-filled roller were used. Tests were performed in triplicate. The NCHRP AAMAS procedure is based on ASTM Method D 3387.[6]

The GSI is the ratio of the maximum angle that occurs at the end of the test to the minimum intermediate angle. It is a measure of shear susceptibility at the refusal density. The minimum intermediate angle is the smallest angle that occurs after the compaction process has started. The GSI at 300 revolutions is close to 1.0 for a stable mixture and is significantly above 1.1 for an unstable mixture.[21] When designing a mixture, the manufacturer states that the optimum binder content should be less than the binder content where the GSI begins to exceed 1.0. The GSI and the Sg are the principal GTM parameters used to evaluate rutting susceptibility.

The GEPI is the ratio of the minimum intermediate angle to the initial machine angle set by the operator. A GEPI of 1.0 indicates high internal friction. A GEPI significantly above 1.0 indicates lower internal friction, generally resulting from the use of rounded aggregates or from moisture damage. The manufacturer suggests using an acceptable range of 1.0 to 1.5. Appendix A provides additional information on the GTM including a photograph of it.

The mixtures were first compacted to an 8 ±1-percent air-void level at 135 °C. They were cooled to 60 °C in an oven over a 3-h period and then compacted and tested until their refusal densities were reached. A trace of the gyratory angle vs. revolutions was obtained to determine the maximum and minimum intermediate angles.

The GTM data are given in table 45. There was very little variation in each parameter from mixture to mixture and no relationship to ALF pavement performance. The tests on the Novophalt surface mixture and AC-20 (PG 70) base mixture were repeated because they had GEPI's significantly less than 1.00, which is the minimum value that can theoretically be obtained. GEPI's below 1.00 were again obtained, and the refusal air voids were not the same as those provided by the original tests. The low GEPI's indicated a machine compliance problem. The GTM was eliminated from further consideration.

5. French PRT

a. Description of the Equipment

The French PRT tests a slab for permanent deformation at 60 °C using a smooth, pneumatic, rubber tire having a diameter of 415 mm and a width of 109 mm. The slabs were compacted by the French Plate Compactor, which is a rolling wheel compactor having the same type of tire as the French PRT. The slabs had a length of 500 mm, a width of 180 mm, and a thickness of 100 mm. The AC-5, AC-10, AC-20, Novophalt, and Styrelf surface mixtures had average air-void levels of 8.4, 7.1, 7.3, 8.1, and 8.4 percent, respectively.

The French PRT tests two slabs simultaneously using two reciprocating tires. The tires are inflated to 600 ±30 kPa. Each slab is confined in a steel mold that rests on a steel base plate. A hydraulic jack underneath the steel base plate pushes upward to provide a load of 5000 ±50 N. The rut depth in each slab is measured at 300, 1000, 3000, 10,000, and 30,000 cycles by averaging measurements taken at 15 standard positions. This rut depth is based on the initial surface elevation of a slab. It does not include any upward heaving outside the wheelpath. One cycle is defined as two passes of the wheel (back and forth). A mixture is acceptable in France if the average percent rut depth at 30,000 cycles is less than or equal to 10 percent of the slab thickness.

Slopes taken from log rut depth vs. log cycle plots can also be compared. Rut-susceptible mixtures generally have higher slopes, but there is no French specification on the slope. When comparing slopes from the French PRT with slopes provided by other tests, it must be remembered that the slopes from the French PRT may be based on cycles and not on passes.

French researchers state that the tester is not valid for mixtures with nominal maximum aggregate sizes greater than 20 mm. The slab width of 180 mm is relatively small compared with the tire width of 110 mm. A space of only 35 mm exists on each side of the slab between the tire and the steel mold. Therefore, mixtures with aggregates greater than 20 mm may be inhibited from shearing laterally and upward. The AC-5 and AC-20 (PG 59 and 70) base mixtures were tested in this study to confirm this principle. Both base mixtures had an average air-void level of 7.6 percent and a nominal maximum aggregate size of 37.5 mm. Appendix A provides additional information on the French PRT including a photograph of it.

b. Results From the French PRT

The French PRT data are given in table 46. The AC-5 and AC-10 (PG 59 and 65) surface mixtures and AC-5 and AC-20 (PG 59 and 70) base mixtures exceeded the 10-mm maximum allowable percent rut depth at 30,000 cycles; the other three surface mixtures met the French criteria. ALF pavement performance in terms of wheel passes and the percent rut depths from the French PRT are shown in figures 31 through 34. As the ALF wheel passes in figures 31 and 32 increase, the percent rut depths from the French PRT in figures 33 and 34 should decrease.

Tables 47 and 48 provide rankings based on the French PRT and ALF pavement performance. The rankings provided by the rut depths and slopes from the French PRT were identical; therefore, only one ranking is shown in each table. The ranking in table 47 shows that the French PRT correctly ranked the five

Table 45. Rutting performance based on the Gyratory Testing Machine (GTM) at 60 °C.

	Surface Mixture					Base Mixture	
Pre-Superpave:	AC-5	AC-10	AC-20	Novophalt	Styrelf	AC-5	AC-20
Superpave PG:	59	65	70	77	88	59	70
Sg, kPa	370	430	370	370	370	400	410
GSI	1.10	1.15	1.15	0.95	1.10	1.10	0.95
GEPI	1.00	1.05	0.90	0.80	0.95	0.95	0.65
Air Voids, %	2.1	2.0	3.3	5.9	6.0	4.2	5.5
Repeated GTM Tests							
Sg, kPa				430			380
GSI				1.00			1.10
GEPI				0.70			0.85
Air Voids, %				7.0			2.6

Table 46. Rutting performance based on the French PRT, Georgia LWT, and Hamburg WTD.

	Surface Mixture					Base Mixture	
Pre-Superpave: Superpave PG:	AC-5 59	AC-10 65	AC-20 70	Novophalt 77	Styrelf 88	AC-5 59	AC-20 70
French PRT at 60 °C and 0.875 rad/s							
Cycles	Percent Rut Depth						
300	3.0	3.0	2.6	1.4	1.8	2.8	2.4
1,000	3.8	4.0	3.2	1.7	2.2	4.5	3.1
3,000	4.9	5.3	4.1	2.2	3.0	7.4	4.0
10,000	8.2	9.2	4.9	2.4	3.2	ND	6.2
30,000 (spec)	15.5	13.8	6.4	2.6	3.7	ND	10.9
Slope, Percent RD vs. Cycles	0.35	0.34	0.19	0.14	0.16	0.42	0.32
G*/sinδ, Pa	212	442	871	2 103	6 444	212	871
Georgia LWT at 40 °C, 0.125 rad/s, and 8,000 cycles							
Rut Depth, mm	7.4	5.4	3.7	1.4	1.9	6.3	3.5
G*/sinδ, Pa	899	2 215	5 060	10 350	21 120	899	5 060
Hamburg WTD at 50 °C and 0.125 rad/s							
RD at 10,000, mm	>30	22.8	6.8	1.4	2.6	24.6	4.9
RD at 20,000, mm	>30	>30	8.5	1.9	2.8	>30	8.6
Creep Slope	300	630	6 220	24 600	17 900	470	3 780
Visual Stripping, %	0	0	0	0	0	0	0
G*/sinδ, Pa	130	348	635	1 744	5 243	130	635

RD at 10,000 = Rut Depth at 10,000 Wheel Passes.
RD at 20,000 = Rut Depth at 20,000 Wheel Passes.
Creep Slope = Wheel Passes per 1-mm Rut Depth.

ND = No data because the mixture failed rapidly.

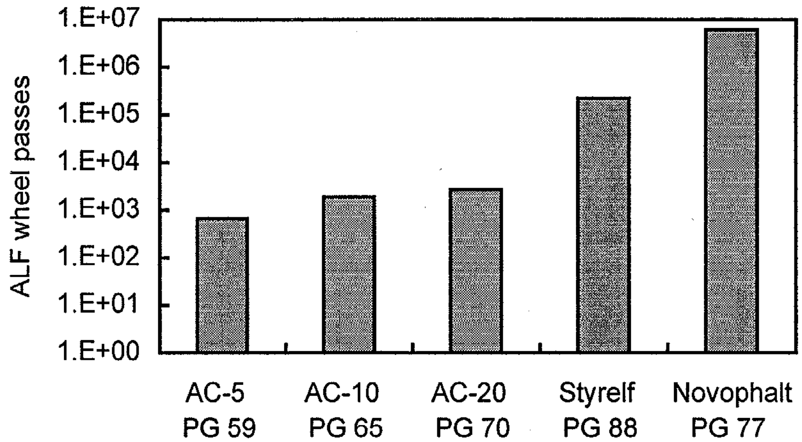

Figure 31. ALF wheel passes at a 20-mm rut depth vs. surface mixture.

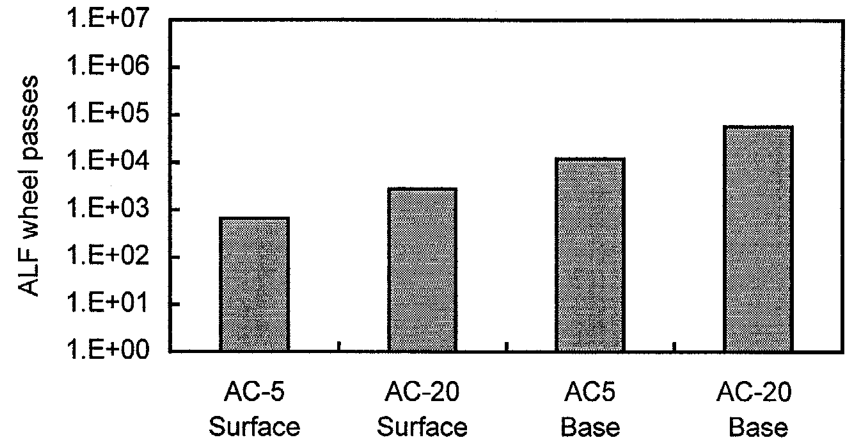

Figure 32. ALF wheel passes at a 20-mm rut depth vs. mixture type.

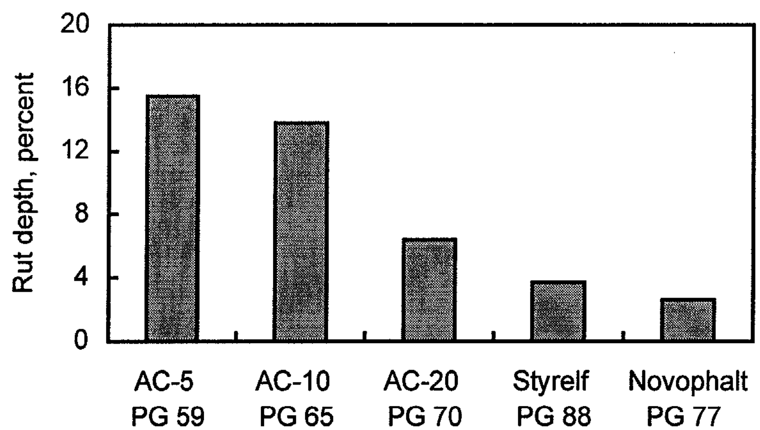

Figure 33. Percent rut depth from the French PRT vs. surface mixture.

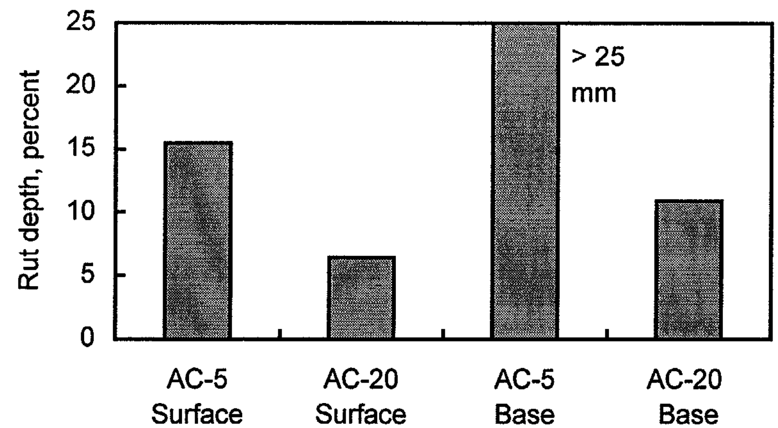

Figure 34. Percent rut depth from the French PRT vs. mixture type.

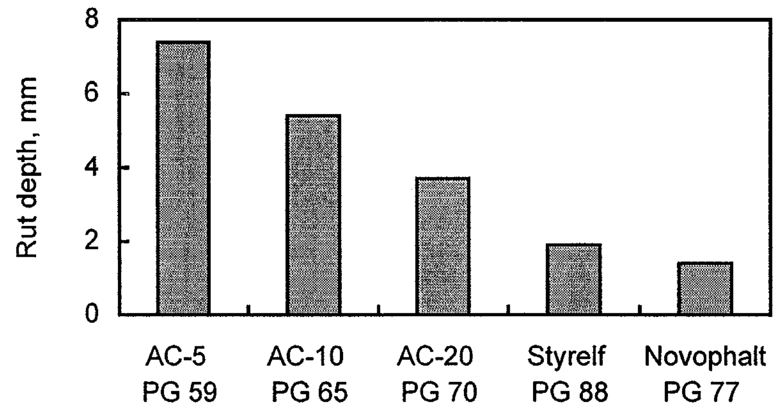

Figure 35. Rut depth from the
Georgia LWT vs. surface mixture.

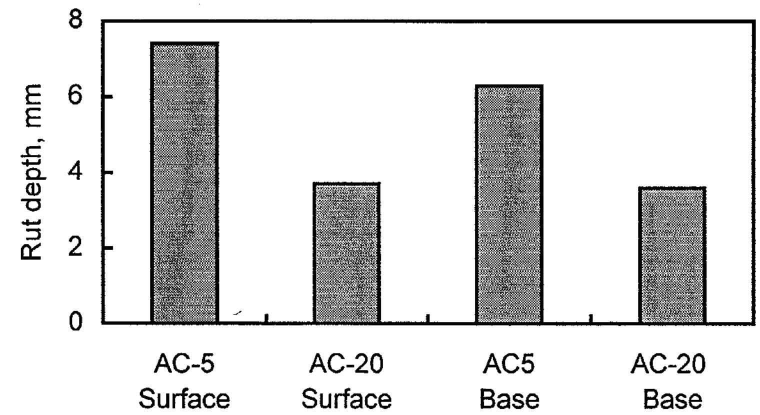

Figure 36. Rut depth from the
Georgia LWT vs. mixture type.

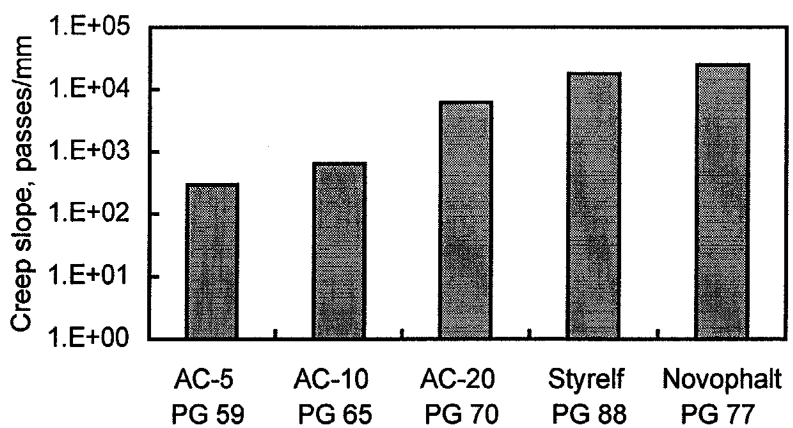

Figure 37. Creep slope from the
Hamburg WTD vs. surface mixture.

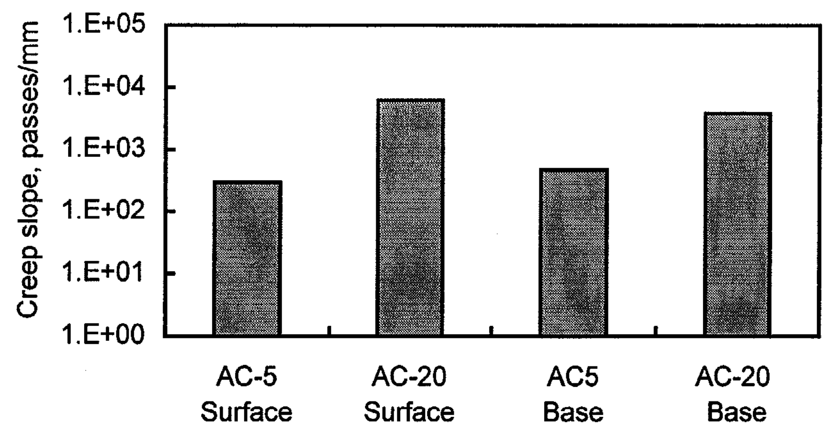

Figure 38. Creep slope from the
Hamburg WTD vs. mixture type.

Table 47. Statistical rankings for the five surface mixtures provided by the ALF and the three wheel-tracking devices.[1]

ALF at 58 °C	French PRT at 60 °C	Georgia LWT at 40 °C	Hamburg WTD at 50 °C
(A) Novophalt	(A) Novophalt	(A) Novophalt	(-) Novophalt[2]
(B) Styrelf	(B) Styrelf	(B) Styrelf	(A) Styrelf
(C) AC-20	(C) AC-20	(BC) AC-20	(B) AC-20
(C) AC-10	(D) AC-10	(C) AC-10	(C) AC-10
(D) AC-5	(D) AC-5	(C) AC-5	(D) AC-5

[1]The letters are the statistical ranking, with "A" denoting the mixture with the lowest susceptibility to rutting.
[2]Not included in the statistical ranking because of high variability.

Table 48. Statistical rankings for the surface and base mixtures provided by the ALF and the three wheel-tracking devices.

ALF at 58 °C		French PRT at 60 °C	Georgia LWT at 40 °C	Hamburg WTD at 50 °C
AC-20 Base	A	AB	A	B
AC-5 Base	B	C	AB	C
AC-20 Surface	C	A	A	A
AC-5 Surface	D	B	B	C

Table 49. Slopes and intercepts provided by the ALF and the French PRT.

Ranking Based on Pavement Rut Depth at 58 °C	Slope		Intercept	
	ALF, 58 °C	French PRT, 60 °C	ALF, 58 °C	French PRT, 60 °C
Novophalt	0.23	0.13	0.6	0.7
Styrelf	0.21	0.15	1.6	0.8
AC-20 Base	0.18	0.39	2.9	0.2
AC-5 Base	0.27	0.43	1.6	0.2
AC-20	0.28	0.20	2.2	0.8
AC-10	0.41	0.37	0.9	0.3
AC-5	0.43	0.45	1.3	0.2

Table 50. Rutting Susceptibility Based Upon the French PRT at 60 °C.

	Surface Mixture					Base Mixture	
Pre-Superpave: Superpave PG:	AC-5 59	AC-10 65	AC-20 70	Novophalt 77	Styrelf 88	AC-5 59	AC-20 70
Cycles	Percent Rut Depth Using 100-mm Slabs, mm						
300	3.0	3.0	2.6	1.4	1.8	2.8	2.4
1,000	3.8	4.0	3.2	1.7	2.2	4.5	3.1
3,000	4.9	5.3	4.1	2.2	3.0	7.4	4.0
10,000	8.2	9.2	4.9	2.4	3.2	ND	6.2
30,000 (spec)	15.5	13.8	6.4	2.6	3.7	ND	10.9
Cycles	Percent Rut Depth Using 50-mm Slabs, mm						
300	3.6	3.4	3.3	1.7	1.8	NT	NT
1,000	5.4	4.5	4.1	2.1	2.3		
3,000 (spec)	8.3	6.0	5.1	2.5	2.6		
10,000	ND	10.1	7.4	3.5	3.2		
30,000	ND	ND	11.2	4.4	4.0		
Ratio of the percent rut depth at 3,000 cycles using 50-mm slabs to the percent rut depth at 30,000 cycles using 100-mm slabs							
	0.5	0.4	0.8	1.0	0.7		
Cycles	Ratios of Rut Depths (50-mm data divided by 100-mm data)						
300	1.2	1.1	1.3	1.2	1.0		
1,000	1.4	1.1	1.3	1.3	1.0		
3,000	1.7	1.1	1.3	1.2	0.9		
10,000	ND	1.1	1.5	1.5	1.0		
30,000	ND	ND	1.8	1.7	1.1		

NT = Not tested because specimens could not be fabricated at this thickness.
ND = No data because the mixture failed rapidly.

surface mixtures based on the average data. The statistical rankings, shown by the letters A through D, were not identical, but they were reasonably close. (The variance for the AC-5 mixture was greater than the variances for the other mixtures. Therefore, the statistical ranking for the surface mixtures tested by the French PRT was based on $\mu \pm 2\sigma_{(n-1)}$.) The ranking provided by the French PRT in table 48 for the surface vs. base mixture study did not agree with ALF pavement performance. (Different presentation styles are used in tables 47 and 48; the style that best facilitated a visual comparison of the rankings was used.)

c. Comparison of the Rut Depths From the French PRT and ALF

The rut depths from the French PRT were significantly lower than those produced by the ALF at 58 °C at an equal number of wheel passes. (This was also found to be true for the Hamburg WTD and Georgia LWT.) For example, less than 1,000 ALF wheel passes at 58 °C were needed to provide rut depths in the five pavements with the surface mixtures equaling those provided by the French PRT at the end of the test. Table 49 shows that the slopes and intercepts from the rut depth curves provided by the French PRT and ALF were not the same. These data, which are regression coefficients, were obtained using the Gauss-Newton statistical method. The main discrepancies were provided by the two base mixtures. The differences in the slopes and intercepts indicate that trying to develop equations that predict pavement rut depths from the French PRT data is not possible. The slopes and intercepts provided by all of the ALF pavement tests are discussed in detail in chapter 3.

d. Comparison of French PRT Data Using 50- and 100-mm-Thick Slabs

A slab thickness of 100 mm is specified in the French method of analysis when the total pavement thickness for the mixture to be placed will be greater than 50 mm. (The mixture can be placed in more than one lift.) A 50-mm-thick slab is specified for mixtures that will be placed at a thickness equal to, or less, than 50 mm. The pavements in this study had a thickness of 200 mm; therefore, a slab thickness of 100 mm was used. However, it was decided to test the five surface mixtures using a thickness of 50 mm to determine the effect of slab thickness on rut depth. The AC-5, AC-10, AC-20, Novophalt, and Styrelf surface mixtures at this thickness had average air-void levels of 7.4, 7.2, 7.9, 8.3, and 8.1 percent, respectively. The AC-5 and AC-20 base mixtures were not tested due to its 37.5-mm nominal maximum aggregate size.

Rut depths are measured at 30, 100, 300, 1,000, and 3,000 cycles when testing 50-mm-thick slabs. The test normally ends at 3,000 cycles, whereas 30,000 cycles are applied when testing 100-mm-thick slabs. When testing 50-m-thick slabs, a mixture is acceptable according to the French procedure if the average rut depth at 1,000 is less than or equal to 5 mm and the average rut depth at 3,000 cycles is less than or equal to 10 mm. In this study, rut depths at 10,000 and 30,000 cycles were also measured when testing 50-mm-thick slabs in order to be consistent with the tests performed on 100-mm-thick slabs.

Table 50 shows the data at both thicknesses and the ratio of the percent rut depth at 3,000 cycles using 50-mm slabs to the percent rut depth at 30,000 cycles using 100-mm slabs. For example, the ratio for the AC-5 (PG 59) surface mixture was 0.5 (8.3 mm divided by 15.5 mm). The ratios were variable, indicating that the two methodologies could provide different conclusions concerning the rutting potential of a mixture. A ratio of 1.0 indicates that the two tests provided the same rut depth at the specified maximum numbers of cycles. Ratios less than 1.0 indicate that the test using thick slabs is a more severe test. Four out of five surface mixtures had ratios less than 1.0. This result is consistent with the French philosophy of allowing little to no rutting to occur in thick, lower pavement layers. The pass/fail criteria also reflect this philosophy. Using 100-mm-thick slabs, both the AC-5 (PG 59) and AC-10 (PG 65) surface mixtures exceeded the 10-mm maximum allowable rut depth at 30,000 cycles. Using 50-mm-thick slabs, only the AC-5 (PG 59) surface mixture exceeded the 5-mm maximum allowable rut depth at 1,000 cycles, and all five mixtures met the 10-mm requirement at 3,000 cycles.

Table 50 also gives the ratios of the rut depths at each number of cycles. A ratio of 1.0 indicates that the two tests provided the same rut depth. A ratio greater than 1.0 indicates that there was more rutting using 50-mm slabs compared with 100-mm slabs. The data show that the rut depths tended to be greater using 50-mm slabs at an equal number of wheel passes, even though the test was more lenient in terms of passing or failing a mixture.

6. Georgia LWT

a. Description of the Equipment

The Georgia LWT tests a beam for permanent deformation at 40 °C. The beams were sawed from slabs compacted using a vibratory tamper and a steel wheel roller. The beams had a length of 320 mm, a width of 120 mm, and a thickness of 80 mm. The AC-5, AC-10, AC-20, Novophalt, and Styrelf surface mixtures had average air-void levels of 7.0, 7.5, 7.1, 7.2, and 7.3 percent, respectively. The AC-5 and AC-20 (PG 59 and 70) base mixtures had average air-void levels of 7.0 and 7.7 percent. Air-void levels closer to the 8-percent target level were not obtainable. Attempts to increase the air-void levels led to increased porosity around the edges and sides of the slabs without a significant increase in air voids in the middle of the slabs.

Each beam is confined by steel plates during testing, except for the top 12.7 mm. A stiff rubber hose pressurized at 0.69 MPa with air is positioned across the top of the beam, and a loaded steel wheel runs back and forth on top of this hose for 8,000 cycles to create a rut. One cycle is defined as two passes of the wheel. The diameter of the hose is 29 mm, and the average load is 700 N.

Deformations are measured at three locations: at the center of the beam and 51 mm left and right of center in the longitudinal direction. The rut depth does not include any upward heaving outside the wheelpath. If the average rut depth exceeds 7.6 mm, the mixture is considered susceptible to rutting by the Georgia Department of Transportation.[22] Appendix A provides additional information on the Georgia LWT including a photograph of it. More advanced models are now being produced.

b. Results From the Georgia LWT

The data from the Georgia LWT are given in table 46. All mixtures met the Georgia Department of Transportation pass/fail specification. As the ALF wheel passes in figures 31 and 32 increase, the rut depths from the Georgia LWT in figures 35 and 36 should decrease.

Tables 47 and 48 provide rankings based on the Georgia LWT and ALF pavement performance. The ranking in table 47 shows that the Georgia LWT ranked the five surface mixtures correctly based on the average data, but the statistical ranking was not the same as ALF. (The variances for the rut depths from the Georgia LWT were not equal; therefore, the statistical ranking for the surface mixtures tested by the Georgia LWT was based on $\mu \pm 2\sigma_{(n-1)}$.) The ranking provided by the Georgia LWT in table 48 for the surface vs. base mixture study did not agree with ALF pavement performance.

7. Hamburg WTD

a. Description of the Equipment

The Hamburg WTD measures the combined effects of rutting and moisture damage by rolling a steel wheel across the surface of a slab that is submerged in water at 50 °C. The slabs were compacted by the same method used to compact slabs for the Georgia LWT. The slabs had a length of 320 mm, a width of 260 mm, and a thickness of 80 mm. The AC-5, AC-10, AC-20, Novophalt, and Styrelf surface mixtures had average air-void levels of 7.3, 6.9, 7.1, 7.4, and 7.4 percent, respectively. The AC-5 and AC-20 (PG 59 and 70) base mixtures had average air-void levels of 6.3 and 7.0 percent.

The device tests two slabs simultaneously using two reciprocating solid steel wheels. The wheels have a diameter of 203.5 mm and a width of 47.0 mm. The applied load is 685 N. The standard, maximum number of wheel passes is 20,000. The measurements are customarily reported vs. wheel passes, unlike the preceding two wheel-tracking devices that use cycles.

The rut depth in each slab is measured by a linear variable differential transformer. Like the French PRT and the Georgia LWT, the rut depth does not include any upward heaving outside the wheelpath. A maximum allowable rut depth of 4 mm at 20,000 wheel passes is specified by the city of Hamburg, Germany. The Colorado Department of Transportation recommends a maximum allowable rut depth of 10 mm at 20,000 wheel passes.[23]

The creep slope, stripping slope, and stripping inflection point can also be evaluated.[24] However, no moisture damage was observed in the slabs, and there was no stripping slope or stripping inflection point. The creep slope is the number of wheel passes required to create a 1-mm rut depth due to viscous flow. It is actually an inverse slope because the slope for this type of relationship is usually defined in terms of rut depth per wheel pass or ESAL. Higher creep slopes indicate less rutting. Creep slopes have been used instead of rut depths to evaluate viscous flow because the number of wheel passes at which moisture damage starts to affect performance varies widely from mixture to mixture. Furthermore, the rut depths often exceed the maximum measurable rut depth of 25 to 30 mm, even if there is no moisture damage. Appendix A provides additional information on the Hamburg WTD including a photograph of it and a drawing that shows the slopes.

b. Results From the Hamburg WTD

The Hamburg WTD data are given in table 46. The AC-5, AC-10, and AC-20 (PG 59, 65, and 70) surface mixtures and the AC-5 and AC-20 (PG 59 and 70) base mixtures exceeded the maximum allowable rut depth of 4 mm at 20,000 wheel passes used in Hamburg, Germany. The AC-5 and AC-10 (PG 59 and 65) surface mixtures and the AC-5 (PG 59) base mixture exceeded the maximum allowable rut depth of 10 mm at 20,000 wheel passes used by the Colorado Department of Transportation.

The rut depths at 20,000 passes could not be evaluated because the rut depths for the AC-5 and AC-10 (PG 59 and 65) surface mixtures and the AC-5 (PG 59) base mixture exceeded the 30-mm limit of the device. Therefore, it was decided to evaluate the rut depths at 10,000 wheel passes. Only the AC-5 (PG 59) surface mixture exceeded the 30-mm limit at 10,000 passes. The AC-20 (PG 70) base mixture and the Novophalt, Styrelf, and AC-20 (PG 70) surface mixtures fell into one statistical group. This indicated that 10,000 wheel passes were inadequate for evaluating the mixtures.

It was concluded that the creep slopes should be used for evaluating rutting susceptibility. These slopes are presented in figures 37 and 38. As the ALF wheel passes in figures 31 and 32 increase, the creep slopes from the Hamburg WTD in figures 37 and 38 should increase.

Tables 47 and 48 provide rankings based on the Hamburg WTD and ALF pavement performance. The ranking in table 47 shows that the Hamburg WTD correctly ranked the five surface mixtures based on the average data. The statistical rankings were difficult to compare. The variance for the Novophalt mixture was very large because the creep slope was very high. This mixture did not rut. Therefore, it was not included in the statistical ranking. The ranking provided by the Hamburg WTD in table 48 for the surface vs. base mixture study did not agree with ALF pavement performance.

8. AAMAS

a. Description of the AAMAS Tests

Unconfined compressive tests were conducted at 40 °C in accordance with AAMAS and a modified AAMAS. The AAMAS procedure for evaluating rutting potential was developed by the Texas Transportation Institute under an NCHRP study.[20] They later modified the procedure under a study for the Texas Department of Transportation.[25] Although the tests conducted for each methodology are identical, the analyses of the data are slightly different.

Specimens with a height and diameter of 152.4 mm were compacted using the GTM. The AC-5, AC-10, AC-20, Novophalt, and Styrelf surface mixtures had average air-void levels of 7.8, 7.6, 7.4, 7.8, and 7.8 percent, respectively. The AC-5 and AC-20 (PG 59 and 70) base mixtures both had an average air-void level of 7.8 percent.

All tests were performed using a Materials Testing System™ having a closed-loop, servo-hydraulic actuator and the Teststar™ program. Three replicate specimens were tested per test. The following properties were measured for the AAMAS:

- Unconfined Compressive Strength Test at 40 °C.
  - Strain at failure, ϵ_{qu}.
- Unconfined Compressive Repeated Load Test at 40 °C and 140 kPa.
  - Total resilient strain at 200 cycles, ϵ_{rt}.
- Unconfined Compressive Creep Test at 40 °C and 140 kPa.
  - Creep modulus vs. time.
  - Total creep strain at 3600 s of loading, ϵ_c.
  - Recoverable creep strain at 3600 s after unloading, ϵ_r.
  - Slope and intercept at 1 s from the linear portion of the log total creep strain vs. log time relationship.

The following properties were measured for the modified AAMAS:

- Unconfined Compressive Strength Test at 40 °C.
  - Strain at failure, ϵ_{qu}.
- Unconfined Compressive Repeated Load Test at 40 °C and 140 kPa.
  - Total resilient strain at 200 cycles, ϵ_{rt}.
- Unconfined Compressive Creep Test at 40 °C and 140 kPa.
  - Creep modulus at 3,600 s of loading.
  - Total creep strain at 3,600 s of loading, ϵ_c.
  - Slope from the log total creep strain vs. log time relationship in the region where the data is linear on an arithmetic plot (generally between 1,000 and 3,000 to 3600 s).

The strength test was performed to measure the strain at failure (ϵ_{qu}) using the specified strain rate of 3.81 mm/min/mm of specimen height. This was calculated to be 580.6 mm/min. The strengths were also recorded to determine the loading stress required for the repeated load and creep tests. According to the AAMAS methodologies, the stress for these two tests must be between 5 and 25 percent of the compressive strength.

The repeated load test was performed to measure the total resilient strain (ϵ_{rt}) at 200 cycles. This strain is the sum of the instantaneous and recoverable viscoelastic strains. A haversine waveform load with a total loading time of 0.1 s, followed by a 0.9-s rest period, was used. The load peaked at 0.05 s. Both AAMAS methodologies terminate the test at 200 cycles.

The creep test was performed by applying a fixed load for 3600 s, and measuring the resulting strains. The load was then released and the rebound strain was recorded for an additional 3600 s. Vertical strains were measured at 1, 3, 10, 30, and 100 s, and then at increments of 100 s until the test was completed at 7200 s.

Both ends of the specimens to be used in the repeated load and creep tests were covered with a 0.25-mm-thick sheet of Teflon™ to reduce platen restraint. AAMAS suggested the use of either a thin Teflon™ layer, silicon grease, or graphite, as a friction-reducing material, but only Teflon™ tape was used in the AAMAS study.[20] The specimens were then preconditioned at 40 °C using a haversine waveform load with a total loading time of 0.1 s, followed by a 0.9-s rest period. Twenty-five cycles were applied using a peak stress of 70 kPa. For the actual repeated load and creep tests, a loading stress of 140 kPa was used. This stress was 22.4, 20.3, 13.7, 12.9, and 9.3 percent of the compressive strengths of the AC-5, AC-10, AC-20, Novophalt, and Styrelf surface mixtures, respectively. It was 13.7 and 11.9 percent of the compressive strengths of the AC-5 and AC-20 (PG 59 and 70) base mixtures.

Vertical compressive strains were measured by averaging the outputs of two Schaevitz model 100 MHR linear variable differential transformers (LVDT's), located on opposites of the specimen. Each LVDT had a full range of 5 mm and a gauge length of 100 mm. A typical instrumented specimen used in the tests is shown in figure 39.

b. AAMAS Analyses

The NCHRP AAMAS has two procedures for evaluating mixtures. The first procedure provides a rough estimate of rutting susceptibility.[20] The creep moduli vs. time relationships are plotted on a chart to determine if they fall in the area of low, moderate, or high rutting susceptibility. The report gives charts for lower, intermediate, and surface layers of asphalt pavements, and for layers placed over rigid pavements or rigid base materials. The methodology does not state what to do if a modulus falls into two areas of rutting susceptibility. The chart for asphalt surface layers, shown in figure 40, was used in this study.

In the second and primary procedure, mixtures are evaluated based on their rutting rates:

$$\epsilon_p = AN^m$$

where:

ϵ_p = rutting rate (mm of rut depth)/(mm of pavement layer thickness),
N = number of 18-kip ESAL's = 10,000,000, and
A,m = regression coefficients.

The coefficients "A" and "m" are normally found by performing long-term repeated load tests and calculating the slope and intercept. In pre-AAMAS studies, rutting rates based on repeated load tests were correlated to field performance data. The NCHRP AAMAS avoided testing difficulties associated with long-term repeated load tests by estimating the coefficients from creep and short-term repeated load test data. Although this procedure avoided the problems with testing, it added another correlation to the relationship between the laboratory data and yield performance. The following two equations were developed:

$$A = a(t_1)^b - \epsilon_{rt}$$

$$m = \frac{\log[a(1-X)/(a(0.1)^b - \epsilon_{rt})] + 3.5563b}{4.5563}$$

where:

a = intercept at 1 s from the steady state portion of the log total creep strain vs. log time relationship;
b = slope from the steady state portion of the log total creep strain vs. log time (s) relationship;
t_1 = traffic load duration = 0.1 s;
ϵ_{rt} = total resilient strain from the repeated load test;
X = recoverable creep strain or recovery efficiency, defined as ϵ_r/ϵ_c;
ϵ_r = recoverable creep strain at 3600 s after unloading, and
ϵ_c = total creep strain at 3600 s of loading.

To use the previous three equations, the creep strains must be in the linear range. To prevent nonlinearity, where the strains increase at an increasing rate, the following limiting compressive strain criteria must be met:

$$\epsilon_p < 0.5\epsilon_{qu} - \epsilon_{rt}$$

The modified AAMAS evaluates rutting susceptibility based on traffic intensity. The slope of the steady state creep curve and the creep strain at 3600 s are used as inputs to table 51, which gives the highest traffic intensity for which a mixture will be acceptable.[25] This intensity is then compared against the user's required traffic intensity. The highest intensity in the table, which is for traffic greater than 1 x 10^6 ESAL's was used in this study. This modified AAMAS uses the following equation to prevent nonlinearity:

$$\epsilon_c + \epsilon_{rt} < 0.5\epsilon_{qu}$$

The modified AAMAS suggests calculating the rutting rate, ϵ_p, as an additional check on rutting susceptibility. The methodology also includes the same charts used by the unmodified NCHRP AAMAS to estimate rutting susceptibility, but only the creep modulus at 3600 s is plotted on them.

c. Results From AAMAS

The NCHRP AAMAS data are given in table 52. The rutting rates, ϵ_p, for the mixtures with AC-5, AC-10, Styrelf, and Novophalt were not statistically different, and all of the rates were low. These low rutting rates indicated that none of the mixtures should be susceptible to rutting. The rates were low primarily because the steady state slopes from the creep tests were very low. The negative "m" coefficients in table 52 indicate the methodology is invalid for the mixtures tested. A negative "m" means that rutting decreases with an increase in traffic level. The traffic intensities using table 51 also showed that the mixtures had low susceptibilities to rutting. All mixtures had traffic intensities greater than 10^6 ESAL's. The strains were in the linear range, which was a requirement of both methodologies.

Since neither methodology could predict performance, the steady state creep slopes "b" were evaluated because they have been used in other studies to determine rutting susceptibility. A higher slope is interpreted to mean a higher potential for rutting. However, the mixtures with Novophalt and Styrelf had the highest slopes.

The stress and strain at failure, creep modulus, total creep strain, and permanent creep strain after unloading were evaluated. ALF pavement performance for the five surface mixtures is shown in figure 41, while the data from the laboratory tests are shown in figures 42 through 46. As the ALF wheel passes at failure in figure 41 increase, the stress at failure in figure 42 and the creep modulus in figure 44 should increase, while the total creep strain in figure 45 and the permanent creep strain in figure 46 should decrease. There is no hypothesis for how the strain at failure from the strength test, shown in figure 43, should relate to rutting performance.

Table 53 shows that the compressive stress at failure reversed the order for the Novophalt and Styrelf mixtures and statistically ranked the Novophalt mixture with the AC-20 mixture. The strain at failure provided a very poor ranking. The creep modulus and total creep strain at 3,600 s did not match ALF pavement performance, but the measurements did separate the mixtures with the modified binders from the mixtures with the unmodified binders. The permanent strains after unloading were highly variable and did not discriminate the mixtures. The variances were also not equal. None of the five measurements differentiated the four mixtures used in the surface vs. base mixture study. The only measurement that ranked the four mixtures correctly based on the averages was the stress at failure. However, the stresses at failure, shown in table 52, for the AC-20 (PG 70) surface and base mixtures and the AC-5 (PG 59) base mixture were not significantly different at a 95-percent confidence level.

The estimates of rutting susceptibility, based on the creep moduli and the chart shown in figure 40, are included in table 52 in terms of low, moderate, and high susceptibility. Although the conclusions that they provided were less than adequate, they agreed with ALF pavement performance better than the primary methods of analysis.

Additional creep tests were performed on the AC-5 (PG 59) and Novophalt surface mixtures to try to obtain data that correlated better with ALF pavement performance. The vertical stress level was increased from 140 to 450 kPa. The rutting rate, ϵ_p, (mm of rut depth per mm of pavement layer thickness) for the AC-5 (PG 59) mixture increased from 665 E-06 to 1580 E-06, while the rate for the Novophalt mixture increased from 449 E-06 to 750 E-06. These new rates were also very low and the "m" coefficients were negative. At either vertical stress, the rutting rates provided by the two mixtures were not significantly different. The mixtures were then retested at 140 kPa, but the average air-void level was reduced from 7.7 percent to 4.0 percent. This provided worse results because the rutting rates decreased. The mixtures were then tested using the original stress and air-void level, but the test temperature was increased from 40 to 50 °C. The rutting rates from these tests provided the erroneous conclusion that the Novophalt mixture was more susceptible to rutting than the AC-5 (PG 59) mixture. The air voids in the specimens, based on bulk specific gravity, did not decrease during testing for any mixture or variation of the test procedure.

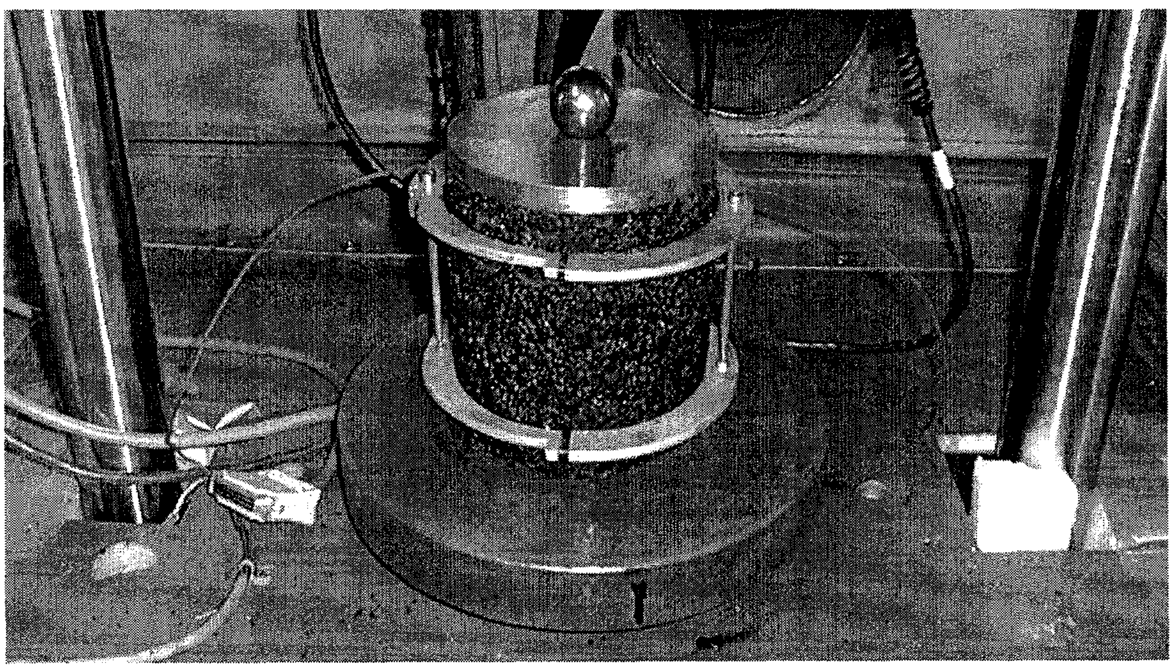

Figure 39. Instrumented specimen for the AAMAS repeated load and creep tests.

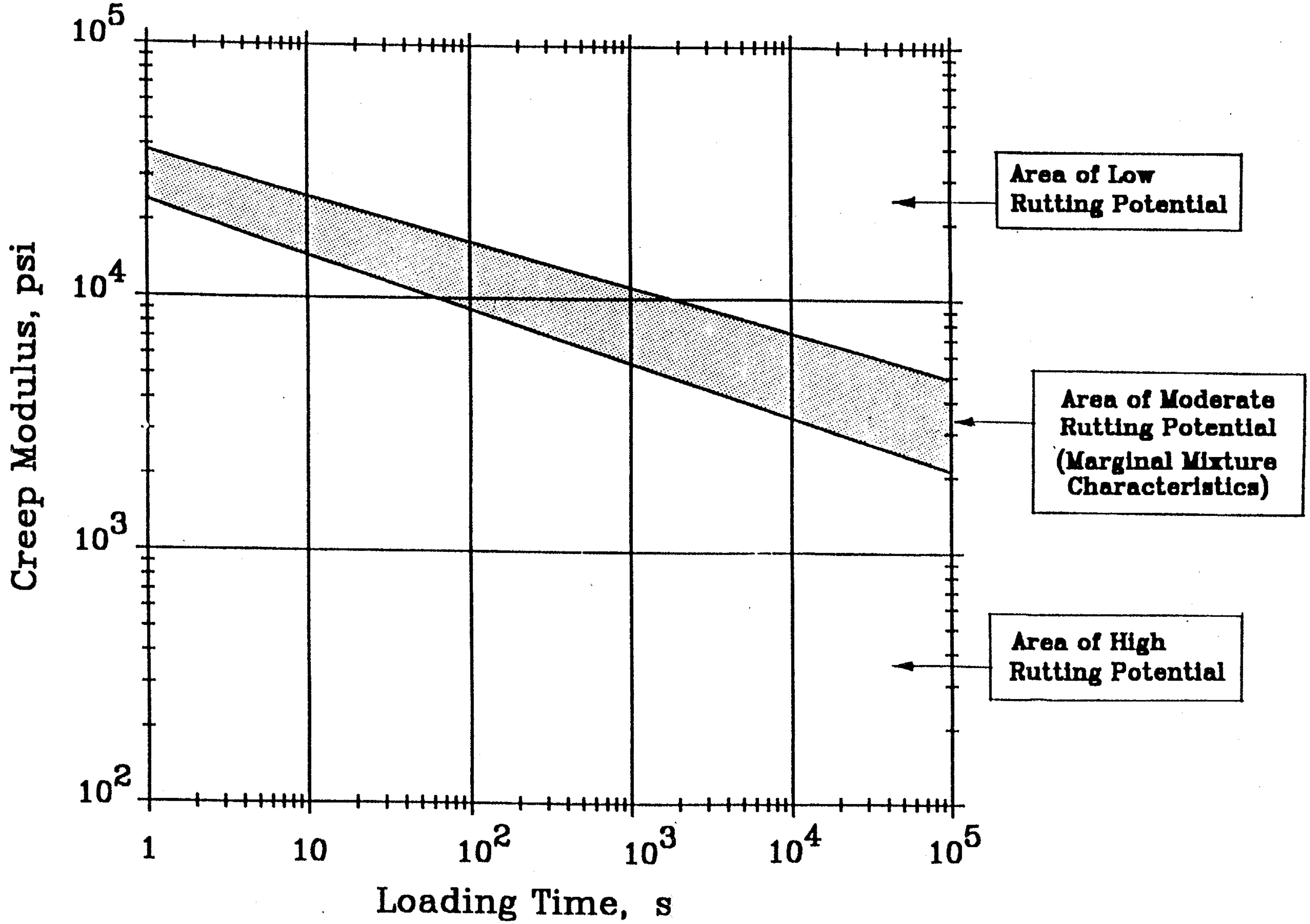

Figure 40. Rutting potential chart for asphalt concrete surface layers.[20]

Table 51. Modified AAMAS traffic intensities.[25]

Total Strain at 3600 s of Loading, %	Slope from the Steady State Portion of the Creep Curve				
	< 0.20	< 0.25	< 0.30	< 0.35	< 0.40
< 0.25	IV[2]	IV[2]	IV[2]	IV[2]	III
< 0.40	IV[2]	IV[2]	III[2]	III[2]	III[2]
< 0.50	IV[2]	III[2]	III[2]	III[2]	II
< 0.80	III[2]	II	II	II	II
< 1.0	I	I	I	I[1]	
< 1.2	I[1]	I[1]			

[1]Must also have $\epsilon_p < 0.8$ percent at 1,800 s of creep loading.
[2]The following criteria should be met: $\epsilon_p + \epsilon_{rt} < 0.5\ \epsilon_{qu}$.

Definitions for Traffic Intensity:[25]

I = < 1 x 10^5 ESAL's	(Low Traffic)
II = 1 x 10^5 to 5 x 10^5 ESAL's	(Moderate Traffic)
III = 5 x 10^5 to 1 x 10^6 ESAL's	(Heavy Traffic)
IV = > 1 x 10^6 ESAL's	(Very Heavy Traffic)

Table 52. Rutting performance based on AAMAS, Modified AAMAS, and the repeated load compression test at 40 °C.

Pre-Superpave: Superpave PG:	AC-5 59	AC-10 65	AC-20 70	Novophalt 77	Styrelf 88
Strength Test					
Stress at Failure, kPa	624	690	1 019	1 084	1 506
Strain at Failure[1], ϵ_{qu}	24 400	28 200	28 200	22 100	34 700
Repeated Load Test					
Total Resilient Strain[1], ϵ_{rt}	310	200	200	110	90
Creep Test					
Creep Modulus, 3600 s, MPa	58.1	68.9	49.3	123.0	85.7
Total Creep Strain[1], ϵ_c	2 500	2 080	2 940	1 180	1 330
Permanent Strain[1]	880	780	1 590	470	400
Recoverable Strain[1], ϵ_r	1 620	1 300	1 350	710	930
Recovery Efficiency, ϵ_r/ϵ_c	0.646	0.613	0.469	0.603	0.738
Intercept[1], a	1 890	1 640	2 130	720	710
Steady State Slope[1], b	32 400	27 390	37 790	58 670	74 190
Coefficient[1] A	1 440	1 340	1 750	520	520
Coefficient[1] m	-48 100	-54 400	-13 100	-9 700	-167 200
NCHRP AAMAS Analysis					
Rutting Potential, Chart	Mod/High	Mod/High	High	Low/Mod	Low/Mod
Rutting Rate[1], ϵ_p	667	612	1 522	449	478
$0.5\epsilon_{qu} - \epsilon_{rt}$	11 890	13 900	13 900	10 940	17 260
Modified AAMAS Analysis					
Rutting Potential, Chart	Mod	Mod	High	Low	Low
Traffic Intensity, ESAL's	$>10^6$	$>10^6$	$>10^6$	$>10^6$	$>10^6$
$\epsilon_c + \epsilon_{rt}$	2 810	2 280	3 140	1 290	1 420
$0.5\epsilon_{qu}$	12 200	14 100	14 100	11 050	17 350
Repeated Load Compression Test					
Dynamic Modulus, MPa	464	800	1 900	1 720	2 760
Cumulative Permanent Strain[1]	7 730	5 150	2 700	630	525
Slope, Linear Region	0.307	0.269	0.281	0.201	0.194
$G^*/\sin(\delta)$	38 640	82 810	159 900	263 600	270 900

[1]These data were multiplied by 10^6. The unit for strain is $\times 10^6$ mm/mm.

Table 52. Rutting performance based on AAMAS, Modified AAMAS, and the repeated load compression test at 40 °C (continued).

Pre-Superpave: Superpave PG:	AC-5 Base 59	AC-20 Base 70
Strength Test		
Stress at Failure, kPa	1 021	1 180
Strain at Failure[1], ϵ_{qu}	24 700	23 300
Repeated Load Test		
Total Resilient Strain[1], ϵ_{rt}	250	140
Creep Test		
Creep Modulus, 3600 s, MPa	46.8	76.8
Total Creep Strain[1], ϵ_c	3 010	2 190
Permanent Strain[1]	620	1 020
Recoverable Strain[1], ϵ_r	2 390	1 170
Recovery Efficiency, ϵ_r/ϵ_c	0.796	0.621
Intercept[1], a	2 480	1 660
Steady State Slope[1], b	24 900	31 900
Coefficient[1] A	2 090	1 400
Coefficient[1] m	-117 300	-94 800
NCHRP AAMAS Analysis		
Rutting Potential, Charts	High	Mod/High
Rutting Rate[1], ϵ_p	327	952
$0.5\epsilon_{qu} - \epsilon_{rt}$	12 100	11 510
Modified AAMAS Analysis		
Rutting Potential, Charts	High	Mod
Traffic Intensity, ESAL's	$>10^6$	$>10^6$
$\epsilon_c + \epsilon_{rt}$	3 260	2 330
$0.5\epsilon_{qu}$	12 350	11 650
Repeated Load Compression Test		
Dynamic Modulus, MPa	600	2 320
Cumulative Permanent Strain[1]	7 540	1 760
Slope, Linear Region	0.320	0.246
$G^*/\sin(\delta)$	38 640	159 900

[1]These data were multiplied by 10^6. The unit for strain is $\times10^6$ mm/mm.

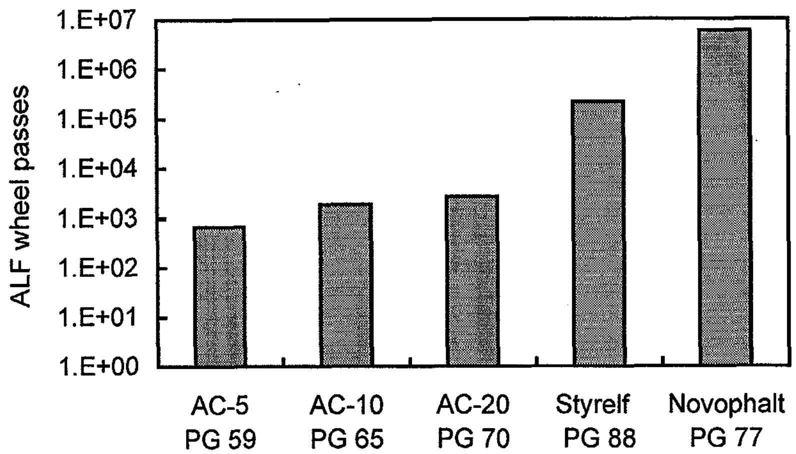

Figure 41. ALF wheel passes at a 20-mm rut depth vs. surface mixture.

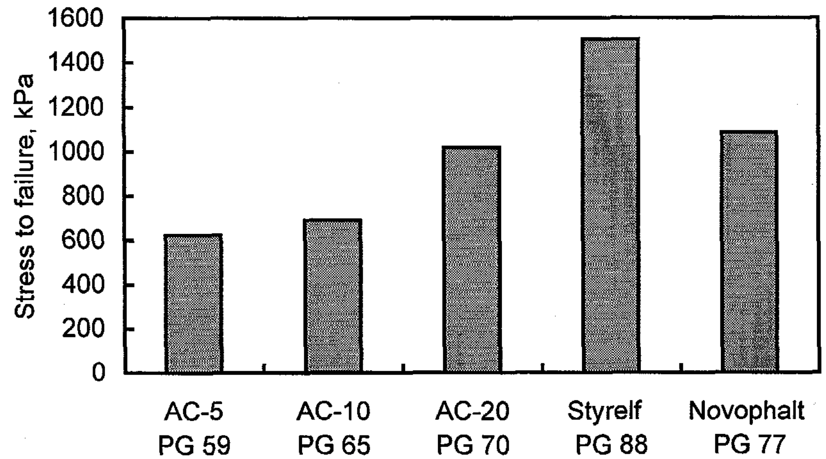

Figure 42. Stress at failure from the strength test vs. surface mixture.

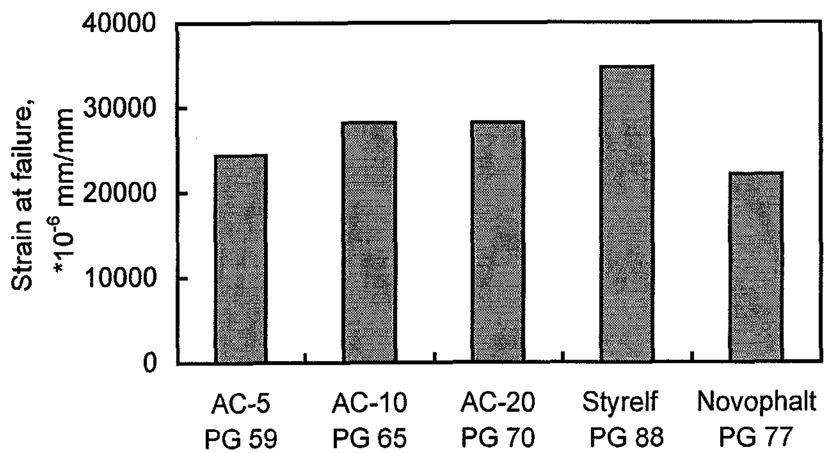

Figure 43. Strain at failure from the strength test vs. surface mixture.

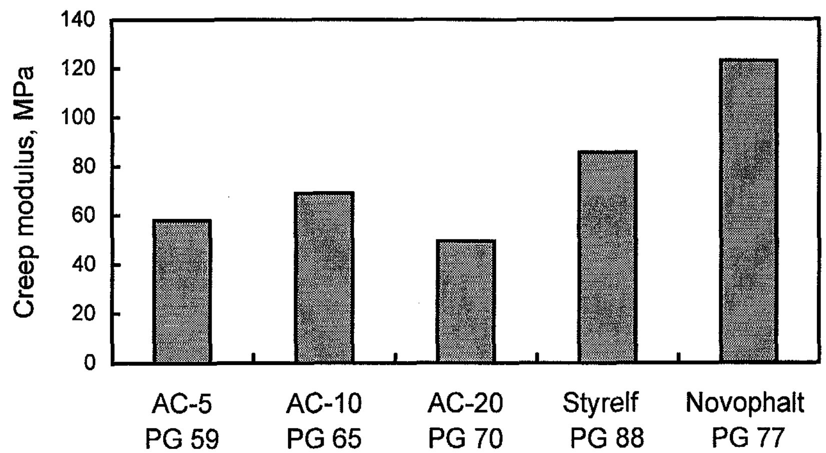

Figure 44. Creep modulus from the creep test vs. surface mixture.

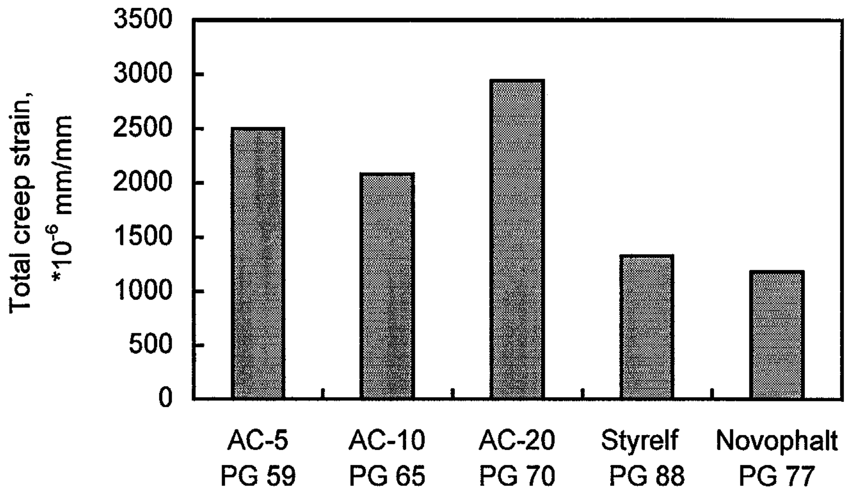

Figure 45. Total creep strain from the creep test vs. surface mixture.

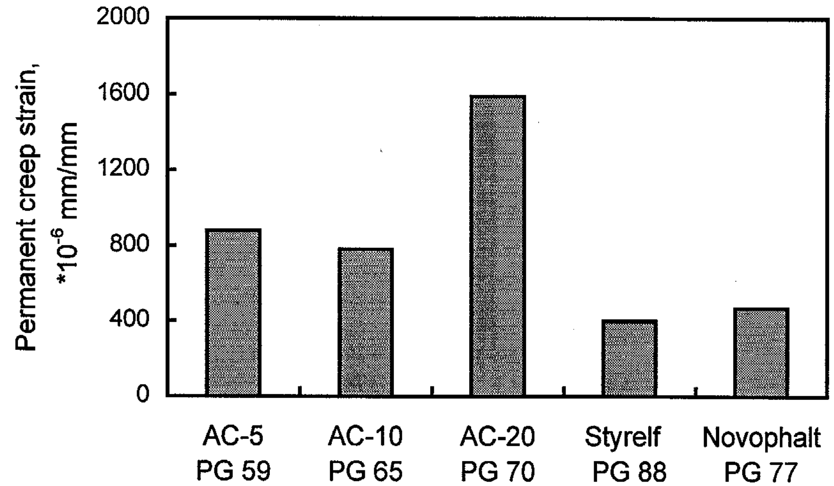

Figure 46. Permanent strain from the creep test vs. surface mixture.

Table 53. Statistical rankings for selected AAMAS tests at 40 °C.[1]

ALF at 58 °C	Compressive Strength Test: Stress at Failure,	Compressive Strength Test: Strain at Failure,	Creep Test: Creep Modulus or Total Creep Strain	Creep Test: Permanent Strain After Unloading
(A) Novophalt	(A) Styrelf	(A) Novophalt	(A) Novophalt	(A) Styrelf
(B) Styrelf	(B) Novophalt	(AB) AC-5	(A) Styrelf	(A) Novophalt
(C) AC-20	(B) AC-20	(B) AC-10	(B) AC-10	(A) AC-10
(C) AC-10	(C) AC-10	(B) AC-20	(BC) AC-5	(A) AC-5
(D) AC-5	(C) AC-5	(C) Styrelf	(C) AC-20	(A) AC-20

[1]The letters are the statistical ranking, with "A" denoting the mixture with the lowest susceptibility to rutting.

Table 54. Statistical rankings for the five surface mixtures provided by the ALF, the wheel-tracking devices, and repeated load compression test.

ALF at 58 °C	French PRT at 60 °C	Georgia LWT at 40 °C	Hamburg WTD at 50 °C	Repeated Load Test at 40 °C
(A) Novophalt	(A) Novophalt	(A) Novophalt	(-) Novophalt	(A) Styrelf
(B) Styrelf	(B) Styrelf	(B) Styrelf	(A) Styrelf	(A) Novophalt
(C) AC-20	(C) AC-20	(BC) AC-20	(B) AC-20	(B) AC-20
(C) AC-10	(D) AC-10	(C) AC-10	(C) AC-10	(C) AC-10
(D) AC-5	(D) AC-5	(C) AC-5	(D) AC-5	(D) AC-5

Table 55. Statistical rankings for the surface and base mixtures provided by the ALF, the wheel-tracking devices, and repeated load compression test.

ALF at 58 °C		French PRT at 60 °C	Georgia LWT at 40 °C	Hamburg WTD at 50 °C	Repeated Load Test at 40 °C
AC-20 Base	A	AB	A	B	A
AC-5 Base	B	C	AB	C	B
AC-20 Surface	C	A	A	A	A
AC-5 Surface	D	B	B	C	B

Table 56. Rankings for the repeated load compression tests at 40 °C.

DSR at 40 °C and 10.0 rad/s: Binder Ranking	DSR at 40 °C and 10.0 rad/s: $G^*/\sin\delta$, kPa	Cumulative Permanent Strain at 10,000 Cycles, Ranking by LSD or $\mu \pm 2\sigma_{(n-1)}$	Dynamic Modulus at 200 Cycles, Ranking by LSD	Dynamic Modulus at 200 Cycles, Ranking by $\mu \pm 2\sigma_{(n-1)}$
(A) Styrelf	270.9	(A) Styrelf	(A) Styrelf	(A) Styrelf
(A) Novophalt	263.6	(A) Novophalt	(B) AC-20	(AB) AC-20
(B) AC-20	159.9	(B) AC-20	(B) Novophalt	(B) Novophalt
(C) AC-10	82.8	(C) AC-10	(C) AC-10	(B) AC-10
(D) AC-5	38.6	(D) AC-5	(C) AC-5	(C) AC-5

Ranking Based on ALF at 58 °C	Ranking Based on the Average Slope, μ		Statistical Ranking Based on $\mu \pm 1\sigma_{(n-1)}$		Statistical Ranking Based on $\mu \pm 2\sigma_{(n-1)}$	
	Slope	All Mixtures	All Mixtures	Surface Mixtures	All Mixtures	Surface Mixtures
Novophalt	0.201	B	A	A	A	A
Styrelf	0.194	A	AB	AB	A	A
AC-20 Base	0.246	C	AC		A	
AC-5 Base	0.320	G	C		A	
AC-20	0.281	E	BC	BC	A	A
AC-10	0.269	D	BC	BC	A	A
AC-5	0.307	F	C	C	A	A

$\mu \pm 2\sigma_{(n-1)}$ = average ± two times the sample standard deviation, where "n" is the number of samples.

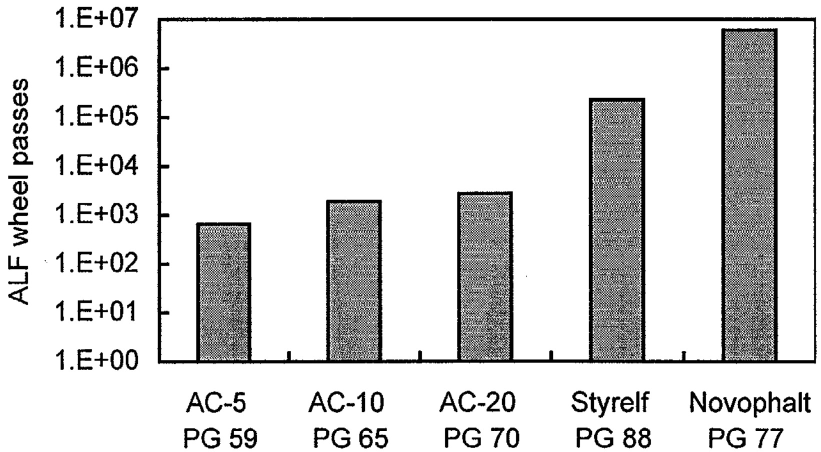

Figure 47. ALF wheel passes at a 20-mm rut depth vs. surface mixture.

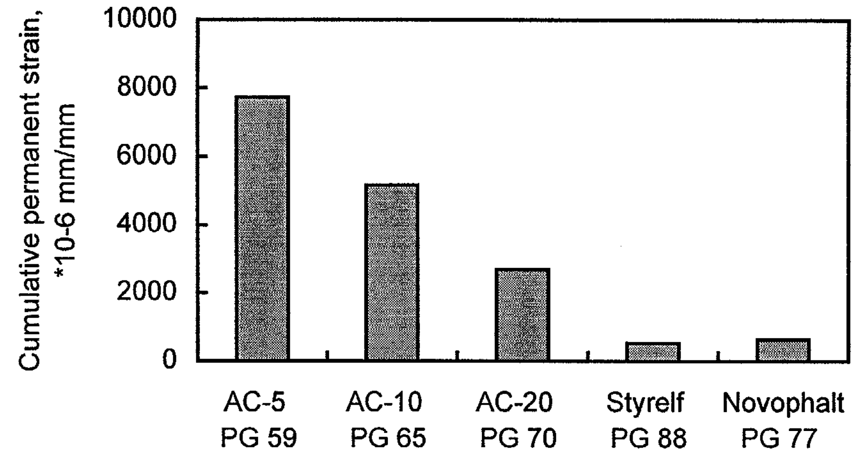

Figure 48. Cumulative permanent strain from the repeated load compression test vs. surface mixture.

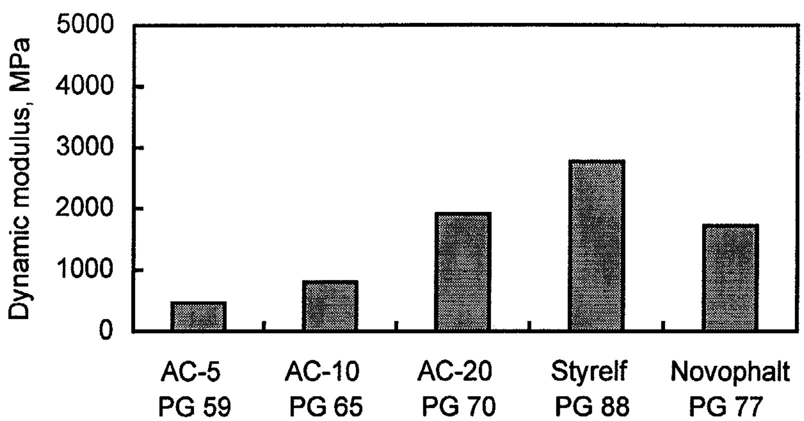

Figure 49. Dynamic modulus from the repeated load compression test vs. surface mixture.

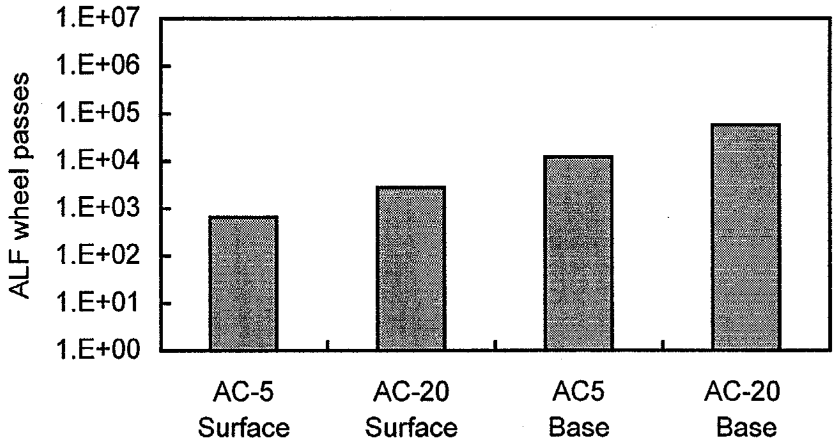

Figure 50. ALF wheel passes at a 20-mm rut depth vs. mixture type.

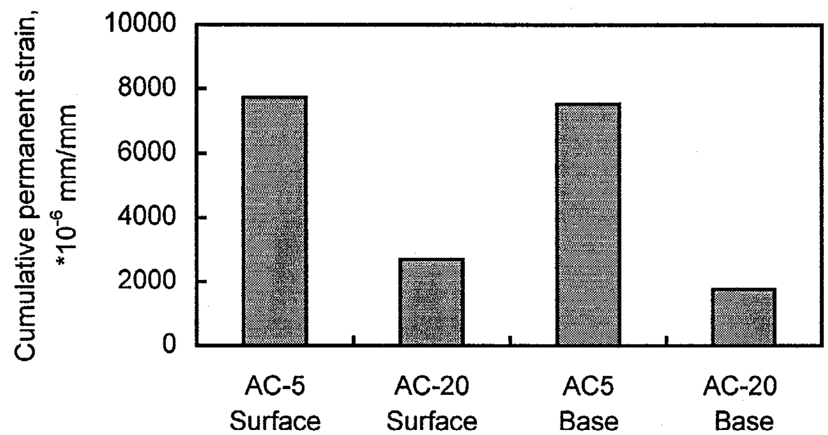

Figure 51. Cumulative permanent strain from the repeated load compression test vs. mixture type.

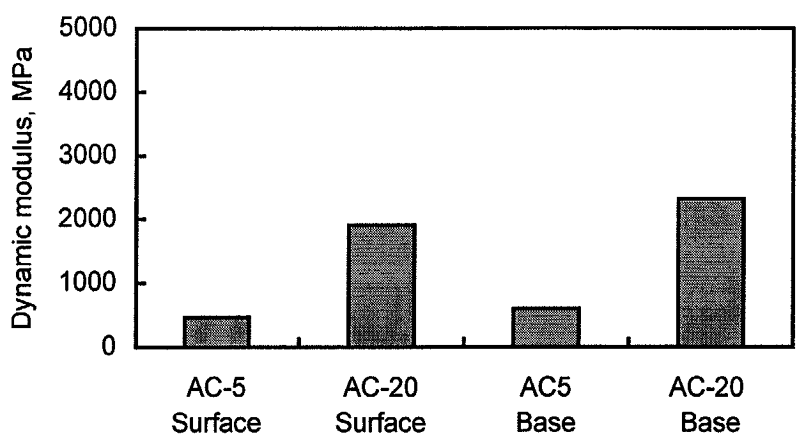

Figure 52. Dynamic modulus from the repeated load compression test vs. mixture type.

The AAMAS methodologies were eliminated from the study. The G*/sinδ's given in table 52 were determined using a frequency of 10.0 rad/s. If the NCHRP AAMAS had not been eliminated, it was not clear what DSR frequency should be used because creep tests do not have a frequency of loading. If the frequency is assumed to be very slow, the G*/sinδ's of the binders would be very low and probably equivalent. However, creep tests are used to predict rutting, or permanent deformation, due to traffic at typical highway traffic speeds.

9. Repeated Load Compression Test

Both AAMAS methodologies included a short-term repeated load test that ended at 200 cycles. This test was extended to 10,000 cycles so that the mixtures could be compared based on cumulative permanent strain.[26] The dynamic modulus at 200 cycles, based on the valley-to-peak total strain, was included in the evaluation. A stress of 140 kPa was applied to the specimens in the form of a haversine wave with a 0.1-s load duration. Each cycle of loading was followed by a 0.9-s rest period. The instrumented specimen is shown in figure 39.

The test data are included in table 52. ALF pavement performance for the five surface mixtures in terms of wheel passes is shown in figure 47, while the cumulative permanent strains and dynamic moduli are shown in figures 48 and 49. As the ALF wheel passes in figure 47 increase, the cumulative permanent strain in figure 48 should decrease. A hypothesis for how the dynamic modulus relates to pavement rutting performance does not exist, although in other studies, an increase in the dynamic modulus has been equated to a decrease in rutting susceptibility. The data for the surface vs. base mixture study are shown in figures 50, 51, and 52. As the ALF wheel passes in figure 50 increase, the cumulative permanent strain in figure 51 should decrease. The air voids in the specimens did not change during testing for any mixture based on the bulk specific gravity of each specimen measured before and after testing.

Tables 54 and 55 provide rankings for the repeated load test based on cumulative permanent strain. Table 54 shows that the ranking for the five surface mixtures was not the same as the rankings provided by the ALF and the three wheel-tracking devices. The order based on the average data was reversed for the Novophalt and Styrelf mixtures. The ranking in table 55 for the surface vs. base mixture study did not agree with ALF pavement performance.

Table 56 shows that the ranking provided by cumulative permanent strain at 40 °C matched the ranking for the five binders based on G*/sinδ at 40 °C. This suggested that the repeated load compression test should be tried at a temperature of 58 °C. Comparisons between G*/sinδ and the other mixture tests are discussed in chapter 6.

Rankings for the dynamic moduli, shown in table 56, did not agree with ALF pavement performance or the cumulative permanent strains. The fallacy of using the dynamic modulus to predict rutting is that it must be assumed that at a given temperature, all mixtures have the same amount of recoverable strain so that the differences in modulus from mixture to mixture are only a function of the differences in permanent strain.

The slopes from the linear portion of the log permanent strain vs. log time relationship were also evaluated. The slopes and the results of statistical analyses performed on them are included in table 56. None of the slopes were significantly different from each other at a 95-percent confidence level. This is shown by the ranking under "$\mu \pm 2\sigma_{(n-1)}$" in table 56. The poor repeatabilities of the slopes make them an inadequate measure of rutting performance.

Based on the findings at 40 °C, the tests were repeated at 58 °C. The data at both 40 and 58 °C are given in table 57. The cumulative permanent strains for the AC-5, AC-10, and AC-20 (PG 59, 65,and 70) surface mixtures and the AC-5 and AC-20 (PG 59 and 70) base mixtures exceeded the range of the LVDT's at 3,000 cycles or less. The data could only be compared at 1,000 cycles. The tests at 58 °C provided rankings for the five surface mixtures that were closer to ALF pavement performance at 58 °C than the rankings provided by the tests at 40 °C. This shows the importance of test temperature. However, no improvement in the rankings was found for the surface vs. base mixture comparisons. The air voids in the AC-5 and AC-10 (PG 59 and 65) surface mixture specimens increased 1.0 percent during testing, which was probably related to the high amount of specimen bulging that occurred. The air voids for the other mixtures did not change during testing.

10. SST[27,28]

a. Description of the SST

The SST was used to test specimens with a diameter of 150 mm that were compacted by the Superpave Gyratory Compactor. Each gyratory specimen was sawed to provide two test specimens, each with a height of 50 mm. The air-void level of each specimen was 7 ±0.5 percent after sawing. Specimens not meeting this requirement were discarded. Three to seven replicate specimens were tested, depending upon the repeatability of the SST data.

All tests were performed at both 40 and 58 °C. A temperature of 40 °C was used because this was the highest temperature used in the Superpave complete mixture analysis. A temperature of 58 °C was used because all seven mixtures were tested by the ALF at this temperature. The SST was operated in accordance with AASHTO Provisional Standard TP7-94, "Standard Test Method for Determining the Permanent Deformation and Fatigue Characteristics of Hot-Mix Asphalt (HMA) Using the Simple Shear Test (SST) Device."[3] Appendix A provides additional information on the SST including a photograph of it.

Table 57. ALF rutting performance vs. the repeated load compression test at 40 and 58 °C.

ALF at 58 °C	Dynamic Modulus, MPa: 200 Cycles and 40 °C	Dynamic Modulus, MPa: 200 Cycles and 58 °C
(A) Novophalt	(A) 2 760 Styrelf	(A) 258 Novophalt
(B) Styrelf	(B) 1 900 AC-20	(B) 176 Styrelf
(C) AC-20	(B) 1 720 Novophalt	(C) 65 AC-20
(C) AC-10	(C) 800 AC-10	(C) 58 AC-10
(D) AC-5	(C) 464 AC-5	(C) 61 AC-5

ALF at 58 °C	Cumulative Permanent Strain x 10^6 mm/mm: 10,000 Cycles and 40 °C	1,000 Cycles and 58 °C	10,000 Cycles and 58 °C
(A) Novophalt	(A) 525 Styrelf	(A) 2 200 Novophalt	(A) 3 120 Novophalt
(B) Styrelf	(A) 630 Novophalt	(A) 3 590 Styrelf	(B) 5 890 Styrelf
(C) AC-20	(B) 2 700 AC-20	(B) 12 840 AC-20	
(C) AC-10	(C) 5 150 AC-10	(C) 15 950 AC-10	
(D) AC-5	(D) 7 730 AC-5	(C) 16 280 AC-5	

ALF at 58 °C		Dynamic Modulus, MPa: 200 Cycles and 40 °C		200 Cycles and 58 °C		Cumulative Permanent Strain x 10^6 mm/mm: 10,000 Cycles and 40 °C		1,000 Cycles and 58 °C	
AC-20 Base	A	2 320	A	80	A	1 760	A	10 170	A
AC-5 Base	B	600	B	55	B	7 540	B	16 020	B
AC-20 Surface	C	1 900	A	65	AB	2 700	A	12 840	AB
AC-5 Surface	D	464	B	61	AB	7 730	B	16 280	B

The following tests were performed:

- Simple Shear at Constant Height (Simple Shear).
  - Compliance parameter (maximum strain /applied stress).
  - Permanent shear strain after unloading.
  - Maximum axial stress.

- Frequency Sweep at Constant Height (Frequency Sweep).
  - Complex shear modulus, G^*, at 10.0 and 2.0 Hz.
  - $G^*/\sin\delta$ at 10.0 and 2.0 Hz.
  - Slope of log G^* vs. log frequency.

- Repeated Shear at Constant Height (Repeated Shear).
  - Slope of cumulative permanent strain vs. cycles.
  - Cumulative permanent strain at 5,000 cycles (load repetitions).

(1) Simple Shear

The Simple Shear test consisted of applying a horizontal shear stress to a specimen at a rate of 70 kPa/s up to a stress level of 35 kPa for tests at 40 °C, and up to a stress level of 15 kPa for the tests at 58 °C. The maximum stress level was maintained for 10 s, after which it was reduced to 0 kPa at a rate of 25 kPa/s. The height of the specimen is kept constant throughout the test to within 0.0013 mm. Because AASHTO TP7-94 did not consider tests with temperatures as high as 58 °C at the time of this study, the stress level for tests at 58 °C was determined by trial-and-error with the goal of determining a stress level that could be applied to all mixtures regardless of their stiffnesses. The 15-kPa stress level met this goal.

The compliance parameter was obtained by dividing the maximum shear strain, which occurred at 10 s, by the applied shear stress. It was hypothesized that as the compliance parameter decreased, rutting susceptibility would decrease.

All tests at a given temperature were performed using the same applied stress history, therefore, the permanent shear strains after loading could be compared. It was hypothesized that as the permanent shear strain decreased, rutting susceptibility would decrease. The permanent shear strain was measured 10 s after unloading.

The SST measures the vertical axial stress needed to maintain a constant specimen height during testing. This axial stress is hypothesized to be the result of aggregates trying to roll past each other as the mixture shears.[29] It is equated to the capability of a mixture to exhibit dilatancy due to shearing. Dilatancy is prohibited in the vertical direction during the test by the application of the axial stress. It was hypothesized that as the vertical axial stress decreased, rutting susceptibility would decrease. A mixture with aggregates having a high degree of interlock should have a low vertical axial stress.

(2) Frequency Sweep

The Frequency Sweep test consisted of applying a sinusoidal shear strain with a peak-to-peak amplitude of 0.1 μm/mm at the following frequencies: 10.0, 5.0, 2.0, 1.0, 0.5, 0.2, 0.1, 0.05, 0.02, and 0.01 Hz. The height of the specimen is kept constant throughout the test to within 0.0013 mm.

The complex shear modulus, G*, was measured as a function of frequency. The G*'s at all frequencies were analyzed, but emphasis was placed on the G*'s at 10.0 and 2.0 Hz because 10.0 Hz is the most widely used frequency for repeated load tests for asphalt mixtures, while 2.0 Hz could be considered the loading frequency of the ALF. A frequency of 2.0 Hz was chosen instead of 2.25 Hz (18 km/h ÷ 8.0 km/(h·Hz) = 2.25 Hz), because 2.0 Hz was one of the standard SST frequencies. It was hypothesized that as G* increased, rutting susceptibility would decrease. However, as discussed for the dynamic moduli from the repeated load compression test, it must be assumed that at a given temperature and frequency, all mixtures have the same amount of recoverable strain so that the differences in modulus from mixture to mixture are only a function of the differences in permanent strain.

The G*/sinδ's of the mixtures at 10.0 and 2.0 Hz were evaluated because the Superpave binder specification uses this parameter to grade binders according to permanent deformation. It is not known if the rheological states of the mixtures at 40 °C allow this parameter to be interpreted in the same manner used when evaluating binders. The rheological state, or rheological model, would have to be the same for all mixtures. For binders, an increase in G*/sinδ should decrease rutting susceptibility.

The slopes from the relationships between log G* and log frequency were also examined. No hypothesis exists for how this slope should relate to pavement performance, although it has been suggested that a lower slope may indicate a greater resistance to rutting.[30] This hypothesis was used to analyze the slopes in this study. Superpave used this slope, defined as the "m-value," in its original performance model for rutting.

(3) Repeated Shear

The Repeated Shear test applies a haversine shear stress of 70 kPa for 0.1 s followed by a 0.6 s rest period. The height of the specimen is kept constant throughout the test to within 0.0013 mm. The process is repeated for 5,000 cycles or until the specimen suffers a permanent shear strain of 5 percent. The slope for each relationship between cumulative permanent shear strain and cycles was determined by fitting the data to a rutting model of the form:

$$PS = aN^b$$

where:

PS = permanent shear strain; N = number of cycles;
a = intercept, and b = slope of cumulative permanent shear strain.

The slope is considered to represent the rate of rutting as a function of load applications. It was hypothesized that as the slope decreased, rutting susceptibility would decrease. However, as discussed in chapter 3, both the slope and the intercept may be needed to predict rutting susceptibility.

The cumulative permanent shear strain at 5,000 cycles is another indicator of the resistance of a mixture to permanent deformation. This strain accounts for both the slope and intercept. It was hypothesized that as the cumulative permanent shear strain at 5,000 cycles decreased, rutting susceptibility would decrease.

b. Results From the SST for the Five Surface Mixtures at 40 °C

The data for all measurements at 40 °C are shown in table 58. Some measurements exhibited heteroscedasticity, where the standard deviation increased with an increase in the average. When this was encountered, the $\log_{10}$ of the measurement was ranked using an analysis of variance and Fisher's LSD.

(1) Simple Shear

Table 59 shows that all three measurements ranked the mixtures the same as ALF pavement performance based on the averages. The statistical rankings provided by the compliance parameter and permanent shear strain matched the ranking provided by ALF. The maximum axial stress provided a lower degree of correlation with ALF based on the statistical rankings. The main discrepancy was that the Novophalt and Styrelf mixtures ranked the same.

(2) Frequency Sweep

Table 59 shows that the rankings based on both G^* and $G^*/\sin\delta$ at 10.0 and 2.0 Hz were the same as ALF pavement performance based on the averages. Figures 53 and 54 show that the rankings were the same at all measured frequencies. The statistical rankings in table 59 for G^* and $G^*/\sin\delta$ were not identical to the ranking provided by ALF, but the degree of correlation was good.

The slopes from the relationship between log G^* and log frequency did not agree with ALF pavement performance. The hypothesis that a lower slope may indicate a greater resistance to rutting was not valid for these data.

(3) Repeated Shear

Table 59 shows that the slopes from the relationship between cumulative permanent strain and cycles did not agree with ALF pavement performance. The cumulative permanent strains at 5,000 cycles ranked the mixtures the same as ALF based on the averages. The statistical ranking provided by these strains was not identical to the ranking provided by ALF, but the degree of correlation was good.

c. Results From the SST for the Five Surface Mixtures at 58 °C

The data at 58 °C are shown in table 60. The Frequency Sweep data are also shown in figures 55 and 56. Table 61 shows that no SST measurement ranked the mixtures the same as ALF based on the averages unless the hypothesis for the Frequency Sweep slope is reversed. The data show that a higher slope indicates a greater resistance to rutting. All of the statistical rankings correlated poorly to ALF pavement performance. The best data were provided by the maximum axial stress from Simple Shear. The Repeated Shear tests at 58 °C were terminated because the data were extremely variable.

Table 62 provides the coefficients of variation for each SST measurement at both 40 and 58 °C. The coefficients of variation were higher at 58 °C compared with 40 °C, except for the maximum axial stresses from Simple Shear, where the coefficients were virtually equal.

The coefficient of variation is used to judge the repeatability of a test. Although there is no standard maximum value, a maximum value of 20 percent is often used. Most measurements at 58 °C had coefficients of 20 percent and above, whereas the measurements at 40 °C were generally less than 20 percent. Even so, the cumulative permanent strains from Repeated Shear provided a coefficient of variation of 33 percent at 40 °C. This test could be considered one of the leading candidate tests for evaluating rutting potential without a performance-predicting model, yet it had a high coefficient of variation. (Note that the coefficients of variation were a function of five binder grades with a single aggregate gradation and binder content.)

d. Results From the SST for the Surface vs. Base Mixture Study at 40 °C

The data for the surface vs. base mixture study at 40 °C are shown in table 63. Table 64 shows that no SST measurement at 40 °C provided a ranking that agreed with ALF pavement performance. (Two formats for presenting the rankings are used in this chapter. The choice of the format depended upon which one best facilitated visual comparisons of the rankings.)

Table 65 shows rankings based only on the averages. The results from the French PRT, Georgia LWT, Hamburg WTD, and repeated load compression test are included. Only the cumulative permanent strain at 5,000 cycles from Repeated Shear provided a ranking that was the same as ALF. The data are also presented in figures 57 and 58. As ALF wheel passes increased, the strains decreased.

Table 66 gives the results of *t*-tests that were used to compare the data from each base mixture with the data from the surface mixture having the same binder grade. The decrease in pavement rutting susceptibility provided by each base mixture was not duplicated by the French PRT, Georgia LWT, Hamburg WTD, or repeated load compression test. Thus, each pair of data for these tests in table 66 has the same ranking "A." The Georgia LWT and the cumulative permanent strains from the repeated load compression test did provide better average data for both base mixtures relative to their associated surface mixture, but the differences in the averages were small.

The results from the *t*-tests for the SST data varied from measurement to measurement. Simple Shear measurements provided better average data for the base mixtures relative to their associated surface mixture in five out of six comparisons. The only exception was the maximum axial stress using the AC-20 (PG 70) binder. Only two of the six comparisons were significantly different. G* and G*/sinδ from Frequency Sweep provided better average data for the base mixtures for all eight comparisons shown in table 66. The differences were significant for five of these eight comparisons. The slopes from Frequency Sweep and Repeated Shear did not give consistent trends. It was concluded that these slopes cannot be used as indicators of rutting performance. The cumulative permanent strains at 5,000 cycles from Repeated Shear provided better average data for both base mixtures relative to their associated surface mixture, but the effect was only significant for the mixtures with AC-20 (PG 70).

The *t*-tests show that some SST measurements were affected by nominal maximum aggregate size, but the rankings for the four mixtures in table 64 show that the effect was not as great as the effect on ALF pavement performance.

e. Results From the SST for the Surface vs. Base Mixture Study at 58 °C

The data for the surface vs. base mixture study at 58 °C are shown in table 67. Only the maximum axial stress ranked the mixtures correctly based on the averages. Figures 57 and 59 present the ALF wheel passes and the maximum axial stresses. As the ALF wheel passes increased, the maximum axial stress decreased. Table 68 shows that no SST measurement at 58 °C provided a statistical ranking that agreed with ALF pavement performance.

f. Results From the SST for the Surface vs. Base Mixture Study at 40 and 58 °C Using Specimens With a Diameter of 150 mm and a Height of 75 mm

AASHTO Provisional Standard TP7-94 stated that specimens with a diameter of 150 mm and height of 75 mm should be used when the maximum aggregate size is 38 mm.[3] Gyratory-compacted specimens were sawed to provide specimens of this size. The data from these tests are given in tables 69 and 70 along with the statistical rankings. One set of specimens was used for all tests shown in both tables. The Repeated Shear test was only performed at 58 °C because this test is destructive. The use of a larger size specimen did not improve the degree of correlation to ALF pavement performance. The best results were provided by the compliance parameter and permanent shear strain from Simple Shear at 40 °C.

Table 58. SST results for the five surface mixtures at 40 °C.

ALF Ranking at 58 °C and a 20-mm Rut Depth	Simple Shear at Constant Height and 40 °C: Compliance Parameter, 1/MPa	Permanent Shear Strain, 10^{-6} mm/mm	Maximum Axial Stress, kPa
(A) Novophalt	0.127	2 020	13.1
(B) Styrelf	0.224	4 020	14.5
(C) AC-20	0.702	19 200	28.9
(C) AC-10	0.766	20 400	40.7
(D) AC-5	1.030	25 500	48.5

ALF Ranking at 58 °C and a 20-mm Rut Depth	Frequency Sweep at Constant Height and 40 °C: Shear Modulus G*, at 10.0 Hz, MPa	Shear Modulus G*, at 2.0 Hz, MPa	G*/sinδ, 10.0 Hz, MPa	G*/sinδ, 2.0 Hz, MPa	Slope of Log G* vs. Log Frequency
(A) Novophalt	409	236	644	378	0.28
(B) Styrelf	281	150	396	212	0.33
(C) AC-20	222	103	256	119	0.35
(C) AC-10	134	60	156	69	0.35
(D) AC-5	62	34	71	39	0.31

ALF Ranking at 58 °C and a 20-mm Rut Depth	Repeated Shear at Constant Height and 40 °C: Slope of Cumulative Permanent Strain	Cumulative Permanent Strain at 5,000 Cycles, 10^{-6} mm/mm
(A) Novophalt	0.30	1 830
(B) Styrelf	0.36	3 480
(C) AC-20	0.35	14 820
(C) AC-10	0.34	17 040
(D) AC-5	0.35	22 200

Table 59. Statistical rankings for the five surface mixtures provided by the SST at 40 °C.[1]

ALF Ranking at 58 °C and a 20-mm Rut Depth	Simple Shear at Constant Height and 40 °C: Log Compliance Parameter, 1/MPa	Log Permanent Shear Strain, 10^{-6} mm/mm	Maximum Axial Stress, kPa
(A) Novo	(A) Novo	(A) Novo	(A) Novo
(B) Sty	(B) Sty	(B) Sty	(A) Sty
(C) AC-20	(C) AC-20	(C) AC-20	(B) AC-20
(C) AC-10	(C) AC-10	(C) AC-10	(C) AC-10
(D) AC-5	(D) AC-5	(D) AC-5	(D) AC-5

ALF Ranking at 58 °C and a 20-mm Rut Depth	Frequency Sweep at Constant Height and 40 °C: Shear Modulus G*, at 10.0 Hz, MPa	Log Shear Modulus G*, at 2.0 Hz, MPa	G*/sinδ, 10.0 Hz, MPa	Log G*/sinδ, 2.0 Hz, MPa	Slope of Log G* vs. Log Frequency
(A) Novo	(A) Novo	(A) Novo	(A) Novo	(A) Novo	(A) Novo
(B) Sty	(B) Sty	(B) Sty	(B) Sty	(B) Sty	(AB) AC-5
(C) AC-20	(C) AC-20	(C) AC-20	(C) AC-20	(C) AC-20	(AB) Sty
(C) AC-10	(D) AC-10	(D) AC-10	(D) AC-10	(D) AC-10	(AB) AC-20
(D) AC-5	(E) AC-5	(E) AC-5	(E) AC-5	(E) AC-5	(B) AC-10

ALF Ranking at 58 °C and a 20-mm Rut Depth	Repeated Shear at Constant Height and 40 °C: Slope of Cumulative Permanent Strain	Log Cumulative Permanent Strain at 5,000 Cycles, 10^{-6} mm/mm
(A) Novo	(A) Novo	(A) Novo
(B) Sty	(A) AC-10	(B) Sty
(C) AC-20	(A) AC-20	(C) AC-20
(C) AC-10	(A) AC-5	(CD) AC-10
(D) AC-5	(A) Sty	(D) AC-5

[1]The letters are the statistical ranking, with "A" denoting the mixture with the lowest susceptibility to rutting.

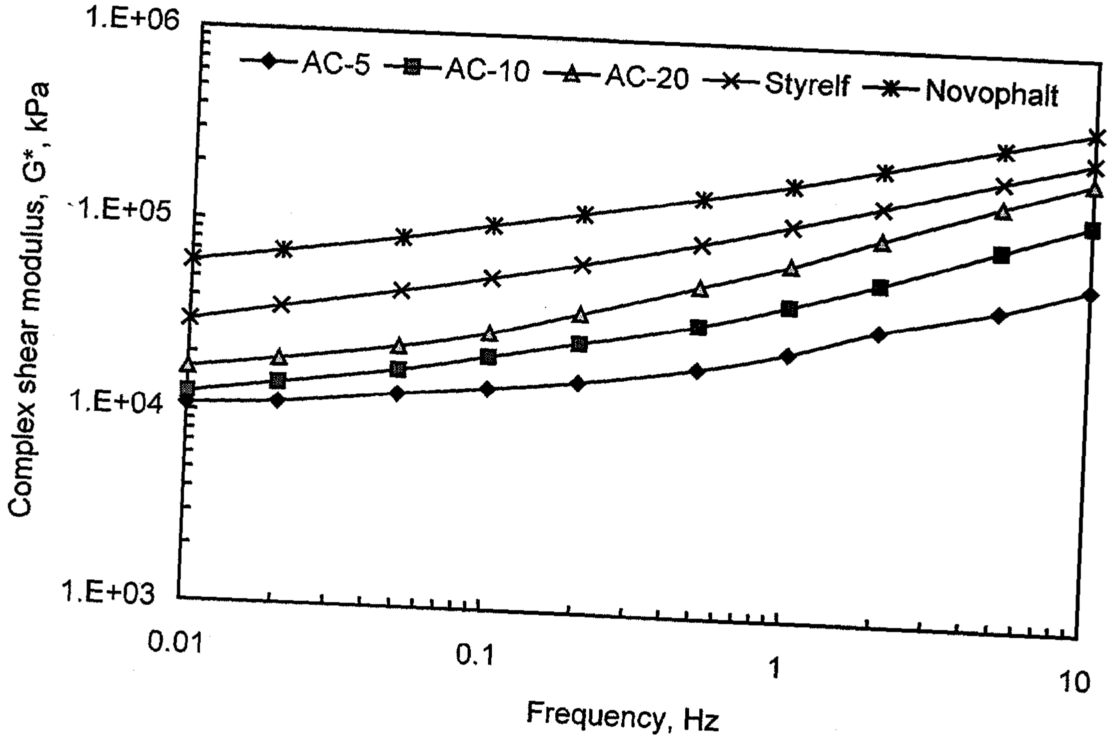

Figure 53. Complex shear modulus, G*, at 40 °C.

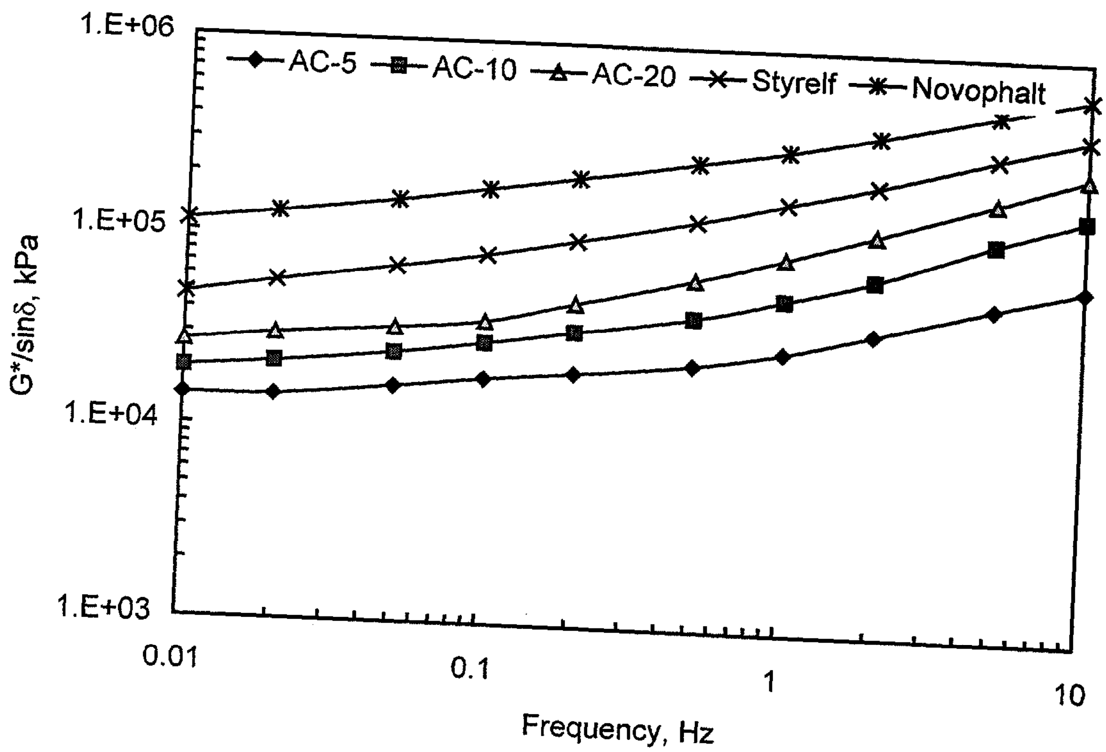

Figure 54. G*/sinδ at 40 °C.

Table 60. SST results for the five surface mixtures at 58 °C.

ALF Ranking at 58 °C and a 20-mm Rut Depth	Simple Shear at Constant Height and 58 °C: Compliance Parameter, 1/MPa	Permanent Shear Strain, 10^{-6} mm/mm	Maximum Axial Stress, kPa
(A) Novophalt	0.351	3 070	4.9
(B) Styrelf	0.910	8 060	10.9
(C) AC-20	1.720	22 700	16.1
(C) AC-10	1.450	16 400	14.2
(D) AC-5	1.390	18 800	17.3

ALF Ranking at 58 °C and a 20-mm Rut Depth	Frequency Sweep at Constant Height and 58 °C: Shear Modulus G*, at 10.0 Hz, MPa	Shear Modulus G*, at 2.0 Hz, MPa	G*/sinδ, 10.0 Hz, MPa	G*/sinδ, 2.0 Hz, MPa	Slope of Log G* vs. Log Frequency
(A) Novophalt	170	124	251	172	0.22
(B) Styrelf	93	61	136	98	0.16
(C) AC-20	89	70	125	116	0.10
(C) AC-10	66	58	111	108	0.09
(D) AC-5	71	60	138	127	0.08

ALF Ranking at 58 °C and a 20-mm Rut Depth	Repeated Shear at Constant Height and 58 °C: Slope of Cumulative Permanent Strain	Cumulative Permanent Strain at 5,000 Cycles, 10^{-6} mm/mm
(A) Novophalt	NT	NT
(B) Styrelf	NT	NT
(C) AC-20	0.35	34 200
(C) AC-10	0.39	31 800
(D) AC-5	NT	NT

NT = Not tested.

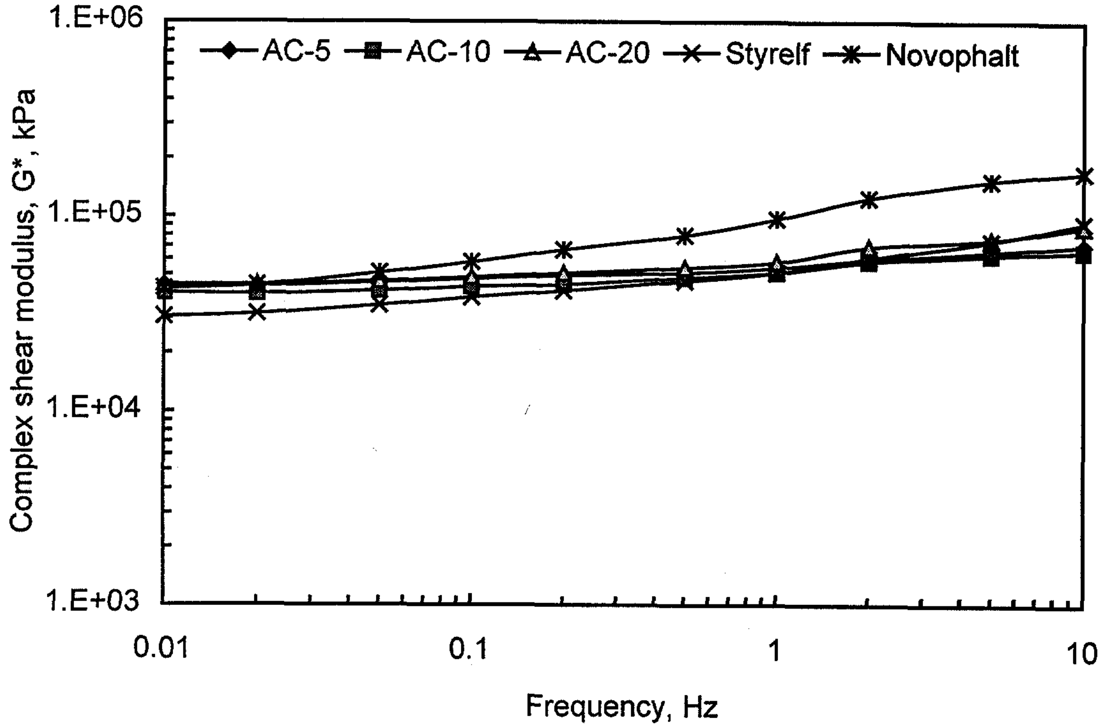

Figure 55. Complex shear modulus, G*, at 58 °C.

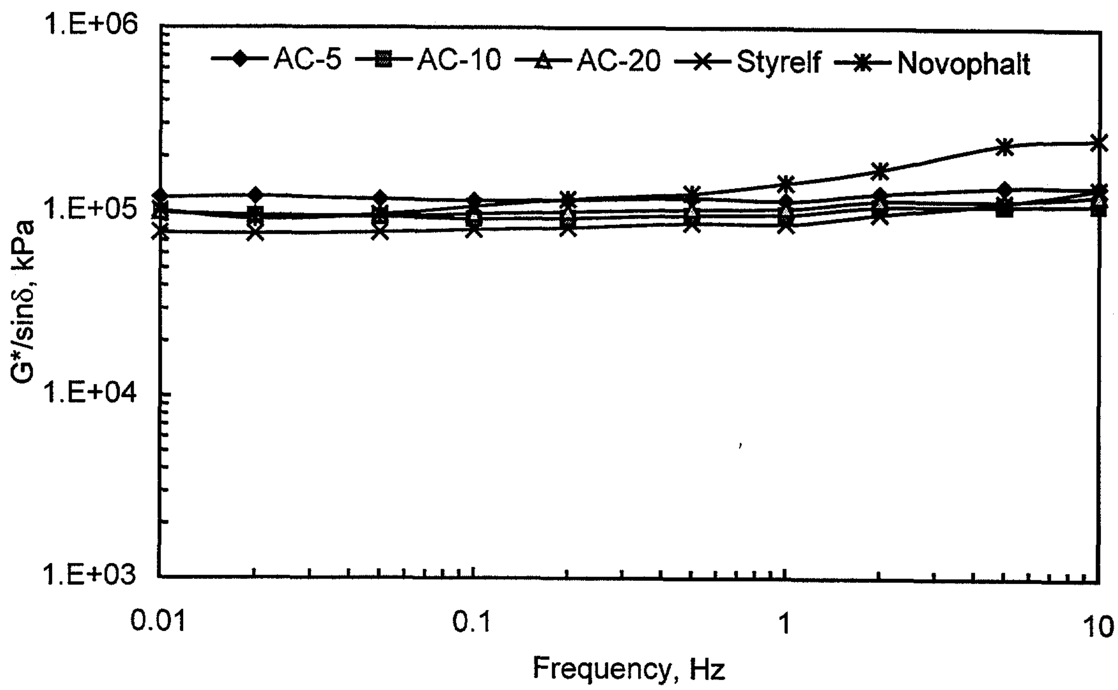

Figure 56. G*/sinδ at 58 °C.

Table 61. Statistical rankings for the five surface mixtures provided by the SST at 58 °C.[1]

ALF Ranking at 58 °C and a 20-mm Rut Depth	Simple Shear at Constant Height and 58 °C: Log Compliance Parameter, 1/MPa	Log Permanent Shear Strain, 10^{-6} mm/mm	Maximum Axial Stress, kPa
(A) Novo	(A) Novo	(A) Novo	(A) Novo
(B) Sty	(B) Sty	(B) Sty	(B) Sty
(C) AC-20	(BC) AC-5	(C) AC-10	(C) AC-10
(C) AC-10	(C) AC-10	(C) AC-5	(C) AC-20
(D) AC-5	(C) AC-20	(C) AC-20	(C) AC-5

ALF Ranking at 58 °C and a 20-mm Rut Depth	Frequency Sweep at Constant Height and 58 °C: Shear Modulus G*, at 10.0 Hz, MPa	Shear Modulus G*, at 2.0 Hz, MPa	G*/sinδ, 10.0 Hz, MPa	G*/sinδ, 2.0 Hz, MPa	Slope of Log G* vs. Log Frequency
(A) Novo	(A) Novo	(A) Novo	(A) Novo	(A) Novo	(A) AC-5
(B) Sty	(BD) Sty	(B) AC-20	(B) AC-5	(AB) AC-5	(A) AC-10
(C) AC-20	(B) AC-20	(B) Sty	(B) Sty	(AB) AC-20	(A) AC-20
(C) AC-10	(BC) AC-5	(B) AC-5	(B) AC-20	(B) AC-10	(B) Sty
(D) AC-5	(CD) AC-10	(B) AC-10	(B) AC-10	(AB) Sty	(C) Novo

ALF Ranking at 58 °C and a 20-mm Rut Depth	Repeated Shear at Constant Height and 58 °C: Slope of Cumulative Permanent Strain	Cumulative Permanent Strain at 5,000 Cycles, 10^{-6} mm/mm
(A) Novo	No Ranking	No Ranking
(B) Sty		
(C) AC-20		
(C) AC-10		
(D) AC-5		

[1]The letters are the statistical ranking, with "A" denoting the mixture with the lowest susceptibility to rutting.

Table 62. Coefficients of variation in terms of percentages for the SST based on the data for the five surface mixtures.

	Simple Shear at Constant Height		
Test Temperature	Compliance Parameter, 1/MPa	Permanent Shear Strain, 10^{-6} mm/mm	Maximum Axial Stress, kPa
40 °C	15	18	18
58 °C	27	43	17

	Frequency Sweep at Constant Height				
Test Temperature	Shear Modulus G*, at 10.0 Hz, MPa	Shear Modulus G*, at 2.0 Hz, MPa	G*/sinδ, 10.0 Hz, MPa	G*/sinδ, 2.0 Hz, MPa	Slope of Log G* vs. Log Frequency
40 °C	14	17	18	24	15
58 °C	20	26	20	38	98

	Repeated Shear at Constant Height	
Test Temperature	Slope of Cumulative Permanent Strain	Cumulative Permanent Strain at 5,000 Cycles, 10^{-6} mm/mm
40 °C	14	33
58 °C	NA	NA

NA = Not applicable because of a lack of sufficient data.

Table 63. SST results for the surface and base mixtures at 40 °C.

ALF Ranking at 58 °C and a 20-mm Rut Depth		Simple Shear at Constant Height and 40 °C: Compliance Parameter, 1/MPa	Permanent Shear Strain, 10^{-6} mm/mm	Maximum Axial Stress, kPa
AC-20 Base	A	0.490	9 370	29.5
AC-5 Base	B	0.794	23 000	31.6
AC-20 Surface	C	0.702	19 200	28.9
AC-5 Surface	D	1.030	25 500	48.5

ALF Ranking at 58 °C and a 20-mm Rut Depth		Frequency Sweep at Constant Height and 40 °C: Shear Modulus G*, at 10.0 Hz, MPa	Shear Modulus G*, at 2.0 Hz, MPa	G*/sinδ, 10.0 Hz, MPa	G*/sinδ, 2.0 Hz, MPa	Slope of Log G* vs. Log Frequency
AC-20 Base	A	291	126	353	147	0.44
AC-5 Base	B	93	48	113	60	0.27
AC-20 Surface	C	222	103	256	119	0.35
AC-5 Surface	D	62	34	71	39	0.31

ALF Ranking at 58 °C and a 20-mm Rut Depth		Repeated Shear at Constant Height and 40 °C: Slope of Cumulative Permanent Strain	Cumulative Permanent Strain at 5,000 Cycles, 10^{-6} mm/mm
AC-20 Base	A	0.30	9 640
AC-5 Base	B	0.45	14 460
AC-20 Surface	C	0.35	14 820
AC-5 Surface	D	0.35	22 200

Table 64. Statistical rankings for the surface and base mixtures provided by the SST at 40 °C.[1]

ALF Ranking at 58 °C and a 20-mm Rut Depth		Simple Shear at Constant Height and 40 °C: Compliance Parameter, 1/MPa	Permanent Shear Strain, 10^{-6} mm/mm	Maximum Axial Stress, kPa
AC-20 Base	A	A	A	A
AC-5 Base	B	BC	BC	A
AC-20 Surface	C	AB	B	A
AC-5 Surface	D	C	C	B

ALF Ranking at 58 °C and a 20-mm Rut Depth		Frequency Sweep at Constant Height and 40 °C: Log Shear Modulus G*, at 10.0 Hz, MPa	Log Shear Modulus G*, at 2.0 Hz, MPa	Log G*/sinδ, 10.0 Hz, MPa	Log G*/sinδ, 2.0 Hz, MPa	Slope of Log G* vs. Log Frequency
AC-20 Base	A	A	A	A	A	B
AC-5 Base	B	C	B	C	B	A
AC-20 Surface	C	B	A	B	A	AB
AC-5 Surface	D	D	C	D	C	A

ALF Ranking at 58 °C and a 20-mm Rut Depth		Repeated Shear at Constant Height and 40 °C: Slope of Cumulative Permanent Strain	Cumulative Permanent Strain at 5,000 Cycles, 10^{-6} mm/mm
AC-20 Base	A	A	A
AC-5 Base	B	A	A
AC-20 Surface	C	A	A
AC-5 Surface	D	B	B

[1]The letters are the statistical ranking, with "A" denoting the mixture with the lowest susceptibility to rutting.

Table 65. Non-statistical rankings for the surface and base mixtures provided by the SST at 40 °C.[1]

ALF Ranking at 58 °C and a 20-mm Rut Depth		French PRT at 60 °C	Georgia LWT at 40 °C	Hamburg WTD at 50 °C	Repeated Load Test at 40 °C or 58 °C
AC-20 Base	A	B	A	B	A
AC-5 Base	B	D	C	C	C
AC-20 Surface	C	A	B	A	B
AC-5 Surface	D	C	D	D	D

Simple Shear at Constant Height and 40 °C

ALF Ranking at 58 °C and a 20-mm Rut Depth		Compliance Parameter, 1/MPa	Permanent Shear Strain, 10^{-6} mm/mm	Maximum Axial Stress, kPa
AC-20 Base	A	A	A	B
AC-5 Base	B	C	C	C
AC-20 Surface	C	B	B	A
AC-5 Surface	D	D	D	D

Frequency Sweep at Constant Height and 40 °C

ALF Ranking at 58 °C and a 20-mm Rut Depth		Shear Modulus G*, at 10.0 Hz, MPa	Shear Modulus G*, at 2.0 Hz, MPa	G*/sinδ, 10.0 Hz, MPa	G*/sinδ, 2.0 Hz, MPa	Slope of Log G* vs. Log Frequency
AC-20 Base	A	A	A	A	A	D
AC-5 Base	B	C	C	C	C	A
AC-20 Surface	C	B	B	B	B	C
AC-5 Surface	D	D	D	D	D	B

[1]The letters are the ranking according to the averages, with "A" denoting the mixture with the lowest susceptibility to rutting.

Table 65. Non-statistical rankings for the surface and base mixtures provided by the SST at 40 °C (continued).[1]

ALF Ranking at 58 °C and a 20-mm Rut Depth		Repeated Shear at Constant Height and 40 °C: Slope of Cumulative Permanent Strain	Repeated Shear at Constant Height and 40 °C: Cumulative Permanent Strain at 5,000 Cycles, 10^{-6} mm/mm
AC-20 Base	A	A	A
AC-5 Base	B	C	B
AC-20 Surface	C	B	C
AC-5 Surface	D	B	D

[1]The letters are the ranking according to the averages, with "A" denoting the mixture with the lowest susceptibility to rutting.

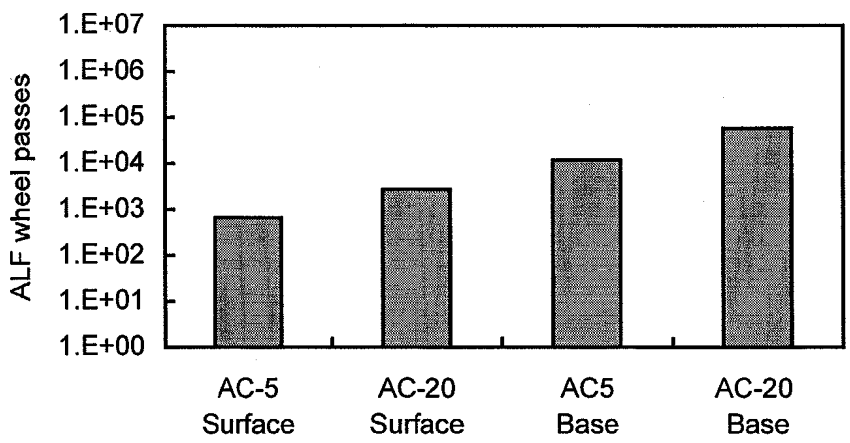

Figure 57. ALF wheel passes at a 20-mm rut depth vs. mixture type.

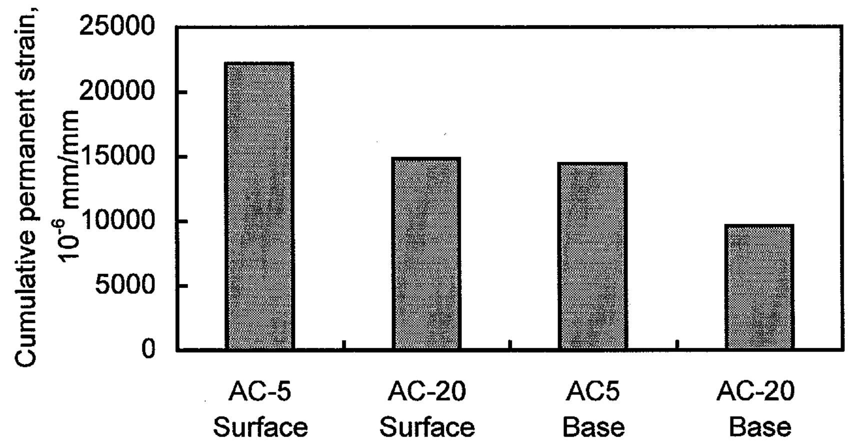

Figure 58. Cumulative permanent strain at 40 °C and 5,000 cycles.

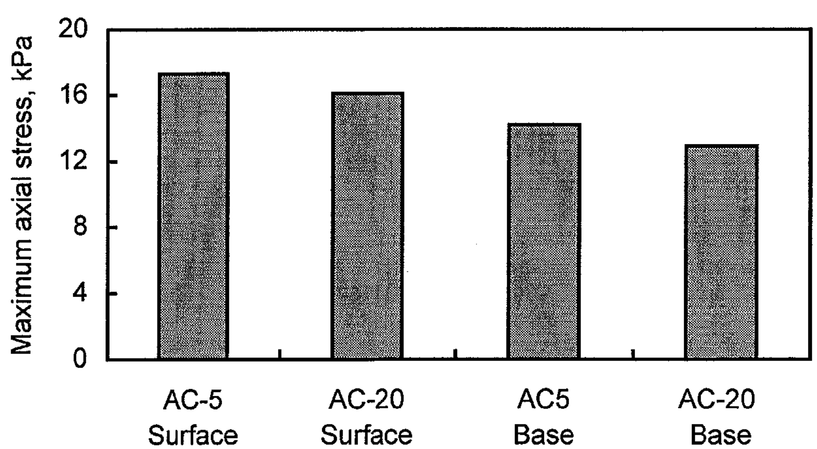

Figure 59. Maximum axial stress at 58 °C.

Table 66. Results from *t*-tests showing the effect of nominal maximum aggregate size and the associated decrease on optimum binder content (continued).[1]

		Frequency Sweep at Constant Height and 40 °C				
ALF Ranking at 58 °C and a 20-mm Rut Depth		Shear Modulus G*, at 10.0 Hz, MPa	Shear Modulus G*, at 2.0 Hz, MPa	G*/sinδ, 10.0 Hz, MPa	G*/sinδ, 2.0 Hz, MPa	Slope of Log G* vs. Log Frequency
AC-20 Base	A	291* A	126* A	353* A	147* A	0.44 B
AC-20 Surface	B	222 A	103 A	256 B	119 A	0.35 A
AC-5 Base	A	93* A	48* A	113* A	60* A	0.27 A
AC-5 Surface	B	62 B	34 B	71 B	39 B	0.31 B

		Repeated Shear at Constant Height and 40 °C	
ALF Ranking at 58 °C and a 20-mm Rut Depth		Slope of Cumulative Permanent Strain	Cumulative Permanent Strain at 5,000 Cycles, 10^{-6} mm/mm
AC-20 Base	A	0.30* A	9 640* A
AC-20 Surface	B	0.35 A	14 820 B
AC-5 Base	A	0.45 B	14 460* A
AC-5 Surface	B	0.35* A	22 200 A

[1]The letters are the statistical ranking, with "A" denoting the mixture with the lowest susceptibility to rutting.

*Better average value in terms of lower rutting susceptibility.

Table 67. SST results for surface and base mixtures at 58 °C.

ALF Ranking at 58 °C and a 20-mm Rut Depth		Simple Shear at Constant Height and 58 °C		
		Compliance Parameter, 1/MPa	Permanent Shear Strain, 10^{-6} mm/mm	Maximum Axial Stress, kPa
AC-20 Base	A	0.876	11 300	12.9
AC-5 Base	B	1.140	14 500	14.2
AC-20 Surface	C	1.720	22 700	16.1
AC-5 Surface	D	1.390	18 800	17.3

ALF Ranking at 58 °C and a 20-mm Rut Depth		Frequency Sweep at Constant Height and 58 °C				
		Shear Modulus G*, at 10.0 Hz, MPa	Shear Modulus G*, at 2.0 Hz, MPa	G*/sinδ, 10.0 Hz, MPa	G*/sinδ, 2.0 Hz, MPa	Slope of Log G* vs. Log Frequency
AC-20 Base	A	95	82	139	101	0.10
AC-5 Base	B	74	114	134	131	0.04
AC-20 Surface	C	89	70	125	116	0.10
AC-5 Surface	D	71	60	138	127	0.08

ALF Ranking at 58 °C and a 20-mm Rut Depth		Repeated Shear at Constant Height and 58 °C	
		Slope of Cumulative Permanent Strain	Cumulative Permanent Strain at 5,000 Cycles, 10^{-6} mm/mm
AC-20 Base	A	0.33	34 020
AC-5 Base	B	NT	NT
AC-20 Surface	C	0.35	34 200
AC-5 Surface	D	NT	NT

NT = Not tested.

Table 68. Statistical rankings for the surface and base mixtures provided by the SST at 58 °C.[1]

ALF Ranking at 58 °C and a 20-mm Rut Depth		Simple Shear at Constant Height and 58 °C: Compliance Parameter, 1/MPa	Permanent Shear Strain, 10^{-6} mm/mm	Maximum Axial Stress, kPa
AC-20 Base	A	A	A	A
AC-5 Base	B	A	AB	AB
AC-20 Surface	C	B	B	B
AC-5 Surface	D	AB	AB	B

ALF Ranking at 58 °C and a 20-mm Rut Depth		Frequency Sweep at Constant Height and 58 °C: Shear Modulus G*, at 10.0 Hz, MPa	Shear Modulus G*, at 2.0 Hz, MPa	G*/sinδ, 10.0 Hz, MPa	G*/sinδ, 2.0 Hz, MPa	Slope of Log G* vs. Log Frequency
AC-20 Base	A	A	A	A	A	B
AC-5 Base	B	A	A	A	A	A
AC-20 Surface	C	A	A	A	A	B
AC-5 Surface	D	A	A	A	A	AB

ALF Ranking at 58 °C and a 20-mm Rut Depth		Repeated Shear at Constant Height and 58 °C: Slope of Cumulative Permanent Strain	Cumulative Permanent Strain at 5,000 Cycles, 10^{-6} mm/mm
AC-20 Base	A	No Ranking	No ranking
AC-5 Base	B		
AC-20 Surface	C		
AC-5 Surface	D		

[1]The letters are the statistical ranking, with "A" denoting the mixture with the lowest susceptibility to rutting.

Table 69. SST results at 40 °C for the surface and base mixtures using specimens prepared in the laboratory with a diameter of 150 mm and a height of 75 mm.

ALF Ranking at 58 °C and a 20-mm Rut Depth		Simple Shear at Constant Height and 40 °C: Compliance Parameter, 1/MPa		Permanent Shear Strain, 10^{-6} mm/mm		Maximum Axial Stress, kPa	
AC-20 Base	A	0.530	A	14 000	A	32.8	A
AC-5 Base	B	1.109	B	29 400	B	46.5	B
AC-20 Surface	C	0.941	B	25 900	B	31.6	A
AC-5 Surface	D	1.521	C	42 200	C	43.5	B

ALF Ranking at 58 °C and a 20-mm Rut Depth		Frequency Sweep at Constant Height and 40 °C: Shear Modulus[1] G*, at 10.0 Hz, MPa		Shear Modulus G*, at 2.0 Hz, MPa		Slope of Log G* vs. Log Frequency	
AC-20 Base	A	279	A	119	A	0.46	C
AC-5 Base	B	85	C	42	C	0.32	B
AC-20 Surface	C	208	B	89	B	0.42	C
AC-5 Surface	D	61	D	31	D	0.27	A

[1]Statistical ranking is based on $\log_{10}$ of the value.

Table 70. SST results at 58 °C for the surface and base mixtures using specimens prepared in the laboratory with a diameter of 150 mm and a height of 75 mm.

ALF Ranking at 58 °C and a 20-mm Rut Depth		Simple Shear at Constant Height and 58 °C: Compliance Parameter, 1/MPa		Permanent Shear Strain, 10^{-6} mm/mm		Maximum Axial Stress, kPa	
AC-20 Base	A	1.228	A	12 500	A	14.0	A
AC-5 Base	B	1.826	A	18 700	A	17.6	BC
AC-20 Surface	C	1.559	A	19 200	A	19.9	C
AC-5 Surface	D	1.506	A	19 300	A	16.9	B

ALF Ranking at 58 °C and a 20-mm Rut Depth		Frequency Sweep at Constant Height and 58 °C: Shear Modulus G*, at 10.0 Hz, MPa		Shear Modulus[1] G*, at 2.0 Hz, MPa		Slope of Log G* vs. Log Frequency	
AC-20 Base	A	69	A	45	A	0.14	C
AC-5 Base	B	48	B	37	B	0.10	B
AC-20 Surface	C	63	A	44	A	0.12	BC
AC-5 Surface	D	60	A	50	A	0.05	A

ALF Ranking at 58 °C and a 20-mm Rut Depth		Repeated Shear at Constant Height and 58 °C: Slope of Cumulative Permanent Strain		Cumulative Permanent Strain at 500 Cycles,[1,2] 10^{-6} mm/mm	
AC-20 Base	A	0.56	A	6 670	A
AC-5 Base	B	0.79	B	15 600	B
AC-20 Surface	C	0.56	A	8 200	A
AC-5 Surface	D	0.76	B	20 100	B

[1]Statistical ranking is based on $\log_{10}$ of the value.
[2]The data were compared at 500 cycles rather than at 5000 cycles because the specimens failed rapidly.

g. Results From the SST for the Surface vs. Base Mixture Study at 40 and 58 °C Using Specimens With a Diameter of 203 mm and a Height of 75 mm

Tables 71 and 72 show data using specimens compacted by the GTM having a diameter of 203 mm and a height of 75 mm. The use of this specimen size did not improve the degree of correlation to ALF pavement performance.

11. Tests Using the Purdue University Wheel Test Device (PURWheel)

a. Description of the Equipment

Slabs from the pavements were tested by Purdue University using the PURWheel. This work was not part of the original work plan but was added when the device became available. Pavement slabs were used for evaluating the PURWheel, while slabs prepared and compacted in the laboratory were used for evaluating the French PRT, Georgia LWT, and Hamburg WTD. However, slabs sawed from lanes 9, 10, 11, and 12 were also tested by the French PRT, Georgia LWT, and Hamburg WTD for the surface vs. base mixture study. The data are given in chapter 5.

The PURWheel was developed by the Purdue University based on the Hamburg WTD, but it was designed to be more versatile. The PURWheel can test slabs as large as 620 mm by 305 mm with a maximum height of 127 mm. Each wheel is moved by an air cylinder that provides a constant speed over the section of the slab where the rut is measured. Sensors in the air cylinders maintain the speed by controlling the air pressure. Speeds from 0.20 to 0.40 m/s can be applied. A solid steel wheel with a width up to 100 mm, or pneumatic rubber tire with an inflation pressure up to 860 kPa, can be used. The rubber tire can be programmed to wander. A load from 500 to 1900 N can be applied. The rut depths are measured at 10 locations along the wheel path at a spacing of 10 mm using LVDT's. Rut depth measurements are made at equal time intervals, such as at every 250 wheel passes.

A test temperature in the range of 25.0 to 60.0 ±0.2 °C can be chosen. Slabs can be tested in a dry state or under water like the Hamburg WTD. When testing in a dry state, water surrounding the steel container is used to heat the slabs from the bottom, while an enclosed chamber allows the air above the slab to be heated. The slabs are conditioned at the test temperature for 2 h. The temperature above and below the slab is recorded every 250 wheel passes.

The slabs tested in this study were cut longitudinally from the wheelpaths of the pavements, but outside of the area where the ALF would test the pavements. The dimensions were 305 by 290 by 76 mm in height. The AC-5, AC-10, AC-20, Novophalt, and Styrelf surface mixture slabs had initial average air-void levels of 6.5, 7.1, 8.0, 9.5, and 8.5 percent, respectively. The AC-5 and AC-20 (PG 59 and 70) base mixtures had initial average air-void levels of 6.1 and 7.2 percent. Four replicate slabs were tested per mixture at 58 °C.

A pneumatic, saw toothed, rubber tire was used with no wheel wander. The contact pressure was 620 kPa, and the inflation pressure was 830 kPa. The load was 1530 N and the speed was 0.33 m/s (1.2 km/h). All slabs were tested in a dry state. Like the other three wheel-tracking devices used in this study, only the downward rut depth was measured.

b. Results From the PURWheel

The average data and statistical rankings are shown in table 73. The statistical rankings show that the PURWheel divided the seven mixtures into three groups. A linear regression between the ALF rut depths at 2,730 wheel passes and the PURWheel rut depths provided an r^2 of 0.78. The r^2 using log ALF wheel passes at a 20-mm rut depth was 0.82. The statistical ranking for the five surface mixtures reasonably agreed with ALF. The statistical rankings for the four mixtures used in the surface vs. base mixture study were not the same as the rankings provided by the other wheel-tracking devices, the repeated load compression test, and the SST. The PURWheel data matched the ALF pavement results in terms of the effect of nominal maximum aggregate size on rutting susceptibility, but it did not measure the effects of binder grade.

12. Comments on the Validation Effort

Pavement performance at 58 °C was used for validating the mixture tests because this was the only temperature at which all seven mixtures were tested. Comparing the data from the wheel-tracking devices to the pavement data at 58 °C seemed reasonable because the French PRT and Hamburg WTD methodologies were based on heavy traffic volumes and a Superpave high-temperature PG of approximately 58 °C. The Georgia LWT methodology was based on heavy traffic volumes and a temperature of approximately 64 °C. Even so, the rankings provided by the ALF would be different at pavement temperatures above and below 58 °C. This is shown by the hypothetical rankings in table 74 for temperatures other than 58 °C. At temperatures of 46 to 52 °C, the two mixtures with the modified binders would not be expected to fail by rutting. At temperatures of 70 to 76 °C, all three surface mixtures with the unmodified binders would be expected to fail rapidly. Less than 2,800 wheel passes were needed to fail these three surface mixtures at 58 °C. The hypothetical rankings are presented to show that there should be more than one statistical ranking for pavement rutting performance.

The loading frequency and test temperature for the ALF and the mixture tests were not always the same. Since the performance of a binder in an asphalt mixture is dependent on frequency and temperature, it should not be expected that the rankings perfectly agree. Even so, the rankings in table 54 point to one problem. The Georgia LWT correctly ranked the five surface mixtures based on the average data, but the statistical rankings indicated that the rutting performances of the Styrelf and AC-20 (PG 70) mixtures were not significantly different. This is not correct based on ALF pavement performance at 58 °C. The ranking indicated that the Georgia LWT may only be able to measure the effect of binder grade when the grades are widely different. Thus, the test can be considered deficient because a mix designer generally has to choose between binders that have relatively close grades, such as between a PG 64-22 and a PG 70-22. However, the Georgia LWT did rank the Styrelf and AC-20 (PG 70) mixtures differently at a 93-percent confidence level. This indicates that either the variability of data has to be reduced, or the testing protocol, such as the test temperature, has to be changed to increase the range in the data.

13. Supplementary Analysis: Shear Modulus vs. Compression Modulus

The shear moduli, $|G^*|$, of the seven mixtures vs. frequency were measured by the SST Frequency Sweep test at 40 and 58 °C. This included the standard frequency of 10.0 Hz. Resilient compression moduli, E_{res}, and dynamic compression moduli, E_{dyn}, were measured by the unconfined repeated load compression test at 10.0 Hz and 40 and 58 °C using a 0.1-s loading time followed by a 0.9-s rest period. E_{res} is calculated using the recovered strain per cycle of loading, while E_{dyn} is calculated using the total strain per cycle of loading. E_{dyn} can also be described as $|E^*|$. Poisson's ratios were calculated using elastic theory:

$$\mu = [E/2G]-1$$

where: μ = Poisson's ratio,
E = Compression modulus, and
G = Shear modulus.

Two sets of Poisson's ratios were calculated. One set was based on $|G^*|$ and E_{res}, while the other set was based on $|G^*|$ and E_{dyn}. The data at 40 °C are given in table 75. E_{res} and E_{dyn} were not significantly different because the percentage of the total strain that was permanent per cycle of loading was generally small for each mixture. The largest difference in these compression moduli was 21 percent, which was provided by the AC-20 (PG 70) surface mixture. The difference for the other mixtures was 10 percent or less. The high Poisson's ratios in table 75 indicate that the shear and compression moduli do not obey the laws of elasticity for isotropic, elastic materials. Theoretically, the ratios cannot be greater than 0.5.

The repeated load compression test was a stress-controlled test, whereas the SST was a strain-controlled test. However, if both modes of loading are performed in the linear range, where the modulus is independent of the applied stress or strain level, both modes should give the same modulus for a given mixture. The repeated load compression test at 40 °C was performed in the linear range. This was determined prior to testing. The small differences between E_{res} and E_{dyn} for most of the mixtures in table 75 also indicate the data were taken in the linear range.

The Frequency Sweep test was performed using a peak strain of ±0.10 μm/mm. When using this test, it is assumed that the data are recorded in the linear range. To determine if this was true, the AC-5 (PG 59) surface mixture was tested using six peak strains (±0.02, ±0.10, ±0.20, ±0.40, ±0.60, and ±0.80 μm/mm) and four frequencies (10.0, 1.0, 0.1, and 0.01 Hz). The total strain applied to each specimen, also called the peak-to-peak strain, is double the peak strain: 0.04, 0.20, 0.40, 0.80, 1.20, and 1.60 μm/mm. The AC-5 (PG 59) surface mixture was chosen because it had the lowest $|G^*|$. It was hypothesized that the response of this mixture should become nonlinear at a strain that is lower than for the other mixtures.

The results are shown in figures 60, 61, and 62. The data indicate that the moduli were relatively high at a peak strain of ±0.02 μm/mm. The data were also highly variable from replicate to replicate. Most likely, the response at ±0.02 μm/mm was the result of the inability of the equipment to accurately apply this strain or measure the resultant stress. For this reason, both a minimum and a maximum strain are normally used to describe the linear range. Figures 60 and 61 indicate that a strain in the range of ±0.40 to ±0.60 μm/mm should be used instead of ±0.10 μm/mm for this mixture. The moduli were virtually the same at these higher strains. This points out a discrepancy in AASHTO TP7-94. This test limits the strain to 0.10 μm/mm, but then states that a strain of 0.50 μm/mm should be applied to the specimen. It is also unclear whether these strains are peak strains or peak-to-peak strains. Based on figures 60 and 61, a peak strain of ±0.40 to ±0.60 μm/mm should be used. Figure 62 shows that the data were also highly variable using a frequency of 0.01 Hz. This indicated that some adjustment in the equipment is needed when using this frequency.

The use of a peak strain greater than ±0.10 μm/mm for the AC-5 (PG 59) surface mixture would decrease $|G^*|$ slightly. A decrease in $|G^*|$ would increase the Poisson's ratio, which was already too high based on the laws of elasticity for isotropic materials. It was concluded that nonlinearity was not the reason for the high Poisson's ratios.

A reason for the high Poisson's ratios was not evident, but if the tension and compression moduli of an asphalt mixture are not equal, the elastic equation used to calculate Poisson's ratio is not valid. To determine whether these moduli are the same, the repeated load compression test would have to be modified so that both compression and tension are applied to the same specimen. Tension moduli were not measured in this study because they are not used to evaluate rutting.

The data for the tests at 58 °C are given in table 76. The E_{dyn}'s are lower than the E_{res}'s because the percentage of the total strain that was permanent per cycle of loading was high for each mixture. The Poisson's ratios are negative using E_{dyn} for the same reason: the permanent deformations were high in the compression test. $|G^*|$ and E_{res} provided more reasonable ratios, except for the ratios using the two larger SST specimen sizes. As specimen size increased, $|G^*|$ decreased, which increased the ratios. Tables 75 and 76 also show that the $|G^*|$'s of the AC-5 (PG 59) surface mixture at 58 °C were higher than or equal to those at 40 °C using SST specimens sizes of 150 by 50 mm and 150 by 75 mm. More extensive research would be needed to provide reasons for these findings.

Table 71. SST results at 40 °C for the surface and base mixtures using specimens prepared in the laboratory with a diameter of 203 mm and a height of 75 mm.

ALF Ranking at 58 °C and a 20-mm Rut Depth		Simple Shear at Constant Height and 40 °C: Compliance Parameter, 1/MPa		Permanent Shear Strain[1], 10^{-6} mm/mm		Maximum Axial Stress, kPa	
AC-20 Base	A	0.350	A	16 600	A	66.2	A
AC-5 Base	B	0.410	A	18 700	A	75.0	A
AC-20 Surface	C	0.397	A	18 600	A	71.8	A
AC-5 Surface	D	0.595	B	31 800	B	83.0	A

ALF Ranking at 58 °C and a 20-mm Rut Depth		Frequency Sweep at Constant Height and 40 °C: Shear Modulus[1] G*, at 10.0 Hz, MPa		Shear Modulus[1] G*, at 2.0 Hz, MPa		Slope of Log G* vs. Log Frequency	
AC-20 Base	A	265	A	108	A	0.57	C
AC-5 Base	B	119	C	49	C	0.44	A
AC-20 Surface	C	213	B	82	B	0.53	BC
AC-5 Surface	D	92	D	36	D	0.46	AB

ALF Ranking at 58 °C and a 20-mm Rut Depth		Repeated Shear at Constant Height and 40 °C: Slope of Cumulative Permanent Strain		Cumulative Permanent Strain at 5000 Cycles, 10^{-6} mm/mm	
AC-20 Base	A	0.41	A	2 560	A
AC-5 Base	B	0.43	A	4 820	B
AC-20 Surface	C	0.42	A	3 270	A
AC-5 Surface	D	0.42	A	5 960	B

[1]Statistical ranking is based on $\log_{10}$ of the value.

Table 72. SST results at 58 °C for the surface and base mixtures using specimens prepared in the laboratory with a diameter of 203 mm and a height of 75 mm.

ALF Ranking at 58 °C and a 20-mm Rut Depth		Frequency Sweep at Constant Height and 58 °C: Log Shear Modulus[1] G*, at 10.0 Hz, MPa		Log Shear Modulus[1] G*, at 2.0 Hz, MPa		Slope of Log G* vs. Log Frequency	
AC-20 Base	A	55	A	32	A	0.16	B
AC-5 Base	B	34	C	24	B	0.10	A
AC-20 Surface	C	44	B	26	B	0.15	B
AC-5 Surface	D	34	C	24	B	0.11	A

ALF Ranking at 58 °C and a 20-mm Rut Depth		Repeated Shear at Constant Height and 58 °C: Slope of Cumulative Permanent Strain		Cumulative Permanent Strain at 500 Cycles,[2] 10^{-6} mm/mm	
AC-20 Base	A	0.53	A	5 310	A
AC-5 Base	B	0.62	B	8 270	B
AC-20 Surface	C	0.59	AB	8 790	B
AC-5 Surface	D	0.60	AB	7 470	AB

[1]Statistical ranking is based on $\log_{10}$ of the value.
[2]The data were compared at 500 cycles rather than at 5000 cycles because the specimens failed rapidly.

Table 73. Rankings for the rut depths from the Purdue University Wheel Test Device (PURWheel) at 20,000 wheel passes and 58 °C.[1]

Ranking Based on ALF at 58 °C	PURWheel Data		Ranking Based on the Average Rut depth, mm	Statistical Rankings at a 95-Percent Confidence Level Based on Log Rut Depth, mm		
	Rut Depth, mm	Log Rut Depth, mm		All Mixtures	Surface Mixtures	Surface vs. Base Mixtures
Novophalt	1.4	0.15	A	A	A	
Styrelf	2.7	0.42	B	B	B	
AC-20 Base	3.6	0.56	D	B		A
AC-5 Base	3.1	0.49	C	B		A
AC-20[2]	6.5	0.80	E	C	C	B
AC-10	7.4	0.85	G	C	C	
AC-5	6.6	0.82	F	C	C	B

[1]The letters are the ranking, with "A" denoting the mixture with the lowest susceptibility to rutting.

[2]The replicate data showed that there may be one outlier for the AC-20 (PG 70) slabs, but eliminating this datum had no effect on the conclusions or statistical rankings.

Table 74. ALF rankings based on the number of wheel passes needed to obtain rut depths of 10, 15, and 20 mm in the asphalt pavement layer.[1]

Hypothetical Ranking at 46 to 52 °C	Actual Ranking at 58 °C	Actual Ranking at 58 °C	Hypothetical Ranking at 70 to 76 °C
Rut Depth of 10 to 20 mm	Rut Depth of of 10 mm	Rut Depth of 15 to 20 mm	Rut Depth of 10 to 20 mm
(A) Novophalt	(A) Novophalt	(A) Novophalt	(A) Novophalt
(A) Styrelf	(B) Styrelf	(B) Styrelf	(B) Styrelf
(B) AC-20	(C) AC-20	(C) AC-20	(C) AC-20
(C) AC-10	(CD) AC-10	(C) AC-10	(C) AC-10
(D) AC-5	(D) AC-5	(D) AC-5	(C) AC-5

[1]The letters are the ranking, with "A" denoting the mixture with the lowest susceptibility to rutting.

Table 75. Poisson's ratios at 40 °C for the seven mixtures calculated using the shear modulus from the SST and the resilient and dynamic moduli from the repeated load compression test.

Mixture	SST Shear Modulus, |G*|, 10.0 Hz, MPa	Compression Moduli, at 10.0 Hz, MPa		Poisson's Ratio μ = [E/2G)]-1, using	
		E_{res}	E_{dyn}	E_{res}	E_{dyn}
Novophalt[1]	409	1720	1720	1.10	1.10
Styrelf[1]	281	2780	2760	3.95	3.91
AC-20[1]	222	2330	1900	4.25	3.28
AC-20[2]	208	2330	1900	4.60	3.57
AC-20[3]	213	2330	1900	4.47	3.46
AC-10[1]	134	725	800	1.71	1.99
AC-5[1]	62	466	464	2.76	2.74
AC-5[2]	61	466	464	2.82	2.80
AC-5[3]	92	466	464	1.53	1.52
AC-20 Base[1]	291	2370	2320	3.07	2.99
AC-20 Base[2]	279	2370	2320	3.25	3.16
AC-20 Base[3]	265	2370	2320	3.47	3.38
AC-5 Base[1]	93	560	600	2.01	2.23
AC-5 Base[2]	85	560	600	2.29	2.53
AC-5 Base[3]	119	560	600	1.35	1.52
Using SST Specimens with a Diameter and Height of 150 mm by 50 mm:					
Novophalt	409	1720	1720	1.10	1.10
Styrelf	281	2780	2760	3.95	3.91
AC-20	222	2330	1900	4.25	3.28
AC-10	134	725	800	1.71	1.99
AC-5	62	466	464	2.76	2.74
AC-20 Base	291	2370	2320	3.07	2.99
AC-5 Base	93	560	600	2.01	2.23

[1]Using SST specimens with a diameter and height of 150 mm by 50 mm.
[2]Using SST specimens with a diameter and height of 150 mm by 75 mm.
[3]Using SST specimens with a diameter and height of 203 mm by 75 mm.

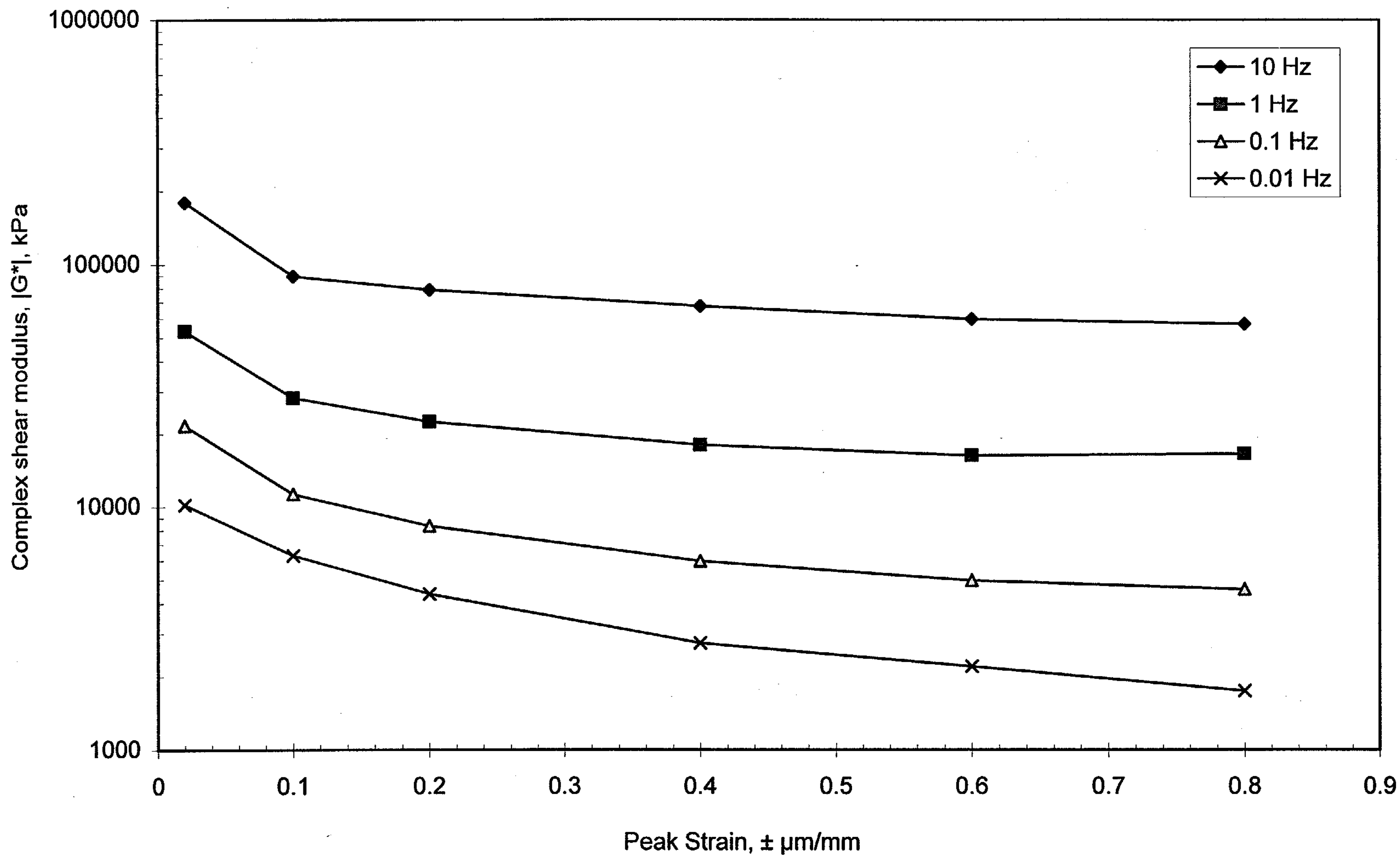

Figure 60. Shear modulus vs. applied strain.

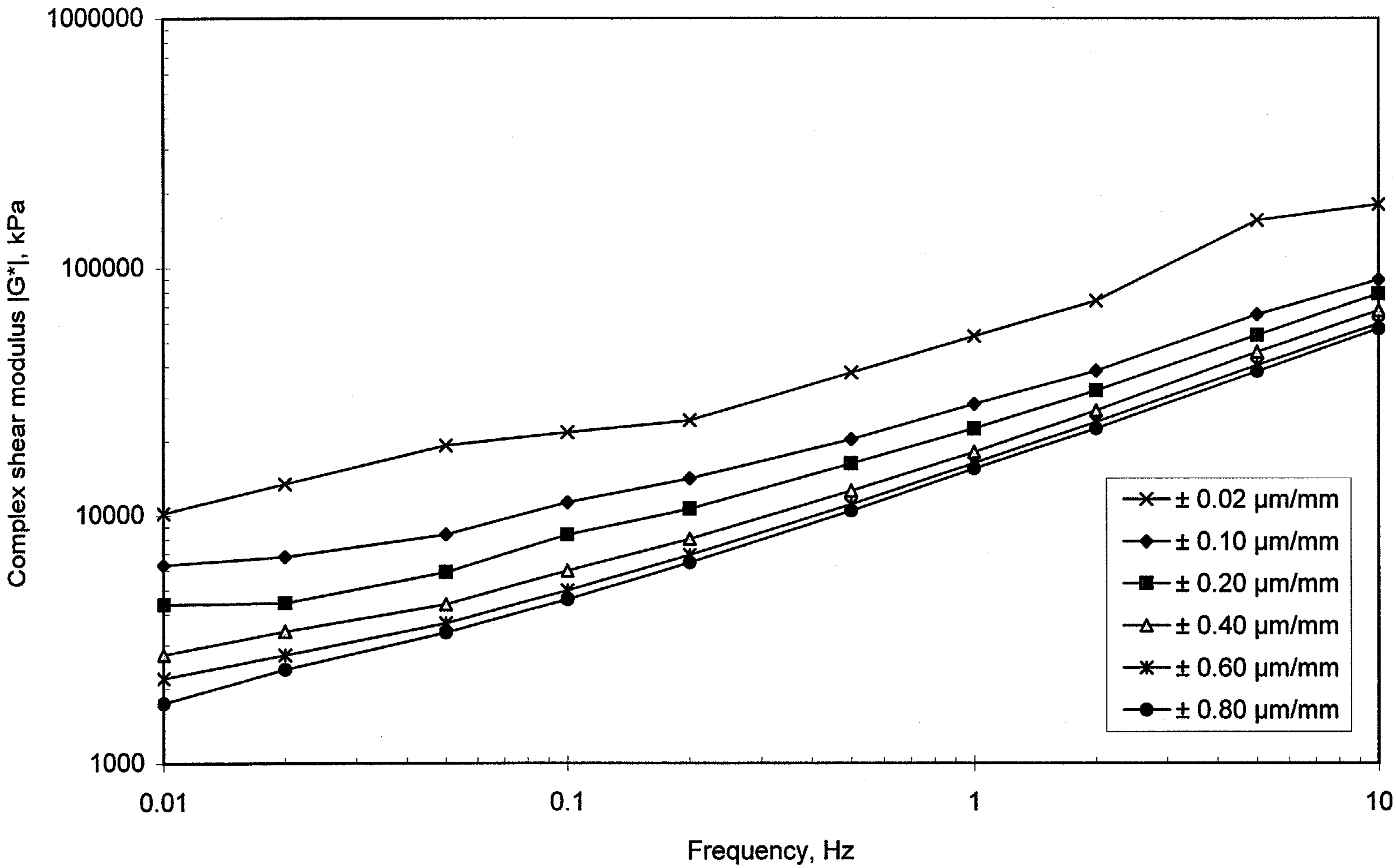

Figure 61. Shear modulus vs. applied frequency.

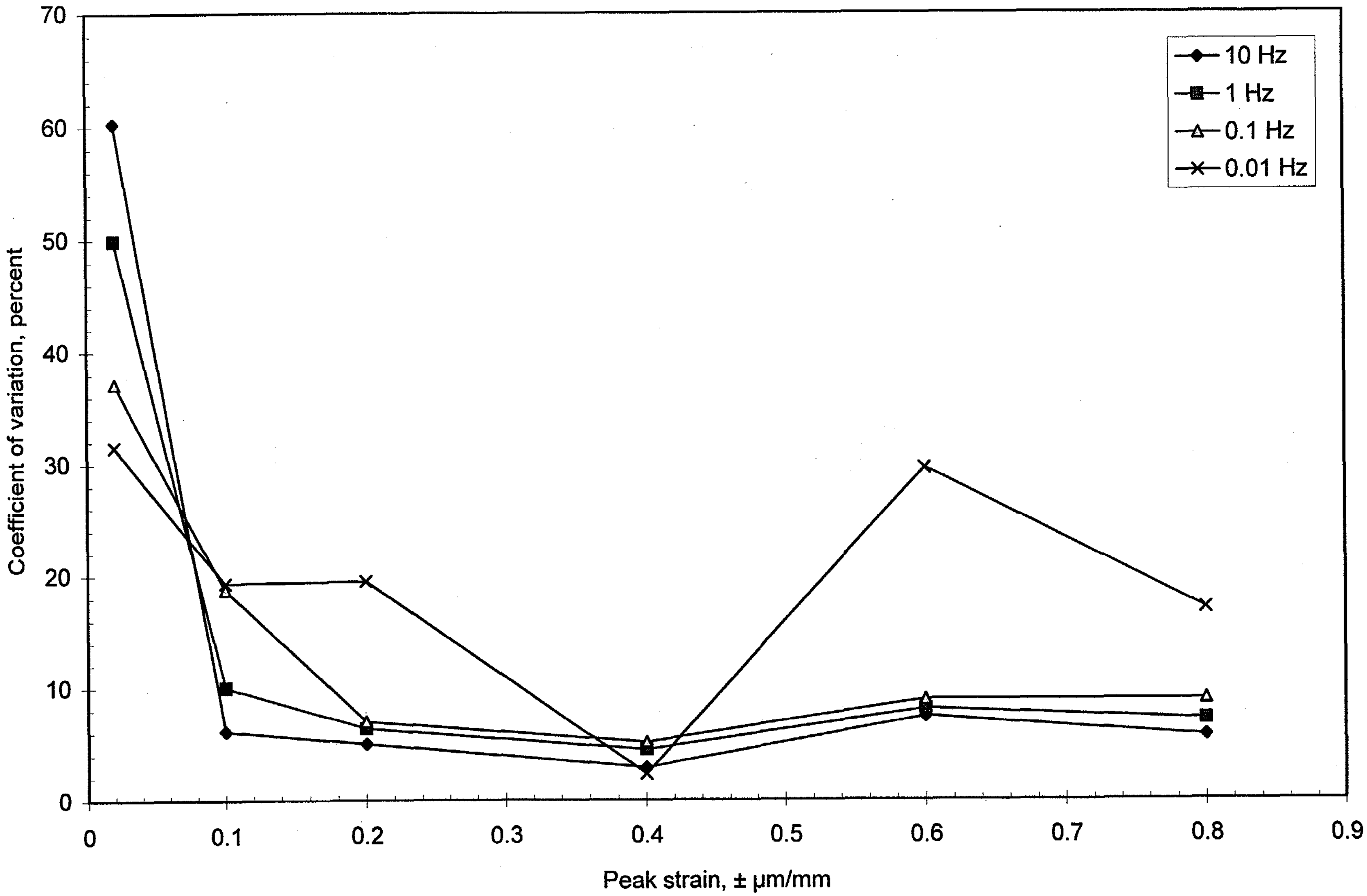

Figure 62. Coefficient of variation for the shear modulus vs. applied strain.

Table 76. Poisson's ratios at 58 °C for the seven mixtures calculated using the shear modulus from the SST and the resilient and dynamic moduli from the repeated load compression test.

Mixture	SST Shear Modulus, |G*|, 10.0 Hz, MPa	Compression Moduli, at 10.0 Hz, MPa		Poisson's Ratio μ = [E/2G)]-1, using	
		E_{res}	E_{dyn}	E_{res}	E_{dyn}
Novophalt[1]	170	427	258	0.26	-0.24
Styrelf[1]	93	370	176	0.99	-0.05
AC-20[1]	89	239	65	0.34	-0.63
AC-20[2]	63	239	65	0.90	-0.48
AC-20[3]	44	239	65	1.72	-0.26
AC-10[1]	66	199	58	0.51	-0.56
AC-5[1]	71	176	61	0.24	-0.57
AC-5[2]	60	176	61	0.47	-0.49
AC-5[3]	34	176	61	1.59	-0.10
AC-20 Base[1]	95	280	80	0.47	-0.58
AC-20 Base[2]	69	280	80	1.03	-0.42
AC-20 Base[3]	55	280	80	1.55	-0.27
AC-5 Base[1]	74	218	55	0.47	-0.63
AC-5 Base[2]	48	218	55	1.27	-0.43
AC-5 Base[3]	34	218	55	2.21	-0.19
Using SST Specimens with a Diameter and Height of 150 mm by 50 mm:					
Novophalt	170	427	258	0.26	-0.24
Styrelf	93	370	176	0.99	-0.05
AC-20	89	239	65	0.34	-0.63
AC-10	66	199	58	0.51	-0.56
AC-5	71	176	61	0.24	-0.57
AC-20 Base	95	280	80	0.47	-0.58
AC-5 Base	74	218	55	0.47	-0.63

[1]Using SST specimens with a diameter and height of 150 mm by 50 mm.
[2]Using SST specimens with a diameter and height of 150 mm by 75 mm.
[3]Using SST specimens with a diameter and height of 203 mm by 75 mm.

14. Conclusions

a. Surface Mixtures

- The French PRT, Georgia LWT, and Hamburg WTD ranked the five surface mixtures the same as ALF based on the averages. Each test provided a slightly different statistical ranking based on Fisher's LSD. The French PRT and Hamburg WTD provided statistical rankings that were slightly better than the Georgia LWT, probably because the range in the data from the best to the worst mixture was smaller for the Georgia LWT.

- The dynamic moduli at 200 cycles and the cumulative permanent strains at 10,000 cycles from the unconfined repeated load compression test at 58 °C ranked the five surface mixtures the same as ALF based on the averages. The statistical rankings were slightly different, but the degree of correlation was good. The slopes from the relationship between cumulative permanent strain and cycles did not differentiate the five surface mixtures according to rutting susceptibility.

- Six of eight SST measurements at 40 °C ranked the five surface mixtures the same as ALF based on the averages: (1) the compliance parameter, permanent shear strain, and maximum axial stress from Simple Shear at Constant Height, (2) G^* and $G^*/\sin\delta$ at all frequencies from Frequency Sweep at Constant Height, and (3) cumulative permanent strain at 5,000 cycles from Repeated Shear at Constant Height.

- The two SST measurements at 40 °C that did not correlate with ALF were the slopes from the relationship between log G^* and log frequency from Frequency Sweep at Constant Height, and the slopes from the relationship between cumulative permanent strain and cycles from Repeated Shear at Constant Height.

- The statistical rankings for the six promising SST measurements at 40 °C were generally different. However, the statistical rankings for the compliance parameter and permanent shear strain from Simple Shear at Constant Height were identical to the statistical ranking provided by the ALF. The statistical rankings provided by G^*, $G^*/\sin\delta$, and cumulative permanent strain at 5,000 cycles were not identical to ALF, but the degree of correlation was good. The maximum axial stress correlated less with ALF pavement performance based on the statistical rankings.

- The degree of correlation between the SST data at 58 °C and ALF pavement performance was poor. Most SST measurements at 58 °C had coefficients of variation (standard deviation divided by the average) of 20 percent and greater, whereas the coefficients at 40 °C were generally less than 20 percent. The coefficients of variation were based on the data from the surface mixtures which consisted of five binder grades, a single aggregate gradation, and a single binder content.

- The PURWheel did not rank the five mixtures the same as ALF based on the averages. However, the statistical ranking was reasonably close to the statistical ranking provided by the ALF.

b. Surface vs. Base Mixture Study (Four Mixtures Consisting of Two Gradations and Two Binders)

- The increase in nominal maximum aggregate size from 19.0 to 37.5 mm, and the associated 0.85-percent decrease in optimum binder content, significantly decreased rutting susceptibility based on ALF pavement performance. Only two mixture tests ranked the four mixtures the same as ALF based on the averages: the cumulative permanent shear strain at 5,000 cycles and 40 °C from Repeated Shear at Constant Height, and the maximum axial stresses at 58 °C from Simple Shear at Constant Height.

- The majority of the specimens tested by the SST had a diameter and height of 150 mm by 50 mm. For the surface vs. base mixture study, tests were also performed on specimens having a diameter and height of 150 mm by 75 mm and 203 by 75 mm. The use of larger specimens did not provide better correlations to ALF pavement performance. Specimens with a height of 75 mm failed rapidly in Repeated Shear at 58 °C and the data had to be compared at 500 cycles rather than at 5,000 cycles.

- The PURWheel provided conclusions that differed from those provided by the French PRT, Georgia LWT, Hamburg WTD, unconfined repeated load compression test, and SST. For the surface vs. base mixture study, the data from the PURWheel were affected by nominal maximum aggregate size, but not by binder grade.

- No laboratory mixture test provided a statistical ranking for the four mixtures that matched ALF pavement performance. Some of the SST data were significantly affected by nominal maximum aggregate size, but the effect was not as great as the effect of nominal maximum aggregate size on ALF pavement performance.

c. Conclusions Using All Mixtures

- Marshall stabilities and flows did not differentiate the mixtures according to rutting susceptibility.

- The rutting parameters from the U.S. Corps of Engineers Gyratory Testing Machine did not differentiate the mixtures according to rutting susceptibility.

- The NCHRP AAMAS did not predict ALF pavement performance. Individual AAMAS test data, including compressive strength, compressive strain at failure, creep modulus, total creep strain, and permanent creep strain after unloading did not adequately predict ALF pavement performance. All tests were performed unconfined.

- The correlation between the PURWheel and ALF for the seven mixtures was reasonably good because the data were affected by nominal maximum aggregate size. A linear regression provided an r^2 of 0.8. The correlations for the other tests were poor because they could not measure the effects of nominal maximum aggregate size.

- The air voids in the specimens tested by the AAMAS creep test and the repeated load compression test did not decrease during testing. Therefore, these tests measured permanent deformation due to viscous flow (called shape distortion) without volume change (densification or volume distortion). The ALF, French PRT, Georgia LWT, Hamburg WTD, and PURWheel measure the combined effects of viscous flow and volume change. The SST was designed so that changes in volume would not occur during testing; thus, it was designed to measure only permanent deformation due to viscous flow.

- The laboratory mixture tests were performed according to customary procedures. However, most of these tests and the ALF pavement tests had different loading frequencies or test temperatures. Since the performance of a binder in an asphalt mixture is dependent on frequency and temperature, it should not be expected that the rankings from these tests agree perfectly.

d. Miscellaneous Conclusions

- A slab thickness of 100 mm is tested by the French PRT when the total pavement thickness for the mixture to be placed will be greater than 50 mm. A slab thickness of 50 mm is tested when the thickness will be equal to, or less than, 50 mm. The data showed that the rut depths tended to be greater using 50-mm slabs at an equal number of wheel passes.

- Even though the French PRT was found to be more severe using 50-mm-thick slabs, the French pass/fail specification was generally found to be more severe when testing 100-mm slabs. This means that the French methodology is more severe for mixtures to be used in thick, lower pavement layers.

- The resilient modulus at 10.0 Hz from the unconfined repeated load compression test and the shear modulus at 10.0 Hz from SST Frequency Sweep were used to calculate Poisson's ratios based on the laws of elasticity for isotropic materials. It was found that one modulus could not be calculated from the other modulus using an assumed Poisson's ratio. The moduli showed that the laws do not apply to the mixtures tested in this study.

15. Recommendations

- Overall, the French PRT at 60 °C, Georgia LWT at 40 °C, Hamburg WTD at 50 °C, unconfined repeated load compression test at 58 °C, and the SST at 40 °C provided similar conclusions. Therefore, any one of these tests can be used to estimate rutting potential at high temperatures. In this evaluation, the data from the unconfined repeated load compression test and SST were not used in a performance prediction model. The test data were directly compared against the ALF pavement test results.

- The correlation between the PURWheel and ALF for the seven mixtures was reasonably good; therefore, this test can also be used. Based on ALF pavement rutting performance, the PURWheel showed the effects of nominal maximum aggregate size, whereas the other tests did not. However, the other tests were more capable of measuring the effects of binder grade. (Note: Only pavement slabs were tested by the PURWheel. Slabs prepared and compacted in the laboratory were not tested.)

- A compression modulus at high temperatures should not be computed from the shear modulus and an assumed Poisson's ratio. Likewise, a shear modulus at high temperatures should not be computed from the compression modulus and an assumed Poisson's ratio.

CHAPTER 5: EFFECT OF COMPACTION METHOD ON RUTTING SUSCEPTIBILITY

1. Background and Objectives

Tables 47 and 59 showed that the data from the ALF and many of the mixture tests provided identical rankings for the five surface mixtures based on the average values, but different statistical rankings based on Fisher's LSD. However, tables 47, 48, 59, and 64 showed that the discrepancies for the five surface mixtures were not as significant as the discrepancies concerning nominal maximum aggregate size. Because of this, it was decided to determine if the method of compaction, mainly laboratory vs. field compaction, could affect the relative laboratory-determined rutting susceptibilities of the surface and base mixtures with AC-5 and AC-20 (PG 59 and 70).[31,32]

Table 77 provides rankings for the laboratory mixture tests and a ranking for ALF pavement performance based on the log wheel passes at a 20-mm rut depth. The ALF pavement ranking was provided by tests on lanes 9, 10, 11, and 12. This ranking represents long-term pavement performance. The rankings for the laboratory tests were previously reported in tables 48 and 64.

A second method of ranking the mixtures, based on the rut depths at 2,730 ALF wheel passes, was also used because mixtures tested by the laboratory wheel-tracking devices are evaluated at specified wheel passes. The rut depths at 2,730 ALF wheel passes were evaluated because this number of wheel passes provided a 20-mm rut depth in the asphalt pavement layer with the AC-20 (PG 70) surface mixture. The AC-20 (PG 70) surface mixture was considered the control mixture and a rut depth of 20 mm was defined as the failure level. (Note: A failure level of 15 mm provided the same ranking as a failure level of 20 mm.) The rut depth of 35 mm for the AC-5 (PG 59) surface mixture in table 77 was obtained through extrapolation.

As discussed in chapter 2, the problem encountered when evaluating the mixtures at a constant number of ALF wheel passes was that either excessive extrapolations had to be performed to obtain the rut depths for pavements that failed quickly, or the pavements had to be compared at wheel passes that were low relative to the lives of longest lasting pavements. Statistical rankings for the four mixtures based on the rut depths at 2,730 wheel passes are given in table 78. The validity of both ranking methods is questionable because the variances were not equal. The heterogeneity of the variances and the closeness of the average rut depths for the two base mixtures at 2,730 wheel passes significantly affected the rankings. Because of this, the rankings shown in table 78 were not used. Instead, the rutting performance of each base mixture relative to the surface mixture having the same binder grade was evaluated using a *t*-test at a 95-percent confidence level.

Both methods for defining ALF pavement performance provided the same conclusion: each base mixture had a significantly lower susceptibility to rutting compared with its associated surface mixture. Table 77 shows that none of the wheel-tracking devices or the SST measurements duplicated this finding.

This study included two potentially confounding factors. All specimens prepared in the laboratory for all mixture tests were short-term oven aged for 2 h at 135 °C. However, the pavement slabs and beams tested by the wheel-tracking devices were taken after the pavements had been inservice for approximately 2 years. The cores to be tested by the SST were taken when the pavements were approximately 3.5 years old. Therefore, there were differences in the degree of age hardening. Furthermore, the level and variability of the air voids for the pavement specimens could not be controlled to the degree they were controlled in the laboratory.

2. French PRT

The slabs previously tested by the French PRT, as discussed in chapter 4, had been compacted using the French Plate Compactor. To determine the effect of compaction method on the data from the French PRT, mixtures were compacted in the laboratory using a SLAB-PAC™ Linear Kneading Compactor. This compactor was purchased after the original tests were performed. To use the Linear Kneading Compactor, vertically aligned steel plates are placed on top of the mixture. A steel roller then transmits a rolling action force through the steel plates, one plate at a time. The mixture is kneaded and compressed into a flat slab of predetermined thickness and density. The compactor is illustrated in figure 63, and additional information is included in appendix A. Slabs were also cut from the ALF pavements, thereby providing three compaction methods. All slabs prepared in the laboratory were tested 3 to 5 days after fabrication. A minimum of two replicate slabs was tested per mixture and compaction method. It was hypothesized that the data from the pavement slabs should correlate best with ALF pavement performance if the method of compaction does affect rutting susceptibility.

The rut depths from the French PRT are presented in table 79. The results of t-tests performed on the data at 30,000 cycles are presented in table 80. These comparisons show whether a change from a surface mixture gradation to a base mixture gradation would either decrease (D), increase (I), or not significantly (NS) affect rutting susceptibility.

The test results using slabs compacted by the French Plate Compactor and the Linear Kneading Compactor did not agree with each other. These data are labeled data set #1 in table 80. Because the data did not agree, and the tests on slabs compacted by the French Plate Compactor were performed 2 years prior to the tests on slabs compacted by the Linear Kneading Compactor, it was decided to retest the mixtures using new slabs. The tests on slabs compacted by the Linear Kneading Compactor were also repeated even though the data for this compactor were new data. The data from the second set of tests are labeled data set #2 in table 80.

Table 77. Statistical rankings for the surface and base mixtures based on rutting susceptibility.[1]

ALF Pavement Performance at 58 °C						
Ranking Based on ALF Wheel Passes at a Rut Depth of 20 mm		ALF Wheel Passes at a Rut Depth of 20 mm	Rut Depth at 2,730 ALF Wheel Passes, mm	**French PRT**	**Georgia LWT**	**Hamburg WTD**
AC-20 Base	A	57,520	12	AB	A	B
AC-5 Base	B	11,990	14	C	AB	C
AC-20 Surface	C	2,730	20	A	A	A
AC-5 Surface	D	670	35	B	B	C

		Simple Shear at Constant Height and 40 °C			**Repeated Shear at Constant Height and 40 °C**	
Ranking Based on ALF Wheel Passes at a Rut Depth of 20 mm		Compliance Parameter	Permanent Shear Strain	Maximum Axial Stress	Slope of Permanent Strain	Cumulative Permanent Strain at 5,000 Cycles
AC-20 Base	A	A	A	A	A	A
AC-5 Base	B	BC	BC	A	A	A
AC-20 Surface	C	AB	B	A	A	A
AC-5 Surface	D	C	C	B	B	B

		Frequency Sweep at Constant Height and 40 °C				
Ranking Based on ALF Wheel Passes at a Rut Depth of 20 mm		Log Shear Modulus, G*, at 10.0 Hz	Log Shear Modulus, G*, at 2.0 Hz	Log G*/sinδ at 10.0 Hz	Log G*/sinδ at 2.0 Hz	Slope of Log G* vs. Log Frequency
AC-20 Base	A	A	A	A	A	B
AC-5 Base	B	C	B	C	B	A
AC-20 Surface	C	B	A	B	A	AB
AC-5 Surface	D	D	C	D	C	A

[1]The letters are the statistical ranking, with "A" denoting the mixture(s) with the lowest susceptibility to rutting.

Table 78. Statistical rankings for the surface and base mixtures.

Mixture Type	Average Rut Depth at 2,730 Wheel Passes, mm	Ranking by Fisher's LSD	Ranking[1] Based on Rut Depth $\pm 2\sigma_{(n-1)}$
AC-20 Base	12	A	A
AC-5 Base	15	A	AB
AC-20 Surface	20	A	B
AC-5 Surface	35	B	C

[1]The rut depths of the mixtures are not significantly different if their $\pm 2\sigma_{(n-1)}$ confidence limits overlap.

Table 79. Rut depths (mm) from the French PRT at 60 °C (data set #2).

	AC-20 Surface Mixture			AC-20 Base Mixture		
Cycles	French Plate Compactor	Linear Kneading Compactor	Pavement Slab	French Plate Compactor	Linear Kneading Compactor	Pavement Slab
300	3.0	2.2	6.3	2.3	1.6	3.9
1,000	3.8	3.0	8.4	2.9	2.2	5.3
3,000	5.1	4.2	10.9	3.4	3.1	6.6
10,000	7.6	6.9	13.9	4.5	4.2	8.7
30,000	10.2	10.7	17.5	6.3	5.9	10.6
Air Voids, %	6.3	7.2	11.3	7.6	7.4	8.9
	AC-5 Surface Mixture			**AC-5 Base Mixture**		
Cycles	French Plate Compactor	Linear Kneading Compactor	Pavement Slab	French Plate Compactor	Linear Kneading Compactor	Pavement Slab
300	3.7	3.5	5.3	2.5	3.1	4.6
1,000	5.0	5.8	6.7	3.9	5.2	6.1
3,000	6.9	8.9	8.8	6.2	9.2	7.8
10,000	12.0	16.8	11.7	10.4	16.8	10.5
30,000	>20	>20	17.6	>20	>20	13.3
Air Voids, %	8.0	6.9	9.9	6.2	7.1	9.3

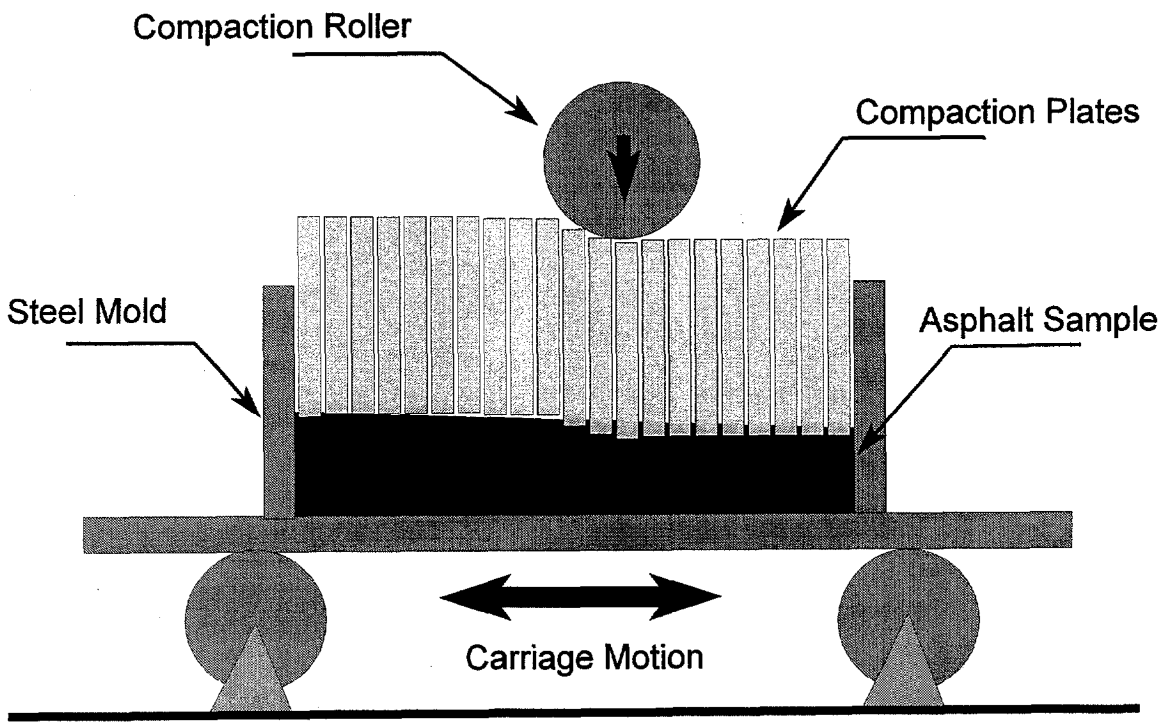

Figure 63. Linear compression provided by the linear kneading compactor.

Table 80. **Results from the French PRT at 60 °C and 30,000 cycles.**

Mix Type, Data Set		Rut Depth at 30,000 Cycles, mm French Plate Compactor	Linear Kneading Compactor	Pavement Slabs	ALF Pavement Rut Depth at 2,730 Passes, mm
AC-20 Base	#1	10.9 *NS*	9.4 *D*		
AC-20 Surface	#1	6.4	14.0		
AC-20 Base	#2	6.3 *NS*	5.9 *D*	10.6 *D*	12 *D*
AC-20 Surface	#2	10.2	10.7	17.5	20
AC-5 Base	#1	>20.0[1]	>20.0[1]		
AC-5 Surface	#1	15.5[1]	>20.0[1]		
AC-5 Base	#2	>20.0[1]	>20.0[1]	13.3 *NS*	14 *D*
AC-5 Surface	#2	>20.0[1]	>20.0[1]	17.6	35

[1]These data could not be statistically analyzed.
NS = Not Significant, and *D* = Decrease.

Table 81. **Results from the French PRT at 60 °C and 10,000 cycles.**

Mix Type, Data Set		Rut Depth at 10,000 Cycles, mm French Plate Compactor	Linear Kneading Compactor	Pavement Slabs	ALF Pavement Rut Depth at 2,730 Passes, mm
AC-20 Base	#1	6.2 *NS*	6.8 *D*		
AC-20 Surface	#1	4.9	9.0		
AC-20 Base	#2	4.5 *NS*	4.2 *D*	8.7 *D*	12 *D*
AC-20 Surface	#2	7.6	6.9	13.9	20
AC-5 Base	#1	16.0 *NS*	>19.0[1]		
AC-5 Surface	#1	8.2	>18.0[1]		
AC-5 Base	#2	10.4 *NS*	16.8 *NS*	10.5 *NS*	14 *D*
AC-5 Surface	#2	12.0	16.8	11.7	35

[1]These data could not be statistically analyzed.
NS = Not Significant, and *D* = Decrease.

Data set #1 shows that the AC-20 (PG 70) surface mixture compacted by the French Plate Compactor had a lower average rut depth than the AC-20 (PG 70) base mixture, while data set #2 shows the reverse. Even so, the pairs of rut depths in either data set were not significantly different. The rut depths for data set #2 using the Linear Kneading Compactor were more than 3 mm lower than those for data set #1 for the AC-20 (PG 70) mixtures. These findings suggested that changes of this magnitude may be typical with the current equipment and laboratory procedures, and further investigations on this subject are needed. The data also showed the importance of using statistical analyses. Conclusions based only on average values could be misleading.

The difference in rut depth provided by the ALF at 2,730 wheel passes was 8 mm (20 mm minus 12 mm) for the mixtures with AC-20 (PG 70). Rutting susceptibility significantly decreased with an increase in nominal maximum aggregate size. Data set #2 showed that the differences provided by the pavement slabs, slabs compacted by the Linear Kneading Compactor, and slabs compacted by the French Plate Compactor were 6.9, 4.8, and 3.9 mm, respectively, but the difference of 3.9 mm provided by the French Plate Compactor was not statistically significant.

In an attempt to increase the difference in rut depth for slabs compacted by the Linear Kneading Compactor, additional slabs were compacted in two layers. This modification decreased the difference from 4.8 to 2.8 mm. The AC-20 (PG 70) surface mixture had a rut depth of 10.5 mm, while the AC-20 (PG 70) base mixture had a rut depth of 7.7 mm. These rut depths were not significantly different.

Most of the rut depths for the two AC-5 (PG 59) mixtures compacted by either laboratory compactor were so deep that they exceeded the range of the measuring device. The laboratory data did not show a decrease in rutting susceptibility with an increase in nominal maximum aggregate size. The AC-5 (PG 59) base mixture did have a lower rut depth than the AC-5 (PG 59) surface mixture for tests performed on pavement slabs, but the difference of 4.3 mm (17.6 mm minus 13.3 mm) was not statistically significant and was not close to the 21-mm difference provided by the ALF.

It was decided to evaluate the data at 10,000 cycles because the data for the AC-5 (PG 59) mixtures at 30,000 cycles could not be statistically analyzed. The data are given in table 81. Only the pavement slabs with AC-20 (PG 70) provided a decrease in rutting susceptibility with an increase in nominal maximum aggregate size. Analyzing the data at 10,000 cycles did not improve the ability of the test to match ALF pavement performance.

Data sets #1 and #2 in table 80 show that the AC-20 (PG 70) surface mixture exceeded the 10-mm maximum allowable rut depth in four of five tests using the French PRT, although the rut depths from two of the failing tests were close to 10 mm. The AC-20 (PG 70) base mixture passed and failed the 10-mm specification depending on the compaction method. All mixtures with AC-5 (PG 59) failed the specification. The AC-5 (PG 59) base mixture was not inhibited from shearing laterally and upward as expected, and there was no evidence that the AC-20 (PG 70) base mixture was inhibited from shearing either.

In summary, the rut depths from the French PRT at 10,000 and 30,000 cycles for the AC-5 (PG 59) surface and base mixtures did not provide a statistically significant decrease in rutting susceptibility with increased nominal maximum aggregate size. This was found for all three compaction methods: French Plate Compactor, Linear Kneading Compactor, and pavement slabs. However, the rut depths at 30,000 cycles for slabs compacted in the laboratory generally exceeded the measuring capability of the machine, which means that differences between the two mixtures could not be established. The rut depths for the AC-20 (PG 70) surface and base mixtures did provide a statistically significant decrease in rutting susceptibility with increased nominal maximum aggregate size when testing pavement slabs and slabs compacted by the Linear Kneading Compactor. A statistically significant decrease was not provided by slabs compacted by the French Plate Compactor.

3. Georgia LWT

All beams previously tested by the Georgia LWT had been compacted in two lifts using a vibratory tamper and a steel wheel roller. In this part of the study, beams were cut from the ALF pavements, thereby providing two compaction methods. All slabs prepared in the laboratory were tested 3 to 5 days after fabrication. A minimum of two replicate slabs was tested per mixture and compaction method.

The rut depths from the Georgia LWT are presented in table 82. Each base mixture had a lower average rut depth compared with its associated surface mixture for both compaction methods. However, the differences were not statistically significant and they did not match the large differences in performance provided by the ALF. All four mixtures met the 7.60-mm maximum allowable rut depth at 8,000 cycles as specified by the Georgia Department of Transportation.

4. Hamburg WTD

All slabs previously tested by the Hamburg WTD had been compacted in two lifts using a vibratory tamper and a steel wheel roller. In this part of the study, slabs were cut from the ALF pavements, thereby providing two compaction methods. All slabs prepared in the laboratory were tested 3 to 5 days after fabrication. A minimum of two replicate slabs was tested per mixture and compaction method.

The Hamburg WTD data are presented in table 83. Lower rut depths and higher creep slopes in terms of passes/mm indicate a greater resistance to rutting. Neither base mixture had a rut depth nor creep slope significantly different from its associated surface mixture when compacted by the vibratory hammer plus steel wheel roller method. Based on the average data from the pavement slabs, each base mixture performed better than its associated surface mixture; however, the differences in the rut depths and creep slopes were only statistically significant for the AC-5 (PG 59) mixtures. The differences were not significant for the AC-20 (PG 70) mixtures.

Because of the large differences in the data provided by the pavement slabs and the slabs compacted by the vibratory hammer plus steel wheel roller, it was decided to compact additional slabs using the Linear Kneading Compactor. As shown in table 83, the results from these slabs did not match the ALF results.

5. SST Using Specimens With a Diameter of 150 mm

All 150-mm-diameter cylindrical specimens tested by the SST were compacted using the Superpave Gyratory Compactor and sawed to obtain specimens with a height of 50 or 75 mm. While the Superpave Gyratory Compactor was developed to simulate the kneading action of rollers in the field, molding specimens to fit a 150-mm-diameter mold can cause uneven aggregate distributions at the edges of the specimen. The aggregates at the edges tend to conform to the curved shape of the cylindrical mold.

In this part of the study, 150-mm-diameter cores were taken from the pavements and from slabs made in the laboratory using the Linear Kneading Compactor. The height of each specimen was 50 mm. Each slab compacted by the Linear Kneading Compactor provided two cores. The target air-void level for the laboratory prepared slabs was 7 ±0.5 percent.

The following tests at 40 °C were evaluated:

- Simple Shear at Constant Height (Simple Shear).
  - Compliance parameter (maximum strain/applied stress).
  - Permanent shear strain after unloading.
  - Maximum axial stress.

- Frequency Sweep at Constant Height (Frequency Sweep)
  - Complex shear modulus, G^*, at 10.0 Hz.
  - $G^*/\sin\delta$ of the mixtures at 10.0 Hz.
  - Slope of log G^* vs. log frequency.

- Repeated Shear at Constant Height (Repeated Shear).
  - Slope of cumulative permanent shear strain vs. cycles.
  - Cumulative permanent shear strain at 5,000 cycles (load repetitions).

The SST data are given in tables 84 and 85. The air voids for the pavement cores, shown in table 84, provided a confounding effect. The air voids of the base mixtures were lower than for their associated surface mixture.

Table 82. Results from the Georgia LWT at 40 °C.

Mixture Type	Vibratory Hammer-Steel Wheel Roller: Rut Depth at 8,000 Cycles, mm	Vibratory Hammer-Steel Wheel Roller: Percent Air Voids	Pavement Beams: Rut Depth at 8,000 Cycles, mm	Pavement Beams: Percent Air Voids	ALF Pavement Rut Depth at 2,730 Passes, mm
AC-20 Base	3.5 *NS*	7.7	2.1 *NS*	6.7	12 *D*
AC-20 Surface	3.7	7.1	2.7	9.1	20
AC-5 Base	6.3 *NS*	7.0	3.5 *NS*	8.8	14 *D*
AC-5 Surface	7.4	7.1	3.9	6.8	35

NS = Not Significant.
D = Decrease.

Table 83. Results from the Hamburg WTD at 50 °C.

Mixture Type	Vibratory Hammer-Steel Wheel Roller: Rut Depth, 20,000 Passes, mm	Creep Slope Passes/mm	Percent Air Voids	Pavement Slabs: Rut Depth, 20,000 Passes, mm	Creep Slope Passes/mm	Percent Air Voids
AC-20 Base	8.6 *NS*	3 780 *NS*	7.0	4.3 *NS*	11 300 *NS*	7.7
AC-20 Surface	8.5	6 220	7.1	6.3	7 340	5.6
AC-5 Base	>25	470 *NS*	6.3	9.1 *D*	4 100 *I*	6.5
AC-5 Surface	>25	300	7.3	21.9	1 340	8.6

Mixture Type	Linear Kneading Compactor: Rut Depth, 20,000 Passes, mm	Creep Slope, Passes/mm	Percent Air Voids	ALF Pavement Rut Depth at 2,730 Passes, mm
AC-20 Base	5.0 *NS*	8 700 *NS*	7.4	12 *D*
AC-20 Surface	7.5	5 150	6.9	20
AC-5 Base	>25	470 *NS*	7.1	14 *D*
AC-5 Surface	>25	630	6.8	35

NS = Not Significant; *D* = Decrease, and *I* = Increase.

Table 84. Average percent air voids of the specimens tested by the SST.

Mixture Type	Superpave Gyratory Compactor	Linear Kneading Compactor	Cores
AC-20 Base	7.3	6.6	5.8
AC-20 Surface	7.2	6.8	8.3
AC-5 Base	7.6	6.3	4.6
AC-5 Surface	6.9	7.0	7.3

Table 85. SST data at 40 °C.

Simple Shear at Constant Height

Mixture Type	Compliance Parameter, 1/MPa			Permanent Shear Strain, 10^{-6} mm/mm			Maximum Axial Stress, kPa		
	SGC	LKC	CORE	SGC	LKC	CORE	SGC	LKC	CORE
AC-20 Base	0.490 *NS*	0.317 *NS*	0.170 *NS*	9370 *D*	5900 *NS*	3900 *NS*	29.5 *NS*	32.5 *NS*	13.1 *NS*
AC-20 Surface	0.702	0.520	0.274	19200	13300	7900	28.9	31.2	16.8
AC-5 Base	0.794 *NS*	0.738 *NS*	0.396 *NS*	23000 *NS*	18100 *NS*	10200 *NS*	31.6 *D*	32.8 *NS*	19.7 *D*
AC-5 Surface	1.030	0.913	0.490	25500	25400	14800	48.5	34.6	29.7

Frequency Sweep at Constant Height

Mixture Type	Shear Modulus, G*, at 10.0 Hz, MPa			G*/sinδ at 10.0 Hz, MPa			Slope of Log G* vs. Log Frequency		
	SGC	LKC	CORE	SGC	LKC	CORE	SGC	LKC	CORE
AC-20 Base	291 *NS*	270 *I*	502 *I*	353 *I*	338 *I*	772 *NS*	0.44 *I*	0.33 *NS*	0.35 *D*
AC-20 Surface	222	214	350	256	266	523	0.35	0.31	0.36
AC-5 Base	93 *I*	99 *NS*	213 *NS*	113 *I*	124 *NS*	293 *NS*	0.27 *D*	0.18 *NS*	0.26 *NS*
AC-5 Surface	62	100	136	71	140	182	0.31	0.14	0.27

Notes: SGC = Superpave Gyratory Compactor.
LKC = Linear Kneading Compactor.
CORE = Pavement Core.

NS = Not Significant.
D = Decrease.
I = Increase.

AC-20 = PG 70.
AC-5 = PG 59.

Table 85. SST data at 40 °C (continued).

	Repeated Shear at Constant Height					
	Slope of Cumulative Permanent Strain			Cumulative Permanent Strain at 5,000 Cycles, 10^{-6} mm/mm		
Mixture Type	SGC	LKC	CORE	SGC	LKC	CORE
AC-20 Base	0.30 *NS*	0.27 *NS*	0.44 *D*	9640 *D*	1410 *NS*	2890 *NS*
AC-20 Surface	0.35	0.35	0.49	14820	4280	5080
AC-5 Base	0.45 *I*	0.41 *NS*	0.37 *NS*	14460 *NS*	8800 *D*	4190 *NS*
AC-5 Surface	0.35	0.43	0.39	22200	16150	9380

Notes: SGC = Superpave Gyratory Compactor. LKC = Linear Kneading Compactor. CORE = Pavement Core.
NS = Not Significant. *D* = Decrease. *I* = Increase.
AC-20 = PG 70. AC-5 = PG 59.

Table 85 shows that the average Simple Shear compliance parameters provided by the base mixtures were lower than the average compliance parameters provided by the surface mixtures in all six comparisons; however, none of them was statistically significant. The average permanent shear strains provided by the base mixtures were also lower in all six comparisons, with only one effect being statistically significant. The average maximum axial stresses provided by the base mixtures were lower in four out of six comparisons, with two effects being statistically significant. Compaction method had little to no effect on the statistical results, although the data for the pavement cores were lower than for the laboratory compacted specimens. The latter result was expected because of the difference in the degree of aging between the pavement cores and the specimens prepared in the laboratory.

The average shear moduli from Frequency Sweep provided by the base mixtures were higher in five out of six comparisons, with three effects being statistically significant. The average $G^*/\sin\delta$'s provided by the base mixtures were also higher in five out of six comparisons, with three effects being statistically significant. The average slopes provided mixed results. The base mixtures provided higher slopes in some comparisons and lower slopes in other comparisons. Compaction method had little to no effect on the statistical results, although the G^*'s and $G^*/\sin\delta$'s for the pavement cores were higher than those provided by the laboratory compacted specimens. Again, the latter result was expected based on the difference in the degree of aging.

The average slopes from Repeated Shear provided by the base mixtures were lower in five of six comparisons, but only one of these five comparisons was statistically significant. The slope was significantly higher for the base mixture in one comparison where the Superpave Gyratory Compactor was used. The average cumulative permanent strains provided by the base mixtures were lower in all six comparisons, with two being statistically significant.

Although some of the data provided trends that matched ALF pavement performance, for example, the lower permanent strains generally provided by the base mixtures relative to their associated surface mixture, none of the compaction methods was clearly better than the others based on ALF pavement rutting performance. The lower air-void levels for the cores from the base mixture pavements appeared to have little to no effect on the statistical results.

6. All Tests

The data from all four mixtures were evaluated as a group using analyses of variance and Fisher's LSD at a 95-percent confidence level. ALF pavement performance was based on the log wheel passes needed to obtain a rut depth of 20 mm. Tables 86 and 87 show the rankings for the wheel-tracking devices based on the averages and Fisher's LSD, respectively. Table 86 shows that only the pavement slabs tested by the French PRT ranked the mixtures the same as ALF based on the averages. Table 87 shows that none of the statistical rankings agreed with ALF pavement performance.

as ALF based on the averages. Table 87 shows that none of the statistical rankings agreed with ALF pavement performance.

Three-way analyses of variance, using binder grade, aggregate gradation, and compaction method as the independent variables, showed that the data from all three wheel-tracking devices were significantly affected by binder grade and compaction method but not by aggregate gradation. The results are given in table 88. The rut depths from the French PRT and Georgia LWT provided an interaction between binder grade and compaction method, while the slopes from the Hamburg WTD provided an interaction between aggregate gradation and compaction method. The French PRT analysis included extrapolated data for tests that exceeded the measurement capability of the machine. If these data were to be excluded, then none of the data from the AC-5 (PG 59) surface mixtures could be used in the analysis. Thus, the effect of binder grade could not be evaluated. An analysis of variance that excluded binder grade showed that both aggregate gradation and compaction method affected the rut depths from the French PRT, but the data in table 80 indicate that binder grade had a greater effect on the rut depths than aggregate gradation.

Table 89 shows the characteristics of the ALF and the laboratory wheel-tracking tests. The numerous differences make it difficult to determine why the rankings provided by the wheel-tracking devices did not match the ranking provided by the ALF. Besides the characteristics shown in table 89, there are other differences such as the sizes of the slabs tested in the laboratory, the type of confinement (steel vs. an actual pavement), and the state of stress.

It was hypothesized that contact area may be one reason for the discrepancies. The contact area for the ALF was much greater than for the French PRT, Hamburg WTD, and Georgia LWT. The larger aggregates may be more difficult to displace laterally under the ALF tire due to the relatively large tire width of 320 mm. The characteristics of the PURWheel are included in table 89. The contact area for this device was between the contact areas for the ALF and the other three wheel-tracking devices. The PURWheel was able to measure the effect of nominal maximum aggregate size but not binder grade. The characteristics shown in table 89 provided no obvious reason for the discrepancies between the machines.

Table 90 provides the rankings for the SST measurements based on the averages. The only measurement that ranked the mixtures the same as ALF was the cumulative permanent strain at 5,000 cycles from Repeated Shear using cores. However, the statistical ranking for this data, which is included in table 90, did not agree with ALF pavement performance.

The results from three-way analyses of variance at a 95-percent confidence level are included in table 88. Only the slope from Repeated Shear was not affected by binder grade, and only the cumulative permanent strain at 5,000 cycles from Repeated Shear was not affected by compaction method. Gradation affected (1) the compliance parameter and permanent shear strain from Simple Shear, (2) cumulative permanent strain at 5,000 cycles from Repeated Shear, and (3) G* and G*/sinδ from Frequency Sweep. However, the effect of gradation on the SST measurements was relatively small compared with the effect of gradation on ALF rutting performance.

7. SST Using Pavement Cores With a Diameter of 203 mm

Cores with a diameter of 203 mm were extracted from the pavements to determine if the use of a larger diameter would improve the degree of correlation between the data from the SST and ALF pavement rutting performance. Specimens with a height of 75 mm were used when testing the two base mixtures, while specimens with a height of 50 mm were used when testing the two surface mixtures. The pavements with the surface mixtures were compacted in four 50-mm lifts. Therefore, the specimens would include a weak shear plane if a height of 75 mm were to be used instead of 50 mm. The base mixtures were compacted in two 100-mm lifts.

The cores were tested using Frequency Sweep at 40 and 58 °C, and Repeated Shear at 58 °C. The data are given in table 91. Based on the results presented in chapter 4, the hypothesis applied to the slopes from Frequency Sweep was that a higher slope indicates lower rutting susceptibility. Tables 91 and 92 show that the tests using the larger diameter pavement cores provided good correlations to ALF pavement performance. The correlations were the best found in this study for any test. Only the slopes from Repeated Shear had no correlation to ALF pavement performance.

Table 93 provides the high-temperature continuous PG's for the four pavements. The PG's for the AC-5 (PG 59) cores from lanes 9 and 11 differed by 4, 4, and 10 °C in 1994, 1995, and 1998, respectively. The PG's for the AC-20 (PG 70) cores from lanes 10 and 12 differed by 6 °C in 1994. The data indicate that the amount of age hardening was greater in the base mixtures. The short-term oven aging period of 2 h was based on the PG's of the binders recovered in 1993. At that time, there were no differences in the amount of aging between lanes 9 and 11, and lanes 10 and 12. Age hardening was a confounding factor in this study.

The SST results in chapter 4 showed that the tests were generally sensitive to changes in binder grade; therefore, it was hypothesized that age hardening was one of the main reasons for the better SST results using the larger diameter cores. These cores were taken from the pavements in 1998. Table 90 shows that the 150- by 50-mm pavement cores did not provide data that correlated with ALF pavement performance except for the average cumulative permanent strains from Repeated Shear. These cores were taken from the pavements in 1996. The results for the larger diameter cores could be a function of differences in both aging and specimen size. The French PRT using pavement slabs was the only other test where the average data provided a ranking that was the same as ALF. The slabs for these tests were taken in 1995.

8. Conclusions

- The ALF provided significant decreases in rutting susceptibility with increased nominal maximum aggregate size and the associated 0.85-percent decrease in optimum binder content. The AC-20 (PG 70) base mixture performed significantly better than the AC-20 (PG 70) surface mixture, and the AC-5 (PG 59) base mixture performed significantly better than the AC-5 (PG 59) surface mixture.

- The effect of aggregate gradation on ALF pavement rutting performance was not duplicated by the laboratory mixture tests, except for the SST using 203-mm-diameter pavement cores and the PURWheel using slabs cut from the pavements. However, the PURWheel did not measure the effect of binder grade.

- The rutting performance of each base mixture provided by the French PRT, Georgia LWT, and Hamburg WTD, relative to the surface mixture having the same grade of binder, varied from test to test and with compaction method. Overall, the data from these devices correlated poorly with ALF pavement rutting performance in terms of measuring the effect of gradation and the associated change in binder content. The data showed that the method of compaction can affect the results from these devices, but it was not the main reason why the devices were insensitive to gradation. It was hypothesized that differences in contact area may be one reason for the discrepancy, but a firm reason was not found.

- The SST using specimens with a diameter and height of 150 by 50 mm provided the same conclusions as the wheel-tracking devices. The average cumulative permanent strains from Repeated Shear using pavement cores was the only measurement that provided a ranking that agreed with ALF pavement rutting performance. Even so, these strains were not significantly different based on statistical analyses.

- Pavement cores with a diameter of 203 mm provided good correlations between the SST and ALF pavement rutting performance. The correlations were the best found in this study for any test. However, the binders in the various pavements age hardened to different degrees over time and these cores were taken near the end of the study. Based on recovered binder properties, it was hypothesized that the differences in age hardening was one of the main reasons for the better SST results using the larger cores. Specimen size could be another reason.

Table 86. Non-statistical rankings for the four mixtures based on the wheel-tracking devices.[1]

ALF Performance		French PRT, Rut Depth at 30,000 Cycles			Georgia LWT, Rut Depth at 8,000 Cycles	
Log ALF Wheel Passes at a Rut Depth of 20 mm		French Plate Compactor	Linear Kneading Compactor	Pavement Slabs	Vibratory-Steel Wheel Roller	Pavement Beams
AC-20 Base	A	A	A	A	A	A
AC-5 Base	B	C	C	B	C	C
AC-20 Surface	C	B	B	C	B	B
AC-5 Surface	D	C	C	D	D	D

ALF Performance		Hamburg WTD, Creep Slope		
Log ALF Wheel Passes at a Rut Depth of 20 mm		Vibratory-Steel Wheel Roller	Linear Kneading Compactor	Pavement Slabs
AC-20 Base	A	B	A	A
AC-5 Base	B	C	D	C
AC-20 Surface	C	A	B	B
AC-5 Surface	D	D	C	D

[1]The letters are the ranking based on the averages with "A" denoting the mixture with the lowest susceptibility to rutting.

Table 87. Statistical rankings for the four mixtures based on the wheel-tracking devices.[1]

ALF Performance		French PRT, Rut Depth at 30,000 Cycles			Georgia LWT, Rut Depth at 8,000 Cycles	
Log ALF Wheel Passes at a Rut Depth of 20 mm		French Plate Compactor	Linear Kneading Compactor	Pavement Slabs	Vibratory-Steel Wheel Roller	Pavement Beams
AC-20 Base	A	A	A	A	A	A
AC-5 Base	B	NA[2]	NA[3]	AB	AB	BC
AC-20 Surface	C	A	B	B	A	AB
AC-5 Surface	D	NA[2]	NA[3]	B	B	C

ALF Performance		Hamburg WTD, Creep Slope		
Log ALF Wheel Passes at a Rut Depth of 20 mm		Vibratory-Steel Wheel Roller	Linear Kneading Compactor	Pavement Slabs
AC-20 Base	A	B	A	A
AC-5 Base	B	C	B	BC
AC-20 Surface	C	A	A	B
AC-5 Surface	D	C	B	C

[1]The letters are the statistical ranking, with "A" denoting the mixture(s) with the lowest susceptibility to rutting.

[2]Not Applicable. The data could not be evaluated using statistics because the rut depths from some of the tests exceeded the measurement capabilities of the equipment. The data could be assigned the letter "B" if desired.

[3]Not Applicable. The data could not be evaluated using statistics because the rut depths from some of the tests exceeded the measurement capabilities of the equipment. The data could be assigned the letter "C" if desired.

Table 88. Significant factors provided by three-way analyses of variance.

French PRT, Rut Depth at 60 °C	Georgia LWT, Rut Depth at 40 °C	Hamburg WTD, Slope at 50 °C
Binder Compaction Binder*Comp	Binder Compaction Binder*Comp	Binder Compaction Grad*Comp

Simple Shear at Constant Height and 40 °C			Repeated Shear at Constant Height and 40 °C	
Compliance Parameter	Permanent Shear Strain	Maximum Axial Stress	Slope of Permanent Strain	Cumulative Permanent Strain at 5,000 Cycles
Binder Gradation Compaction	Binder Gradation Compaction Binder*Comp	Binder Compaction	Compaction Binder*Comp	Binder Gradation

Frequency Sweep at Constant Height and 40 °C

Shear Modulus, G*, at 10.0 Hz	Shear Modulus, G*, at 2.0 Hz	G*/sinδ at 10.0 Hz	G*/sinδ at 2.0 Hz	Slope of Log G* vs. Log Frequency
Binder Gradation Compaction	Binder Gradation Compaction Binder*Comp	Binder Gradation Compaction Binder*Comp	Binder Gradation Compaction Binder*Comp Grad*Comp	Binder Compaction Binder*Comp

Independent Variables:

Binder = Binder Grade
Gradation or Grad = Aggregate Gradation
Compaction or Comp = Compaction Method

Table 89. Characteristics of the ALF and wheel-tracking tests.

	Thickness of Slab, mm	Load, N	Stress, MPa	Contact Area, mm^2	Speed, km/h	Test Temp, °C
ALF	200	44 500	0.690	64 500	18.0	58
PURWheel	76	1 530	0.62	20 640	1.2	58
French PRT	100	5 000	0.57	8 770	7.0	60
Hamburg WTD	80	660	0.73	900[1]	1.1	50
Georgia LWT	80	700	1.0	700[1]	2.0	40

[1]Maximum contact area; the contact area increases during the test and can vary from mixture to mixture.

Table 90. Non-statistical rankings for the four mixtures based on the SST at 40 °C.[1]

Simple Shear at Constant Height and 40 °C

ALF at 58 °C		Compliance Parameter			Permanent Shear Strain			Maximum Axial Stress		
		SGC	LKC	CORE	SGC	LKC	CORE	SGC	LKC	CORE
AC-20 Base	A	A	A	A	A	A	A	B	B	A
AC-5 Base	B	C	C	C	C	C	C	C	C	C
AC-20 Surface	C	B	B	B	B	B	B	A	A	B
AC-5 Surface	D	D	D	D	D	D	D	D	D	D

Frequency Sweep at Constant Height and 40 °C

ALF at 58 °C		Shear Modulus, G* at 10.0 Hz			G*/sinδ at 10.0 Hz			Slope of Log G* vs. Log Frequency		
		SGC	LKC	CORE	SGC	LKC	CORE	SGC	LKC	CORE
AC-20 Base	A	A	A	A	A	A	A	A	A	B
AC-5 Base	B	C	C	C	C	D	C	D	C	D
AC-20 Surface	C	B	B	B	B	B	B	B	B	A
AC-5 Surface	D	D	D	D	D	C	D	C	D	C

Repeated Shear at Constant Height and 40 °C

ALF at 58 °C		Slope of Cumulative Permanent Strain			Cumulative Permanent Strain at 5,000 Cycles: Non-statistical Rankings			Cumulative Permanent Strain at 5,000 Cycles: Statistical Rankings	
		SGC	LKC	CORE	SGC	LKC	CORE	SCG	CORE
AC-20 Base	A	C	A	B	A	A	A	A	A
AC-5 Base	B	A	C	D	B	C	B	A	A
AC-20 Surface	C	B	B	A	C	B	C	A	AB
AC-5 Surface	D	B	D	C	D	D	D	B	B

[1]The letters are the ranking, with "A" denoting the mixture(s) with the lowest susceptibility to rutting.

Table 91. SST results using pavement cores with a diameter of 203 mm and a height of 50 mm for surface mixtures and 75 mm for base mixtures.

ALF Ranking at 58 °C and a 20-mm Rut Depth		Shear Modulus[1] G*, at 10.0 Hz, MPa		Shear Modulus[1] G*, at 2.0 Hz, MPa		Slope of Log G* vs. Log Frequency	
		Frequency Sweep at Constant Height and 40 °C					
AC-20 Base	A	715	A	347	A	0.47	A
AC-5 Base	B	385	B	191	B	0.42	B
AC-20 Surface	C	286	B	141	B	0.42	B
AC-5 Surface	D	85	C	40	C	0.35	C

ALF Ranking at 58 °C and a 20-mm Rut Depth		Shear Modulus G*, at 10.0 Hz, MPa		Shear Modulus G*, at 2.0 Hz, MPa		Slope of Log G* vs. Log Frequency	
		Frequency Sweep at Constant Height and 58 °C					
AC-20 Base	A	161	A	73	A	0.34	A
AC-5 Base	B	79	B	43	B	0.22	B
AC-20 Surface	C	56	C	33	C	0.20	B
AC-5 Surface	D	27	D	20	D	0.12	C

ALF Ranking at 58 °C and a 20-mm Rut Depth		Slope of Cumulative Permanent Strain		Cumulative Permanent Strain at 5,000 Cycles,[1] 10^{-6} mm/mm	
		Repeated Shear at Constant Height and 58 °C			
AC-20 Base	A	0.44	A	4 320	A
AC-5 Base	B	0.45	A	5 360	A
AC-20 Surface	C	0.43	A	14 400	B
AC-5 Surface	D	0.47	A	28 000	C

[1]Statistical ranking is based on $\log_{10}$ of the value.

Table 92. Effect of specimen size and type on the SST results.

ALF Ranking at 58 °C and a 20-mm Rut Depth		Frequency Sweep at Constant Height and 40 °C Shear Modulus, G*, at 10.0 Hz, MPa									
		Pavement Core D = 203 mm H = 75 mm[1]		Pavement Core D = 150 mm H = 50 mm		Gyratory Testing Machine D = 203 mm H = 75 mm		Superpave Gyratory Compactor D = 150 mm H = 75 mm		Superpave Gyratory Compactor D = 150 mm H = 50 mm	
AC-20 Base	A	715	A	502	A	265	A	279	A	291	A
AC-5 Base	B	385	B	213	C	119	C	85	C	93	C
AC-20 Surface	C	286	B	350	B	213	B	208	B	222	B
AC-5 Surface	D	85	C	136	D	92	D	61	D	62	D

ALF Ranking at 58 °C and a 20-mm Rut Depth		Frequency Sweep at Constant Height and 58 °C Shear Modulus, G*, at 10.0 Hz, MPa							
		Pavement Core D = 203 mm H = 75 mm[1]		Gyratory Testing Machine D = 203 mm H = 75 mm		Superpave Gyratory Compactor D = 150 mm H = 75 mm		Superpave Gyratory Compactor D = 150 mm H = 50 mm	
AC-20 Base	A	161	A	55	A	69	A	95	A
AC-5 Base	B	79	B	34	C	48	B	74	A
AC-20 Surface	C	56	C	44	B	63	A	89	A
AC-5 Surface	D	27	D	34	C	60	A	71	A

ALF Ranking at 58 °C and a 20-mm Rut Depth		Repeated Shear at Constant Height and 58 °C Cumulative Permanent Strain at 5,000 Cycles, 10^{-6} mm/mm				
		Pavement Core D = 203 mm H = 75 mm[1]		Gyratory Testing Machine D = 203 mm H = 75 mm	Superpave Gyratory Compactor D = 150 mm H = 75 mm	Superpave Gyratory Compactor D = 150 mm H = 50 mm
AC-20 Base	A	4 320	A	Failed	Failed	34 020
AC-5 Base	B	5 360	A	Failed	Failed	Failed
AC-20 Surface	C	14 400	B	Failed	Failed	34 200
AC-5 Surface	D	28 000	C	Failed	Failed	Failed

[1]The height was 75 mm for the base mixtures and 50 mm for the surface mixtures.

Table 93. High-temperature continuous PG's at 10 rad/s for the binders used in the surface vs. base mixture study.

Mixture	Lane	PG of Neat Binder after RTFO	PG of Binder Recovered From Laboratory Mixtures After STOA	PG of Binder Recovered From Pavement Samples			
				1993	1994	1995	1998
AC-20 Base	12	70	67	68	78	NT	NT
AC-5 Base	11	59	61	60	67	72	74
AC-20 Surface	10	70	67	68	72	78	78
AC-5 Surface	9	59	61	59	63	68	64
				Fractional Difference in Asphalt Binder Grade Where 1.0 Indicates a Change of One PG (Pavement PG - Lab PG) ÷ 6 °C			
AC-20 Base	12	-	67	0.2	1.8	-	-
AC-5 Base	11	-	61	-0.2	1.0	1.8	2.2
AC-20 Surface	10	-	67	0.2	0.8	1.8	1.8
AC-5 Surface	9	-	61	-0.3	0.3	1.2	0.5

NT = Not tested by the ALF in 1995 and 1998; therefore, there are no data.

STOA = After 2 h of short-term oven aging.

CHAPTER 6: G*/SINδ VERSUS LABORATORY MIXTURE TESTS FOR RUTTING

1. Background

ALF pavement performance was the principal means used to validate G*/sinδ. Rankings for the five binders based on G*/sinδ were also compared with the rankings for the five surface mixtures provided by the laboratory mixture tests for rutting listed in chapter 4. Mixture tests that did not correlate with ALF pavement performance were excluded.

The G*/sinδ's at the temperature and angular frequency of each laboratory mixture test are given in table 94. The DSR angular frequencies were based on a speed of 80 km/h being equivalent to 10.0 rad/s. The speed of each mixture test was divided by eight to obtain the DSR angular frequency to be used. The loading frequency of 10.0 Hz used by the repeated load compression test and SST is generally equated to 80 km/h. Therefore, the data from these tests were compared with the G*/sinδ's at 10.0 rad/s. As discussed in chapter 2, Superpave equates 10.0 rad/s to approximately 10 Hz. The Frequency Sweep data at a frequency of 2.0 Hz were also evaluated because this could be considered the loading frequency of the ALF. A frequency of 2.0 Hz was used in lieu of 2.25 Hz (18.0 km/h ÷ 8) because 2.0 Hz is one of the standard SST frequencies and the conversion from km/h to Hz is approximate.

ALF pavement performance was based on the wheel passes at a 20-mm rut depth and on the rut depths at 2,370 and 10,000 wheel passes. Pavement performances based on rut depths at constant numbers of ALF wheel passes were used in this part of the study so that the rut depths from the ALF and the three wheel-tracking devices could be examined together. The ALF pavement rut depths are given in table 95.

The rut depths at 2,370 wheel passes were evaluated because this number of wheel passes provided an average rut depth of 20 mm in the pavement with the AC-20 (PG 70) surface mixture. This mixture was considered the control mixture, and a rut depth of 20 mm was defined as the failure level. The rut depths at 10,000 wheel passes were also evaluated. This was the maximum number of wheel passes that could be used because at higher numbers of wheel passes, the rut depths for three out of the five mixtures would have to be obtained by extrapolation. At 2,370 wheel passes, the rut depth for the AC-5 (PG 59) surface mixture had to be calculated by extrapolation. At 10,000 wheel passes, the rut depths for the AC-5 (PG 59) and AC-10 (PG 65) surface mixtures had to be calculated by extrapolation.

2. French PRT, Georgia LWT, and Hamburg WTD

The statistical rankings in table 96 show a reversed order for Novophalt and Styrelf based on the average values. According to G*/sinδ, the Styrelf

Table 94. G*/sinδ and binder rankings at the angular frequencies and temperatures used in the ALF pavement and laboratory mixture tests.[1]

Pre-Superpave Designation:	AC-5	AC-10	AC-20	Novophalt	Styrelf
Superpave PG:	58-34	58-28	64-22	76-22	82-22
	G*/sinδ's of the RTFO Residues, Pa				
ALF Pavement Tests, G*/sinδ at 2.25 rad/s (18.0 km/h) and 58 °C	664 E	1 384 D	2 702 C	6 826 B	13 710 A
French PRT, G*/sinδ at 0.875 rad/s (7.0 km/h) and 60 °C	212 E	442 D	871 C	2 103 B	6 444 A
Georgia LWT, G*/sinδ at 0.125 rad/s (1.0 km/h) and 40 °C	899 E	2 215 D	5 060 C	10 350 B	21 120 A
Hamburg WTD, G*/sinδ at 0.125 rad/s (1.0 km/h) and 50 °C	130 D	348 DC	635 C	1 744 B	5 243 A
Repeated Load Test, G*/sinδ at 10.0 rad/s (80.0 km/h) and 40 °C	38 640 D	82 800 C	159 900 B	263 600 A	270 900 A
Repeated Load Test, G*/sinδ at 10.0 rad/s (80.0 km/h) and 58 °C	2 600 E	5 285 D	10 010 C	21 090 B	35 170 A
SST, G*/sinδ at 10.0 rad/s (80.0 km/h) and 40 °C	38 640 D	82 800 C	159 900 B	263 600 A	270 900 A
SST, G*/sinδ at 2.0 rad/s (18.0 km/h) and 40 °C	11 910 E	26 350 D	54 470 C	92 470 B	117 700 A

[1]The letters are the statistical ranking, with "A" denoting the binder(s) with the highest G*/sinδ.

Table 95. Rut depths in the asphalt pavement layer at 2,370 and 10,000 ALF wheel passes.

Surface Mixture	Rut Depth at 2,370 Wheel Passes, mm	Rut Depth at 10,000 Wheel Passes, mm
Novophalt	4	5
Styrelf	8	10
AC-20	20	29
AC-10	23	39[1]
AC-5	37[1]	65[1]

[1]From extrapolation.

Table 96. Rankings for the five surface mixtures vs. rankings based on the G*/sinδ's of the binders at the angular frequency and temperature corresponding to the ALF pavement and laboratory mixture tests.[1]

ALF Pavements at 2.25 rad/s, 58 °C

Binder, G*/sinδ	Wheel Passes at a 20-mm Rut Depth
(A) Styrelf	(A) Novophalt
(B) Novophalt	(B) Styrelf
(C) AC-20	(C) AC-20
(D) AC-10	(C) AC-10
(E) AC-5	(D) AC-5

French PRT at 0.875 rad/s, 60 °C

Binder, G*/sinδ	Percent Rut Depth	Slope
(A) Styrelf	(A) Novophalt	(A) Novophalt
(B) Novophalt	(B) Styrelf	(B) Styrelf
(C) AC-20	(C) AC-20	(C) AC-20
(D) AC-10	(D) AC-10	(D) AC-10
(E) AC-5	(D) AC-5	(D) AC-5

Georgia LWT at 0.125 rad/s, 40 °C

Binder, G*/sinδ	Rut Depth
(A) Styrelf	(A) Novophalt
(B) Novophalt	(B) Styrelf
(C) AC-20	(BC) AC-20
(D) AC-10	(C) AC-10
(E) AC-5	(C) AC-5

Hamburg WTD at 0.125 rad/s, 50 °C

Binder, G*/sinδ	Creep Slope
(A) Styrelf	(-) Novophalt[2]
(B) Novophalt	(A) Styrelf
(C) AC-20	(B) AC-20
(CD) AC-10	(C) AC-10
(D) AC-5	(D) AC-5

Repeated Load Compression Test at 10.0 rad/s, 40 °C

Binder, G*/sinδ	Cumulative Permanent Strain, 10,000 Cycles
(A) Styrelf	(A) Styrelf
(A) Novophalt	(A) Novophalt
(B) AC-20	(B) AC-20
(C) AC-10	(C) AC-10
(D) AC-5	(D) AC-5

Repeated Load Compression Test at 10.0 rad/s, 58 °C

Binder, G*/sinδ	Cumulative Permanent Strain, 1,000 Cycles
(A) Styrelf	(A) Novophalt
(B) Novophalt	(A) Styrelf
(C) AC-20	(B) AC-20
(D) AC-10	(C) AC-10
(E) AC-5	(C) AC-5

[1]The letters are the statistical ranking, with "A" denoting the binder(s) or mixture(s) with the lowest susceptibility to rutting.

[2]This mixture had the lowest susceptibility to rutting but it was not included in the statistical ranking because of high variability.

Table 96. Rankings for the five surface mixtures vs. rankings based on the G*/sinδ's of the binders at the angular frequency and temperature corresponding to the ALF pavement and laboratory mixture tests (continued).[1]

Simple Shear at Constant Height and 40 °C

Binder, G*/sinδ at 10.0 rad/s	Compliance Parameter	Permanent Shear Strain	Maximum Axial Stress
(A) Styrelf	(A) Novophalt	(A) Styrelf	(A) Novophalt
(A) Novophalt	(B) Styrelf	(AB) Novophalt	(AB) Styrelf
(B) AC-20	(C) AC-20	(B) AC-20	(AC) AC-20
(C) AC-10	(D) AC-10	(C) AC-5	(BCD) AC-10
(D) AC-5	(D) AC-5	(C) AC-10	(AD) AC-5

Frequency Sweep at Constant Height and 40 °C

Binder, G*/sinδ at 10.0 rad/s	Shear Modulus, G*, at 10.0 Hz	Mixture G*/sinδ at 10.0 Hz	Slope of Log G* vs. Log Frequency
(A) Styrelf	(A) Novophalt	(A) Novophalt	(A) Novophalt
(A) Novophalt	(B) Styrelf	(B) Styrelf	(AB) AC-5
(B) AC-20	(C) AC-20	(C) AC-20	(AB) Styrelf
(C) AC-10	(D) AC-10	(D) AC-10	(AB) AC-20
(D) AC-5	(E) AC-5	(E) AC-5	(B) AC-10

Frequency Sweep at Constant Height and 40 °C

Binder, G*/sinδ at 2.0 rad/s	Shear Modulus, G*, at 2.0 Hz	G*/sinδ at 2.0 Hz
(A) Styrelf	(A) Novophalt	(A) Novophalt
(B) Novophalt	(B) Styrelf	(B) Styrelf
(C) AC-20	(C) AC-20	(C) AC-20
(D) AC-10	(D) AC-10	(CD) AC-10
(E) AC-5	(D) AC-5	(D) AC-5

[1]The letters are the statistical ranking, with "A" denoting the binder(s) or mixture(s) with the lowest susceptibility to rutting.

Table 96. Rankings for the five surface mixtures vs. rankings based on the G*/sinδ's of the binders at the angular frequency and temperature corresponding to the ALF pavement and laboratory mixture tests (continued).[1]

Repeated Shear at Constant Height and 40 °C		
Binder, G*/sinδ at 10.0 rad/s	Slope of Cumulative Permanent Strain	Cumulative Permanent Strain at 5,000 cycles
(A) Styrelf	(A) Novophalt	(A) Novophalt
(A) Novophalt	(A) AC-20	(A) Styrelf
(B) AC-20	(A) AC-10	(AB) AC-20
(C) AC-10	(A) AC-5	(B) AC-10
(D) AC-5	(A) Styrelf	(C) AC-5

[1]The letters are the statistical ranking, with "A" denoting the binder(s) or mixture(s) with the lowest susceptibility to rutting.

binder should provide the most resistance to rutting, followed by Novophalt. All three wheel-tracking tests and ALF show that the mixture with Novophalt was most resistant to rutting, followed by the mixture with Styrelf. The degree of correlation between G*/sinδ and the wheel-tracking tests, based on the statistical rankings, varied from test to test.

Figures 64 and 65 show the rut depths from the ALF and the wheel-tracking devices vs. G*/sinδ after RTFO. The rut depths from the three wheel-tracking devices provided a single relationship with G*/sinδ. The rut depths from the ALF were greater than the rut depths from the wheel-tracking devices for a given mixture at both 2,730 and 10,000 ALF wheel passes.

The rut depths provided by the wheel-tracking devices suggest that the 2.20-kPa minimum specification level for G*/sinδ after RTFO is valid. The failure level rut depths of 10 mm for the French PRT and Hamburg WTD and 7.6 mm for the Georgia LWT indicate that 2.20 kPa is conservative. The rut depths provided by the ALF suggest that 2.20 kPa is low, but a firm relationship was not provided because the number of data points was too low. Figures 64 and 65 each show two possible relationships for the rut depths provided by the ALF vs. G*/sinδ. The reversal for the Novophalt and Styrelf materials was less pronounced when performance was based on 2,370 or 10,000 ALF wheel passes rather than on the number of wheel passes at a rut depth of 20 mm.

3. Repeated Load Compression Test

The rankings in table 96 based on G*/sinδ and cumulative permanent strain at 40 °C are identical. The rankings at 58 °C provided the same discrepancy for Novophalt and Styrelf that was provided by the wheel-tracking devices.

4. SST

The G*/sinδ's of the binders at 40 °C were compared with the rankings provided by the following tests performed at 40 °C. Specimens compacted by the Superpave Gyratory Compactor were used. Each specimen had a diameter and height of 150 and 50 mm, respectively.

- Simple Shear at Constant Height (Simple Shear).
  - Compliance parameter (maximum strain/applied stress).
  - Permanent shear strain after unloading.
  - Maximum axial stress.

- Frequency Sweep at Constant Height (Frequency Sweep).
  - Complex shear modulus, G*, at 10.0 and 2.0 Hz.
  - G*/sinδ of the mixtures at 10.0 and 2.0 Hz.
  - Slope of log G* vs. log frequency.

- Repeated Shear at Constant Height (Repeated Shear).
  - Slope of cumulative permanent shear strain vs. cycles.
  - Cumulative permanent shear strain at 5,000 cycles (load repetitions).

The Simple Shear test had no associated frequency so the data were compared with the G*/sinδ's at the standard DSR angular frequency of 10.0 rad/s. The rankings for the SST measurements are included in table 96. The mixtures were also tested at 58 °C, but the results were not used because the data did not correlate to ALF pavement performance and was highly variable.

How the mixtures grouped together based on statistics, and how each statistical ranking compared to the ranking based on G*/sinδ, depended on the particular SST measurement. In general, the SST provided the same conclusion as the laboratory wheel-tracking tests. Most rankings show a reversed order for the Novophalt and Styrelf materials.

5. Rankings Based on an Angular Frequency of 10.0 rad/s

The five binders were ranked based on G*/sinδ at the standard DSR angular frequency of 10.0 rad/s and the test temperatures used in the ALF, French PRT, Georgia LWT, and Hamburg WTD tests. These G*/sinδ's are given in table 97. Tables 94 and 97 show that the change in frequency did not change the rankings for the G*/sinδ's used in the ALF and French PRT comparisons. Therefore, the change in angular frequency had no effect on the degree of correlation between G*/sinδ and these two tests.

Different rankings for G*/sinδ were obtained using 10.0 rad/s for the Georgia LWT and Hamburg WTD comparisons. Tables 96 and 98 show that the use of 10.0 rad/s, at best, marginally improved the relationship with the Hamburg WTD, but it did not improve the relationship with the Georgia LWT.

Normally, 10.0 Hz is equated to 62.8 rad/s. If 62.8 rad/s were to be equated to 80 to 100 km/h instead of 10.0 rad/s, the DSR angular frequency for the ALF comparison would be in the range of 11 to 14 rad/s. Angular frequencies in this range provided the same ranking for G*/sinδ as 2.25 and 10.0 rad/s. Thus, angular frequencies from 2 to 14 rad/s did not affect the degree of correlation between G*/sinδ and ALF pavement performance.

6. Comment on Loading Time and Frequency

The loading time for a point on a pavement is generally based on vehicle speed and on the deflection basin or some other measure that shows how the stresses at the point change as a tire rolls over it. Stresses at the point will start to occur before the tire reaches it and will not completely relax until the tire is some distance past it. Thus, the loading time for a pavement is a function of vehicle speed and the size of the deflection basin. An additional complication that arises when calculating loading times is that the size of the deflection basin should vary with vehicle speed.

The stress patterns in the ALF pavements and specimens tested by the wheel-tracking tests were not known. Furthermore, the specimens tested by the wheel-tracking devices could not deflect because the underlying support in each device was rigid. The DSR angular frequencies used to represent these machines were based solely on speed; thus, they can only be considered approximate angular frequencies. This comment also applies to the standard DSR test. The standard frequency of 10.0 rad/s only represents some average pavement condition even if the resulting high-temperature PG is adjusted based on vehicle speed.

7. Conclusions

- The French PRT, Georgia LWT, Hamburg WTD, the cumulative permanent strains from the repeated load compression test at 58 °C, and most of the SST data ranked the five surface mixtures the same as ALF based on the average data. The mixture with Novophalt had the greatest resistance to rutting, followed by the mixture with Styrelf. According to G*/sinδ, the Styrelf binder should have provided the most resistance to rutting, followed by Novophalt. The degree of correlation between the mixture tests and G*/sinδ using statistical rankings varied from mixture test to mixture test. However, the reversal for the Novophalt and Styrelf materials was the most significant discrepancy found.

- The rankings based on G*/sinδ and the cumulative permanent strains from the repeated load compression test at 40 °C were identical.

- A DSR angular frequency of 2.25 rad/s was used in this study to account for the relatively slow speed of the ALF. The range of possible angular frequencies that could be used to represent the ALF is 2 to 14 rad/s. Angular frequencies in this range did not change the ranking for the binders based on G*/sinδ. Thus, angular frequency did not affect the degree of correlation between G*/sinδ and ALF pavement performance.

- Use of the standard DSR angular frequency of 10.0 rad/s, in lieu of lower angular frequencies that account for the relatively slow speeds of the ALF and the three wheel-tracking devices, had no overall negative or positive effect on the degree of correlation between of G*/sinδ and rutting susceptibility. Changing the angular frequency changed the G*/sinδ's, but not the degree of correlation.

- The data from the French PRT, Hamburg WTD, and Georgia LWT indicated that the 2.20-kPa minimum specification level for G*/sinδ after RTFO is valid. The rut depths provided by the ALF suggested that 2.20 kPa is low, but a different minimum specification level could not be suggested due to the limited number of mixtures tested.

8. Recommendations

- Because of the limited number of mixtures tested in this study, it is recommended that the speeds of full-scale accelerated pavement testers and laboratory wheel-tracking devices be taken into account when making comparisons to G*/sinδ, even though the data in this study did not show this to be of benefit. Theoretically, adjustments should be made.

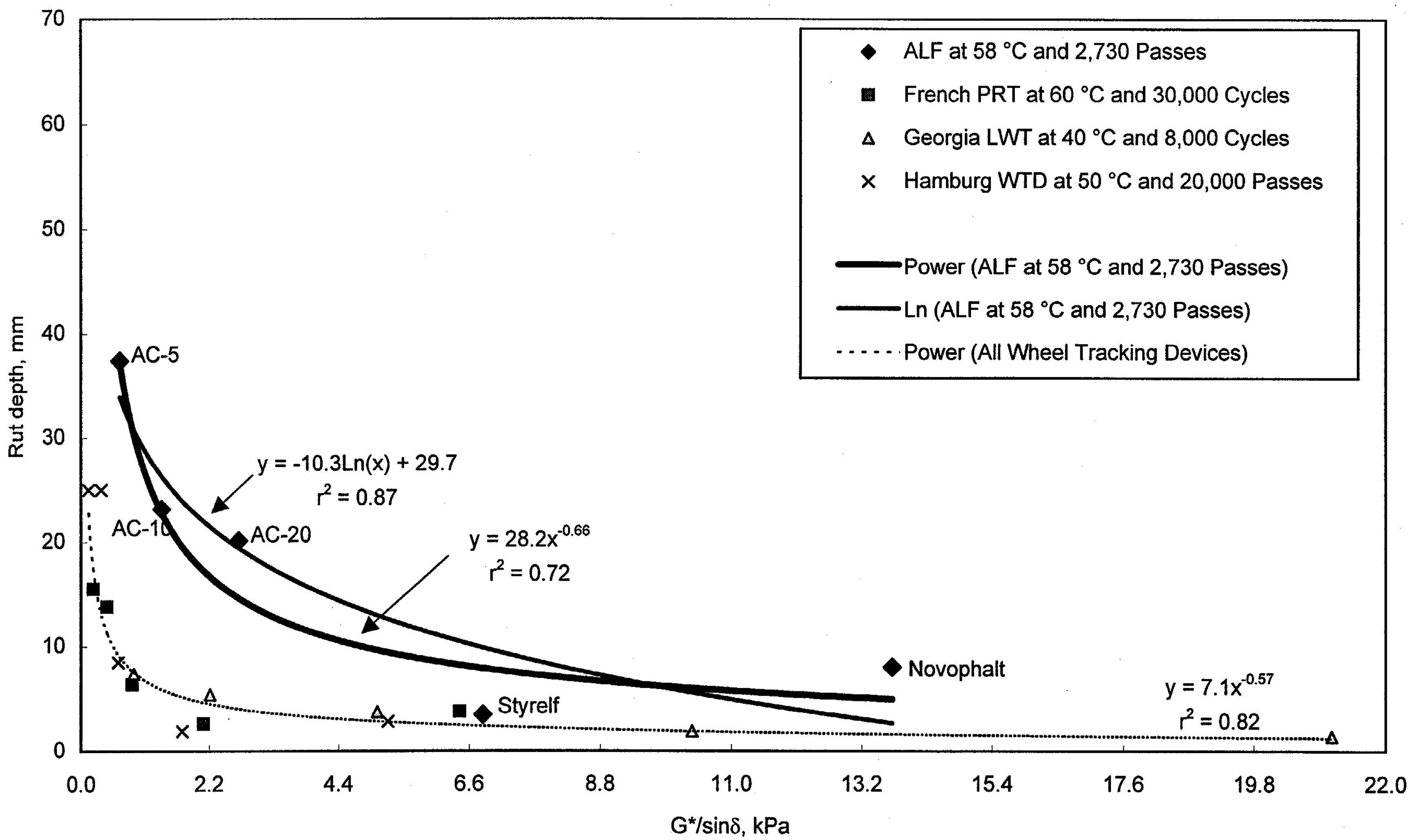

Figure 64. Rut depths at 2,730 ALF wheel passes and from the wheel-tracking devices vs. G*/sinδ after RTFO.

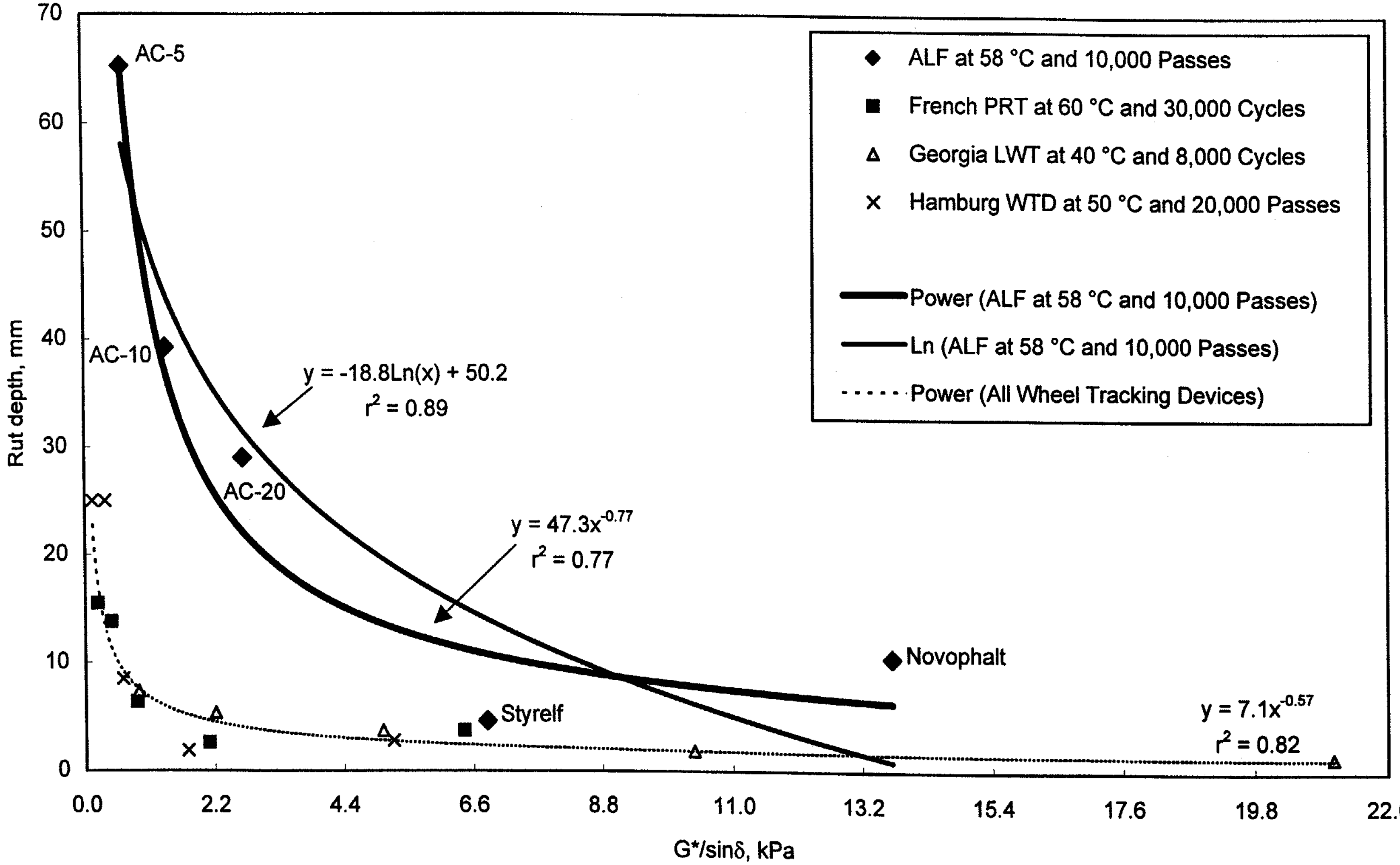

Figure 65. Rut depths at 10, 000 ALF wheel passes and from the wheel-tracking devices vs. G*/sinδ after RTFO.

Table 97. G*/sinδ and binder rankings at 10.0 rad/s and the temperatures used in the ALF pavement and laboratory wheel-tracking tests.[1]

Pre-Superpave Designation:	AC-5	AC-10	AC-20	Novo-phalt	Styrelf
Superpave PG:	58-34	58-28	64-22	76-22	82-22
	G*/sinδ's of the RTFO Residues, Pa				
ALF Pavement Tests, 58 °C	2 600 E	5 285 D	10 010 C	21 090 B	35 170 A
French PRT, 60 °C	2 096 E	4 202 D	7 897 C	16 580 B	28 504 A
Georgia LWT, 40 °C	38 640 D	82 800 C	159 900 B	263 600 A	270 900 A
Hamburg WTD, 50 °C	7 528 E	15 880 D	30 660 C	60 150 B	75 960 A

[1]The letters are the statistical ranking, with "A" denoting the binder(s) with the highest G*/sinδ.

Table 98. Rankings for the five surface mixtures vs. rankings based on the G*/sinδ's of the binders at 10.0 rad/s and the temperature used in the ALF pavement and laboratory wheel-tracking tests.[1]

ALF, 58 °C

Binder, G*/sinδ at 10.0 rad/s	Pavement Performance
(A) Styrelf	(A) Novophalt
(B) Novophalt	(B) Styrelf
(C) AC-20	(C) AC-20
(D) AC-10	(C) AC-10
(E) AC-5	(D) AC-5

French PRT, 60 °C

Binder, G*/sinδ at 10.0 rad/s	Percent Rut Depth	Slope
(A) Styrelf	(A) Novophalt	(A) Novophalt
(B) Novophalt	(B) Styrelf	(B) Styrelf
(C) AC-20	(C) AC-20	(C) AC-20
(D) AC-10	(D) AC-10	(D) AC-10
(E) AC-5	(D) AC-5	(D) AC-5

Georgia LWT, 40 °C

Binder, G*/sinδ at 10.0 rad/s	Rut Depth
(A) Styrelf	(A) Novophalt
(A) Novophalt	(B) Styrelf
(B) AC-20	(BC) AC-20
(C) AC-10	(C) AC-10
(D) AC-5	(C) AC-5

Hamburg WTD, 50 °C

Binder, G*/sinδ at 10.0 rad/s	Creep Slope
(A) Styrelf	(-) Novophalt[2]
(B) Novophalt	(A) Styrelf
(C) AC-20	(B) AC-20
(D) AC-10	(C) AC-10
(E) AC-5	(D) AC-5

[1]The letters are the statistical ranking, with "A" denoting the binder(s) or mixture(s) with the lowest susceptibility to rutting.

[2]This mixture had the lowest susceptibility to rutting but it was not included in the statistical ranking because of high variability.

CHAPTER 7: EFFECT OF AGE HARDENING ON PAVEMENT RUTTING SUSCEPTIBILITY

1. Background and Objectives

The pavement rutting data given in chapter 3 indicated that binder age hardening may have affected the results of the pavement tests, which were performed from 1994 to 1997. However, most of the pavement tests consisted of testing the five surface mixtures at three different temperatures with no replication. The conclusion that age hardening affected the data was based on a comparison of the data collected in 1997 with the data collected in prior years. The G*/sinδ's of binders recovered from pavement cores taken after failure did not conclusively indicate that binder age hardening was a problem.

Lanes 9, 10, and 11 were the only lanes that were tested more than once at a given test temperature. These lanes were tested at 58 °C in both 1994 and 1995. To further examine the effect that age hardening can have on rutting susceptibility, these lanes were retested at 58 °C in 1998.

One additional site, namely, site 4 of lane 10, was tested in 1998 using a tire pressure of 520 kPa compared with the pressure of 690 kPa that was used when testing all other sites. Testing this site at a reduced tire pressure was a mini-study added to the project after the main experiments were completed. The data from this site were compared with the data from site 3 of lane 10, which was also tested in 1998, but at a tire pressure of 690 kPa.

2. Results and Conclusions for the Age-Hardening Study

The high-temperature continuous PG's of the neat binders and binders recovered from the pavements are given in table 99. Table 100 gives the G*/sinδ's of the binders at the pavement test temperature of 58 °C. The data show that the AC-20 (PG 70) surface mixture and the AC-5 (PG 59) base mixture hardened approximately one high-temperature PG over the 4-year period. (The increment between PG's is 6 °C.) The AC-5 (PG 59) surface mixture exhibited no trend in age hardening with time.

The pavement data are presented in table 101. The air voids show that densification generally decreased with an increase in age, although the air voids of cores taken from out of the wheelpath, which were considered the initial air-void levels, tended to be lower for the sites tested in 1998.

The wheel passes needed to produce rut depths of 10, 15, and 20 mm at 58 °C are given in table 101. Figures 66, 67, and 68 show the relationships using the rut depths in the asphalt pavement layer. The wheel passes for lane 9 were low and showed no trend with time. The wheel passes for lane 10 were substantially higher in 1998 compared with 1994 and 1995, while the wheel passes in 1994 and 1995 were close to each other. The wheel passes for lane 11 increased with time, except for the 1994 and 1995 wheel passes based on total rut depth. The data show that the time between the pavement tests can significantly affect the results provided by the ALF. For example, the wheel passes needed to obtain a 20-mm rut depth in the AC-5 (PG 59) base mixture layer increased from 8,984 in 1994 to 61,400 in 1998.

The increases in wheel passes over time were attributed to binder age hardening. Therefore, the wheel passes in table 101 were linearly regressed against the PG's in table 99 and the G*/sinδ's at 10 rad/s in table 100. The coefficients of determination, r^2, are given in table 102 with high coefficients shown in bold type. The wheel passes at rut depths of 15 and 20 mm for lane 9 highly correlated with both PG and G*/sinδ, even though there was no trend in the wheel passes with time. Therefore, the wheel passes were a function the variation in PG and G*/sinδ from test site to test site for this lane. The correlations were poor for lane 10 because the wheel passes in 1995 were relatively low compared with the PG and G*/sinδ of the recovered binder. The wheel passes for lane 11 highly correlated with G*/sinδ, while the correlations with PG were generally mediocre. Higher r^2's could be expected using G*/sinδ because the actual pavement test temperature of 58 °C was used when determining G*/sinδ. In conclusion, G*/sinδ highly correlated with the rutting data for two out of the three pavement tests.

The binder contents, aggregate gradations, and air voids of the mixtures did not explain the discrepancies provided by the 1997 pavement data. The data presented in this chapter indicated that binder age hardening could possibly be the reason, although a reason why the properties of the binders recovered from the pavements in 1997 did not explain the discrepancies was not found.

3. Results and Conclusions for the Tire Pressure Study

The high-temperature continuous PG's of the binders recovered from sites 3 and 4 of lane 10 were both 78 °C. The G*/sinδ's of the recovered binders at 58 °C were 10.4 and 10.7 °C using 2.25 rad/s, and 33.6 and 34.8 °C using 10 rad/s. The binder properties for these two sites were not significantly different.

A comparison of the pavement data in table 101 showed that the decrease in tire pressure from 690 kPa (site 3) to 520 kPa (site 4) only provided a 3.6-percent increase in wheel passes based on a 20-mm rut depth in the asphalt pavement layer. The wheel passes increased from 12,720 to 13,182. Most likely, this difference is smaller than the repeatability of the ALF data.

The decrease in tire pressure increased the wheel passes from 6,206 to 7,926 based on a total rut depth of 20 mm. This is a 28-percent increase in wheel passes. Whether this increase was at least partially due to differences in the properties of the underlying crushed aggregate base layer was not known. Therefore, a firm conclusion regarding this increase could not be made.

Table 99. High-temperature continuous PG's at three different ages.

Mixture	Lane	High-Temperature Continuous PG's of Neat Binders at 10 rad/s after RTFO, °C	Year of ALF Pavement Test and High-Temperature Continuous PG's of Recovered Binders at 10 rad/s,		
			1994	1995	1998
AC-5 Surface	9	59	63	68	64
AC-20 Surface	10	70	72	78	78
AC-5 Base	11	59	67	72	74

Table 100. G*/sinδ's at three different ages.

Mixture	Lane	G*/sinδ's of the Neat Binders after RTFO at 58 °C, kPa	Year of ALF Pavement Test and the G*/sinδ's of the Recovered Binders at 58 °C, kPa		
			1994	1995	1998
		DSR Frequency = 2.25 rad/s			
AC-5 Surface	9	0.66	1.3	ND	1.4
AC-20 Surface	10	2.70	4.3	ND	10.4
AC-5 Base	11	0.66	1.7	5.5	6.4
		DSR Frequency = 10.0 rad/s			
AC-5 Surface	9	2.6	4.3	7.9	5.2
AC-20 Surface	10	10.0	12.4	25.0	33.6
AC-5 Base	11	2.6	6.9	12.7	19.7

ND = No data; binder samples were tested.
Note: AC-5 = PG 59; AC-20 = PG 70.

Table 101. ALF pavement data at 58 °C and three ages.

	Surface Mixture AC-5 (PG 59) Lane 9 Year and Site			Surface Mixture AC-20 (PG 70) Lane 10 Year and Site				Base Mixture AC-5 (PG 59) Lane 11 Year and Site		
	1994 2	1995 1	1998 4	1994 2	1995 1	1998 3	1998 4	1994 2	1995 1	1998 3
Pavement Depth				**Pavement Temperature, °C**						
0 mm	62	61	57	61	59	64	64	62	58	62
20 mm	59	57	56	59	57	60	60	60	56	59
102 mm	55	55	55	55	55	57	58	58	55	55
197 mm	51	52	53	51	51	54	57	52	50	54
Difference, 0 to 197 mm	11	9	4	10	8	10	7	10	8	8
				Air Voids, Top 100 mm of Pavement, Percent						
OWP	7.7	7.8	5.8	9.3	8.8	7.4	8.4	6.0	7.3	5.7
IWP	3.6	3.2	4.0	3.4	3.9	5.3	5.8	2.2	4.0	4.1
Densification	4.1	4.6	1.8	5.9	4.9	2.1	2.6	3.8	3.3	1.6
				Air Voids, Bottom 100 mm of Pavement, Percent						
OWP	7.9	6.1	5.2	9.5	7.2	6.0	6.7	6.0	6.1	4.2
IWP	3.1	2.5	2.6	3.7	3.2	3.0	3.2	1.9	2.6	3.1
Densification	4.8	3.6	2.6	5.8	4.0	3.0	3.5	4.1	3.5	1.1
Average Densification	4.4	4.1	2.2	5.8	4.4	2.6	3.0	4.0	3.4	1.4
Rut Depth in Asphalt Layer				**Number of ALF Wheel Passes**						
10 mm	115	143	87	262	206	1010	1344	612	1363	2217
15 mm	279	395	275	1031	937	4445	5111	2946	5544	15472
20 mm	521	814	619	2724	2741	12720	13182	8984	15000	61400
Total Rut Depth				**Number of ALF Wheel Passes**						
10 mm	85	140	56	226	169	546	982	707	676	914
15 mm	212	310	186	739	687	2263	3331	2224	2399	5217
20 mm	407	546	435	1713	1859	6206	7926	5012	5895	17950

OWP = Out of wheelpath.
IWP = In wheelpath.

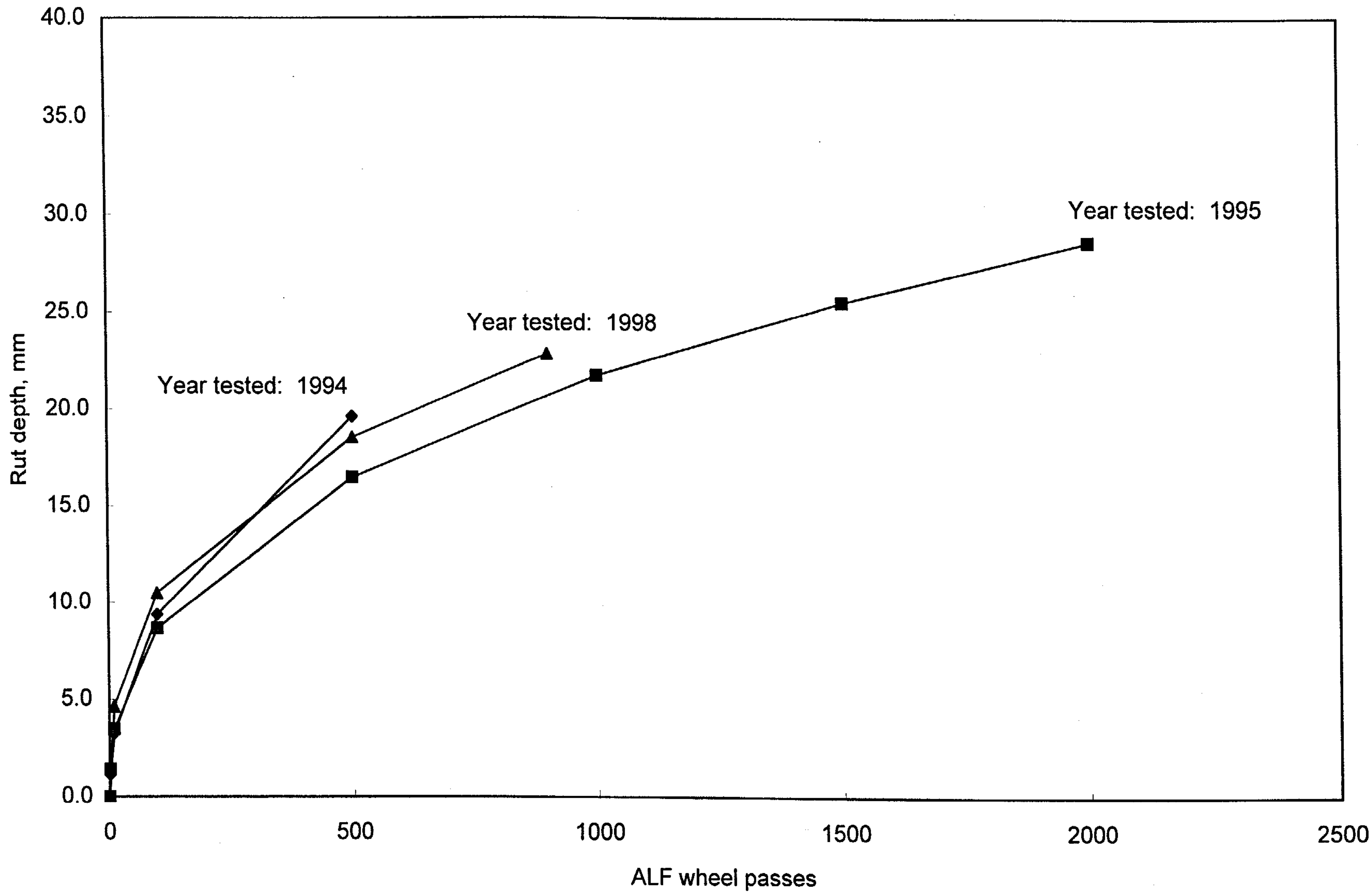

Figure 66. Rut depth in the asphalt pavement layer from the model vs. ALF wheel passes for lane 9.

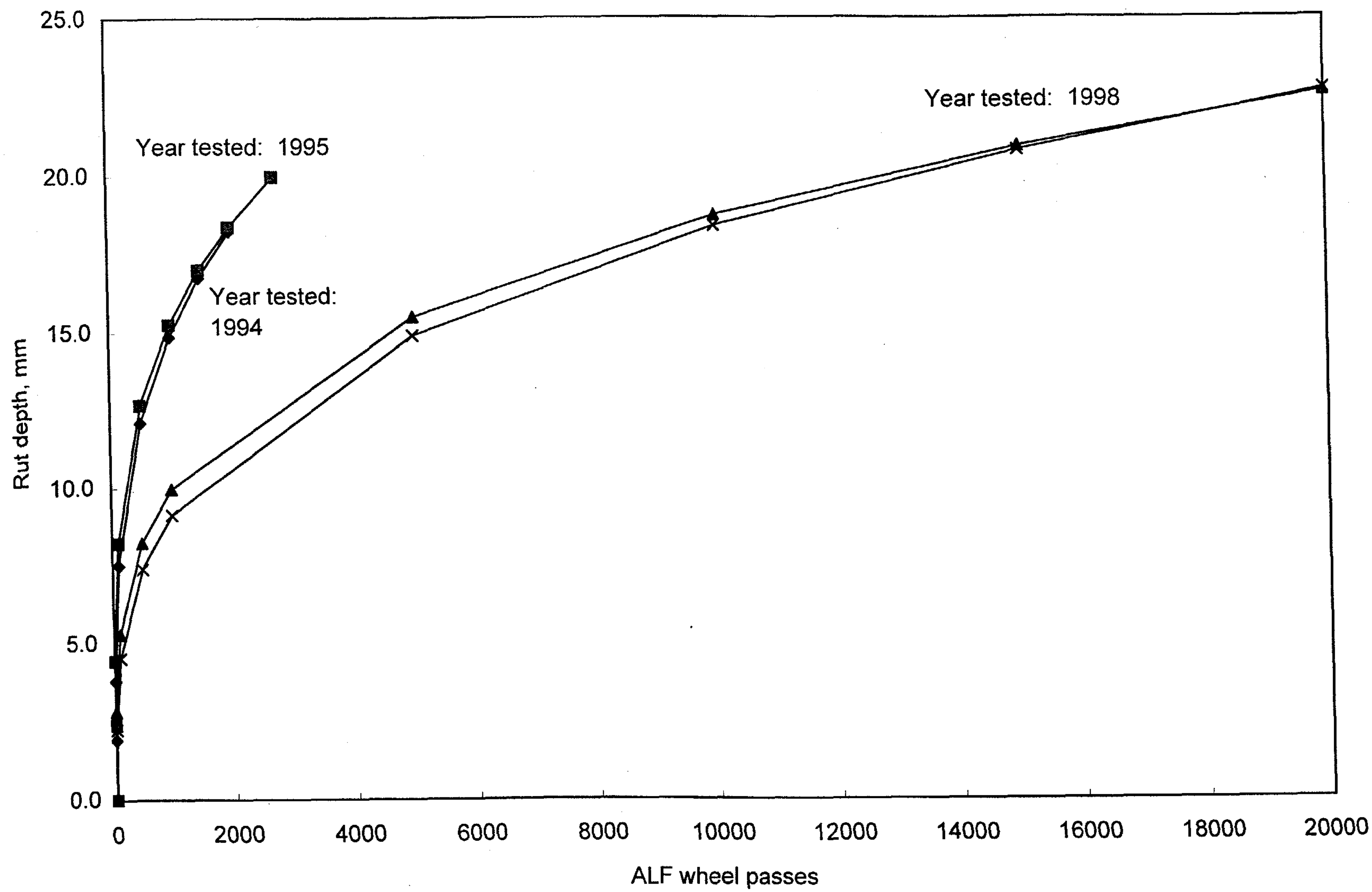

Figure 67. Rut depth in the asphalt pavement layer from the model vs. ALF wheel passes for lane 10.

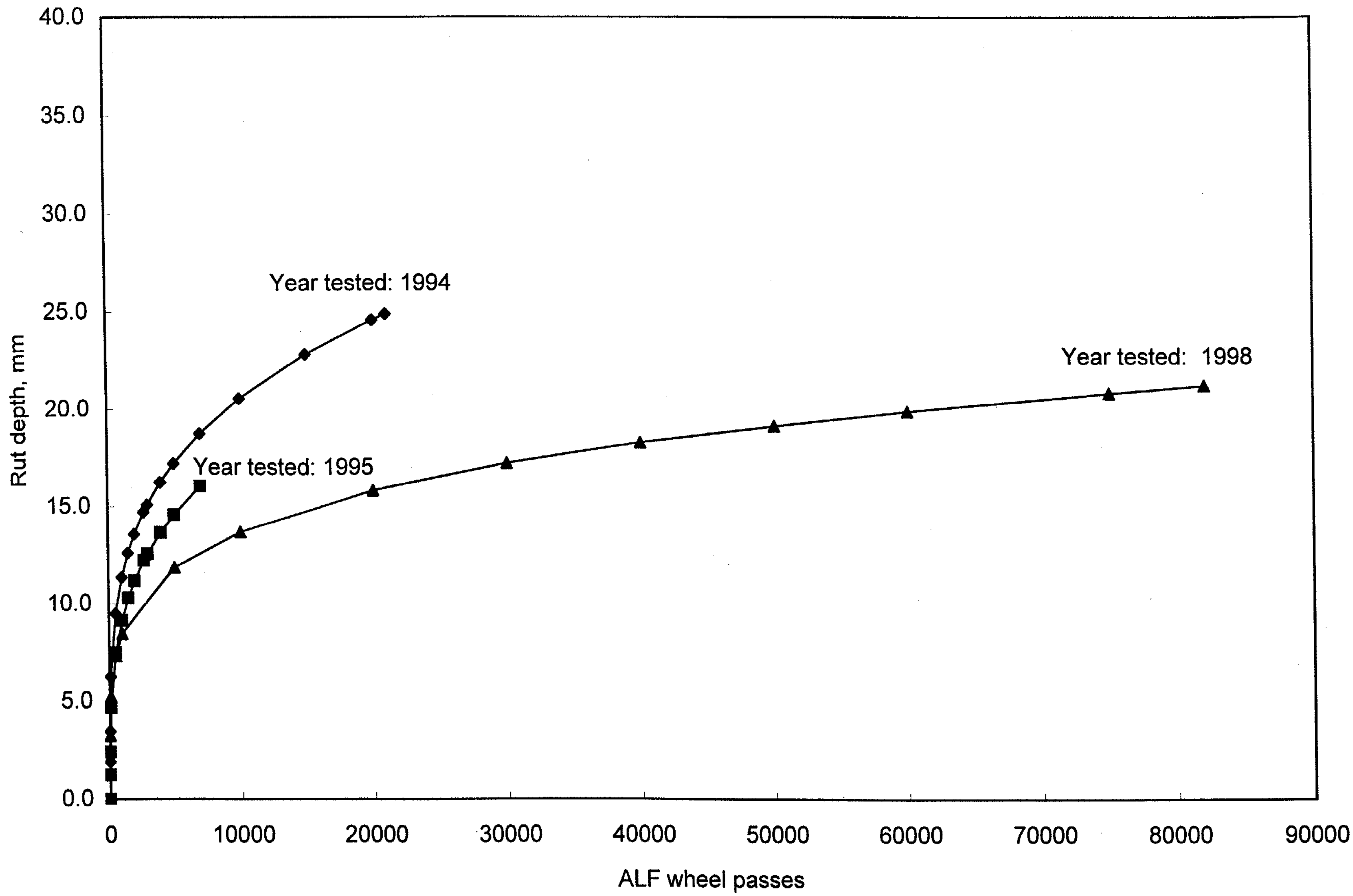

Figure 68. Rut depth in the asphalt pavement layer from the model vs. ALF wheel passes for lane 11.

Table 102. Coefficient of determination, r^2, between the ALF wheel passes at rut depths of 10, 15, and 20 mm and the PG or $G^*/\sin\delta$ at 10 rad/s.

	Surface Mixture AC-5 (PG 59) Lane 9		Surface Mixture AC-20 (PG 70) Lane 10		Base Mixture AC-5 (PG 59) Lane 11	
	PG	$G^*/\sin\delta$	PG	$G^*/\sin\delta$	PG	$G^*/\sin\delta$
Rut Depth in Asphalt Layer						
10 mm	0.58	0.52	0.20	0.61	**0.92**	**0.99**
15 mm	**0.96**	**0.92**	0.23	0.64	0.71	**0.92**
20 mm	**0.98**	**0.98**	0.25	0.67	0.62	**0.86**
Total Rut Depth						
10 mm	0.74	0.69	0.14	0.53	0.40	0.69
15 mm	**0.85**	**0.81**	0.22	0.64	0.58	**0.83**
20 mm	**0.99**	**0.99**	0.27	0.69	0.58	**0.88**

CHAPTER 8: CONCLUSIONS AND RECOMMENDATIONS

1. Validation of G*/sinδ From the DSR Based on ALF Pavement Rutting Performance at 58 °C

- Unmodified binders with higher G*/sinδ's after RTFO aging provided mixtures with lower pavement rutting susceptibilities for a given nominal maximum aggregate size.

- A discrepancy between G*/sinδ at 58 °C after RTFO aging and ALF pavement rutting performance at 58 °C was found. The G*/sinδ of the Styrelf binder was significantly higher than for Novophalt (13.7 kPa vs.6.83 kPa), but the asphalt pavement layer with Novophalt had a significantly lower susceptibility to rutting. The ALF produced a rut depth of 20 mm in the asphalt pavement layer with Styrelf at 220,000 wheel passes. The rut depth in the asphalt pavement layer with Novophalt was 9.4 mm at 220,000 wheel passes. The rutting performances of both mixtures were excellent at 58 °C.

- The following binder parameters measured at 58 °C using the DSR provided the same discrepancy for the Novophalt and Styrelf materials: G*, δ, sinδ, tanδ, zero shear viscosity, δ using RTFO/PAV residues, cumulative permanent strain after four cycles of repeated loading, and the G*/sinδ's of binders recovered from pavement cores after failure. The use of DSR angular frequencies ranging from 2.5 to 63.0 rad/s was not beneficial. Absolute viscosity also provided the same discrepancy.

- The French PRT at 60 °C, Georgia LWT at 40 °C, Hamburg WTD at 50 °C, unconfined repeated load compression test at 58 °C, and the SST at 40 °C provided the same discrepancy between G*/sinδ and rutting performance for the Novophalt and Styrelf materials. Test temperature and loading frequency were taken into account in these correlations.

- The use of the standard DSR angular frequency of 10.0 rad/s, in lieu of lower angular frequencies that account for the relatively slow speeds of the ALF and the three wheel-tracking devices compared with highway traffic, had no significant negative or positive effect on the degree of correlation between G*/sinδ and ALF pavement rutting performance. Changing the angular frequency changed the G*/sinδ's, but not the degree of correlation.

- An increase in nominal maximum aggregate size from 19.0 to 37.5 mm, and the associated 0.85-percent decrease in optimum binder content, significantly decreased rutting susceptibility based on ALF pavement rutting performance at 58 °C for a given binder. No binder property can be expected to provide the effects of mixture composition and aggregate properties on pavement performance. Binder properties should provide some minimal level of performance.

- Part of the decrease in pavement rutting susceptibility provided by the increase in nominal maximum aggregate size could have been due to differences in binder age hardening. The high-temperature continuous PG of the binder recovered from the AC-5 (PG 59) base mixture was higher than for the AC-5 (PG 59) surface mixture. The same result was found for the two gradations containing the AC-20 (PG 70) binder. Most likely, the 0.85-percent lower binder content used in the base mixtures allowed more aging to occur during construction and early pavement life, even though the air voids were not higher in the base mixtures.

- Although the increase in nominal maximum aggregate size decreased rutting susceptibility, it did not reduce the influence of binder grade on rutting performance on a percentage basis. The increase in ALF wheel passes due to an increase in the high-temperature continuous PG from 59 to 70 was 310 percent for the surface mixtures and 380 percent for the base mixtures.

- The rut depths from the French PRT, Hamburg WTD, and Georgia LWT indicated that rutting should not occur when the G*/sinδ of the binder is greater than the minimum Superpave binder specification criterion of 2.20 kPa. Therefore, the results from these devices supported the current criterion. The number of binders used in this study was not sufficient for determining whether this criterion was valid based on ALF pavement rutting performance at 58 °C. ALF provided a large gap in performance between the unmodified and modified binders.

2. **Validation of G*/sinδ Based on ALF Pavement Rutting Performance at All Temperatures**

- The overall relationship between G*/sinδ after RTFO aging and ALF pavement rutting performance was poor, although the trend was correct for the unmodified binders.

- The G*/sinδ of the Styrelf binder after RTFO aging was higher than for the Novophalt binder at each pavement test temperature, but the pavement with Novophalt was always more resistant to rutting. This was the major discrepancy that was found.

- When the data from the Novophalt and Styrelf pavement tests were excluded from the analysis, a minimum allowable G*/sinδ of 4.4 kPa eliminated the poorest performing mixtures. Even so, pavement life still varied significantly when the G*/sinδ's of the binders after RTFO aging were above 4.4 kPa.

- Discrepancies between rutting performance and test temperature for the pavements with the Novophalt, Styrelf, and AC-20 binders manifested themselves in 1997, which was 3.5 years after construction. These discrepancies were attributed to asphalt binder age hardening. However, eliminating the 1997 data from the analyses did not change the conclusions concerning G*/sinδ.

- The $G^*/\sin\delta$'s of binders recovered from the pavements after failure were greater than the $G^*/\sin\delta$'s after RTFO aging. This included the initial, 1994 pavement tests. However, these $G^*/\sin\delta$'s did not completely explain the discrepancies between pavement performance and test temperature, and they did not provide a better correlation with pavement performance. Also, some of the pavements failed rapidly even though the $G^*/\sin\delta$'s of the recovered binders were above the minimum criterion of 2.20 kPa.

- The downward only rut depths, based on the initial surface elevations of the pavements, were used to validate $G^*/\sin\delta$. However, the peak-to-valley rut depths were also examined. These rut depths provided the same discrepancy for the Novophalt and Styrelf materials.

3. **Validation of Mixture Tests Based on the ALF Pavement Rutting Performances of the Five Surface Mixtures at 58 °C**

- The French PRT at 60 °C, Georgia LWT at 40 °C, and Hamburg WTD at 50 °C ranked the five surface mixtures the same as ALF at 58 °C based on the averages. Each test provided a slightly different statistical ranking based on Fisher's LSD. The French PRT and Hamburg WTD provided statistical rankings that were slightly better than the Georgia LWT, probably because the range in the data from the best to the worst mixture was smaller for the Georgia LWT.

- The dynamic moduli at 200 cycles and the cumulative permanent strains at 10,000 cycles from an unconfined repeated load compression test at 58 °C ranked the five surface mixtures the same as ALF at 58 °C based on the averages. The statistical rankings were slightly different, but the degree of correlation to ALF was good. The slopes from the relationship between cumulative permanent strain and cycles did not differentiate the five surface mixtures according to rutting susceptibility.

- The degree of correlation between the SST data at 58 °C and ALF pavement rutting performance at 58 °C was poor. Most SST measurements at 58 °C had coefficients of variation (standard deviation divided by the average) of 20 percent and greater, whereas the coefficients at 40 °C were generally less than 20 percent. The coefficients of variation were based on the data from the surface mixtures, which consisted of five binder grades, a single aggregate gradation, and a single binder content. The use of additional mixtures may increase these coefficients.

- Six of eight SST measurements at 40 °C ranked the five surface mixtures the same as ALF at 58 °C based on the averages: (1) the compliance parameter, permanent shear strain, and maximum axial stress from Simple Shear at Constant Height, (2) G^* and $G^*/\sin\delta$ at all frequencies from Frequency Sweep at Constant Height, and (3) cumulative permanent strain at 5,000 cycles from Repeated Shear at Constant Height.

- The statistical rankings for the compliance parameter and permanent shear strain from Simple Shear at Constant Height at 40 °C were identical to the statistical ranking provided by the ALF at 58 °C. The statistical rankings provided by G*, G*/sinδ, and cumulative permanent strain at 5,000 cycles were not identical to ALF, but the degree of correlation was good. The maximum axial stress correlated less with ALF pavement rutting performance based on the statistical rankings.

- The two SST measurements at 40 °C that did not correlate with ALF at 58 °C were the slopes from the relationship between log G* and log frequency from Frequency Sweep at Constant Height, and the slopes from the relationship between cumulative permanent strain and cycles from Repeated Shear at Constant Height.

- The PURWheel at 58 °C did not rank the mixtures the same as ALF at 58 °C based on the averages. However, the statistical ranking was reasonably close to the statistical ranking provided by the ALF.

4. **Validation of Mixture Tests Based on the ALF Pavement Rutting Performances of the Surface and Base Mixtures With AC-5 and AC-20 (PG 59 and PG 70) at 58 °C**

   a. **Validation Using Laboratory-Prepared Specimens**

- The increase in nominal maximum aggregate size from 19.0 to 37.5 mm and the associated 0.85-percent decrease in optimum binder content significantly decreased rutting susceptibility based on ALF pavement rutting performance at 58 °C.

- Only two mixture tests ranked the four mixtures the same as ALF pavement rutting performance at 58 °C based on the averages: the cumulative permanent shear strain at 5,000 cycles and 40 °C from Repeated Shear at Constant Height, and the maximum axial stress at 58 °C from Simple Shear at Constant Height. The averages from the other SST measurements, the wheel-tracking.devices, and the unconfined repeated load compression test did not provide a ranking that was the same as that provided by the ALF.

- No laboratory mixture test provided a statistical ranking for the four mixtures that matched ALF pavement rutting performance at 58 °C. Some of the data from the SST were significantly affected by nominal maximum aggregate size, but the effect was not as great as the effect on pavement performance.

- The majority of the specimens tested by the SST had a diameter and height of 150 mm by 50 mm. However, tests at 40 and 58 °C were also performed on specimens having a diameter and height of 150 mm by 75 mm and 203 by 75 mm. The use of larger specimens did not provide better correlations to ALF pavement rutting performance. Specimens with a height of 75 mm failed rapidly in Repeated Shear at Constant Height at 58 °C; thus, the data had to be compared at 500 cycles rather than at 5,000 cycles.

b. Validation Using Both Laboratory-Prepared and Pavement Specimens

- The method of compaction was evaluated using both laboratory and pavement specimens to determine if it could affect the conclusions from the French PRT, Georgia LWT, and Hamburg WTD. It was found that the method of compaction can affect the data from these tests, but it was not the main reason why these devices were generally insensitive to gradation. It was hypothesized that differences in contact area may be one reason for the discrepancy, but the cause of the discrepancy was not found.

- The SST using specimens with a diameter and height of 150 by 50 mm provided the same conclusions as the wheel-tracking devices. The method of compaction can affect the data, but it was not the main reason why the tests were generally insensitive to gradation. The average cumulative permanent strains from Repeated Shear at Constant Height at 40 °C using pavement cores was the only measurement that provided a ranking that agreed with ALF pavement rutting performance at 58 °C. Even so, these strains were not significantly different based on statistical analyses.

- Pavement cores with a diameter of 203 mm provided good correlations between the SST data at 40 and 58 °C and ALF pavement rutting performance at 58 °C. These correlations were the best correlations obtained in this study for any mixture test. Correlations using cores with a diameter of 150 mm were not as good. However, the binders in the base mixtures hardened more rapidly than in the surface mixtures, and the 203-mm diameter cores were taken at the end of the study in January 1999. The 150-mm diameter cores were taken during the summer of 1997. Based on recovered binder properties, it appeared that differences in age hardening led to the seemingly good correlations.

- The PURWheel provided conclusions that were different from those provided by the French PRT, Georgia LWT, Hamburg WTD, unconfined repeated load compression test, and SST. The data from the PURWheel were significantly affected by nominal maximum aggregate size, but not by binder grade.

5. Validation of Mixture Tests Based on the ALF Pavement Rutting Performances of All Seven Mixtures

- The results from the following tests did not correlate with pavement rutting susceptibility: (1) Marshall stability and flow, (2) U.S. Corps of Engineers Gyratory Testing Machine, (3) NCHRP AAMAS prediction model, and (4) individual AAMAS tests, including compressive strength, compressive strain at failure, creep modulus, total creep strain, and permanent creep strain after unloading. No confining pressure is used when performing AAMAS compression tests.

- The correlation between the PURWheel and ALF for the seven mixtures was reasonably good, primarily because the data were affected by nominal maximum aggregate size. A linear regression provided an r^2 of 0.8. The correlations for the other tests were generally poor because they could not measure the effects of nominal maximum aggregate size.

- The air voids in the specimens tested by the AAMAS creep test and the unconfined repeated load compression test did not decrease during testing. Therefore, these tests measured permanent deformation due to viscous flow (also called shape distortion) without volume change (densification or volume distortion). The ALF, French PRT, Georgia LWT, Hamburg WTD, and PURWheel measure the combined effects of viscous flow and volume change. The SST was designed so that changes in volume would not occur during testing; thus, it was designed to measure only permanent deformation due to viscous flow.

- The laboratory mixture tests were performed according to customary procedures. However, most of these tests and the ALF tests had different loading frequencies or test temperatures. Since the performance of a binder in an asphalt mixture is dependent on frequency and temperature, it should not be expected that the rankings from these tests perfectly agree.

6. Additional Conclusions Concerning the Laboratory Mixture Tests

- A slab thickness of 100 mm is tested by the French PRT when the total pavement thickness for the mixture to be placed will be greater than 50 mm. A slab thickness of 50 mm is tested when the thickness will be equal to, or less than, 50 mm. The data showed that the rut depths tended to be greater using 50-mm slabs at an equal number of wheel passes.

- Even though the French PRT was found to be more severe using 50-mm-thick slabs, the French pass/fail specification was generally found to be more severe when testing 100-mm slabs. This means that the French methodology is more severe for mixtures to be used in thick, lower pavement layers.

- The resilient modulus at 10.0 Hz from the unconfined repeated load compression test and the shear modulus at 10.0 Hz from SST Frequency Sweep were used to calculate Poisson's ratios based on the laws of elasticity for isotropic materials. The ratios ranged from 1.10 to 4.60 at 40 °C and from 0.24 to 2.21 at 58 °C. Theoretically, these ratios cannot be greater than 0.5 for an isotropic, elastic material. This indicated that the elastic laws are not valid for these tests, and one modulus cannot be calculated from the other modulus using an assumed Poisson's ratio.

7. **Additional Conclusions Concerning the ALF Pavement Rutting Tests**

- The reductions in air voids due to trafficking (densification) in the top and bottom halves of the 200-mm-thick asphalt pavement layer were not significantly different at a 95-percent confidence level for any pavement test. Based on the average densification in the top and bottom halves, it was found that the average densification in the bottom half could be greater than, equal to, or less than the average densification in the top half.

- The decreases in air voids due to trafficking indicated that when the rut depth in the asphalt pavement layer was 20 mm, the range in the percent densification was approximately 20 to 55 percent, which is 4 to 11 mm.

- Based on the rutting data from all pavements, rutting occurred in all asphalt pavement lifts. No particular lift or group of lifts consistently rutted the most. (The surface mixtures were placed in four 50-mm lifts, while the base mixtures were placed in two 100-mm lifts.) The rut depths used in this analysis consisted of both the rut depth due to densification and to viscous flow.

- By dividing the total rut depth into the percent rut depth in the asphalt pavement layer and the percent rut depth in the underlying layers, as expected, it was found that the percent rut depth in the underlying layers increased as the asphalt pavement layer became thinner due to lateral shearing and flow.

- The slopes and intercepts provided by the relationships between pavement rut depth and wheel passes are not fundamental material properties: they are regression coefficients that depend on the type of regression used to calculate them. The slope or intercept alone cannot be used as a rutting performance indicator. Additional conclusions concerning the slope and intercept are given at the end of chapter 3.

8. **Recommendations**

- The relationship between $G^*/\sin\delta$ after RTFO aging and ALF pavement rutting performance for the unmodified binders suggested that the Superpave $G^*/\sin\delta$ criterion of 2.20 kPa is low. The data indicated that a criterion around 4.40 kPa may be needed. However, the 1997 Superpave binder specification recommended an increase of one high-temperature PG for the ALF traffic level, which was above 10 million ESAL's based on a 20-year design life.[3] An increase of one high-temperature PG is equivalent to doubling the criterion from 2.20 to 4.40 kPa. Thus, the data supported the current criterion of 2.20 kPa if the PG can be adjusted based on both traffic loading (speed) and ESAL's. A potential flaw in this analysis is that it is unknown how the number of ALF wheel passes applied to a pavement at a constant, high temperature relates to Superpave ESAL's.

- If the five binders were to be used in mixtures other than the mixtures tested in this study, different pavement performances would be obtained for a given PG. These mixtures could provide a different criterion. Therefore, additional studies are needed to determine the applicability of the 2.20-kPa criterion even though the data in this study provided no definitive reason for changing the criterion.

- The cause of the discrepancy between G*/sinδ and the pavement rutting performances provided by Novophalt and Styrelf needs to be determined. The average total strain and the average percent permanent strain provided by the DSR were found to be much greater than the average strains for the composite mixture. See appendix D. If the discrepancy is related to an interaction between the effects of the binders and the aggregates, then a binder test may not always be able to properly rank all binders according to relative pavement performance. Appendix E provides DSR data where mastics were tested. These data show an interaction. The G*/sinδ's of four mastics, consisting of the AC-10, AC-20, Novophalt, and Styrelf (PG 58-28, 64-22, 76-22, and 82-22) binders with diabase and hydrated lime, matched ALF pavement rutting performance.

- The French PRT at 60 °C, Georgia LWT at 40 °C, Hamburg WTD at 50 °C, unconfined repeated load compression test at 58 °C, and the SST at 40 °C provided similar conclusions regarding the effects of the five binders on rutting performance. Based on these results, any of these tests can be used to determine the relative effects of asphalt binders on rutting performance. However, the sensitivities of these tests to all key mixture variables need to be determined in future studies.

- The PURWheel and ALF correlated very well. Compared with the other mixture tests, the PURWheel was better at measuring the effects of nominal maximum aggregate size, but less capable of measuring the effects of asphalt binder grade. Each mixture test may be valid for measuring the effects of some variables on rutting performance, but may not be valid for measuring the effects of other variables. A more fundamental study is needed to determine a reason for the differences. (Note: Only pavement slabs were tested by the PURWheel, while both laboratory and pavement specimens were tested by the French PRT, Georgia LWT, Hamburg WTD, and SST. The degree of correlation between ALF and the PURWheel using specimens prepared in the laboratory was not determined.)

- It is recommended that the speeds of full-scale accelerated pavement testers and laboratory wheel-tracking devices be taken into account when validating G*/sinδ. The data obtained in this study did not show this to be of benefit, but the number of mixtures was limited. Theoretically, adjustments should be made.

- The compression modulus at a high temperature should not be computed from a measured shear modulus and an assumed Poisson's ratio. Likewise, a shear modulus should not be computed from a compression modulus.

REFERENCES

1. "Standard Specifications for Transportation Materials and Methods of Sampling and Testing—Part I Specifications," American Association of State Highway and Transportation Officials, 444 North Capital Street, N.W., Suite 225, Washington, D.C., 1993.

2. Road and Bridge Specifications, Virginia Department of Transportation, Richmond, VA, January 1991.

3. "AASHTO Provisional Standards," American Association of State Highway and Transportation Officials, 444 North Capital Street, N.W., Suite 225, Washington, D.C., March 1995 and June 1998.

4. "Standard Specifications for Transportation Materials and Methods of Sampling and Testing—Part II Methods of Sampling and Testing," American Association of State Highway and Transportation Officials, 444 North Capital Street, N.W., Suite 225, Washington, D.C., 1993.

5. R. B. McGennis, R. M. Anderson, T. W. Kennedy, and M. Solaimanian, Background of Superpave Asphalt Mixture Design and Analysis, FHWA-SA-95-003, The Asphalt Institute, Lexington, KY, November 1994, 160 pp.

6. American Society for Testing and Materials, *1994 Annual Book of ASTM Standards*, Section 4—Volume 04.03, 1916 Race Street, Philadelphia, PA, April 1994.

7. Standard Test Method for Uncompacted Void Content of Fine Aggregate (As Influenced by Particle Shape, Surface Texture, and Grading), National Aggregates Association, Silver Spring, MD, June 1993.

8. K. D. Stuart and R. P. Izzo, "Hot-Mix Asphalt Pavement Construction Report for the 1993-2000 FHWA Accelerated Loading Facility Project," FHWA-RD-99-083, Federal Highway Administration, McLean, VA, April 1999, 56 pp.

9. Asphalt Institute, *Mix Design Methods for Asphalt Concrete and Other Hot-Mix Types*, Manual Series NO.2 (MS-2), Lexington, KY, 1988.

10. American Society for Testing and Materials, "Proposed Standard Test Method for Resistance to Plastic Flow of Bituminous Mixtures Using Marshall Apparatus (6-Inch-Diameter Specimen)," Draft No. 8, 1916 Race Street, Philadelphia, PA, December 1992.

11. K. D. Stuart and R. P. Izzo, "Correlation of Superpave™ $G^*/\sin\delta$ With Rutting Susceptibility From Laboratory Mixture Tests," In *Transportation Research Record 1492*, Transportation Research Board, National Research Council, Washington, D.C., 1995, pp. 176-183.

12. K. D. Stuart, "Evaluation of Procedures Used to Predict Moisture Damage in Asphalt Mixtures," Final Report, FHWA/RD-86/091, Federal Highway Administration, Washington, D.C., March 1986, 117 pp.

13. L. H. Van Vlack, *Materials Science for Engineers*, Addison-Wesley Publishing Company, Inc, Reading, MA, 1970.

14. K. D. Stuart and W. S. Mogawer, "Validation of Asphalt Binder and Mixture Tests that Predict Rutting Susceptibility Using the Federal Highway Administration's Accelerated Loading Facility," Presented at the 1997 Annual Meeting of the Association of Asphalt Paving Technologists, Salt Lake City, UT, March 17, 1997.

15. T. W. Kennedy, G. A. Huber, E. T. Harrigan, R. J. Cominsky, C. S. Hughes, H. Von Quintus, and J. S. Moulthrop, "Superior Performing Asphalt Pavements (Superpave): The Product of the SHRP Asphalt Research Program," SHRP-A-410, Strategic Highway Research Program, National Research Council, Washington D.C., 1994.

16. "Distress Identification Manual for the Long-Term Pavement Performance Project," SHRP-P-338, Strategic Highway Research Program, National Research Council, Washington, D.C., 1993.

17. R. Bonaquist and W. S. Mogawer, "Analysis of Pavement Rutting Data from the FHWA Pavement Testing Facility Superpave Validation Study," Presented at the 76th Annual Meeting of the Transportation Research Board, Washington, D.C., 1997.

18. R. Bonaquist, J. A. Sherwood, and K. D. Stuart, "Accelerated Pavement Testing at the Federal Highway Administration Pavement Testing Facility," Prepared and Accepted for Presentation at the 1998 Annual Meeting of the Association of Asphalt Paving Technologists, Boston, MA, March 16-18, 1998.

19. Strategic Highway Research Program (SHRP), *SHRP Designation: M-007, Short- and Long-Term Aging of Bituminous Mixes*, Report SHRP-A-379, National Research Council, Washington, D.C., 1994.

20. H. L. Von Quintus, J. A. Scherocman, C. S. Hughes, and T. W. Kennedy, *Asphalt-Aggregate Mixture Analysis System*, NCHRP Report 338, Transportation Research Board, National Research Council, Washington, D.C., 1991.

21. F. L. Roberts, P. S. Kandhal, E. R. Brown, D. Y. Lee, and T. W. Kennedy, *Hot Mix Asphalt Materials, Mixture Design, and Construction*, National Asphalt Pavement Association (NAPA) Education Foundation, Lanham, MD, 1991.

22. GDT-115, Method of Test for Determining Rutting Susceptibility Using the Loaded Wheel Tester, Georgia Department of Transportation, Atlanta, GA, August 1994.

23. T. Aschenbrener, R. Terrel, and R. Zamora, *Comparison of Hamburg Wheel-Tracking Device and the Environmental Conditioning System to Pavements of Known Stripping Performance*, CDOT-DTD-R-94-1, Colorado Department of Transportation, Denver, CO, January 1994.

24. M. Hines, The Hamburg Wheel-Tracking Device, In *Proceedings of the Twenty-Eighth Paving and Transportation Conference*, Civil Engineering Department, The University of New Mexico, Albuquerque, NM, 1991.

25. D. N. Little, and Y. Hisham, *Improved ACP Mixture Design: Development and Verification*, FHWA/TX-92/1170-1F, Texas Department of Transportation, Austin, TX, March 1992.

26. W. J. Kenis, *Predictive Design Procedures, VESYS Users Manual*, FHWA/RD-77/154, Federal Highway Administration, Washington, D.C., January 1978.

27. P. Romero and W. S. Mogawer, "Evaluation of the Superpave Shear Tester Using 19-mm Mixtures From the Federal Highway Administration's Accelerated Loading Facility," Presented at the 1998 Annual Meeting of the Association of Asphalt Paving Technologists, Boston, MA, March 16-18, 1998.

28. P. Romero and W. S. Mogawer, "Evaluation of the Superpave Shear Tester's Ability to Discern Two Mixtures with Different Size Aggregates Using the Federal Highway Administration's Accelerated Loading Facility," Presented at the 1998 Annual Meeting of the Transportation Research Board, Washington, D.C., 1998.

29. J. B. Sousa, and S. L. Weissman, "Modeling Permanent Deformation in Asphalt-Aggregate Mixes," *Journal of the Association of Asphalt Paving Technologists*, Volume 63, 1994.

30. X. Zhang, and G. Huber, "Effect of Asphalt Binder on Pavement Performance: An Investigation Using the Superpave Mix Design System," *Journal of the Association of Asphalt Paving Technologists*, Volume 65, 1996.

31. K. D. Stuart and W. S. Mogawer, "Effect of Compaction Method on Rutting Susceptibility Measured by Three Laboratory Wheel-Tracking Devices" Presented at the 76th Annual Meeting of the Transportation Research Board, Washington, D.C., 1997.

32. P. Romero, "Effect of Sample Compaction Method on Superpave Shear tester Results," FHWA In-house Report, 1998, 4 pp.

APPENDIX A: DESCRIPTIONS OF THE ACCELERATED LOADING FACILITY (ALF), SELECTED LABORATORY MIXTURE TESTS USED TO MEASURE RUTTING POTENTIAL, AND THE LINEAR KNEADING COMPACTOR

The fliers given in this appendix are intended to be stand alone fliers; therefore, each flier has its own set of table and figure numbers that start at table 1 and figure 1. The numbers do not match the numbers for the rest of the report.

ALF Puts Superpave to the Test

Bituminous Mixtures Laboratory
Federal Highway Administration
Turner-Fairbank Highway Research Center
6300 Georgetown Pike
McLean, VA 22101-2296

June 4, 1998

The Federal Highway Administration (FHWA) has undertaken the lead in implementing Superpave (Superior Performance Asphalt Pavements), the main product of the Strategic Highway Research Program in the area of asphalt binders and hot-mix asphalt. Superpave is a performance-based mixture design and analysis system. A significant component of the implementation program is to validate the Superpave binder tests, mixture tests, and performance prediction models for rutting and fatigue cracking using the FHWA Accelerated Loading Facility (ALF). The FHWA is also using the ALF to validate other laboratory mixture tests that are used to predict rutting or fatigue cracking performance. The FHWA owns two ALF's, shown in figure 1, that are located at the FHWA Pavement Testing Facility, Turner-Fairbank Highway Research Center, McLean, VA. Figure 2 shows the ALF wheel.

The ALF is a full-scale pavement tester that applies 20 years of traffic loadings in less than 6 months. It applies a load, ranging from 43 to 100 kN, through a wheel assembly that models one-half of a single truck axle. A dual tire or wide base (super single) tire can be used. It travels at a maximum speed of 18.5 km/h over a 10-m test section. Approximately 8,600 wheel passes can be applied per day; 50,000 wheel passes can be applied per week, which includes time for maintenance. To simulate highway traffic, the ALF loads the pavement in one direction, and the load can be laterally distributed to simulate traffic wander.

Twelve lanes, each having a length of 44 m and a width of 4 m were constructed in 1993 at the Pavement Testing Facility to assist in the validation of Superpave. Each lane has four test sites; therefore, 48 sites are available for the validation effort. The lanes were constructed using five different asphalt binders with a wide range of expected performance. Table 1 shows the Superpave Performance Grade and Conventional Designation of each binder.

Two gradations were used in the mixtures: a surface mixture gradation that met the 1991 Virginia Department of Transportation (VDOT) specification for an SM-3B mixture and a base mixture gradation that met the VDOT specification for a BM-3 mixture. The nominal maximum aggregate sizes for the surface and base mixtures are 19 mm and 37.5 mm. The purpose of including the base mixtures is to determine the effect of nominal maximum aggregate size on rutting susceptibility and to determine if the influence of binder type on rutting susceptibility decreases with an increase in nominal maximum aggregate size and the associated decrease in optimum binder content. The surface mixtures include all five binders, while the base mixtures include two of the five binders. The asphalt layer of each lane consists of a single mixture so that rutting and fatigue performance is a function of a single mixture. Each mixture contains 1-percent hydrated lime to eliminate moisture damage. Table 1 presents the pavement sections for this study.

Two thicknesses were constructed for the fatigue cracking study. The thickness of the asphalt layer in lanes 1 and 2 is 100 mm. The asphalt layers in the other 10 lanes have a thickness of 200 mm. Two thicknesses are included to determine if the influence of binder grade on fatigue cracking performance is dependent on thickness.

The pavement tests are being performed so that each site fails by a single distress mode, either by rutting or by fatigue cracking. For both evaluations, a 425/65/R22.5, super single tire with a pressure of 690 kPa are being used. For the rutting evaluation, the load is 43 kN and the wheel is not allowed to wander laterally. The target test temperatures are 46, 52, 58, 64, 70, and 76 °C at a pavement depth of 20 mm. For the fatigue evaluation, the load is 53 kN and the total lateral wander is 1070 mm. The target temperatures are 10, 19, and 28 °C at the pavement surface. Superpave evaluates mixtures for their resistance to rutting based on the temperature at a depth of 20 mm, while the surface temperature is used when evaluating mixtures for their resistances to fatigue and low-temperature cracking. The pavements are heated using infrared lamps located underneath the ALF frame.

The following properties are being measured: temperature and moisture content of the crushed aggregate base and subgrade layers, temperature vs. depth in the asphalt layer, air temperature, rainfall, and pavement deflection using a falling-weight deflectometer. Fatigue cracks and rut depths are being measured by performing distress surveys at specified numbers of wheel passes. Post mortem evaluations that include analyses of pavement cores are performed after each pavement fails.

The results from the Superpave binder and mixture tests for rutting and fatigue cracking are being compared to ALF pavement performance. Superpave employs the Dynamic Shear Rheometer to test binders for rutting and fatigue cracking performance. The Superpave Shear Tester and Indirect Tensile Test are used to evaluate mixtures. To validate the Superpave performance models, ALF pavement performance will be compared to the predictions provided by these models. The raw materials needed to perform the laboratory tests are stored at the facility.

Besides validating Superpave, the FHWA is evaluating other laboratory tests used to predict the rutting and fatigue cracking susceptibilities of asphalt mixtures. The resistance to rutting is being predicted using wheel-tracking devices, a creep test, and a repeated load test. The resistance to fatigue cracking is being predicted by subjecting beam specimens to flexural, repeated load tests. The results from these tests will also be compared to ALF pavement performance.

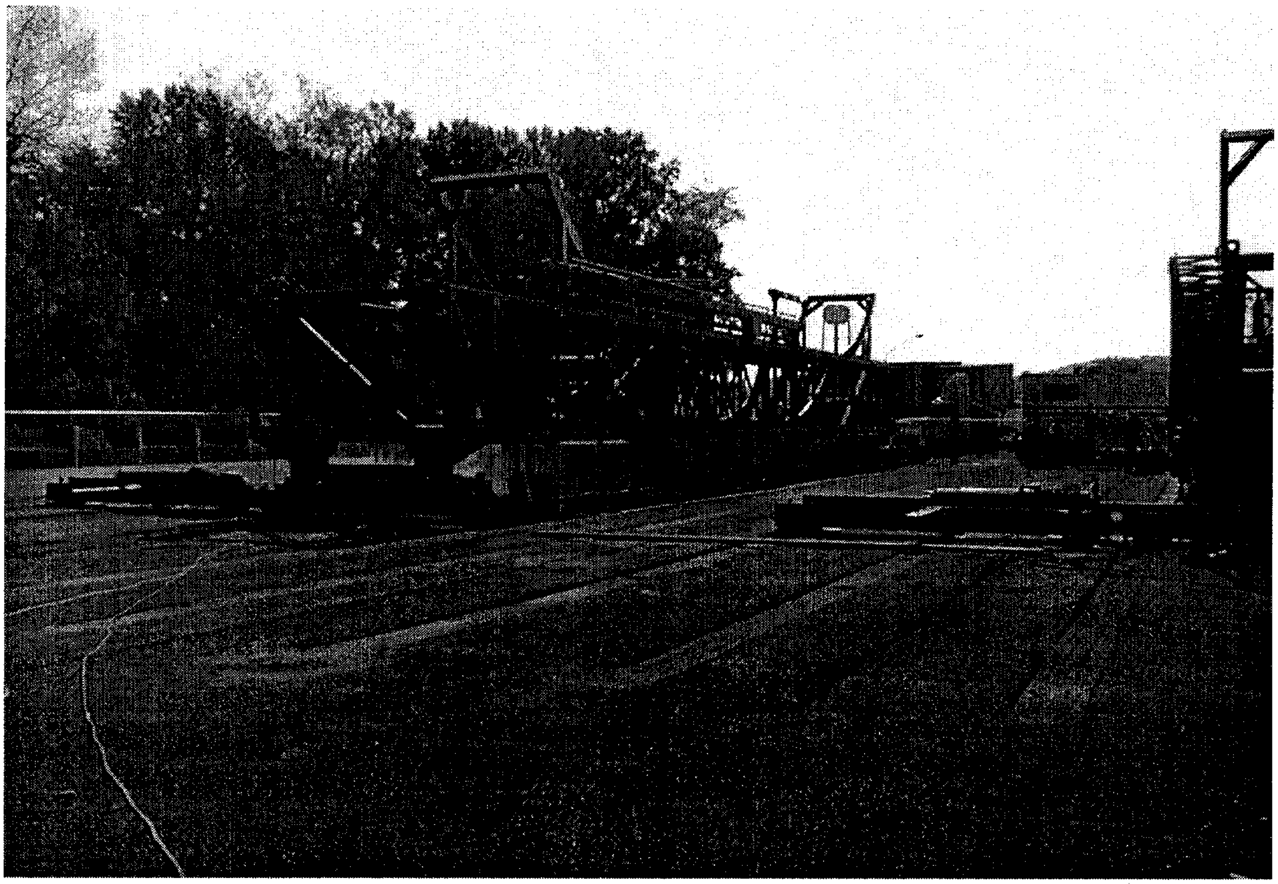

Figure 1. Accelerated Loading Facility.

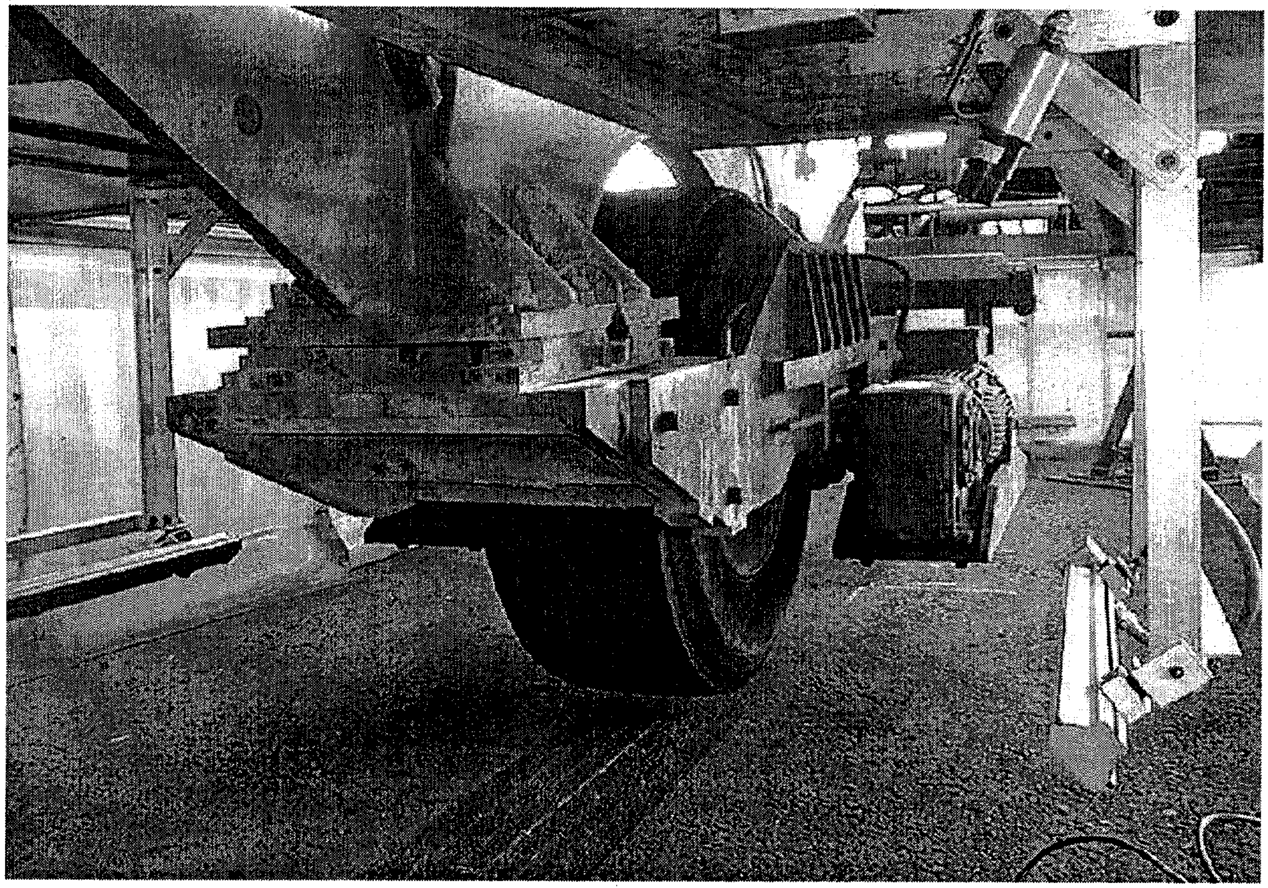

Figure 2. Close-up of the ALF wheel.

Table 1. Pavement lanes for the Superpave validation study.

	Hot-Mix Asphalt Pavement Layer						VDOT 21-A Unbound Crushed Aggregate Base	AASHTO A-4 Uniform Subgrade
Lane	Layer Thickness, mm	VDOT Aggregate Gradation	Pre-Superpave Binder Designation	Superpave Performance Grade (PG)	High Temperature Continuous Grade After RTFO Aging	Intermediate Temperature Continuous Grade After RTFO/PAV	Layer Thickness, mm	Layer Thickness, mm
1	100	SM-3	AC-5	58-34	59	9	560	610
2	100	SM-3	AC-20	64-22	70	17	560	610
3	200	SM-3	AC-5	58-34	59	9	460	610
4	200	SM-3	AC-20	64-22	70	17	460	610
5	200	SM-3	AC-10	58-28	65	15	460	610
6	200	SM-3	AC-20	64-22	70	17	460	610
7	200	SM-3	Styrelf™ I-D	82-22	88	18	460	610
8	200	SM-3	Novophalt™	76-22	77	20	460	610
9	200	SM-3	AC-5	58-34	59	9	460	610
10	200	SM-3	AC-20	64-22	70	17	460	610
11	200	BM-3	AC-5	58-34	59	9	460	610
12	200	BM-3	AC-20	64-22	70	17	460	610

U.S. Corps of Engineers Gyratory Testing Machine

Bituminous Mixtures Laboratory
Federal Highway Administration
Turner-Fairbank Highway Research Center
6300 Georgetown Pike
McLean, VA 22101-2296

January 23, 1996

1. Operational Principles of the Gyratory Testing Machine (GTM)

The Gyratory Testing Machine (GTM) is a combination compaction and plane strain shear testing machine that applies a stress equal to a chosen tire pressure. The GTM monitors the shear strain in an asphalt mixture and its shear strength while it is being compacted. The GTM Model 8A-6B-4C used by the Federal Highway Administration (FHWA) at the Turner-Fairbank Highway Research Center can test specimens with diameters of 101.6, 152.4, or 203.2 mm. Specimens that are 101.6 mm in diameter by 63.5 mm in height or 152.4 mm in diameter by 95.2 mm in height are normally tested. The FHWA GTM automatically measures and calculates the parameters used to determine the shear, or rutting, susceptibility of asphalt mixtures. Besides evaluating asphalt mixtures, the GTM has been used to evaluate subgrades and unbound aggregate base courses. This model costs $145,000 and is shown in figure 1.

A gyratory angle of compaction is chosen and manually set by the operator using two rollers that circle around the upper flange of the mold chuck. This angle is called the initial angle, or machine angle. The rollers, which are 3.14159 rad apart, are offset in vertical elevation to provide this angle. One roller is adjusted up or down prior to the test to set the angle. The second roller compresses a gauge that measures the gyratory pressure. This pressure is proportional to the shear strength of the mixture. The two rollers knead a mixture in its steel mold as they circle around the upper flange of the mold chuck at 1.26 rad/s.

The second roller can be either an oil-filled roller or an air-filled roller. These two rollers can place slightly different stresses on the mixture; therefore, they may not always provide equivalent effects. When the oil-filled roller is used, the initial gyratory angle set by the operator is maintained on the axis of the rollers throughout the test because oil is incompressible. When the air-filled roller is used, the angle on the axis of the rollers may drop lower than the initial angle during the test because air is slightly compressible. It has been hypothesized that the air-filled roller may more realistically simulate the changes in the level of strain in a pavement as it densifies under traffic. This also implies that the oil-filled roller provides a more severe testing condition. Although the air-filled roller has been available for many years, its use has been very limited until recently. Current standardized procedures for evaluating the parameters provided by the GTM are based on using the oil-filled roller.

Angles on axes other than the axis of the rollers are not fixed. The mold chuck is able to tilt (wobble) to larger angles on other axes. If a mixture shears while it is being compacted, it moves away from under the rollers, causing the mold and mold chuck to tilt to a larger angle on some other axis. (The mold chuck clamps the mold firmly.) The upper and lower platens remain parallel during the test, but the upper platen is free to slide sideways in a horizontal plane during the test. This allows the mixture to shear and the mold and mold chuck to tilt. The cross section of the GTM is shown in figure 2.

The GTM records the largest angle produced during each revolution. This angle, which may occur on any axis, is a measure of the magnitude of the shear strain in the mixture. After the compaction process is started, the recorded angle is normally higher than the initial angle because the loose mixture shears, causing the mold and mold chuck to tilt. With further compaction, the recorded angle will generally start to decrease because the shear strengths of most mixtures increase with an increase in density.

When a mixture is not shear-susceptible, the angles recorded by the GTM vs. revolutions will be equal to, or close to, the initial angle. The mold and mold chuck tilt will be very little. An angle greater than the initial angle is produced when the mixture is shear-susceptible. A mixture containing rounded, smooth, coarse aggregates may immediately produce a significantly greater angle because these aggregates provide low internal friction and no interlock. With excessive binder contents, the angle at some number of revolutions will start to increase as the mixture approaches its refusal, or ultimate, density. This will occur when testing mixtures containing either rounded or crushed coarse aggregates.

2. GTM Parameters

The three principal GTM parameters used to evaluate asphalt mixtures are the gyratory stability index (GSI), gyratory elasto-plastic index (GEPI), and shear strength (Sg). Other parameters that have been evaluated are the gyratory shear factor (GSF), gyratory strain classification index (GSCI), gyratory compatibility index (GCI), and the density of the aggregate.

The GSI is the ratio of the final angle at the end of the test to the minimum intermediate angle. It is a measure of shear susceptibility at the refusal density. The minimum intermediate angle is the smallest angle that occurs after the compaction process has started. It can be greater than the initial angle. The GSI at 300 revolutions is close to 1.0 for a stable mixture and is significantly above 1.1 for an unstable mixture.(1) (A more definitive criterion for the GSI has not been established. The manufacturer suggests using 1.00 as the maximum allowable GSI to eliminate rutting completely and because some test methods terminate the test at revolutions much lower than 300. When designing a mixture, binder contents that provide a GSI above 1.00 will be susceptible to rutting.)

The GEPI is the ratio of the minimum intermediate angle to the initial angle. It is a measure of internal friction. A GEPI of 1.00 indicates high internal friction. A GEPI significantly above 1.00 indicates low internal friction, generally due to the use of rounded coarse aggregates. (More definitive criteria for the GEPI have not been established. The manufacturer suggests using an acceptable range of 1.00 to 1.50 and a marginal range of 1.51 to 1.65.)

The Sg of a mixture is calculated from the roller pressure. The GTM Model 8A-6B-4C continuously monitors the Sg during compaction, but current test methods only evaluate the Sg at the refusal density. Reportedly, the Sg should peak and then start to decrease rapidly with increasing binder content. Binder contents higher than the content at the peak Sg may lead to mixtures that are susceptible to rutting.

The GSF is the ratio of the Sg to the theoretical maximum shear stress that will be applied to the mixture in a pavement. The theoretical maximum shear stress is obtained by performing a mechanistic analysis of the pavement. A ratio greater than 1.0 indicates that the mixture may fail in shear. If a mechanistic analysis is not available, then a tentative minimum allowable Sg of 350 kPa can be used.

The GSCI is the ratio of the angle at 30 revolutions to the final angle. This approximates the ratio of the strain in the mixture after pavement construction to the strain after densification by traffic. The GSCI is a more recently developed parameter. The benefit of this parameter has not been established. A high GSCI may indicate a susceptibility to rutting. A low GSCI, caused by a decreasing angle during compaction, may indicate that either the aggregate is deteriorating, or, when pavement cores are tested, they may have been damaged by moisture.

The GCI is the ratio of the unit mass of the mixture at 50 revolutions to the unit mass of the mixture at 100 revolutions. This parameter has been used to evaluate the workabilities of mixtures, but the use of 50 and 100 revolutions to compute this parameter is arbitrary.

The density of the aggregate only, as opposed to the density of the total mixture, is evaluated because this is a measure of aggregate structure. Binder contents higher than the content at the peak aggregate density may provide mixtures that are susceptible to rutting.

The height of the specimen is also monitored during compaction. After the compaction process is completed, the specimen is then removed from the mold and tested for bulk specific gravity. This gravity and the maximum specific gravity of the loose mixture are used to calculate the air voids in the specimen. A relationship between air voids and revolutions, which provides the compaction history of the mixture, can be calculated using the heights. The air voids at the beginning of the compaction history have the greatest amount of error because the bulk specific gravities determined after compaction do not account for the greater volumes of surface voids that are present at the beginning of the test. The height measurements include these voids.

3. GTM Procedures Used by the FHWA

Two test methods have been used by the FHWA, both employing the oil-filled roller. The first procedure is American Society for Testing and Materials (ASTM) Method D 3387, "Compaction and Shear Properties of Bituminous Mixtures by Means of the U.S. Corps of Engineers Gyratory Testing Machine (GTM)."[2] This procedure uses a vertical pressure equal to the anticipated maximum tire pressure and a 0.014-rad gyratory angle. The FHWA uses a vertical pressure of 0.827 MPa. Mixtures are compacted at typical compaction temperatures to equilibrium, defined as the number of revolutions where the change in density becomes less than 16 kg/m^3 per 100 revolutions. This point of equilibrium is usually well below 300 revolutions and is often around 200 revolutions. A trace of the gyratory angle vs. revolutions is obtained to determine the minimum intermediate and final angles.

The second procedure is given in the National Cooperative Highway Research Program (NCHRP) Asphalt-Aggregate Mixture Analysis System (AAMAS), which is based on ASTM Method D 3387.[2,3] This procedure uses a vertical pressure of 0.827 MPa and a 0.035-rad gyratory angle. However, this angle was found to produce specimens with excessively low air-void levels; therefore, a 0.014-rad angle has been used by the FHWA. The specimens are first compacted to the estimated air-void level that will be obtained in the field after construction, usually between 5 and 8 percent. The number of gyratory revolutions is varied to obtain this air-void level. Trial tests are used to determine the needed number of revolutions. After initial compaction, the specimens in their molds are placed in an oven at 60 °C for 3 h. They are then compacted to refusal density at 60 °C, using 300 revolutions. A trace of the gyratory angle vs. revolutions is obtained to determine the minimum intermediate and final angles. This procedure was developed so that mixtures would be tested at the typically used high pavement temperature of 60 °C.

4. References

1. Roberts, F.L., P.S. Kandhal, E.R. Brown, D.Y. Lee, and T.W. Kennedy. *Hot Mix Asphalt Materials, Mixture Design, and Construction*. National Asphalt Pavement Association (NAPA) Education Foundation, Lanham, MD, 1991.

2. American Society for Testing and Materials. *1994 Annual Book of ASTM Standards, Section 4, Volume 04.03*. 1916 Race Street, Philadelphia, PA, April 1994.

3. Von Quintus, H.L, J.A. Scherocman, C.S. Hughes, and T.W. Kennedy. *Asphalt-Aggregate Mixture Analysis System*. NCHRP Report 338, Transportation Research Board, National Research Council, Washington, DC, 1991.

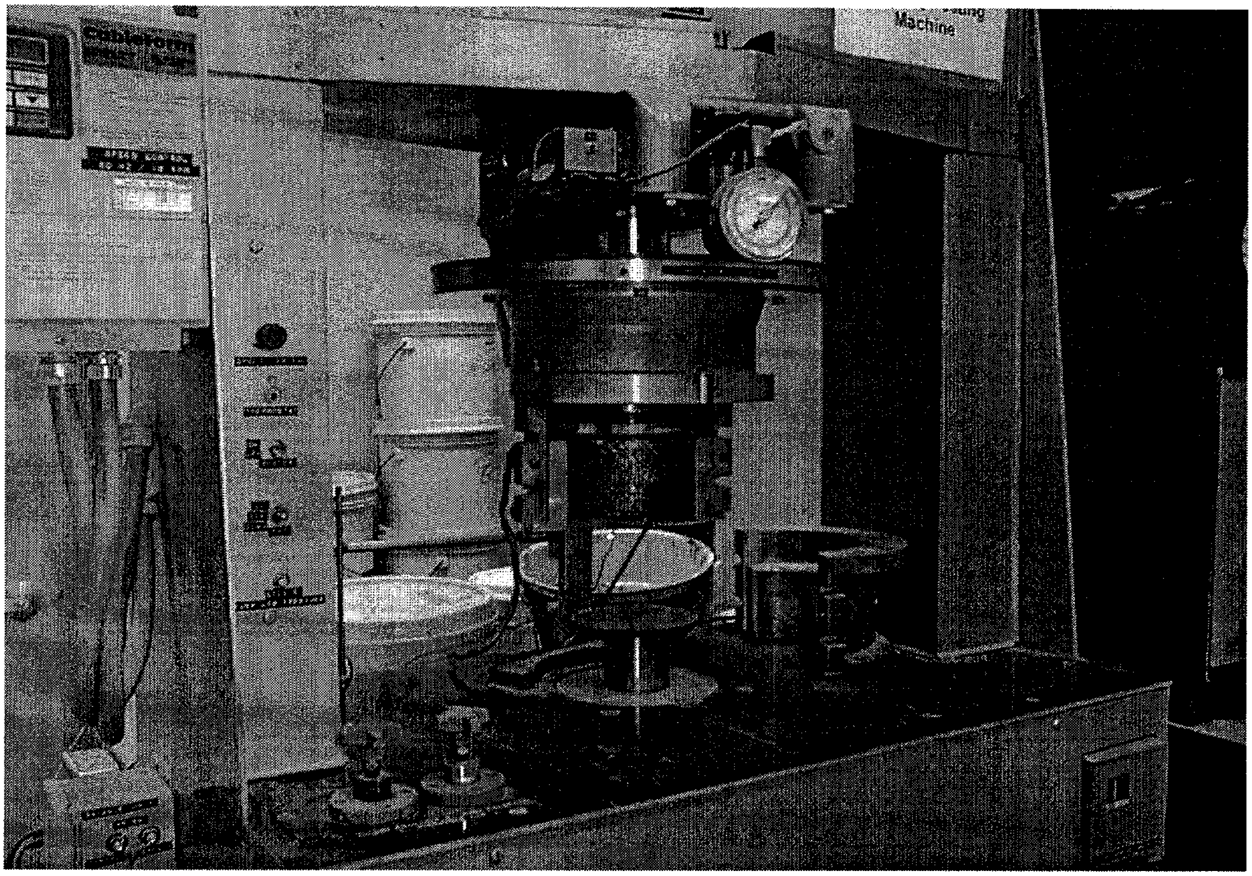

Figure 1. U.S. Corps of Engineers Gyratory Testing Machine.

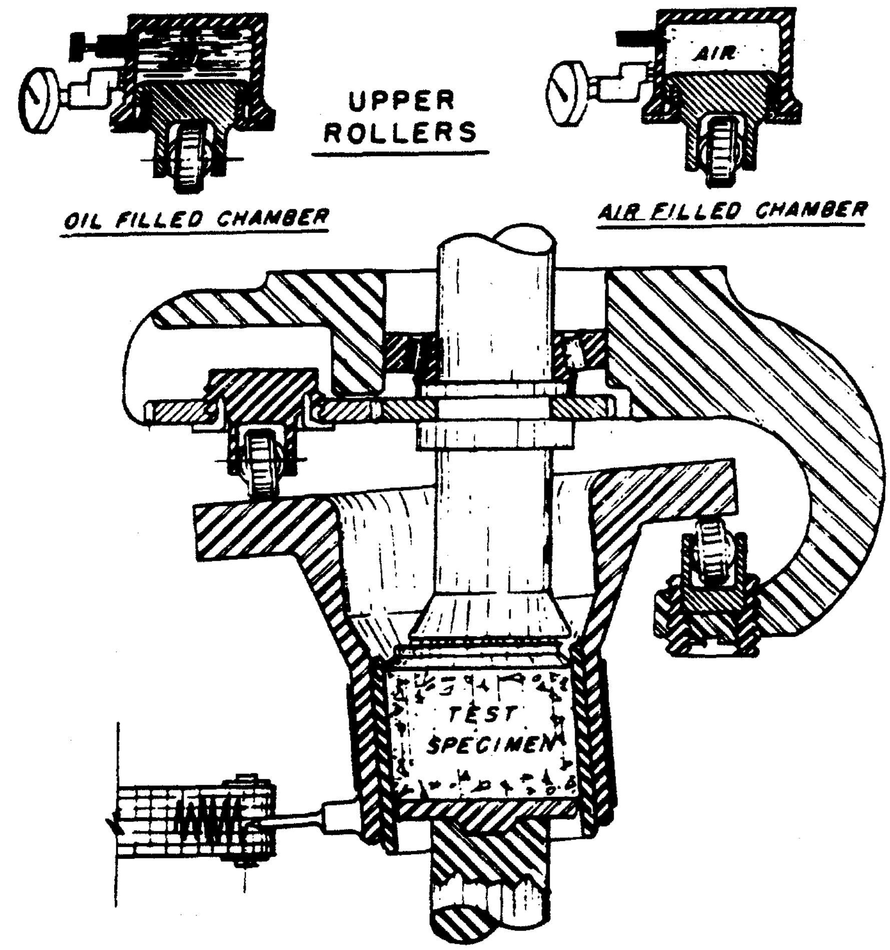

Figure 2. Cross section of the GTM.

French Pavement Rutting Tester

Bituminous Mixtures Laboratory
Federal Highway Administration
Turner-Fairbank Highway Research Center
6300 Georgetown Pike
McLean, VA 22101-2296

December 19, 1996

The French (Laboratoires des Ponts et Chaussees) Pavement Rutting Tester tests slabs for permanent deformation at 60 °C using a smooth, reciprocating, pneumatic rubber tire inflated to 0.60 ±0.03 MPa. This tester is used in France to evaluate mixtures subjected to heavy traffic; mixtures that incorporate materials that tend to lead to rutting, such as some natural sands; and mixtures that have no performance history. It is also used for quality control purposes during construction. This tester costs $85,000 and is shown in figures 1 and 2.

This machine tests a slab with a length of 500 mm, a width of 180 mm, and a thickness of either 50 mm or 100 mm. Other thicknesses between 20 and 100 mm can be tested by fabricating a nonstandard-sized mold or by putting the slab on plaster of paris or steel plates. A thickness of 50 mm is specified for mixtures that will be used in surface course layers less than or equal to 50 mm. Thin surface course layers in France are generally placed at thicknesses ranging from 30 to 40 mm. The 100-mm thickness is specified for mixtures that will be used in surface or base course layers greater than 50 mm. In France, these layers are generally placed at thicknesses ranging from 60 to 80 mm. A slab cut from a pavement can also be tested, but it must be cut to fit the mold. Cut slabs having small gaps between the slab and the mold must be secured in some way, such as with plaster of paris. The allowable deviation in thickness for a cut slab is the average thickness ±5 mm. The mass of the slab with a thickness of 100 mm is approximately 22 kg.

Slabs are compacted to two to three air-void levels in France. After compaction, the slab is aged at room temperature for up to 7 days. The density of the slab is obtained after compaction, but the slab is then placed back into the mold for testing.

The machine tests two slabs simultaneously using two reciprocating tires. The wheel load on both slabs must be equal to avoid asymmetric pressures on the tire assembly. However, the two slabs do not have to be replicates and, in fact, the French recommend testing mixtures in random order to account for variabilities associated with the machine over time. Replicate slabs are tested at different times using both sides of the machine.

Hydraulic jacks underneath the slabs push them upward to create the load. The standard load is 5,000 ±50 N; the maximum load is 5,500 N. Pressure gauges on the control panel of the machine give the pressure in each jack. Each pressure gauge is calibrated in increments of 0.1 MPa using a load cell. A graph of pressure vs. load is constructed and used to apply the desired load. The weight of the mold and slab are not included in the applied load. The average pressure provided by 5,000 N was determined to be 0.59 MPa for the left tire of the Federal Highway Administration machine and 0.55 MPa for the right tire. The tires were inflated to 0.60 MPa and loaded on flat steel plates to obtain the contact area.

The French Pavement Rutting Tester uses the same type of tire as the French Plate Compactor. Each tire has a diameter of 415 mm and a width of 110 mm. The standard tire pressure is 0.60 ±0.03 MPa; the maximum pressure is 0.71 MPa. It takes approximately 0.1 s for the tires to travel from one end of a slab to the center with the speed being fastest at the center. The tires remain at a fixed elevation as they travel back and forth across the slabs. The average speed of each wheel is approximately 7 km/h; each wheel travels approximately 380 mm before reversing direction, and the device operates at approximately 67 cycles/min (134 passes/min). One cycle is defined as two passes of the tire (back and forth).

Initially, 1,000 cycles are applied at 15 to 25 °C to densify the mixture and to provide a smoother surface. This requires approximately 15 min. The thickness of each slab is then calculated by averaging 15 thickness measurements taken at 15 standard positions using a gauge with a minimum accuracy of 0.1 mm. This thickness is considered the initial thickness of the slab. The slabs are then heated to the test temperature of 60 ±2 °C for 12 h. A test temperature of 50 ±2 °C is sometimes used in France for base courses. The test is started, and the average rut depth in each slab is measured manually at 30, 100, 300, 1,000, and 3,000 cycles when testing 50-mm slabs, and at 300, 1,000, 3,000, 10,000, and 30,000 cycles when testing 100-mm slabs. Rut depth measurements at 30, 100, and 300 cycles are included in the 100-mm slab test if it is hypothesized that the slab will fail before 3,000 cycles. The average percent rut depth based on the initial thickness of the slab is calculated.

The application of 3,000 cycles requires 1.5 h, whereas 30,000 cycles require 9 h. The tester can apply 3,000 cycles in approximately 45 min, but after each rut depth measurement, the temperature of the slab must be reestablished. Rut depths are measured manually, which requires the environmental chamber to be opened.

When testing 50-mm slabs, a mixture is acceptable according to the French specification if the average percent rut depths at 1,000 and 3,000 cycles are less than or equal to 10 and 20 percent, respectively. When testing 100-mm slabs, a mixture is acceptable if the average percent rut depth at 30,000 cycles is less than or equal to 10 percent. Slopes for different mixtures taken from log rut depth vs. log cycle plots can also be compared. Rut-susceptible mixtures generally have higher slopes, but there is no French specification on the slope.

The test method reportedly is not valid for mixtures with nominal maximum aggregate sizes greater than 20 mm. The slab width of 180 mm is relatively small compared to the tire width of 110 mm. A space of only 35 mm exists on each side of the slab between the tire and the steel mold. Therefore, mixtures with aggregates greater than 20 mm may be inhibited from shearing outward and upward. Aggregates larger than 20 mm may also wear the tires severely, and often cannot be compacted properly using the French Plate Compactor. The machine was developed primarily for testing surface layer mixtures. It was later used in France to test surface treatments for chip retention and elasticity. Surface treatments are often placed on stabilized soils when tested.

Disadvantages of the French Pavement Rutting Tester are that the data cannot be used in mechanistic pavement analyses and cannot be used to determine the modulus of the mixture or layer coefficients used by American Association of State Highway and Transportation Officials thickness design procedures. This is due to the complex and unknown state of stress in the slab.

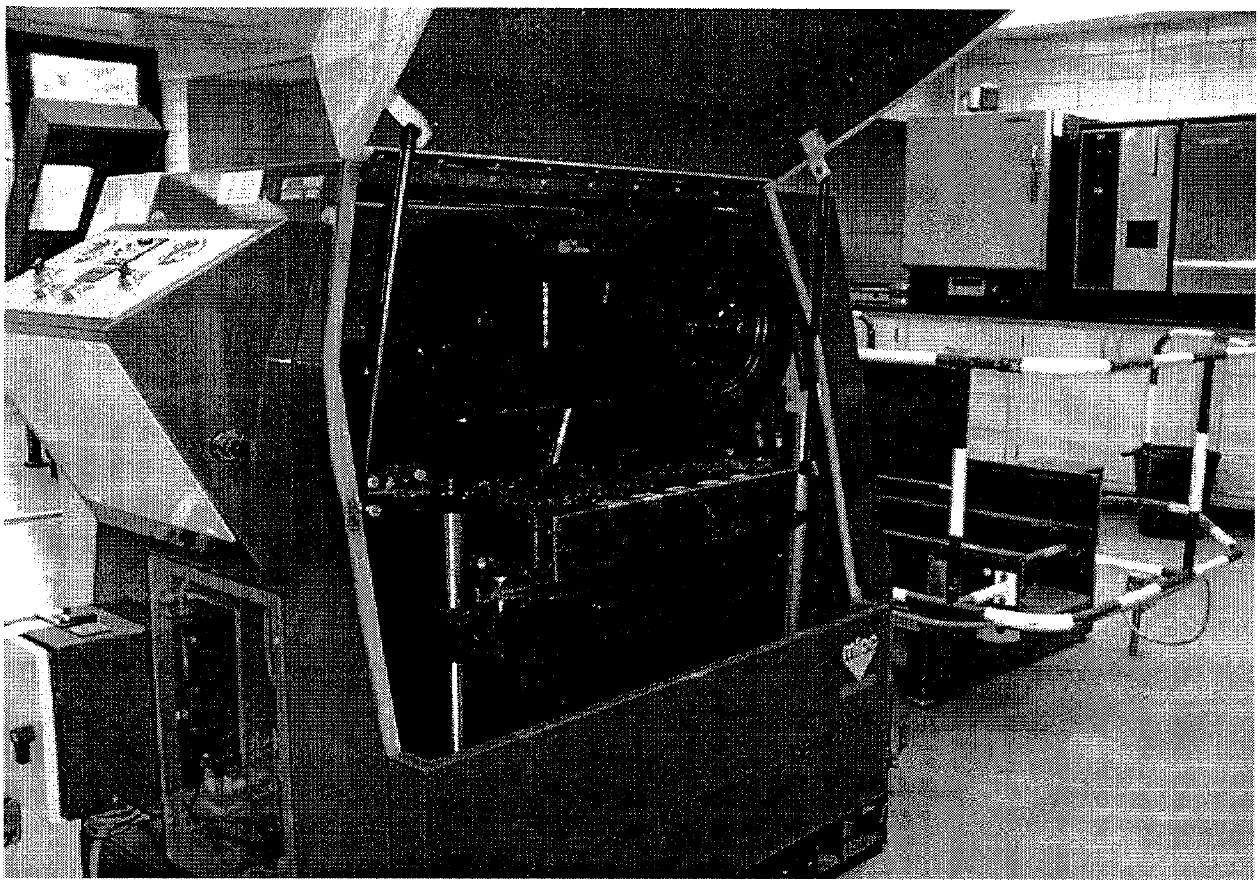

Figure 1. French Pavement Rutting Tester.

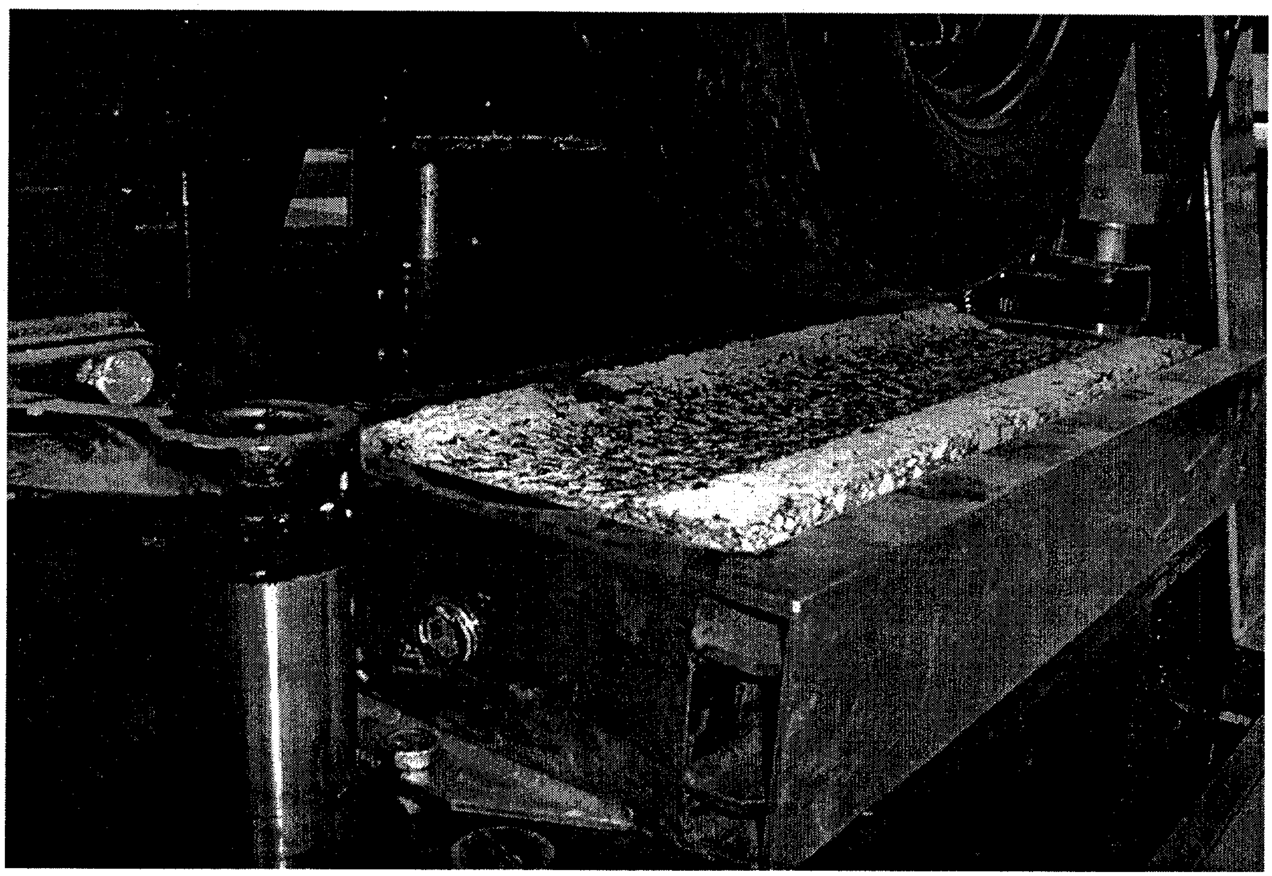

Figure 2. Close-up of tire and slab.

Georgia Loaded-Wheel Tester

Bituminous Mixtures Laboratory
Federal Highway Administration
Turner-Fairbank Highway Research Center
6300 Georgetown Pike
McLean, VA 22101-2296

September 28, 1998

The Georgia Loaded-Wheel Tester (GLWT) measures rutting susceptibility by rolling a steel wheel across a pressurized hose positioned on top of an asphalt concrete beam at 41 °C. The GLWT was developed by the Georgia Department of Transportation (GDOT) and has been refined several times. The model currently used by the Federal Highway Administration (FHWA) at the Turner-Fairbank Highway Research Center cost $10,000 and is shown in figure 1.

Each beam is 125 mm in width, 75 mm in thickness, and 380 mm in length. The mass of a beam is 8.5 kg. Mixtures with maximum aggregate sizes up to 37.5 mm are tested by GDOT, although the maximum aggregate size applicable to this test is not known.

Each beam is aged for 24 h at room temperature and for 24 h at the test temperature of 40.6 °C. After aging, a beam is positioned in the GLWT and a stiff, 29-mm diameter, rubber hose pressurized at 0.69 MPa with air is positioned across the top of the beam. A steel wheel loaded with weights rolls back and forth on top of this hose for 8,000 cycles to create a rut. The sides of the beam during the test are confined by steel plates except for the top 12.7 mm. The average speed of the wheel is approximately 2 km/h; the wheel travels approximately 330 mm before reversing in direction, and the device operates at 33 ±1 cycles/min (67 ±2 passes/min). One cycle is two wheel passes.

The FHWA found that the load varies with the direction of travel. When the wheel is moving from right to left, when viewed from the front of the machine, the load is approximately 740 N at the center of the beam, while it is 630 N when moving from left to right. Across the central region of the beam where the deformations are recorded, each of these loads has a variation of less then ±2.5 percent. The load varies because the two arms that connect the wheel to the motor undergo a circular action at the motor. This "locomotion effect" shifts the distribution of the load during the test. (The load may also vary if the height of the beam were to be significantly changed.)

The deformations are measured at three positions: at the center of the beam, 51 mm left of center, and 51 mm right of center. The deformations are averaged. If the average rut depth for three replicate beams exceeds 7.6 mm, the mixture is considered by GDOT to be susceptible to rutting. Testing one beam requires 4 h. The total time to perform a test from start to finish, including specimen fabrication and aging, is 4 days.

Disadvantages of the GLWT are that the data cannot be used in mechanistic pavement analyses and cannot be used to determine the modulus of the mixture or layer coefficients used by American Association of State Highway and Transportation Officials thickness design procedures. This is due to the complex and unknown state of stress in the beam. Little documentation is available that compares the results of this test to long-term pavement performance.

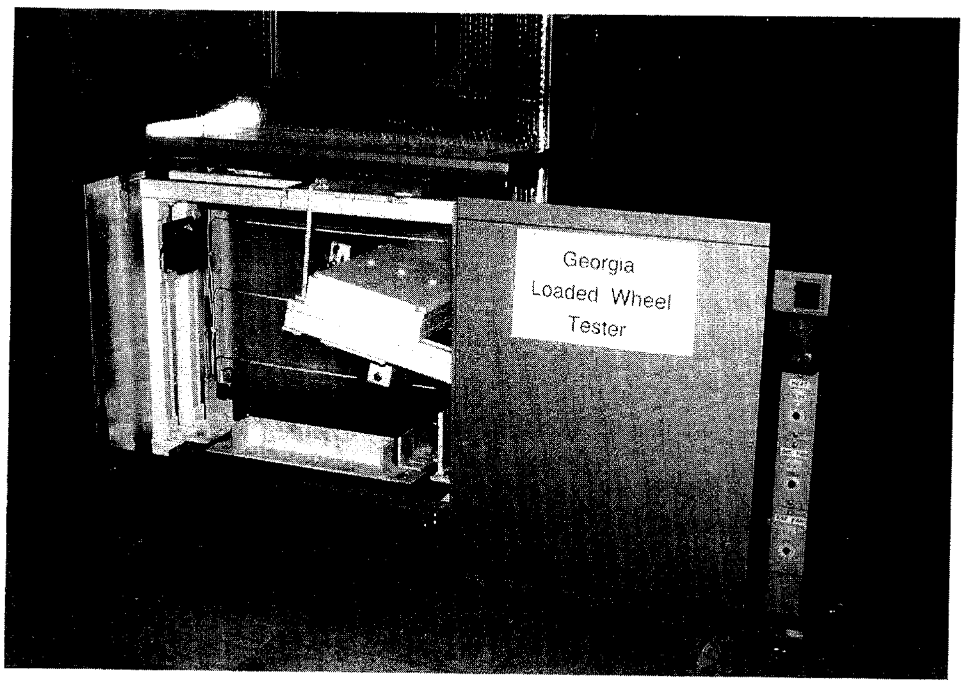

Figure 1. Georgia Loaded-Wheel Tester.

Hamburg Wheel-Tracking Device

Bituminous Mixtures Laboratory
Federal Highway Administration
Turner-Fairbank Highway Research Center
6300 Georgetown Pike
McLean, VA 22101-2296

February 10, 1997

The Hamburg Wheel-Tracking Device measures the combined effects of rutting and moisture damage by rolling a steel wheel across the surface of an asphalt concrete slab that is immersed in hot water. The device was developed in the 1970's by Esso A.G. of Hamburg, Germany, based on a similar British device that had a rubber tire. The machine was originally called the Esso Wheel-Tracking Device. The City of Hamburg finalized the test method and developed a pass/fail criterion to guarantee that mixtures that pass the test have a very low susceptibility to rutting.[1] This device costs $60,000 and is shown in figures 1 and 2.

The device was originally used by the City of Hamburg to measure rutting susceptibility. The test was performed for 9,540 wheel passes at either 40 or 50 °C. Water was used to obtain the required test temperature instead of an environmental air chamber. The City of Hamburg later increased the number of wheel passes to 19,200 and found that some mixtures began to deteriorate from moisture damage. Greater than 10,000 wheel passes was generally needed to show the effects of moisture damage.

The machine tests slabs that typically have a length of 320 mm, a width of 260 mm, and a thickness of either 40, 80, or 120 mm. Thicknesses up to 150 mm can be tested. The thickness of the slab is specified to be a minimum of three times the nominal maximum aggregate size.[A] The mass of a slab having a thickness of 80 mm is approximately 15 kg. Pavement cores having a minimum diameter of 250 mm can also be tested.

The required air-void level for laboratory-prepared specimens is not given by the City of Hamburg procedure. The Federal Highway Administration at the Turner-Fairbank Highway Research Center is using 7 ± 1 percent air voids for dense-graded hot-mix asphalts, and 5.5 ± 0.5 percent for stone matrix asphalts. The Colorado Department of Transportation (CDOT) also uses 7 ± 1 percent air voids for dense-graded hot-mix asphalts.[2]

Specimens are secured in reusable steel containers using plaster of paris. Each specimen is placed into a container so that its surface is level with the top edge of the container. This allows the full range of the rut depth measurement system to be utilized. Containers are manufactured in heights of 40, 80, and 120 mm. Steel spacers can be placed under cores and pavement slabs if needed. The container with the specimen is then placed into the wheel-tracking device. The container rests on steel; this provides a rigid, load-bearing base for the specimen.

The temperature of the water bath can be set from 25 to 70 °C. The most commonly used test temperature in Hamburg is 50 °C, although 40 °C has been used when testing certain base mixtures. A water temperature of 50 °C is reached within 45 min. Specimens are conditioned at the test temperature for a minimum of 30 min. Heat is provided by heated coils in the water. The temperature of the water is then maintained by these heating coils and by introducing cold water from a faucet.[B]

The device tests two slabs simultaneously using two reciprocating solid steel wheels. The wheels have a diameter of 203.5 mm and a width of 47.0 mm. The load is fixed at 685 N and the average contact stress given by the manufacturer is 0.73 MPa. This assumes an average contact area of 970 mm^2, which is based on the 47.0-mm wheel width and an average contact length of 20.6 mm in the direction of travel. However, the contact area increases with rut depth, and thus the contact stress is variable. The manufacturer states that a contact stress of 0.73-MPa approximates the stress produced by one rear tire of a double-axle truck. The average speed of each wheel is approximately 1.1 km/h; each wheel travels approximately 230 mm before reversing direction, and the device operates at approximately 53 ± 2 wheel passes/min.

The number of wheel passes being used in the United States is 20,000, although up to 100,000 wheel passes can be applied. CDOT recommends maximum allowable rut depths of 4 mm at 10,000 wheel passes and 10 mm at 20,000 wheel passes, based on correlations between the test results and moisture damage in dense-graded hot-mix asphalt pavements.[3] The City of Hamburg uses a maximum allowable rut depth of 4 mm at 19,200 wheel passes. The rut depth in each slab is measured automatically and continuously by a linear variable differential transformer that has an accuracy of 0.01 mm. A printout of the data can be obtained at every 20, 50, 100, or 200 wheel passes. Approximately 6.5 h are needed to apply 20,000 wheel passes; however, the device will automatically stop if the rut depth in one of the slabs exceeds 30 mm. The total time to perform a test from start to finish, including specimen fabrication, is 3 days.

The post-compaction consolidation, creep slope, stripping inflection point, and stripping slope, shown in figure 3, can also be analyzed.[4] The post-compaction consolidation is the deformation (mm) at 1,000 wheel passes. It is called post-compaction consolidation because it is assumed that the wheel is densifying the mixture within the first 1,000 wheel passes.

The creep slope is used to measure rutting susceptibility. It measures the accumulation of permanent deformation primarily due to mechanisms other than moisture damage. It is the inverse of the rate of deformation (wheel passes per 1-mm rut depth) in the linear region of the plot between the post-compaction consolidation and the stripping inflection point. Creep slopes have been used to evaluate rutting susceptibility instead of rut depths because the number of wheel passes at which moisture damage starts to affect performance varies widely from mixture to mixture. Furthermore, the rut depths often exceed the maximum measurable rut depth of 25 to 30 mm, even if there is no moisture damage.

The stripping inflection point and the stripping slope are used to measure moisture damage. The stripping inflection point is the number of wheel passes at the intersection of the creep slope and the stripping slope. This is the number of wheel passes at which moisture damage starts to dominate performance. CDOT reports that an inflection point below 10,000 wheel passes indicates moisture susceptibility.[3] The stripping slope measures the accumulation of permanent deformation primarily due to moisture damage. It is the inverse of the rate of deformation (wheel passes per 1-mm rut depth) after the stripping inflection point.

Inverse slopes are used for both the creep slope and the stripping slope so that these slopes can be reported in terms of wheel passes along with the number of wheel passes at the stripping inflection point. Higher creep slopes, stripping inflection points, and stripping slopes indicate less damage.[4]

The shape of the curve in figure 2 is the same as typical permanent deformation curves provided by creep and repeated load tests. The curves from these tests are also broken down into three regions. The final region, called the tertiary region, is where the specimen is rapidly failing. Based on the examination of many slabs and pavement cores, the tertiary regions of the curves produced by the Hamburg Wheel-Tracking Device appear to be primarily related to moisture damage, rather than to other mechanisms that cause permanent deformation, such as viscous flow. Mixtures that are susceptible to moisture damage also tend to start losing fine aggregates around the stripping inflection point, and coarse aggregate particles may become dislodged. However, there is no method for separating the deformation due to viscous flow from the deformation due to moisture damage, because dry specimens cannot be tested. There is also no method for determining the amount of deformation and the amount of fine particles generated if any of the aggregate particles are crushed by the steel wheel.[C]

Additional disadvantages are that the data cannot be used in mechanistic pavement analyses and cannot be used to determine the modulus of the mixture or layer coefficients used by American Association of State Highway and Transportation Officials thickness design procedures. This is due to the complex and unknown state of stress in the slab.

Footnotes

A. The effect of thickness on the test results has not been determined.

B. There may be some variability in the data resulting from the use of tap water. Distilled water is specified in most test methods used to determine the moisture susceptibility of asphalt mixtures in order to reduce the between-laboratory testing variability.

C. Correlating the test data to field performance is difficult since the test combines two distress modes and the steel wheel can crush some aggregates.

References

1. *Tracking Test, Determination of the Track Depth of High-Stability Binding Layers.* Construction Bureau, Civil Engineering Office, Department of City Traffic, Hamburg, Germany, 1991.

2. Aschenbrener, T. "Evaluation of the Hamburg Wheel-Tracking Device to Predict Moisture Damage in Hot-Mix Asphalt." *Transportation Research Record 1492,* Transportation Research Board, Washington, D.C., 1995, pp. 193-201.

3. Aschenbrener, T., R. Terrel, and R. Zamora. *Comparison of the Hamburg Wheel-Tracking Device and the Environmental Conditioning System to Pavements of Known Stripping Performance* (CDOT-DTD-R-94-1) Colorado Department of Transportation, Denver, CO, January 1994.

4. Hines, M. "The Hamburg Wheel-Tracking Device." *Proceedings of the Twenty-Eighth Paving and Transportation Conference.* Civil Engineering Department, The University of New Mexico, Albuquerque, NM, 1991.

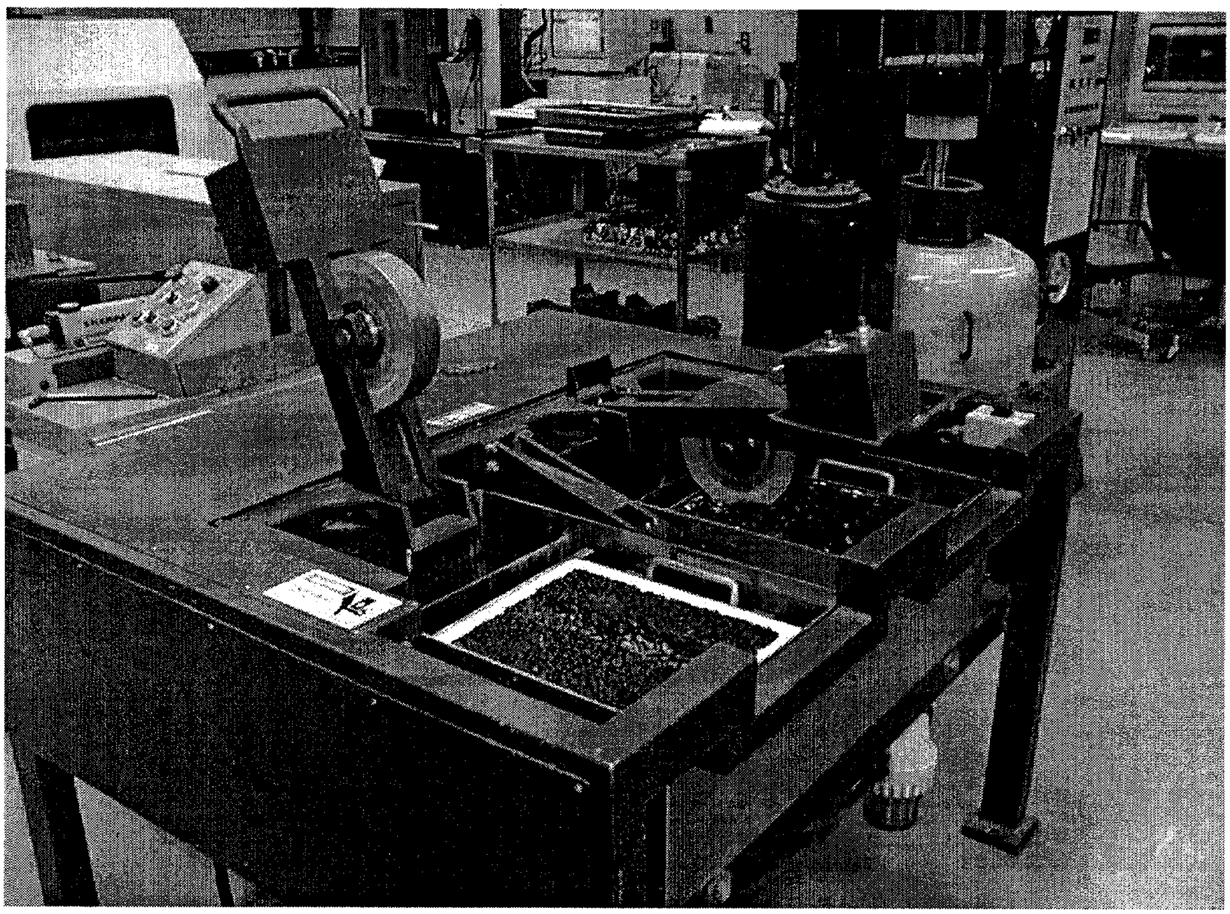

Figure 1. Hamburg Wheel-Tracking Device.

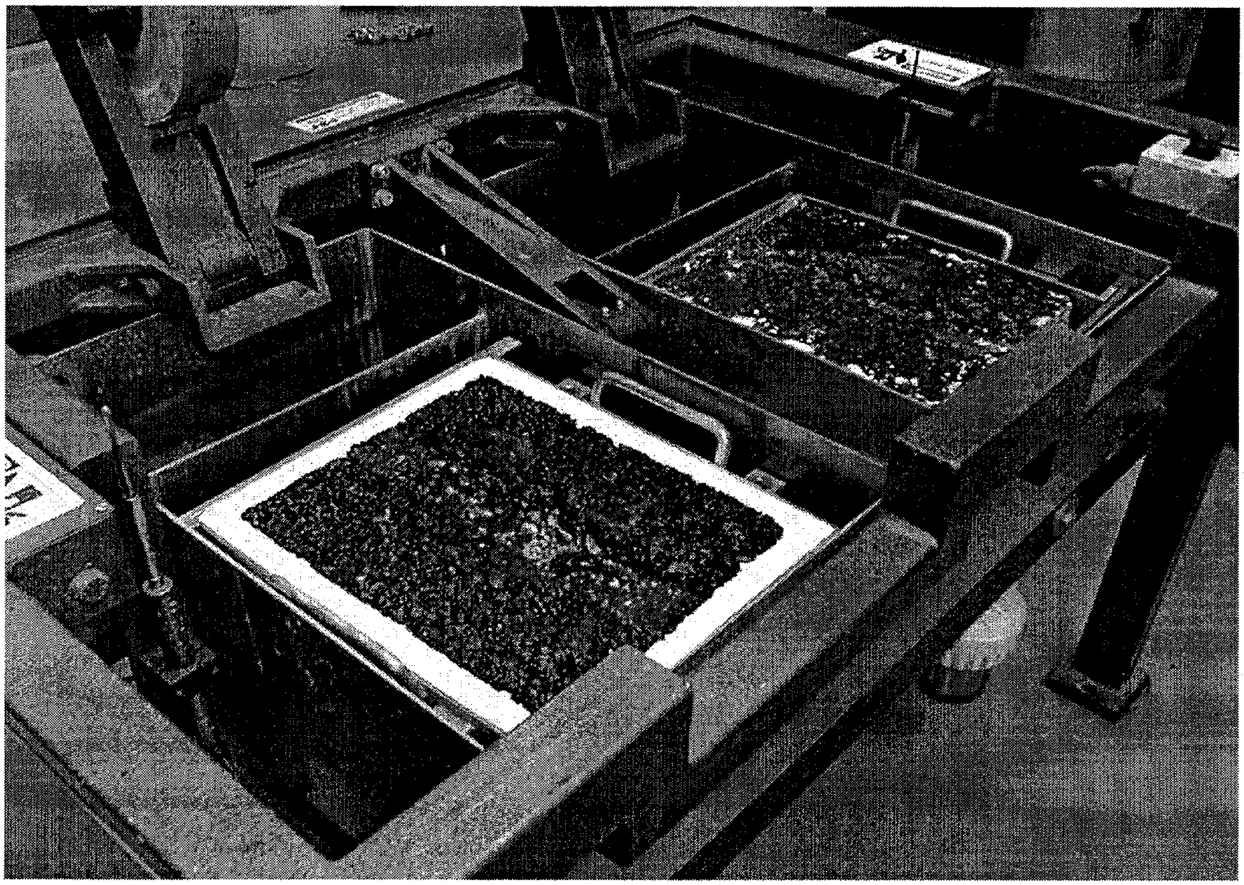

Figure 2. Close-up of slabs without water.

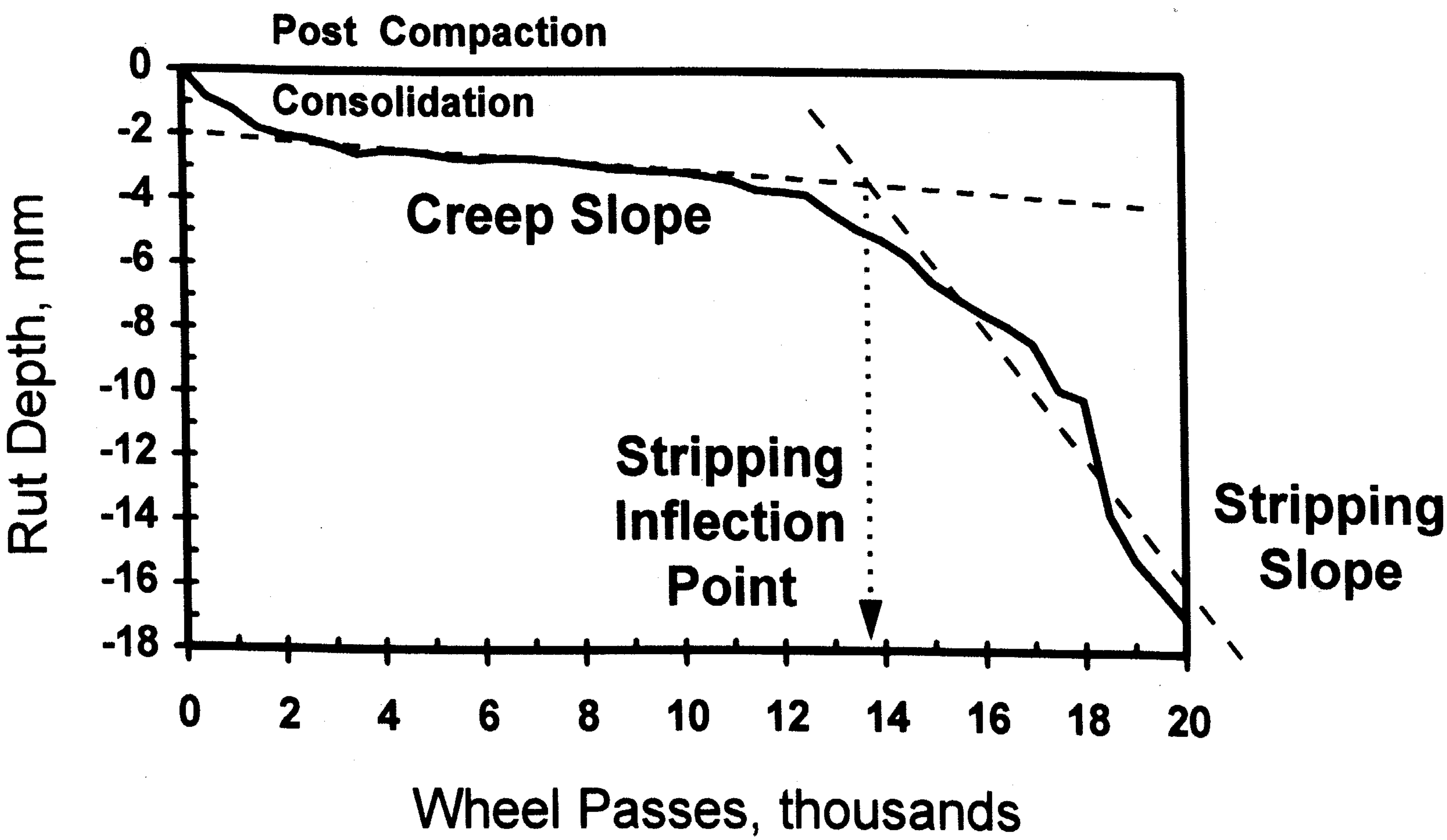

Figure 3. Rut depth vs. number of wheel passes.

Superpave Shear Tester

Bituminous Mixtures Laboratory
Federal Highway Administration
Turner-Fairbank Highway Research Center
6300 Georgetown Pike
McLean, VA 22101-2296

September 23, 1998

The Superpave Shear Tester (SST) is a closed-loop feedback, servo-hydraulic system that can apply axial loads, shear loads, and confinement pressures to asphalt concrete specimens at controlled temperatures. The response of asphalt concrete to these loads can be used as inputs to performance prediction models such as Superpave.

The SST has six main components: testing chamber, test control system, environmental system, hydraulic system, air pressurization system, and measurement transducers.

The testing chamber includes a reaction frame and a shear table. It also houses various components that are driven by other systems such as temperature control, pressure control, hydraulic actuators, and input and output transducers. The reaction frame is extremely rigid so that precise specimen displacement measurements can be achieved without problems related to displacements in the frame itself, which is called machine compliance. The shear table holds a specimen during testing and is capable of applying shear loads. The specimens normally have a diameter of 150 mm and a height of 50 mm; however, specimens with diameters and heights up 200 mm can be tested with only minor modifications to the system. The temperature inside the testing chamber is precisely controlled by the environmental system. A diagram of the testing chamber is shown in figure 1.

The test control system consists of hardware and software. The hardware interfaces with the testing chamber through input and output transducers. It consists of controllers, signal conditioners, and a computer and its peripherals. The software consists of preprogramed algorithms required to provide the load and acquire the data during testing. Closed-looped feedback control allows the SST to make adjustments during testing so that the machine precisely performs the test.

The environmental system is a forced-air conditioning unit and an insulated enclosure surrounding the testing chamber. Temperatures from 0 to 70 °C can be provided. The unit can be controlled through the SST computer. The insulated enclosure keeps the temperature constant during testing.

The hydraulic system provides the loads. Interlaken Series 3410 hydraulic motors power two actuators, each with a capacity of approximately 32 kN. One actuator applies the vertical, axial force. A horizontal actuator moves the shear table, which applies the shear loads.

The air pressurization system consists of an air compressor, a storage tank for pressurized air, hoses, and filters. The storage tank is needed because pressurized air must be supplied to the testing chamber at high rates. A rate of 70 kPa/s is used in some Superpave tests.

The measurement transducers consist of two load cells, one for the vertical axial load and one for the horizontal shear load, several linear variable differential transformers (LVDT's) with ranges from 0.05 to 50 mm, and a pressure cell with a range from 0 to 1000 kPa. LVDT's mounted on the specimens measure the response of the specimen to the applied testing loads. Three types of LVDT's are employed: shear LVDT's that measure the relative deformation of the specimen at two heights; axial LVDT's that measure the relative motion of the upper and lower platens, and circumferential LVDT's that measure changes in the diameter of the specimen. Any of these LVDT's can be used as feedback signals for the closed loop control. The system is designed to compensate for the effects of the moving masses of the machine on the load measurements during testing because these effects can be relatively high compared to the load measurements.

Six Superpave tests were preprogramed when the SST was purchased:

- volumetric,
- uniaxial strain,
- repeated shear at constant height,
- repeated shear at constant stress ratio,
- simple shear at constant height, and
- frequency sweep at constant height.

These tests are described in detailed in AASHTO Provisional Standard TP 7. Other tests can be programmed using the QuikTest™ software provided with the SST.

The SST in the Bituminous Mixtures Laboratory, shown in figure 2, was purchased from Interlaken Technologies in 1995 at a cost of $230,000. Identical SST's were purchased for the five Superpave Centers located in the United States.

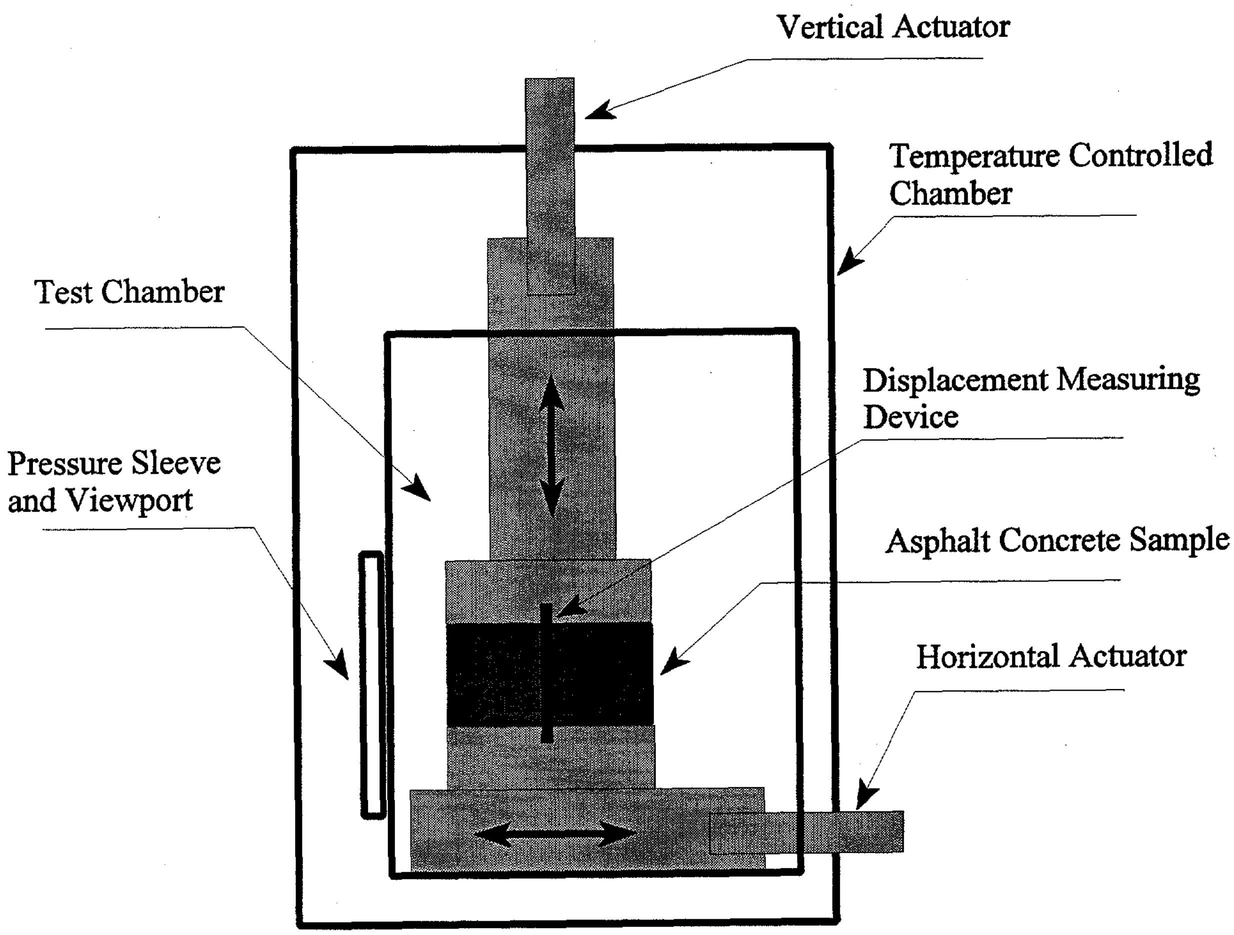

Figure 1. Diagram of testing chamber.

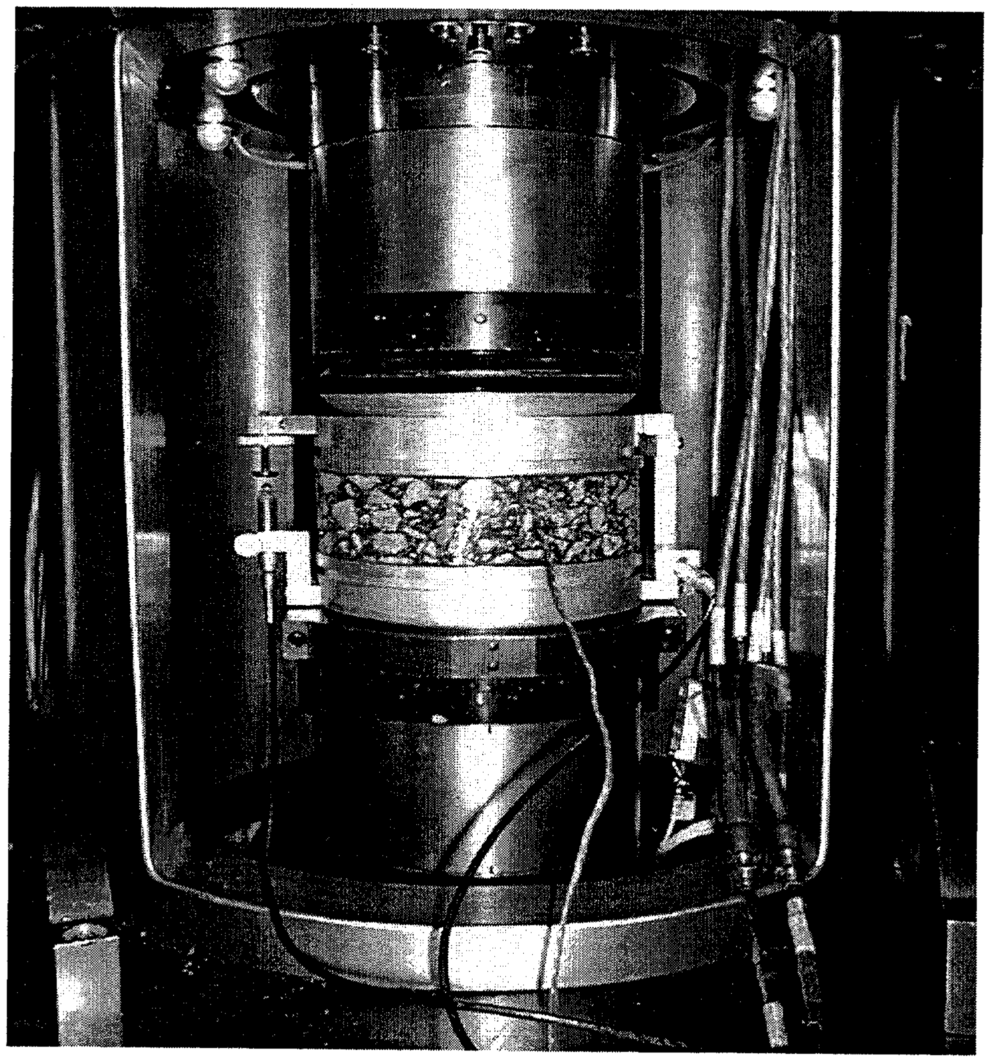

Figure 2. Superpave Shear Tester.

Linear Kneading Compactor

Bituminous Mixtures Laboratory
Federal Highway Administration
Turner-Fairbank Highway Research Center
6300 Georgetown Pike
McLean, VA 22101-2296

January 23, 1996

The Linear Kneading Compactor produces slabs that are used for testing asphalt mixtures for various properties. A mixture is placed in a steel mold in the compactor and a series of vertically aligned steel plates are positioned on top of it. A steel roller then transmits a rolling action force through the steel plates, one plate at a time. The mixture is kneaded and compressed into a flat slab of predetermined thickness and density. The trade name for this compactor is HasDek SLAB-PAC. It is manufactured by R/H Specialty & Machine, Terre Haute, IN. This compactor costs $66,000 and is shown in figure 1.

The Linear Kneading Compactor is called "linear" because of the lateral motion involved. The mold, mixture, and steel plates move back and forth on a sliding table under the roller. It is called "kneading" because only a fraction of the mixture is compacted at any given time. This kneading action allows the mixture to be compacted without excessively fracturing the aggregate. The linear compression wave provided by the compactor is shown in figure 2.

The density of the mixture at the required air-void level and the dimensions of the slab are used to calculate the mass of mixture needed. Once the mixture is placed in the mold, 5 to 15 min are required to achieve the desired density. Two different mold sizes are available—a 260- by 320-mm mold that provides slabs used by the Hamburg Wheel-Tracking Device, and a 180- by 500-mm mold that provides slabs used by the French Pavement Rutting Tester. Other mold sizes can be easily accommodated. The slabs produced by this compactor can also be cored or sawed into beams. Beam specimens needed for the Georgia Loaded-Wheel Tester are provided by cutting the slab for the Hamburg Wheel-Tracking Device in half.

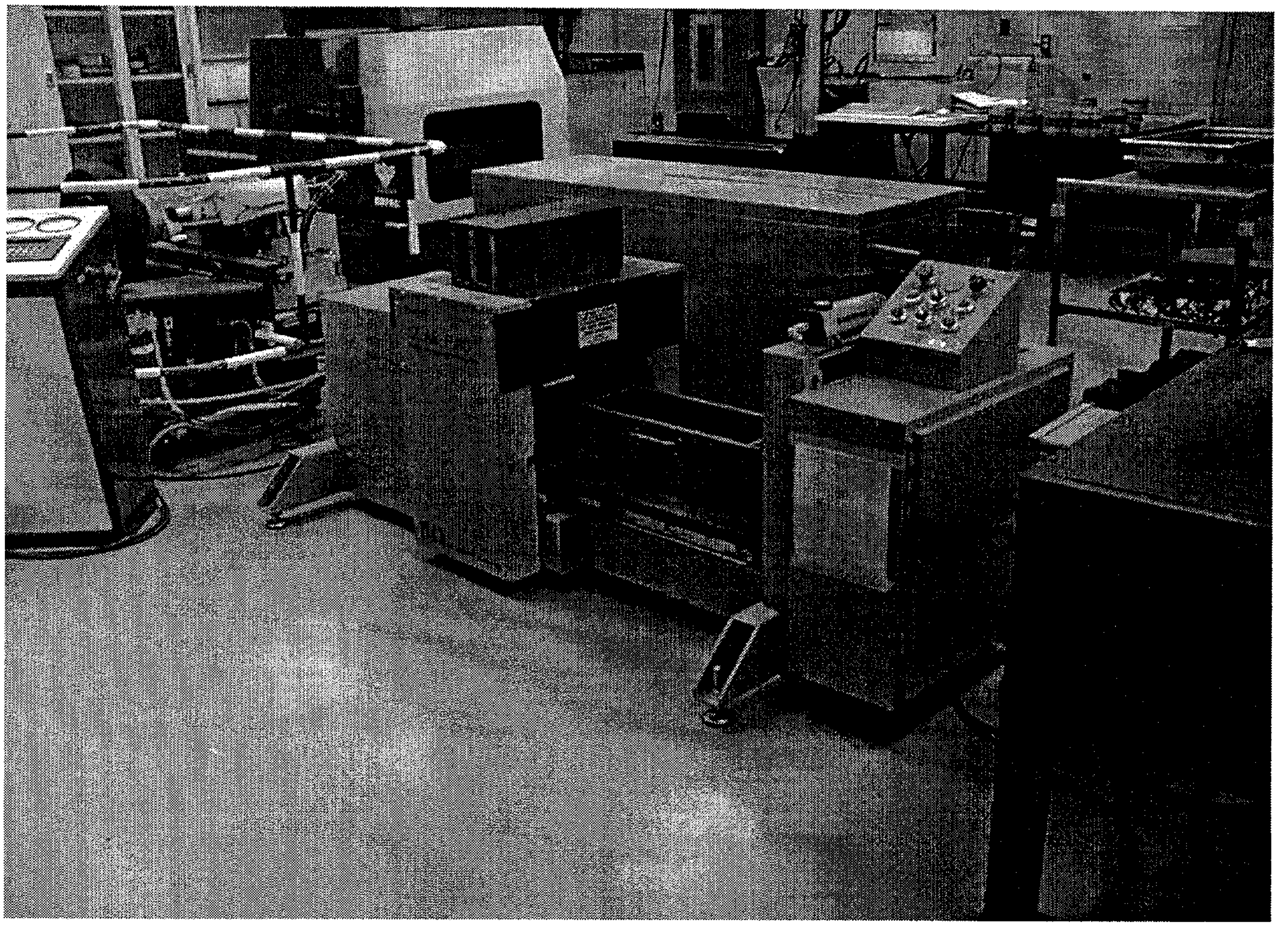

Figure 1. SLAB-PAC Linear Kneading Compactor.

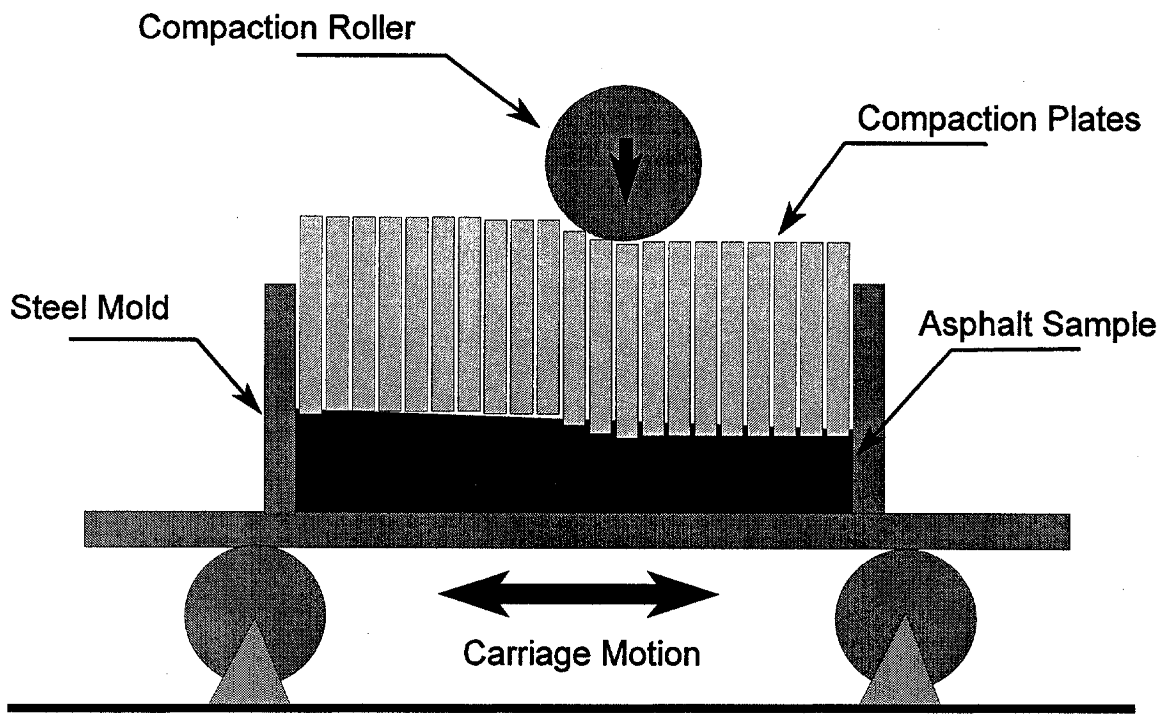

Figure 2. Linear compression wave.

APPENDIX B: AGGREGATE GRADATIONS, BINDER CONTENTS, AND MAXIMUM SPECIFIC GRAVITIES PROVIDED BY LOOSE MIXTURES ACQUIRED DURING CONSTRUCTION AND FROM PAVEMENT CORES TAKEN AFTER PAVEMENT FAILURE

Laboratory Abbreviations:

SPC = Superior Paving Corporation; eight tests per lane during construction, 1993

EFLHD = Eastern Federal Lands Highway Division; one test per lane during construction, 1993

BML = Bituminous Mixtures Laboratory (FHWA); two tests on lanes 3, 6, and 8 during construction, and one test on lanes 7, 9, and 12 during construction, 1993. Four tests were performed after each site was tested by the ALF (two cores were each split to obtain four samples).

FHWA = Combined tests performed by EFLHD and BML during construction, 1993.

AAT = Advanced Asphalt Technologies, Sterling VA; four tests were performed after each site was tested by the ALF (two cores were each split to obtain four samples).

Notes for appendix B tables:

Lanes 1, 3, 9, and 11 contain AC-5, PG 58-34.
Lane 5 contains AC-10, PG 58-28.
Lanes 2, 4, 6, 10, and 12 contain AC-20, PG 64-22.
Lane 7 contains Styrelf, PG 82-22.
Lane 8 contains Novophalt, PG 76-22.

Lanes 1 through 10 contain the surface mixtures.
Lanes 11 and 12 contain the base mixtures.

Table 103. Aggregate gradations.

Lane 1, AC-5, PG 58-34

Sieve Size (mm)	Construction SPC	EFLHD	Avg[1]	Site 1 AAT Mar96	Site 3 BML Jun98	Site 4 BML Jun98	Site 3[2] BML Jul98	Site 4[2] BML Jul98
25.0	100.0	100.0	100.0	100.0	100.0	100.0	100.0	100.0
19.0	98.7	100.0	98.7	98.0	99.3	98.6	100.0	99.4
12.5	76.4	79.0	76.0	73.6	80.1	75.1	79.8	80.4
9.5	62.6	63.0	62.0	59.3	67.1	61.6	65.7	67.4
4.75	44.3	42.0	44.0	41.4	48.1	43.9	48.7	48.8
2.36	**32.8**	**31.0**	**32.5**	**29.7**	**35.5**	**32.8**	**36.0**	**36.1**
1.18	--	23.0	23.5	22.8	26.5	24.7	27.1	27.2
0.600	17.2	17.0	17.5	17.2	19.4	18.1	20.0	20.3
0.300	11.4	11.0	11.5	11.9	13.6	12.5	13.7	14.2
0.150	--	7.0	8.0	8.4	9.7	8.8	9.7	10.1
0.075	**4.9**	**4.6**	**5.1**	**5.9**	**6.9**	**6.2**	**7.0**	**7.2**

Lane 2, AC-20, PG 64-22

Sieve Size (mm)	Construction SPC	EFLHD	Avg[1]	Site 1 AAT Mar96	Site 3 BML Jun98	Site 4 BML Jun98	Site 3[2] BML Jul98	Site 4[2] BML Jul98
25.0	100.0	100.0	100.0	100.0	100.0	100.0	100.0	100.0
19.0	98.8	99.0	98.7	98.9	98.1	99.7	100.0	99.2
12.5	74.9	80.0	76.0	74.5	77.4	76.9	80.2	79.8
9.5	61.3	61.0	62.0	58.8	61.7	61.4	66.5	65.4
4.75	43.7	41.0	44.0	40.3	41.7	40.7	46.4	44.6
2.36	**33.2**	**30.0**	**32.5**	**29.7**	**30.7**	**29.6**	**34.0**	**31.8**
1.18	--	22.0	23.5	22.9	23.4	22.8	25.6	24.1
0.600	17.3	16.0	17.5	17.4	17.4	17.0	19.1	18.1
0.300	11.9	11.0	11.5	11.8	12.2	11.9	13.2	12.7
0.150	--	7.0	8.0	8.3	8.6	8.3	9.4	9.1
0.075	**5.4**	**4.5**	**5.1**	**5.7**	**6.1**	**5.8**	**6.8**	**6.4**

[1]Overall average for the 10 pavements with the surface mixtures.
[2]These cores were taken from wheelpath after completion of the ALF test.

Table 103. Aggregate gradations (continued).

Lane 3, AC-5, PG 58-34

Sieve Size (mm)	Construction SPC	EFLHD	BML	Avg[1]	Site 1 AAT Nov96	Site 2[2] BML Aug97	Site 2[3] BML Aug97	Site 3 BML Oct97	Site 3 BML Repeat	Site 4
25.0	100.0	100.0	100.0	100.0	100.0	100.0	100.0	100.0	100.0	Not Tested by the ALF
19.0	98.1	99.0	97.0	98.7	99.1	100.0	98.6	98.9	99.4	
12.5	76.7	71.0	78.1	76.0	81.2	79.6	78.4	79.6	81.6	
9.5	62.5	56.0	60.5	62.0	63.9	63.7	64.6	64.3	64.7	
4.75	43.9	37.0	41.6	44.0	42.1	42.5	46.5	40.2	41.0	
2.36	**32.3**	**24.0**	**30.0**	**32.5**	**31.6**	**31.8**	**33.6**	**28.8**	**29.6**	
1.18	--	18.0	22.8	23.5	24.5	24.5	25.1	21.8	22.4	
0.600	17.1	13.0	16.6	17.5	18.6	18.4	18.2	16.4	16.8	
0.300	11.3	9.0	11.1	11.5	12.7	12.8	12.3	11.6	11.8	
0.150	--	6.0	7.6	8.0	8.6	8.9	8.4	8.2	8.4	
0.075	**4.8**	**3.9**	**5.1**	**5.1**	**5.5**	**6.1**	**5.8**	**5.9**	**5.8**	

[1]Overall average for the 10 pavements with the surface mixtures.
[2]Top Lift.
[3]Bottom Lift.

Table 103. Aggregate gradations (continued).

Lane 4, AC-20, PG 64-22

Sieve Size (mm)	Construction SPC	Construction EFLHD	Construction Avg[1]	Site 1 AAT Nov96	Site 2 BML Aug97	Site 3	Site 4
25.0	100.0	100.0	100.0	100.0	100.0	Not Tested by the ALF	Not Tested by the ALF
19.0	98.7	99.0	98.7	98.5	99.2		
12.5	76.2	78.0	76.0	78.5	76.3		
9.5	62.9	62.0	62.0	60.8	60.8		
4.75	44.3	43.0	44.0	41.2	42.2		
2.36	**32.9**	**29.0**	**32.5**	**32.0**	**33.0**		
1.18	--	22.0	23.5	25.0	25.6		
0.600	17.4	16.0	17.5	19.1	19.4		
0.300	11.6	10.0	11.5	13.2	13.6		
0.150	--	7.0	8.0	9.3	9.9		
0.075	**5.0**	**4.4**	**5.1**	**6.4**	**7.0**		

Lane 5, AC-10, PG 58-28

Sieve Size (mm)	Construction SPC	Construction EFLHD	Construction Avg[1]	Site 2 AAT Aug95	Site 1 BML Aug97	Site 4 BML Oct97	Site 3
25.0	100.0	100.0	100.0	100.0	100.0	100.0	Not Tested by the ALF
19.0	98.4	98.0	98.7	99.6	99.6	100.0	
12.5	76.0	72.0	76.0	79.0	79.6	81.7	
9.5	62.0	58.0	62.0	61.0	62.0	66.0	
4.75	43.5	41.0	44.0	36.4	38.0	42.6	
2.36	**32.3**	**30.0**	**32.5**	**26.3**	**27.6**	**30.8**	
1.18	--	23.0	23.5	20.1	20.9	22.8	
0.600	17.4	17.0	17.5	15.3	15.5	17.2	
0.300	11.5	11.0	11.5	10.5	10.9	11.0	
0.150	--	8.0	8.0	7.3	7.8	7.8	
0.075	**5.0**	**5.2**	**5.1**	**4.9**	**5.6**	**5.6**	

[1]Overall average for the 10 pavements with the surface mixtures.

Table 103. Aggregate gradations (continued).

Lane 6, AC-20, PG 64-22

Sieve Size (mm)	Construction SPC	EFLHD	BML	Avg[1]	Site 1 AAT Jul97	Site 2 BML Aug97	Site 3	Site 4
25.0	100.0	100.0	100.0	100.0	100.0	100.0	Not Tested by the ALF	Not Tested by the ALF
19.0	98.8	99.0	97.8	98.7	98.7	100.0		
12.5	76.0	75.0	77.1	76.0	77.6	78.0		
9.5	62.4	58.0	60.6	62.0	61.7	61.0		
4.75	44.9	41.0	41.4	44.0	41.6	40.3		
2.36	**34.4**	**30.0**	**29.8**	**32.5**	**30.3**	**30.0**		
1.18	--	23.0	22.3	23.5	23.2	23.0		
0.600	17.3	17.0	16.3	17.5	17.4	17.4		
0.300	11.9	11.0	11.2	11.5	11.9	12.2		
0.150	--	8.0	8.0	8.0	8.3	8.8		
0.075	**5.0**	**5.2**	**5.6**	**5.1**	**5.6**	**6.3**		

Lane 7, Styrelf, PG 82-22

Sieve Size (mm)	Construction SPC	EFLHD	BML	Avg[1]	Site 2 AAT Aug95	Site 1 AAT Mar96	Site 3 BML Jan98	Site 3 BML Repeat	Site 4
25.0	100.0	100.0	100.0	100.0	100.0	100.0	100.0	100.0	Not Tested by the ALF
19.0	99.5	100.0	98.6	98.7	97.5	98.4	98.6	99.2	
12.5	76.2	80.0	77.5	76.0	75.4	78.1	78.4	80.0	
9.5	22.5	62.0	63.4	62.0	60.4	61.8	62.0	66.0	
4.75	44.4	46.0	46.0	44.0	42.4	43.9	43.4	46.8	
2.36	**32.7**	**35.0**	**33.4**	**32.5**	**31.4**	**33.4**	**32.8**	**34.7**	
1.18	--	26.0	24.5	23.5	23.7	25.3	24.6	25.6	
0.600	17.9	19.0	17.7	17.5	17.2	18.7	18.0	18.2	
0.300	11.8	12.0	11.9	11.5	10.7	12.0	12.0	11.6	
0.150	--	8.0	8.3	8.0	6.6	7.7	8.0	7.4	
0.075	**5.1**	**4.7**	**6.0**	**5.1**	**3.7**	**4.7**	**5.2**	**4.6**	

[1]Overall average for the 10 pavements with the surface mixtures.

Table 103. Aggregate gradations (continued).

Lane 8, Novophalt, PG 76-22

Sieve Size (mm)	Construction SPC	EFLHD	BML	Avg[1]	Site 2 AAT Aug95	Site 1 AAT Mar96	Site 3 BML Jan98	Site 3 BML Repeat	Site 4
25.0	100.0	100.0	100.0	100.0	100.0	100.0	100.0	100.0	Not Tested by the ALF
19.0	98.7	99.0	99.0	98.7	98.4	99.5	99.2	99.7	
12.5	76.0	76.0	78.3	76.0	77.1	75.5	79.2	81.3	
9.5	61.7	53.0	58.9	62.0	60.0	59.1	61.1	65.0	
4.75	43.9	31.0	38.9	44.0	40.3	40.4	36.6	39.2	
2.36	**32.8**	**21.0**	**28.0**	**32.5**	**30.7**	**31.1**	**26.1**	**27.4**	
1.18	--	17.0	21.2	23.5	24.0	24.3	20.2	20.6	
0.600	17.5	12.0	15.4	17.5	18.5	18.5	15.2	15.5	
0.300	11.7	8.0	10.2	11.5	12.9	12.7	10.4	10.6	
0.150	--	6.0	6.9	8.0	8.9	8.8	6.8	6.8	
0.075	**5.0**	**3.5**	**4.5**	**5.1**	**5.5**	**5.4**	**4.2**	**3.9**	

[1]Overall average for the 10 pavements with the surface mixtures.

Table 103. Aggregate gradations (continued).

Lane 9, AC-5, PG 58-34

Sieve Size (mm)	Construction SPC	EFLHD	BML	Avg[1]	Site 2 AAT Aug95	Site 1 AAT Mar96	Site 2[2] BML Jan98	Site 3 BML Feb98	Site 3 BML Repeat	Site 4 BML Sep98	Site 4[2] BML Sep98
25.0	100.0	100.0	100.0	100.0	100.0	100.0	100.0	100.0	100.0	100.0	100.0
19.0	98.9	100.0	97.4	98.7	97.8	99.0	99.1	98.9	99.7	100.0	100.0
12.5	75.5	82.0	75.9	76.0	77.4	76.6	79.5	79.6	79.4	78.6	78.6
9.5	62.7	66.0	62.2	62.0	61.3	60.9	65.8	64.7	64.4	63.1	64.0
4.75	44.6	48.0	45.6	44.0	41.2	41.0	46.2	44.8	44.7	44.0	44.6
2.36	**33.9**	**35.0**	**33.6**	**32.5**	**30.2**	**30.8**	**34.6**	**33.0**	**33.3**	**32.4**	**33.2**
1.18	--	26.0	25.2	23.5	23.1	23.7	25.6	24.6	24.8	24.8	25.5
0.600	17.6	19.0	17.8	17.5	17.3	17.7	18.9	17.9	18.2	18.0	18.6
0.300	11.5	12.0	11.6	11.5	11.5	11.9	12.8	11.8	12.2	12.0	12.4
0.150	--	8.0	7.8	8.0	7.8	8.0	8.9	8.0	8.6	8.2	8.7
0.075	**4.9**	**5.1**	**5.4**	**5.1**	**5.1**	**5.3**	**6.2**	**5.5**	**5.9**	**5.7**	**6.0**

[1]Overall average for the 10 pavements with the surface mixtures.
[2]These cores were taken from wheelpath after completion of the ALF test.

Table 103. Aggregate gradations (continued).

Lane 10, AC-20, PG 64-22

Sieve Size (mm)	Construction SPC			Site 2 AAT Aug95	Site 1 AAT Mar96	Site 2[2] BML Feb98	Site 4 BML Aug98	Site 4 BML Aug98	Site 3 BML Sep98	Site 3[2] BML Sep98
	SPC	EFLHD	Avg[1]							
25.0	100.0	99.0	100.0	100.0	100.0	100.0	100.0	100.0	100.0	100.0
19.0	98.6	99.0	98.7	98.3	99.2	98.9	98.4	99.1	100.0	100.0
12.5	75.8	79.0	76.0	83.4	76.0	78.8	78.3	77.6	77.2	80.7
9.5	62.4	64.0	62.0	67.1	59.9	64.0	61.2	61.3	61.8	61.8
4.75	44.9	47.0	44.0	46.3	40.8	46.0	39.8	41.4	40.4	40.8
2.36	**34.2**	**34.0**	**32.5**	**34.4**	**30.2**	**35.1**	**29.3**	**30.6**	**29.5**	**30.0**
1.18	--	26.0	23.5	26.4	23.1	26.6	22.6	23.6	23.0	22.3
0.600	18.1	18.0	17.5	19.9	17.2	19.8	17.0	17.8	17.1	17.5
0.300	12.1	12.0	11.5	13.4	10.9	13.4	11.8	12.4	11.8	12.2
0.150	--	8.0	8.0	9.3	7.0	9.5	8.3	8.8	8.4	8.8
0.075	**5.0**	**5.0**	**5.1**	**6.2**	**4.1**	**6.6**	**5.9**	**6.3**	**6.0**	**6.3**

[1]Overall average for the 10 pavements with the surface mixtures.
[2]These cores were taken from wheelpath after completion of the ALF test.

Table 103. Aggregate Gradations (continued).

Lane 11, AC-5, PG 58-34

Sieve Size (mm)	Construction			Site 2 AAT Aug95	Site 1 AAT Mar96	Site 3 BML May97	Site 4 BML May97	Site 2[2] BML Feb98	Site 3 BML Aug98	Site 3[2] BML Aug98	Site 4
	SPC	EFLHD	Avg[1]								
37.5	100.0	100.0	100.0	100.0	100.0	100.0	100.0	100.0	100.0	100.0	Not Tested by the ALF
25.0	85.7	90.0	85.6	90.1	84.3	90.4	85.0	87.4	85.2	87.4	
19.0	73.0	75.0	73.9	78.8	76.0	80.5	72.4	75.4	72.8	77.3	
12.5	64.3	64.0	65.1	70.3	65.7	69.6	63.6	67.1	62.1	68.2	
9.5	--	--	59.0	64.8	53.3	64.4	59.4	63.2	56.8	63.3	
4.75	47.3	45.0	47.6	50.2	47.7	50.5	47.2	50.4	44.3	49.4	
2.36	**--**	**29.0**	**32.5**	**34.6**	**33.0**	**35.6**	**32.6**	**35.0**	**31.3**	**34.7**	
1.18	--	22.0	24.0	24.9	23.8	25.6	23.3	24.8	22.8	25.0	
0.600	17.2	16.0	17.4	18.3	17.6	19.0	17.3	18.2	16.9	18.4	
0.300	12.4	12.0	12.3	12.4	12.1	13.4	12.0	12.6	12.0	13.0	
0.150	--	9.0	8.0	8.6	8.5	9.6	8.6	9.0	8.5	9.2	
0.075	**5.6**	**6.3**	**5.7**	**5.5**	**5.7**	**6.7**	**5.9**	**6.3**	**5.9**	**6.5**	

[1]Overall average for the two pavements with the base mixtures.
[2]These cores were taken from wheelpath after completion of the ALF test.

Table 103. Aggregate gradations (continued).

Lane 12, AC-20, PG 64-22

Sieve Size (mm)	Construction SPC	EFLHD	BML	Avg[1]	Site 1 AAT Aug95	Site 3 BML May97	Site 4 BML May97	Site 3
37.5	100.0	100.0	100.0	100.0	100.0	100.0	100.0	Not Tested by the ALF
25.0	85.6	88.0	82.4	85.6	80.8	85.6	86.7	
19.0	74.8	76.0	74.4	73.9	67.1	74.0	79.0	
12.5	65.9	68.0	67.2	65.1	56.1	66.8	70.2	
9.5	--	--	62.7	59.0	51.9	62.9	66.6	
4.75	47.9	48.0	48.1	47.6	40.1	50.7	53.6	
2.36	**--**	**32.0**	**31.0**	**32.5**	**28.3**	**35.2**	**37.2**	
1.18	--	23.0	22.4	24.0	21.2	25.3	26.6	
0.600	17.3	17.0	18.4	17.4	16.2	18.8	19.6	
0.300	12.2	11.0	11.7	12.3	11.6	13.2	13.9	
0.150	--	8.0	8.4	8.0	8.3	9.4	10.0	
0.075	**5.5**	**5.1**	**5.9**	**5.7**	**5.6**	**6.6**	**7.2**	

[1]Overall average for the two pavements with the base mixtures.

Table 104. Binder contents.

Lane	Construction SPC[1]	Construction FHWA	AAT Aug95	AAT Mar95	AAT Nov96	BML May97	AAT Jul97	BML Aug97	BML Aug97	BML Oct97
1	4.7	4.9 (1)[2]	---	4.6	---	---	---	---	---	---
2	4.8	5.0 (1)	---	4.5	---	---	---	---	---	---
3	4.8	4.8 (3)	---	---	5.2	---	---	5.0[3]	5.6[4]	5.1
4	4.9	4.9 (1)	---	---	4.9	---	---	4.8	---	---
5	4.8	4.9 (1)	4.8	---	---	---	---	4.8	---	5.1
6	4.9	4.8 (3)	---	---	---	---	4.8	4.8	---	---
7	4.9	4.85(2)	4.9	4.6	---	---	---	---	---	---
8	4.7	4.6 (3)	4.9	4.8	---	---	---	---	---	---
9	4.9	5.1 (2)	4.8	4.7	---	---	---	---	---	---
10	4.9	4.9 (1)	5.0	4.8	---	---	---	---	---	---
11	4.0	4.2 (1)	4.1	3.8	---	4.0	---	---	---	---
12	4.1	4.15(2)	3.4	---	---	4.1	---	---	---	---

Lane	BML Jan98	BML Feb98	BML Jun98	BML[5] Jul98	BML[5] Jul98	BML Aug98	BML[5] Aug98	BML Sep98	Core AVG[6]
1	---	---	5.0	5.1	4.9	---	---	---	4.9
2	---	---	4.8	5.0	5.0	---	---	---	4.8
3	---	---	4.9	---	---	---	---	---	5.2
4	---	---	5.0	---	---	---	---	---	4.9
5	---	---	---	---	---	---	---	---	4.9
6	---	---	---	---	---	---	---	---	4.8
7	4.8	---	---	---	---	---	---	---	4.8
8	4.8	---	---	---	---	---	---	---	4.8
9	4.9	5.0	---	---	---	---	---	5.3	4.9
10	---	5.1	---	---	---	4.9	5.1	5.2	5.0
11	---	4.3	---	---	---	3.8	4.2	---	4.0
12	---	---	---	---	---	---	---	---	3.8

[1]Average of 10 replicate tests per lane.
[2]Indicates the number of samples tested per lane: 1, 2, or 3 samples.
[3]Top lift.
[4]Bottom lift. This lift was tested because it appeared to be high in binder content when cored.
[5]These cores were taken from wheelpath after completion of the ALF test.
[6]Average from cores taken after construction.

Table 105. Maximum specific gravities of the mixtures.

Lane Number	FHWA Const	AAT Aug95	AAT Mar95	AAT Nov96	BML May97	AAT Jul97	BML Aug97	BML Oct97	BML Jan98	BML Jun98	BML Aug98	BML Sep98	Core AVG[1]
1	2.686	---	2.679	---	---	---	---	---	---	2.671	---	---	2.679
2	2.686	---	2.677	---	---	---	---	---	---	2.686	---	---	2.683
3	2.678	---	---	2.678	---	---	2.676	2.678	---	2.684	---	---	2.679
4	2.692	---	---	2.680	---	---	2.686	---	---	2.679	---	---	2.684
5	2.691	2.688	---	---	2.688	---	2.696	2.675	---	---	---	---	2.688
6	2.686	---	---	---	2.690	2.666	2.692	---	---	---	---	---	2.684
7	2.684	2.694	2.701	---	2.681	---	---	---	2.682	---	---	---	2.690
8	2.686	2.700	2.695	---	2.682	---	---	---	2.698	---	---	---	2.694
9	2.684	2.680	2.681	---	2.657	---	---	---	2.674	---	---	2.668	2.672
10	2.680	2.688	2.686	---	2.692	---	---	---	---	---	2.687	2.675	2.686
11	2.746	2.724	2.753	---	2.717	---	---	---	---	---	2.756	---	2.738
12	2.755	2.774	---	---	2.728	---	---	---	---	---	---	---	2.752

[1]Average from cores taken after construction. Did not use law of partial fractions.

APPENDIX C: ALF PAVEMENT RUT DEPTH DATA

1. Rut Depth Data

Tables 106 to 119 provide the rut depth data for each ALF pavement test. Both the raw data and the data from the Gauss-Newton model are provided. Figure 69 graphically shows the rut depths in the asphalt pavement layer, including confidence bands based on $\pm 2\sigma$ for the pavement tests at 58 °C. Figure 70 shows the rut depths in the asphalt pavement layer for the mixtures with unmodified binders at all pavement test temperatures. Figure 71 shows the rut depths in the asphalt pavement layer for the mixtures with modified binders at all pavement test temperatures.

2. Downward Only Rut Depth vs. Peak-to-Valley Rut Depth

The downward only rut depths using the survey rod and level and the peak-to-valley rut depths from the transverse profiles were compared to determine if they would provide the same conclusions regarding the relative rutting performances of the asphalt pavement layers. The downward only rut depth is the rut depth based on the original surface elevation of the pavement. The peak-to-valley rut depth is the rut depth that includes any uplift of mixture outside the wheelpath. The transverse profile data were extensive. However, these profiles alone could not be used to determine the rutting performances of the various asphalt mixtures because of the variable amount of rutting in the crushed aggregate base layer from test to test. The asphalt mixtures were compared using the data from the rod and level technique. These data were measured at only three locations. The usefulness of the transverse profiles was also diminished by the computer program used to obtain and store the data. Some of the profiles were not usable because of hardware and software problems.

The transverse profiles for each ALF test site were measured at eight stations during each distress survey. The profile was measured five times at each station and the data averaged. For each of the eight average profiles, the minimum value was considered the valley. The average of the two maximum values on each side of the wheelpath was considered the peak. Six of the eight profiles were used in the analysis. The profiles from the first and eighth stations were not used because these stations were not close to the pins used by the rod and level technique. The average transverse profiles for 14 test sites are shown in figures 72 to 85. The unit for the transverse points in these figures is inches, where 1 inch equals 25.4 mm.

Table 120 provides the wheel passes at total rut depth of 20 mm for the 14 test sites. The total rut depth is the rut depth from all pavement layers. The rankings provided by the two techniques are not identical, but they are close. The two sets of wheel passes provided an r^2 of 0.90. Table 120 shows that the number of wheel passes for lane 7, site 1 was higher using the peak-to-valley rut depth (10,650 vs. 11,030). This lane contained the Styrelf surface mixture. The wheel passes for the peak-to-valley rut depth should always be equal to or lower than the wheel passes for the downward only rut depth. This discrepancy was attributed to the difference in the number of survey locations: three locations were used for the rod and level technique while six locations were used for the transverse profiles. Based on this finding, it is recommended that a minimum of six locations be used for the rod and level technique in future studies.

The two methods provided wheel passes for lane 5, site 1 that were not close to each other (6,070 vs. 1,910). This lane contained the AC-10 (PG 65) surface mixture. Differences in how the peaks developed in relationship to the valley was found to be the main reason for this. For example, figure 80 shows that there was a sharp increase in the heights of the peaks around 5,000 wheel passes, especially for the peak on the right side of the wheelpath. A reason for why this pavement deformed differently than the other pavements could not be established.

Figures 72, 73, 74, 76, and 77 show that the amount of uplift outside the wheelpath was very low for the pavements with the modified binders, even though the percent rut depth from viscous flow, which does not include the rut depth from densification, was significant in all five tests. The percent rut depth from viscous flow ranged from 45 to 75 percent. As expected, this percentage increased as the susceptibilities of the mixtures to rutting increased. Another observation was that when an asphalt pavement layer rutted quickly, the uplift outside the wheelpath started to occur at less than 100 ALF wheel passes. An example of this is shown in figure 85. This indicates that rutting from viscous flow and densification occurred at the same time.

Table 121 shows the wheel passes that provided a rut depth of 20 mm in the asphalt pavement layer. The amount of rutting in the lower layers was subtracted from the total rut depth provided by both the rod and level technique and the transverse profiles. The rutting in the lower layers was provided by the rod and level technique. The wheel passes were dissimilar for the three best performing pavements. The relationships between rut depth and wheel passes were relatively flat for these mixture at a rut depth of 20 mm. This meant that the error in the number of wheel passes was potentially very large. The two sets of wheel passes provided an r^2 of 0.96 without these three mixtures. The rankings also differed for Lane 5, site 1, containing the AC-10 (PG 65) surface mixture (21,720 vs. 3,780).

Table 122 shows the data for the Novophalt and Styrelf pavement tests at 58 and 70 °C. The Novophalt surface mixture performed better than the Styrelf surface mixture using both the downward only and the peak-to-valley rut depths. Therefore, the discrepancy between $G^*/\sin\delta$ and ALF pavement rutting performance was not related to the type of rut depth measurement.

The eight transverse profiles also provide longitudinal profiles with a distance of 1.2 m between the points. These data are not included in this report. The amount of variability in the longitudinal direction and the changes in this variability with wheel passes indicated that at least six locations should be used for the rod and level technique.

Table 106. Rut depth, lane 5 site 4 at 46 °C.

Passes	AC-10			
	Asphalt Layer, mm		Total, mm	
	Raw	Model	Raw	Model
0	0.0	0.0	0.0	0.0
10	1.8	3.1	1.8	2.6
100	4.1	4.9	4.2	4.9
500	6.5	6.9	6.8	7.7
1000	7.6	8.0	8.1	9.4
5000	11.7	11.1	15.0	14.8
10000	13.5	12.9	18.0	18.0
15000	14.5	14.0	20.2	20.1
25000	16.3	15.6	24.5	23.3
40000	18.1	17.2	27.9	26.5
50000	18.7	18.0	29.7	28.3
75000	19.2	19.6	31.8	31.7
100000	19.9	20.8	33.8	34.4
125000	20.8	21.8	34.6	36.6

Table 107. Rut depth, lane 3 site 3 at 46 °C.

Passes	AC-5			
	Asphalt Layer, mm		Total, mm	
	Raw	Model	Raw	Model
0	0.0	0.0	0.0	0.0
10	1.8	4.0	2.5	4.7
100	4.6	5.8	5.9	7.4
500	7.3	7.5	9.8	10.1
1000	8.4	8.4	11.3	11.5
5000	11.8	11.0	16.8	15.8
10000	13.3	12.3	19.4	18.1
15000	13.9	13.2	20.4	19.6
25000	15.3	14.3	22.7	21.7
50000	16.6	16.0	25.5	24.8
75000	17.4	17.1	26.6	26.9
100000	18.1	18.0	28.2	28.5
125000	18.6	18.6	29.4	29.7
150000	19.1	19.2	30.8	30.8
175000	19.4	19.7	31.8	31.8
200000	19.5	20.1	31.9	32.6
225000	20.1	20.5	33.2	33.4
250000	20.2	20.9	33.7	34.1

Table 108. Rut depth, lane 5 site 1 at 52 °C.

Passes	AC-10			
	Asphalt Layer, mm		Total, mm	
	Raw	Model	Raw	Model
0	0.0	0.0	0.0	0.0
1	0.1	1.0	0.1	0.8
10	1.3	2.0	1.4	1.9
100	4.3	4.0	4.7	4.5
500	7.5	6.5	8.7	8.0
5000	12.1	12.9	17.7	18.6
10000	16.2	15.9	24.1	24.0
15000	18.2	17.9	28.2	27.8
20000	19.7	19.5	30.7	30.9
25000	20.6	20.9	33.5	33.5

Table 110. Rut depth, lane 9 site 3 at 52 °C.

Passes	AC -5			
	Asphalt Layer, mm		Total, mm	
	Raw	Model	Raw	Model
0	0.0	0.0	0.0	0.0
10	5.1	4.1	4.9	3.2
100	7.8	8.2	8.2	7.9
1000	15.7	16.4	17.7	19.6
2500	21.7	21.6	29.0	28.2
3500	24.1	23.8	32.4	32.2

Table 109. Rut depth, lane 6 site 1 at 52 °C.

Passes	AC-20			
	Asphalt Layer, mm		Total, mm	
	Raw	Model	Raw	Model
0	0.0	0.0	0.0	0.0
1	0.1	2.0	0.2	2.0
10	2.0	3.2	2.2	3.4
100	4.9	4.9	5.3	5.8
500	6.1	6.7	7.7	8.5
5000	10.3	10.3	14.4	14.6
10000	12.6	11.8	18.2	17.2
15000	13.8	12.7	19.7	18.9
25000	14.6	14.0	21.9	21.3
40000	16.2	15.3	25.3	23.8
65000	17.1	16.8	27.7	26.7
90000	18.0	17.9	29.4	28.9
115000	19.0	18.8	31.1	30.6
140000	18.9	19.5	32.3	32.0
158300	19.3	19.9	32.4	33.0
165000	19.3	20.1	32.7	33.3
190000	20.1	20.6	34.1	34.4
215000	20.6	21.1	34.7	35.4

Table 111. Asphalt layer rut depth at 58° C, mm, raw data.

Passes	Lane number																
	9				5	10					7	8	11				12
	AC-5				AC-10	AC-20					Styrelf	Novophalt	AC-5 B				AC-20 B
	S1	S2	Avg.	S4	S2	S1	S2	Avg.	S3	S4	S2	S2	S1	S2	Avg.	S3	S1
0	0.0	0.0	0.0		0.0	0.0	0.0	0.0			0.0	0.0	0.0	0.0	0.0		0.0
1	0.2	0.2	0.2		0.2	1.9	0.6	1.3			0.2	0.2	-0.2	0.3	0.1		0.5
10	4.3	3.0	3.7	4.8	2.9	4.6	2.8	3.7	2.3	1.7	1.5	0.7	2.1	2.4	2.2	2.6	3.4
100	10.1	9.6	9.8	10.0	6.3	8.8	8.0	8.4	5.5	4.6	3.5	2.2	5.4	5.7	5.6	4.6	5.8
500	16.0	14.5	15.2	19.4	11.9	12.3	13.8	13.1	7.8	7.6	5.6	3.4	8.8	10.1	9.4	7.6	9.3
900				22.4													
1000	21.1	9.8	15.4		14.7	14.2	15.5	14.9	9.9	9.3	6.3	2.9	9.3	10.6	10.0	8.6	10.6
1500	23.5				NA												
2000	30.9	22.3	26.6		20.7									13.4			
3000					23.8	19.8							11.9	15.2	13.6		10.6
4000					27.4									16.9			
5000						27.2	27.4	27.3	16.5	14.0	7.1	2.9	13.8	18.1	16.0	11.3	14.4
7000						24.9							15.7				
10000						27.1	36.3	31.7	19.3	19.6	12.0	4.4	17.7	22.3	20.0	13.5	15.2
15000									19.9	20.7			20.8	23.6	22.2		
20000									22.7	22.3			21.6	24.1	22.9	16.7	
21000														25.0			
22000														24.6			
23000														24.3			
24000														24.9			
25000											14.3		23.4				
25100																	18.2
35500												5.8					
50000											16.6					19.0	20.6
60000																19.5	20.9
75000											17.0					20.2	21.2
82000																20.3	
85500												7.7					21.9
100000											16.9						
110500												7.6					
125000											17.6						22.9
135500												8.5					
150000											17.9						23.5
160500												8.9					
175000											18.2						
176735																	23.5
185500												9.2					
200000											18.1						24.1
208805												9.2					

Avg. = The average of sites 1 and 2.

Table 112. Asphalt layer rut depth at 58° C, mm, model data.

Passes	Lane Number																
	9				5	10					7	8	11				12
	AC-5				AC-10	AC-20					Styrelf	Novophalt	AC-5 B				AC-20 B
	S1	S2	Avg.	S4	S2	S1	S2	Avg.	S3	S4	S2	S2	S1	S2	Avg.	S3	S1
0	0.0	0.0	0.0	0.0	0.0	0.0	0.0	0.0	0.0	0.0	0.0	0.0	0.0	0.0	0.0	0.0	0.0
1	1.4	1.1	1.3	2.1	0.9	2.4	1.9	2.2	1.5	1.1	1.5	0.6	1.2	1.9	1.6	2.0	2.9
10	3.5	3.3	3.4	4.6	2.4	4.4	3.8	4.1	2.8	2.3	2.5	1.0	2.4	3.5	3.0	3.2	4.4
100	8.7	9.4	9.1	10.5	6.1	8.2	7.5	7.9	5.3	4.5	4.0	1.6	4.7	6.3	5.6	5.2	6.5
500	16.5	19.6	18.1	18.5	11.6	12.7	12.1	12.5	8.3	7.4	5.6	2.4	7.5	9.5	8.6	7.3	8.7
1000	21.7	27.0	24.3	23.7	15.4	15.3	14.9	15.2	10.0	9.1	6.5	2.8	9.1	11.4	10.4	8.5	9.8
1500	25.5	32.5	28.9	27.4	18.2	17.0	16.8	17.0	11.1	10.3	7.1	3.0	10.3	12.6	11.6	9.2	10.5
2000	28.6	37.1	32.7	30.3	20.4	18.4	18.3	18.4	12.1	11.3	7.5	3.2	11.2	13.6	12.6	9.8	11.1
2730	32.4	42.8	37.4	33.8	23.2	20.0	20.0	20.1	13.1	12.4	8.0	3.5	12.2	14.7	13.7	10.4	11.7
3000	33.6	44.7	38.9	35.0	24.1	20.5	20.6	20.7	13.5	12.8	8.2	3.5	12.6	15.1	14.1	10.7	11.9
4000	37.7	51.0	44.1	38.7	27.1	22.1	22.4	22.4	14.6	13.9	8.7	3.8	13.6	16.2	15.2	11.3	12.5
5000	41.2	56.5	48.5	41.9	29.6	23.5	23.9	23.9	15.5	14.9	9.1	4.0	14.6	17.2	16.2	11.8	13.0
7000	47.1	65.9	56.0	47.2	34.0	25.7	26.4	26.2	17.0	16.5	9.7	4.3	16.0	18.8	17.7	12.7	13.8
10000	54.3	77.6	65.2	53.6	39.3	28.3	29.4	29.0	18.7	18.4	10.5	4.6	17.8	20.6	19.6	13.7	14.7
15000	63.8	93.5	77.6	61.9	46.3	31.5	33.1	32.5	20.9	20.8	11.4	5.1	20.0	22.8	21.9	14.9	15.8
20000	71.5	106.7	87.8	68.5	52.0	34.1	36.1	35.3	22.6	22.7	12.1	5.4	21.7	24.6	23.7	15.8	16.6
21000	72.9	109.1	89.7	69.7	53.1	34.5	36.6	35.8	22.9	23.0	12.3	5.5	22.0	24.9	24.0	16.0	16.7
22000	74.3	111.4	91.5	70.8	54.1	34.9	37.1	36.2	23.2	23.4	12.4	5.6	22.3	25.2	24.3	16.1	16.9
23000	75.6	113.7	93.2	72.0	55.0	35.4	37.6	36.7	23.5	23.7	12.5	5.6	22.6	25.5	24.6	16.3	17.0
24000	76.9	116.0	94.9	73.1	56.0	35.8	38.1	37.1	23.8	24.0	12.6	5.7	22.9	25.8	24.9	16.4	17.1
25000	78.2	118.2	96.6	74.1	56.9	36.2	38.5	37.6	24.1	24.3	12.7	5.7	23.2	26.0	25.1	16.6	17.3
25100	78.3	118.4	96.8	74.2	57.0	36.2	38.6	37.6	24.1	24.3	12.7	5.7	23.2	26.1	25.2	16.6	17.3
35500	89.9	138.8	112.3	83.9	65.7	39.7	42.8	41.5	26.5	27.0	13.7	6.2	25.7	28.5	27.7	17.8	18.4
50000	103.0	162.4	130.0	94.7	75.5	43.6	47.3	45.7	29.1	30.0	14.7	6.7	28.3	31.1	30.4	19.2	19.5
60000	110.8	176.6	140.6	101.1	81.2	45.7	50.0	48.1	30.6	31.7	15.2	7.0	29.9	32.6	31.9	19.9	20.1
75000	121.1	195.7	154.7	109.4	89.0	48.5	53.4	51.2	32.5	33.9	16.0	7.3	31.8	34.6	34.0	20.9	21.0
85500	127.5	207.8	163.6	114.6	93.8	50.3	55.5	53.1	33.7	35.3	16.4	7.6	33.1	35.8	35.2	21.4	21.4
100000	135.7	223.3	175.0	121.1	100.0	52.4	58.1	55.5	35.2	37.0	17.0	7.8	34.6	37.2	36.7	22.1	22.0
110500	141.2	233.7	182.7	125.5	104.1	53.9	59.8	57.1	36.1	38.1	17.3	8.0	35.6	38.2	37.7	22.6	22.4
125000	148.3	247.4	192.6	131.1	109.5	55.7	62.1	59.1	37.4	39.6	17.8	8.2	36.9	39.4	39.0	23.2	22.9
135500	153.2	256.7	199.3	134.9	113.1	56.9	63.6	60.5	38.2	40.6	18.1	8.4	37.8	40.3	39.9	23.6	23.3
150000	159.5	269.0	208.2	139.8	117.9	58.5	65.5	62.3	39.3	41.8	18.4	8.6	38.9	41.3	41.0	24.1	23.7
160500	163.9	277.4	214.3	143.2	121.1	59.5	66.8	63.5	40.0	42.7	18.7	8.7	39.7	42.1	41.8	24.4	24.0
175000	169.6	288.7	222.4	147.6	125.5	60.9	68.6	65.0	41.0	43.9	19.0	8.9	40.7	43.0	42.8	24.9	24.3
176735	170.3	290.0	223.4	148.2	126.0	61.1	68.8	65.2	41.1	44.0	19.1	8.9	40.8	43.1	42.9	24.9	24.4
185500	173.6	296.5	228.0	150.7	128.5	61.9	69.8	66.1	41.6	44.6	19.3	9.0	41.4	43.7	43.5	25.2	24.6
200000	178.9	306.9	235.5	154.8	132.5	63.1	71.3	67.5	42.5	45.7	19.6	9.2	42.3	44.5	44.4	25.6	24.9
208805	182.0	313.0	239.9	157.2	134.8	63.9	72.3	68.3	43.0	46.3	19.8	9.3	42.8	45.0	44.9	25.8	25.1
1000000	339.4	642.5	469.4	273.7	254.6	97.2	114.9	106.3	66.0	74.4	27.4	13.2	67.3	67.5	69.0	35.8	33.1

Avg. = The average of sites 1 and 2.

Table 113. Total rut depth at 58 °C, mm, raw data.

Passes	Lane Number																
	9				5	10					7	8	11				12
	AC-5				AC-10	AC-20					Styrelf	Novophalt	AC-5 B				AC-20 B
	S1	S2	Avg.	S4	S2	S1	S2	Avg.	S3	S4	S2	S2	S1	S2	Avg.	S3	S1
0	0.0	0.0	0.0		0.0	0.0	0.0	0.0			0.0	0.0	0.0	0.0	0.0		0.0
1	0.2	0.2	0.2		0.3	2.0	0.7	1.4			0.3	0.3	0.1	0.5	0.3		0.6
10	4.3	4.1	4.2	5.9	3.1	4.8	2.9	3.9	3.1	1.7	1.8	2.4	2.3	2.6	2.5	3.0	3.6
100	10.5	10.8	10.6	11.5	7.2	8.9	8.1	8.5	6.5	4.6	3.8	5.1	5.7	6.0	5.8	5.0	6.3
500	18.2	21.6	19.9	21.8	13.8	13.5	14.0	13.8	9.0	8.0	6.8	7.5	9.0	10.4	9.7	9.2	9.7
900				25.1													
1000	26.0	30.3	28.2		18.8	16.6	16.2	16.4	11.7	10.5	8.2	9.6	11.3	11.4	11.3	10.2	11.0
1500	31.6																
2000	41.5	40.1	40.8		25.5									14.2			
3000					29.8	22.7							16.3	16.5	16.4		11.0
4000					34.0									18.3			
5000						26.4	28.0	27.2	19.5	16.8	11.0	11.0	18.6	19.5	19.1	14.4	15.7
7000						29.2							21.4				
10000						32.8	36.9	34.8	23.7	22.6	18.1	15.2	23.9	24.4	24.1	18.0	17.3
15000									24.7	23.7			27.6	28.4	28.0		
20000									28.0	27.5			29.2	32.2		21.1	
21000														33.8			
22000														34.6			
23000														34.8			
24000														35.7			
25000											22.8	0.0	31.3				
25100																	21.0
35500												18.6					
50000											26.4					25.3	24.4
60000																26.3	25.3
75000											28.2					27.8	26.1
82000																27.8	
85500												22.3					27.2
100000											29.8						
110500												26.6					
125000											30.7						28.8
135500												29.1					
150000											31.2						29.7
160500												27.7					
175000											32.0						
176735																	30.0
185500												28.0					
200000											32.3						30.7
208805												29.3					

Avg. = The average of sites 1 and 2.

Table 114. Total rut depth at 58 °C, mm, model data.

Passes	Lane Number																
	9				5	10					7	8	11				12
	AC-5				AC-10	AC-20					Styrelf	Novophalt	AC-5 B				AC-20 B
	S1	S2	Avg.	S4	S2	S1	S2	Avg.	S3	S4	S2	S2	S1	S2	Avg.	S3	S1
0	0.0	0.0	0.0	0.0	0.0	0.0	0.0	0.0	0.0	0.0	0.0	0.0	0.0	0.0	0.0	0.0	0.0
1	0.8	1.4	1.1	2.6	1.0	2.3	1.6	1.9	1.7	1.0	1.6	1.6	1.2	1.0	1.1	2.0	2.5
10	2.6	3.9	3.3	5.6	2.7	4.4	3.4	4.0	3.2	2.2	2.8	2.8	2.6	2.2	2.4	3.5	4.0
100	8.4	10.7	9.9	12.2	7.1	8.6	7.6	8.2	6.2	4.7	5.1	4.8	5.4	5.0	5.2	6.0	6.5
500	19.1	21.9	21.2	21.0	14.0	13.7	13.1	13.6	9.8	8.0	7.6	7.1	9.1	8.8	9.0	8.7	9.1
1000	27.2	29.8	29.6	26.5	18.8	16.7	16.6	17.0	11.9	10.1	9.1	8.4	11.3	11.3	11.4	10.2	10.5
1500	33.5	35.7	35.8	30.4	22.3	18.8	19.1	19.3	13.3	11.5	10.0	9.2	12.9	13.0	13.1	11.2	11.4
2000	38.7	40.5	41.1	33.5	25.2	20.4	21.1	21.1	14.5	12.7	10.8	9.9	14.2	14.4	14.4	12.0	12.1
2730	45.4	46.5	47.7	37.2	28.7	22.3	23.5	23.3	15.8	14.0	11.7	10.6	15.6	16.1	16.0	12.9	12.9
3000	47.6	48.5	49.9	38.4	29.9	23.0	24.2	24.0	16.3	14.5	11.9	10.9	16.1	16.7	16.5	13.2	13.2
4000	55.1	55.1	57.2	42.3	33.8	25.0	26.7	26.3	17.6	15.9	12.8	11.6	17.7	18.5	18.2	14.1	14.0
5000	61.8	60.8	63.6	45.6	37.1	26.6	28.8	28.2	18.8	17.2	13.6	12.2	19.0	20.0	19.6	14.9	14.7
7000	73.3	70.6	74.6	51.1	42.8	29.3	32.4	31.3	20.7	19.2	14.8	13.3	21.1	22.5	22.0	16.1	15.7
10000	87.9	82.6	88.4	57.6	49.8	32.5	36.6	35.1	22.9	21.6	16.2	14.4	23.7	25.5	24.8	17.5	17.0
15000	108.0	98.9	107.2	66.1	59.2	36.6	42.0	39.9	25.7	24.7	17.9	15.9	27.0	29.5	28.4	19.2	18.5
20000	125.1	112.3	123.0	72.8	66.8	39.7	46.3	43.7	27.9	27.2	19.3	17.0	29.6	32.6	31.3	20.5	19.6
21000	128.2	114.8	125.9	74.0	68.2	40.3	47.1	44.3	28.3	27.6	19.5	17.2	30.0	33.2	31.8	20.7	19.8
22000	131.3	117.2	128.7	75.2	69.6	40.8	47.9	45.0	28.7	28.1	19.7	17.4	30.5	33.8	32.3	21.0	20.0
23000	134.3	119.5	131.4	76.3	70.9	41.4	48.6	45.6	29.1	28.5	20.0	17.6	30.9	34.3	32.8	21.2	20.2
24000	137.2	121.8	134.1	77.5	72.2	41.9	49.3	46.2	29.4	28.9	20.2	17.8	31.3	34.8	33.3	21.4	20.3
25000	140.1	124.0	136.8	78.5	73.5	42.4	50.0	46.8	29.8	29.3	20.4	17.9	31.8	35.3	33.7	21.6	20.5
25100	140.4	124.2	137.0	78.6	73.6	42.4	50.1	46.9	29.8	29.3	20.4	18.0	31.8	35.4	33.8	21.6	20.5
35500	167.5	144.9	161.6	88.4	85.2	46.9	56.4	52.3	32.9	32.9	22.3	19.5	35.5	40.0	38.0	23.4	22.1
50000	199.4	168.6	190.2	99.2	98.6	51.8	63.4	58.3	36.3	36.9	24.3	21.1	39.6	45.2	42.6	25.4	23.7
60000	218.8	182.8	207.5	105.5	106.5	54.6	67.5	61.7	38.2	39.2	25.4	22.1	42.0	48.2	45.3	26.5	24.6
75000	245.1	201.8	230.7	113.8	117.0	58.2	72.8	66.2	40.7	42.2	26.9	23.3	45.1	52.1	48.8	27.9	25.8
85500	262.0	213.8	245.6	118.9	123.7	60.5	76.2	69.0	42.3	44.0	27.8	24.0	47.1	54.6	51.0	28.8	26.5
100000	283.8	229.2	264.6	125.4	132.2	63.3	80.4	72.5	44.2	46.4	28.9	24.9	49.5	57.7	53.8	29.8	27.4
110500	298.6	239.6	277.5	129.7	137.9	65.1	83.2	74.9	45.5	47.9	29.7	25.5	51.1	59.8	55.7	30.5	28.0
125000	317.9	253.0	294.2	135.2	145.3	67.5	86.7	77.8	47.1	50.0	30.6	26.3	53.1	62.4	58.0	31.4	28.7
135500	331.2	262.2	305.8	139.0	150.4	69.1	89.2	79.8	48.2	51.3	31.2	26.8	54.5	64.3	59.6	32.0	29.2
150000	348.8	274.3	320.9	143.8	157.0	71.1	92.3	82.4	49.6	53.1	32.0	27.4	56.3	66.6	61.7	32.8	29.8
160500	361.0	282.6	331.4	147.1	161.6	72.5	94.5	84.2	50.6	54.3	32.6	27.9	57.6	68.2	63.1	33.3	30.2
175000	377.3	293.7	345.4	151.5	167.6	74.4	97.3	86.5	51.8	55.9	33.3	28.4	59.2	70.3	65.0	34.0	30.8
176735	379.2	295.0	347.0	152.0	168.3	74.6	97.6	86.8	52.0	56.0	33.4	28.5	59.4	70.6	65.2	34.1	30.8
185500	388.6	301.4	355.1	154.5	171.8	75.6	99.3	88.2	52.7	56.9	33.8	28.8	60.3	71.8	66.3	34.4	31.1
200000	403.8	311.6	368.0	158.5	177.4	77.3	101.9	90.3	53.8	58.4	34.4	29.4	61.8	73.8	68.0	35.1	31.6
208805	412.8	317.6	375.6	160.8	180.7	78.3	103.4	91.5	54.5	59.2	34.8	29.7	62.6	74.9	69.0	35.4	31.9
1000000	916.1	635.6	791.7	272.9	351.0	123.1	176.6	150.0	85.2	99.6	51.7	43.0	103.4	130.4	116.9	51.0	44.2

Avg. = The average of sites 1 and 2.

Table 115. Rut depth, lane 6 site 2 at 64 °C.

Passes	AC-20			
	Asphalt Layer, mm		Total, mm	
	Raw	Model	Raw	Model
0	0.0	0.0	0.0	0.0
10	2.9	2.9	3.0	3.9
30	3.9	4.0	5.5	5.4
100	5.3	5.7	7.5	7.8
300	7.4	7.9	10.8	10.8
1000	12.3	11.3	16.2	15.4
3000	16.4	15.6	22.3	21.4
4000	16.8	17.0	23.0	23.3
5000	17.5	18.1	24.2	24.9
6000	18.5	19.1	25.5	26.3
8000	21.2	20.8	29.1	28.6

Table 116. Asphalt layer rut depth at 70 °C, mm.

Passes	Lane Number			
	7		8	
	Styrelf		Novophalt	
	Site 1		Site 1	
	Raw	Model	Raw	Model
0	0.0	0.0	0.0	0.0
1	0.8	3.0	1.4	2.3
10	2.5	4.3	3.5	3.4
100	6.3	6.4	5.6	5.0
500	8.7	8.3	7.7	6.6
1000	10.1	9.3	8.2	7.4
5000	13.6	12.2	9.1	9.8
10000	14.9	13.7	10.7	11.0
25000	17.0	15.9	11.3	12.8
50000	18.3	17.9	14.0	14.4
75000	18.6	19.1	15.3	15.5
100000	19.1	20.1	16.2	16.2
125000	19.7	20.8	18.3	16.9

Table 117. Total rut depth at 70 °C, mm.

Passes	Lane number			
	7		8	
	Styrelf		Novophalt	
	Site 1		Site 1	
	Raw	Model	Raw	Model
0	0.0	0.0	0.0	0.0
1	0.9	2.8	1.5	1.6
10	3.1	4.5	3.7	2.8
100	7.1	7.4	6.4	5.0
500	10.5	10.4	8.8	7.3
1000	12.2	12.1	10.1	8.7
5000	17.9	17.0	12.5	12.8
10000	20.1	19.7	13.9	15.2
25000	25.1	24.0	15.7	19.0
50000	28.8	27.8	21.2	22.5
75000	30.3	30.3	24.6	24.8
100000	31.3	32.2	26.9	26.6
125000	32.8	33.8	31.1	28.1

Table 118. Asphalt layer rut depth at 76 °C, mm.

Passes	Lane Number			
	7		8	
	Styrelf		Novophalt	
	Site 1		Site 2	
	Raw	Model	Raw	Model
0	0.0	0.0	0.0	0.0
10	2.8	4.0	2.7	2.6
100	5.4	5.8	4.6	3.8
500	7.4	7.5	5.8	5.0
1000	9.7	8.4	6.7	5.6
5000	11.5	10.8	7.6	7.3
10000	12.6	12.1	8.2	8.2
25000	13.6	14.0	8.9	9.6
50000	15.6	15.6	9.6	10.8
75000	16.5	16.6	9.9	11.6
100000	16.9	17.4	11.7	12.2
125000	17.3	18.0	12.4	12.6
150000	18.3	18.6	12.6	13.0
175000	18.9	19.0	13.3	13.4
200000	19.9	19.4	13.5	13.7
225000	20.7	19.8	13.6	13.9
250000			14.1	14.2
275000			14.8	14.4
300000			14.8	14.6
325000			14.9	14.8
350000			15.1	15.0
375000			15.5	15.2
400000			15.6	15.4
425000			16.4	15.5
450000			15.6	15.7
475000			15.7	15.8
500000			15.4	16.0
525000			15.6	16.1
550000			16.4	16.2
575000			16.1	16.3
600000			16.8	16.5
625000			16.9	16.6
650000			17.1	16.7
675000			17.2	16.8
700000			17.0	16.9

Table 119. Total rut depth at 76 °C, mm.

Passes	Lane Number			
	7		8	
	Styrelf		Novophalt	
	Site 1		Site 1	
	Raw	Model	Raw	Model
0	0.0	0.0	0.0	0.0
10	3.8	4.1	3.6	1.8
100	7.8	6.9	6.1	3.4
500	10.6	9.9	8.0	5.3
1000	12.8	11.6	8.5	6.4
5000	16.7	16.7	11.2	10.1
10000	18.5	19.5	12.2	12.2
25000	22.5	24.0	14.6	15.8
50000	28.7	28.1	16.8	19.2
75000	30.0	30.8	19.0	21.5
100000	32.4	32.9	22.6	23.3
125000	34.4	34.6	24.3	24.8
150000	36.2	36.0	25.7	26.1
175000	37.9	37.3	26.3	27.3
200000	38.4	38.4	27.9	28.3
225000	40.0	39.5	29.2	29.3
250000			30.5	30.2
275000			31.4	31.0
300000			31.4	31.7
325000			32.8	32.5
350000			33.0	33.1
375000			34.0	33.8
400000			34.2	34.4
425000			35.4	35.0
450000			35.5	35.6
475000			35.6	36.1
500000			35.8	36.6
525000			36.6	37.1
550000			37.7	37.6
575000			38.1	38.1
600000			39.4	38.5
625000			39.5	39.0
650000			39.4	39.4
675000			40.0	39.8
700000			40.6	40.2

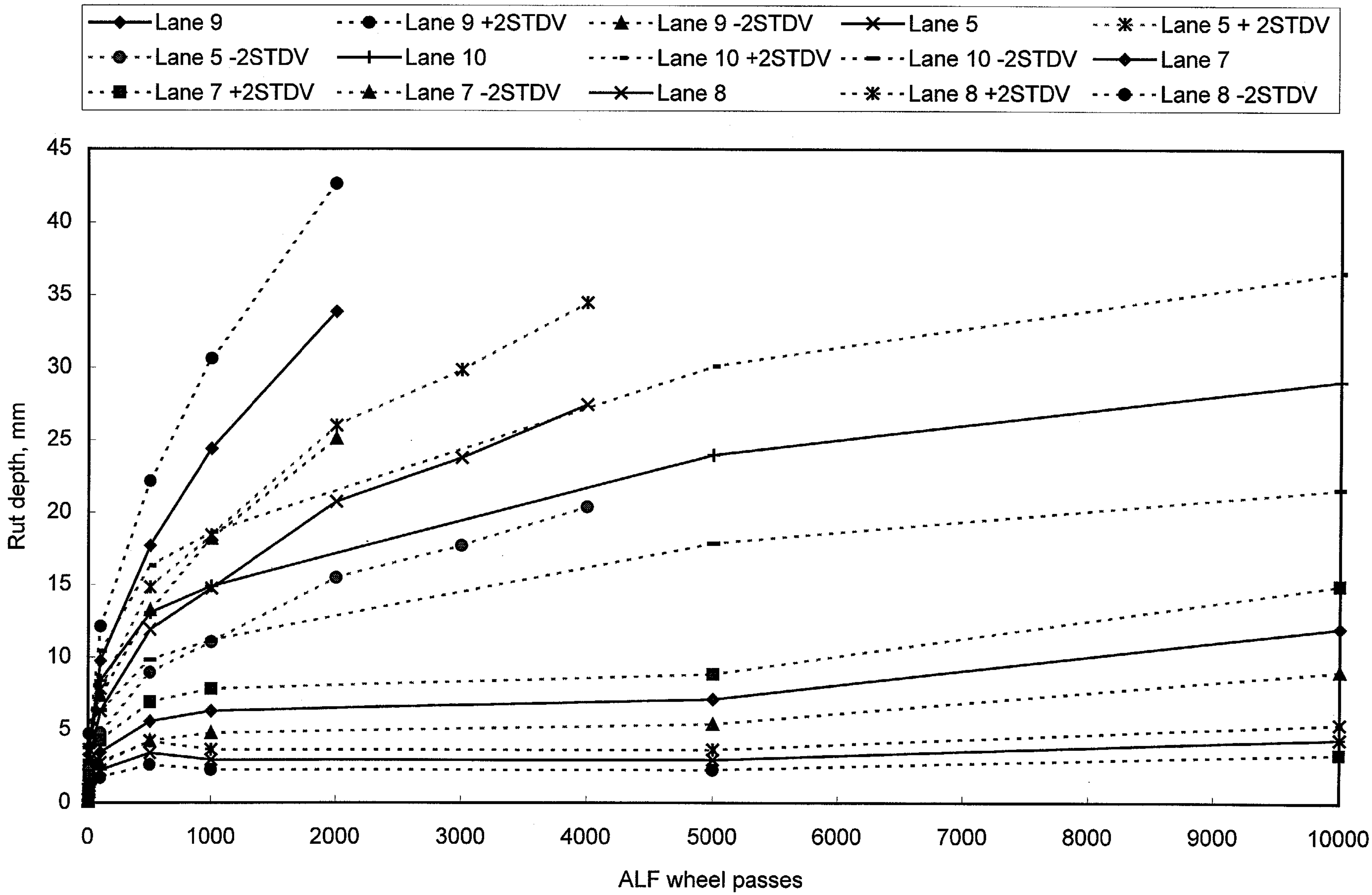

Figure 69. Rut depth ± two standard deviation (± 2STDV) at 58 °C.

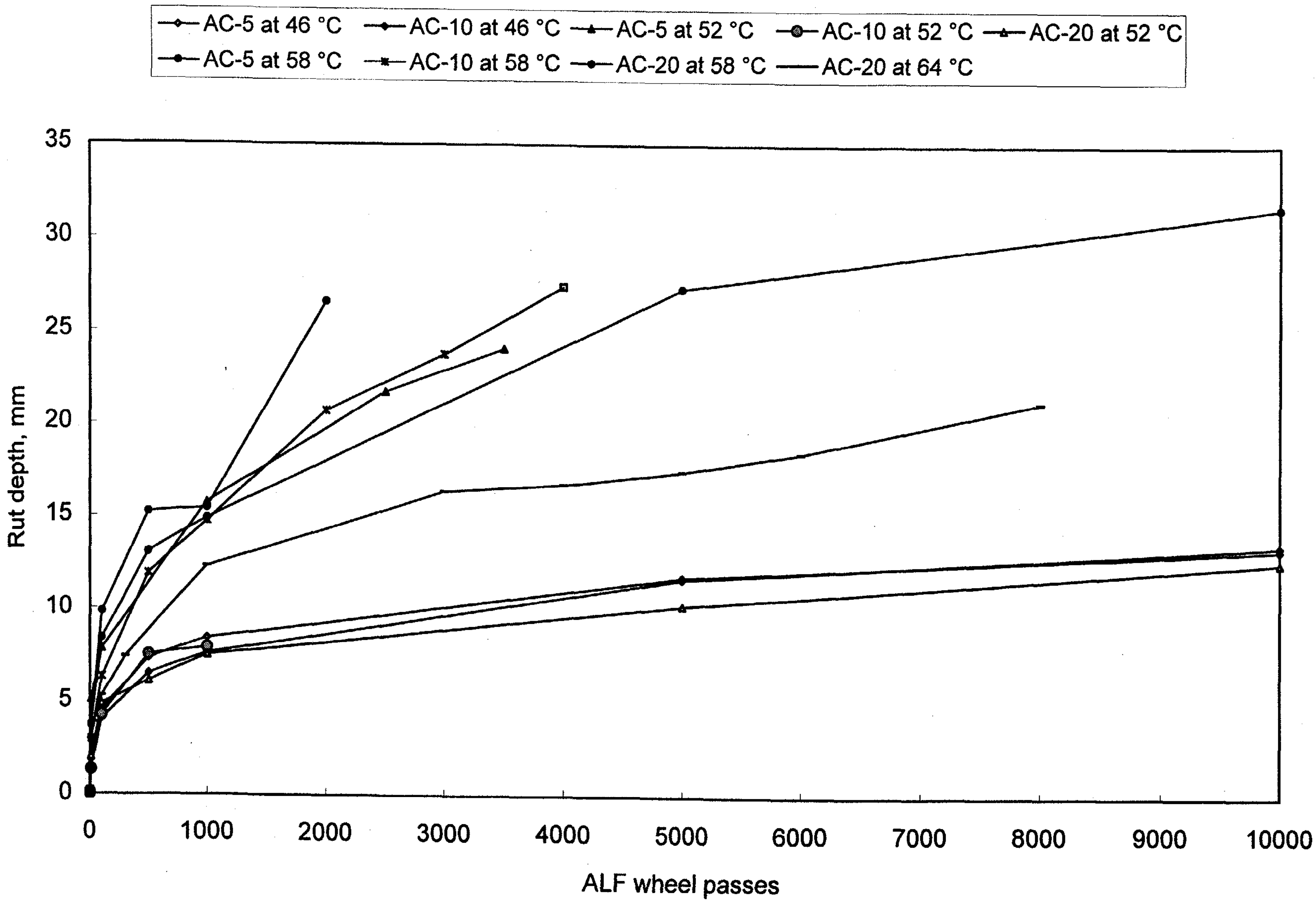

Figure 70. Measured rut depths in the asphalt pavement layer vs. ALF wheel passes.

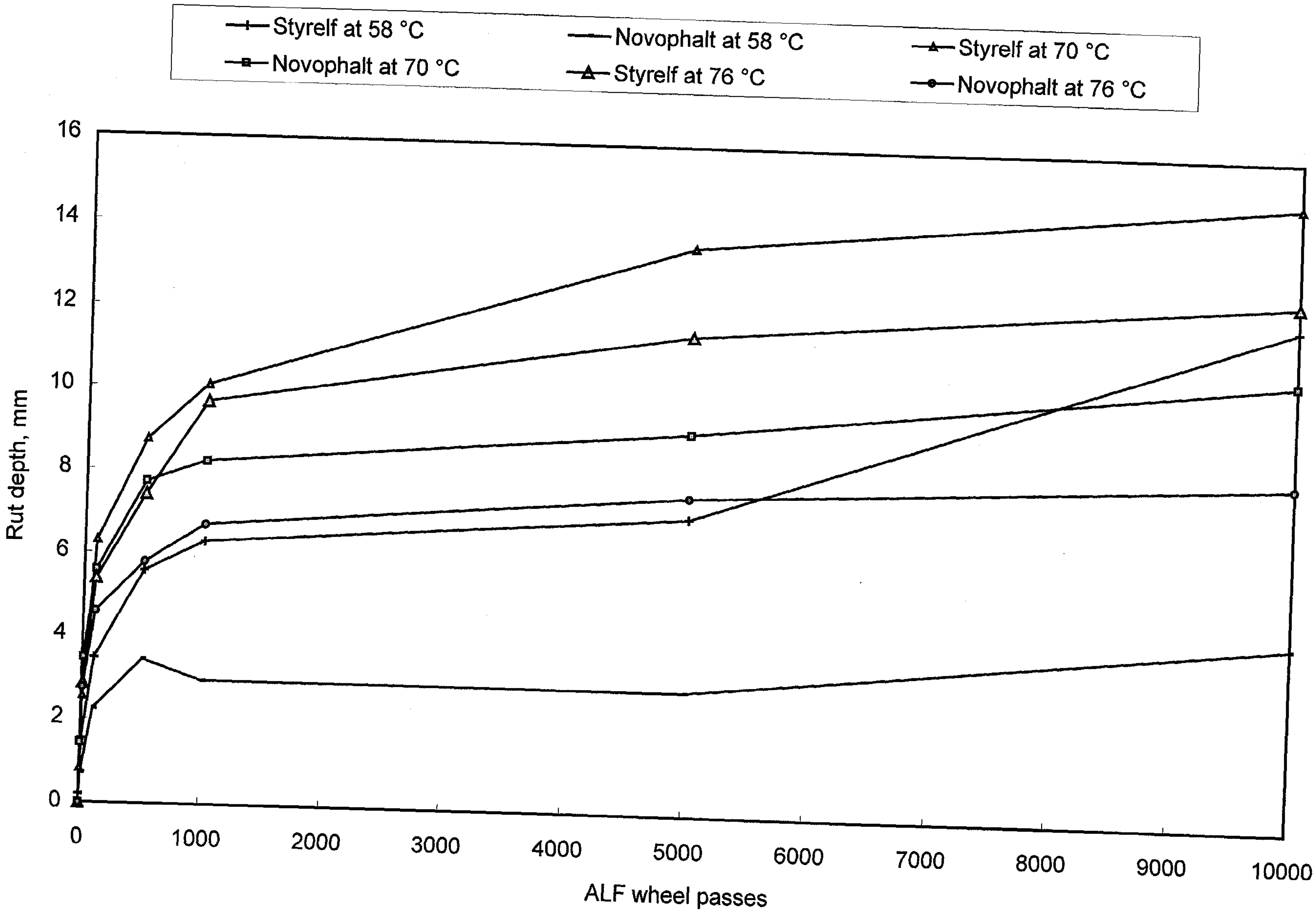

Figure 71. Measured rut depths in the asphalt pavement layer with modified binders vs. ALF wheel passes.

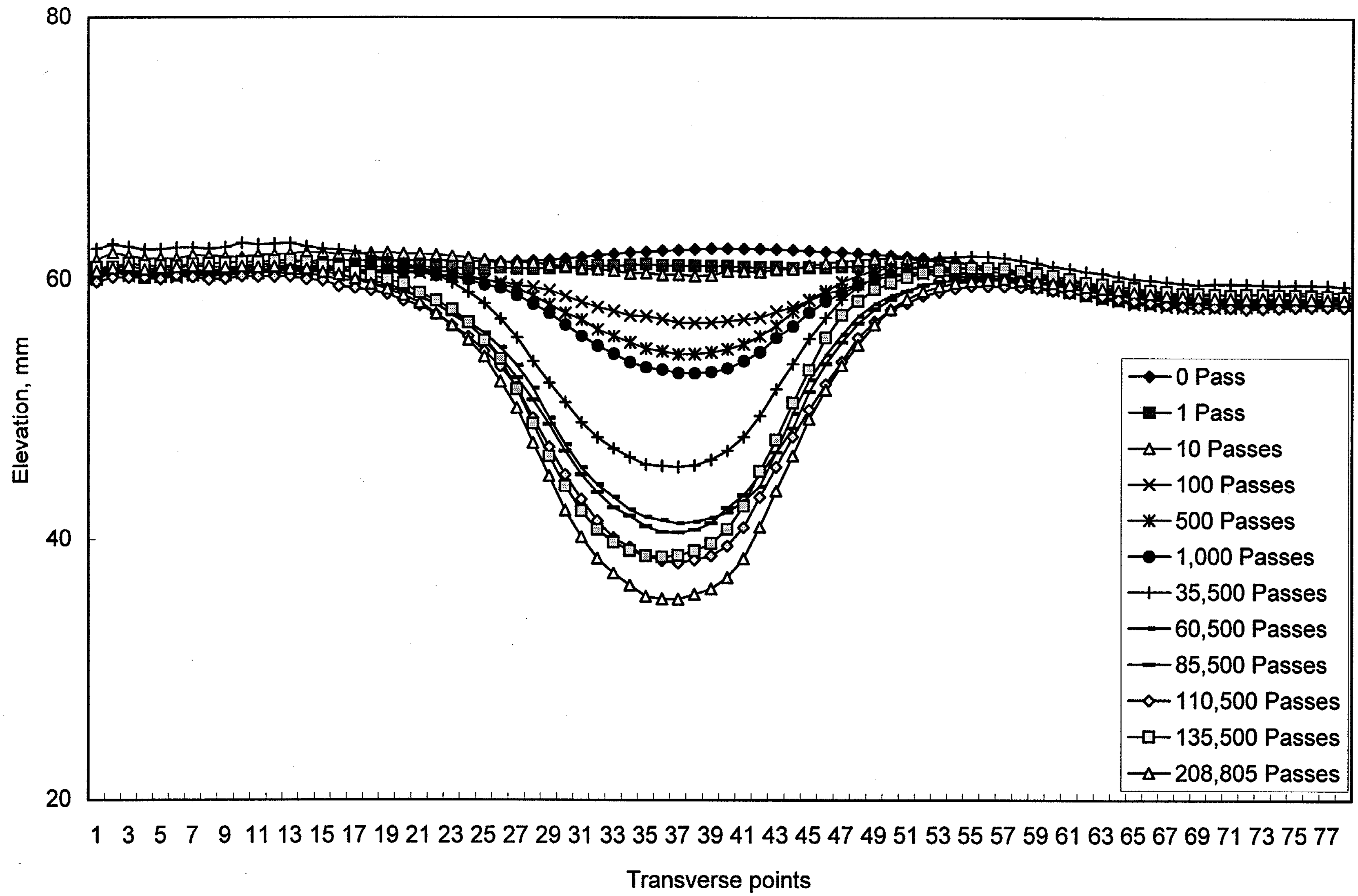

Figure 72. Transverse profiles for lane 8, site 2, Novophalt (PG 77) surface mixture at 58 °C.

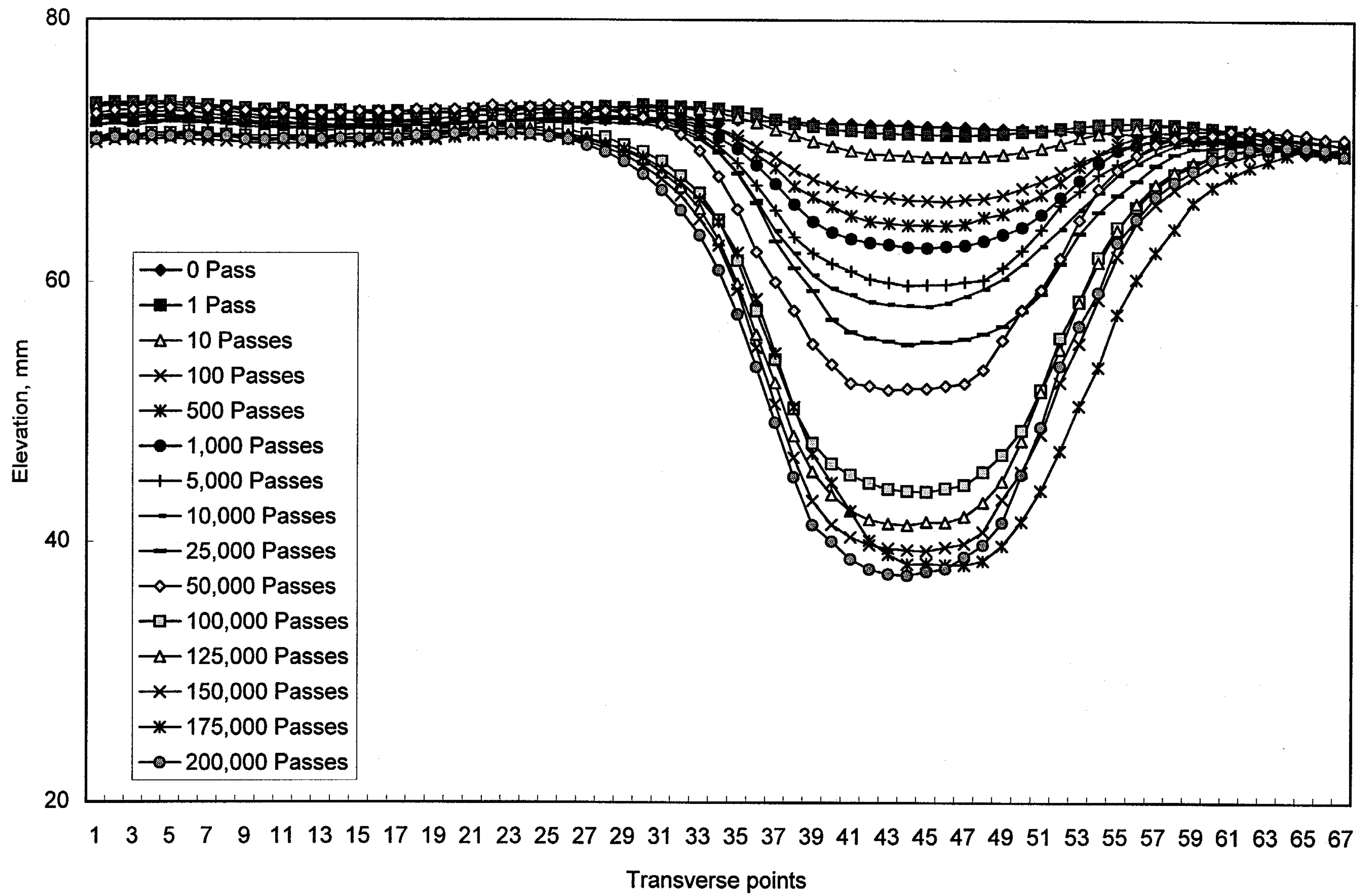

Figure 73. Transverse profiles for lane 8, site 1, Novophalt (PG 77) surface mixture at 70 °C.

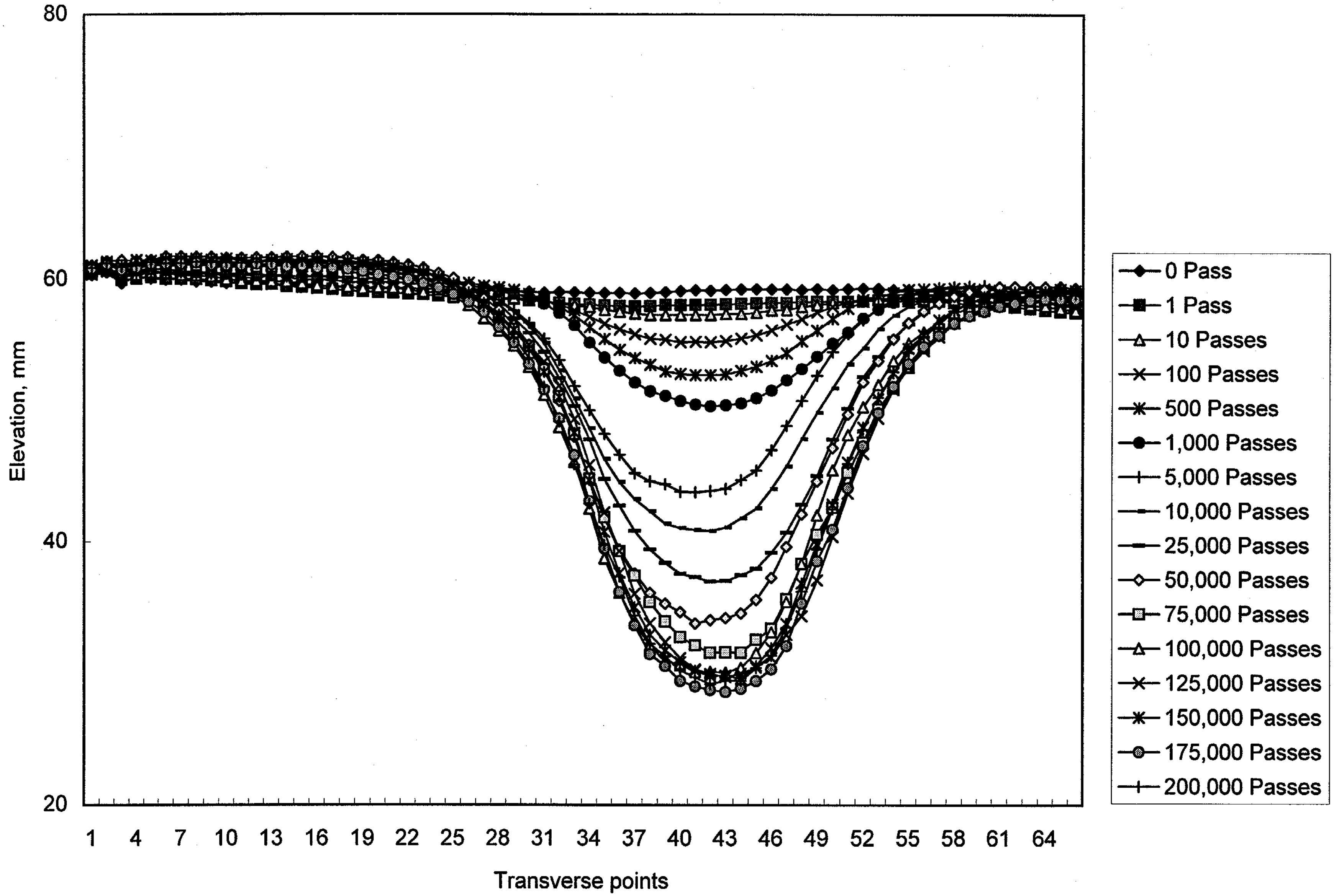

Figure 74. Transverse profiles for lane 7, site 2, Styrelf (PG 88) surface mixture at 58 °C.

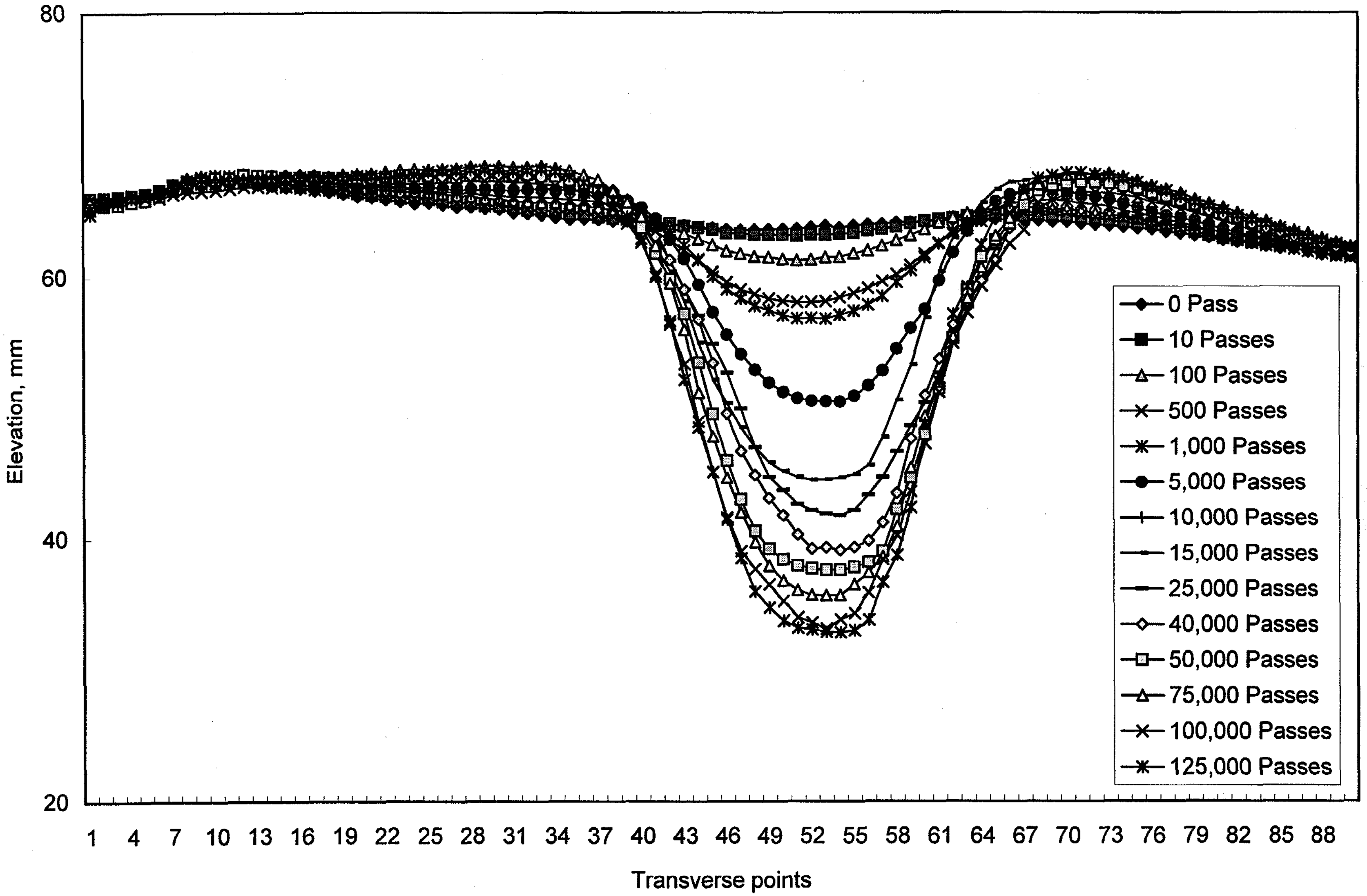

Figure 75. Transverse profiles for lane 5, site 4, AC-10 (PG 65) surface mixture at 46 °C.

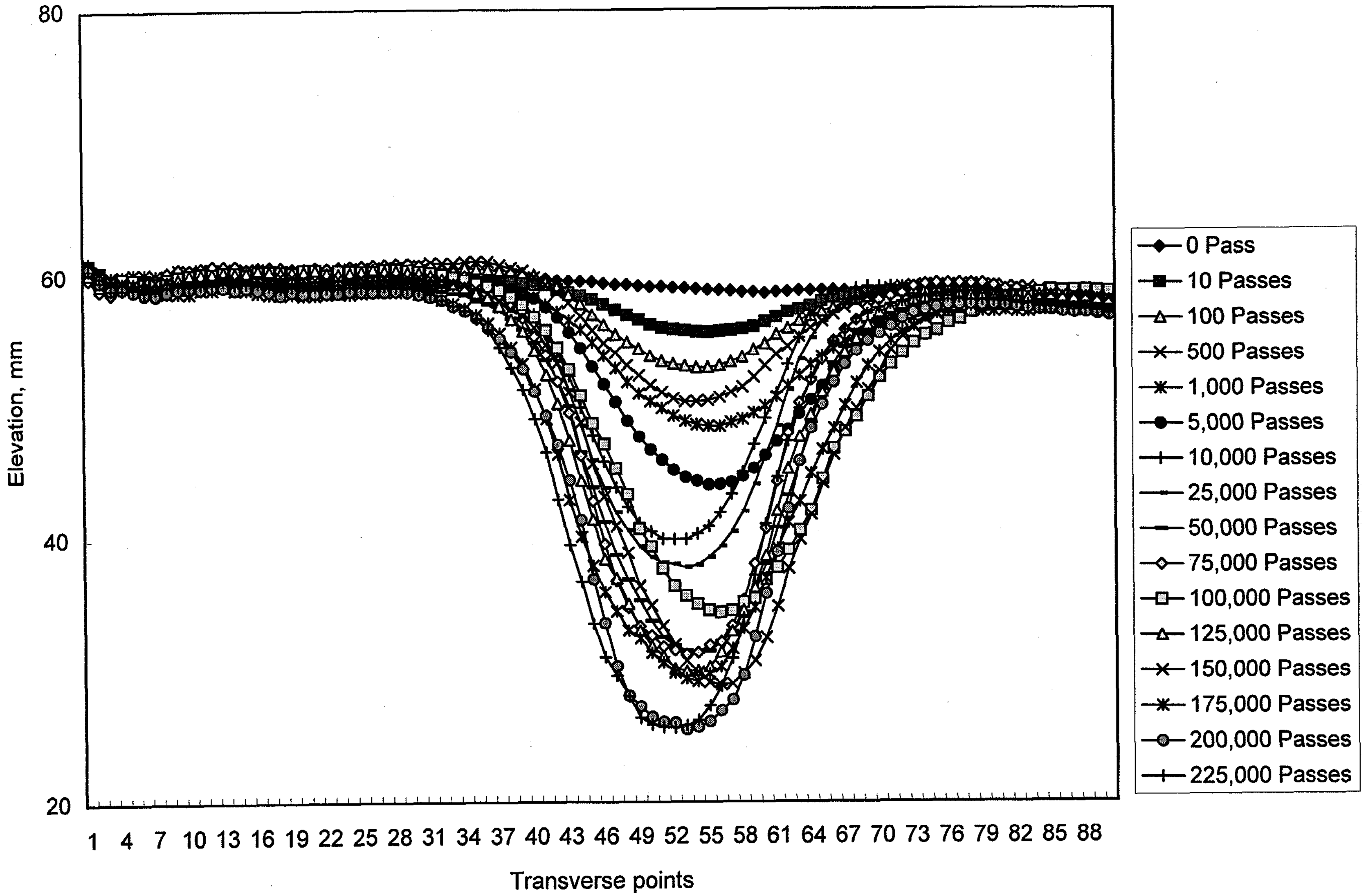

Figure 76. Transverse profiles for lane 7, site 3, Styrelf (PG 88) surface mixture at 76 °C.

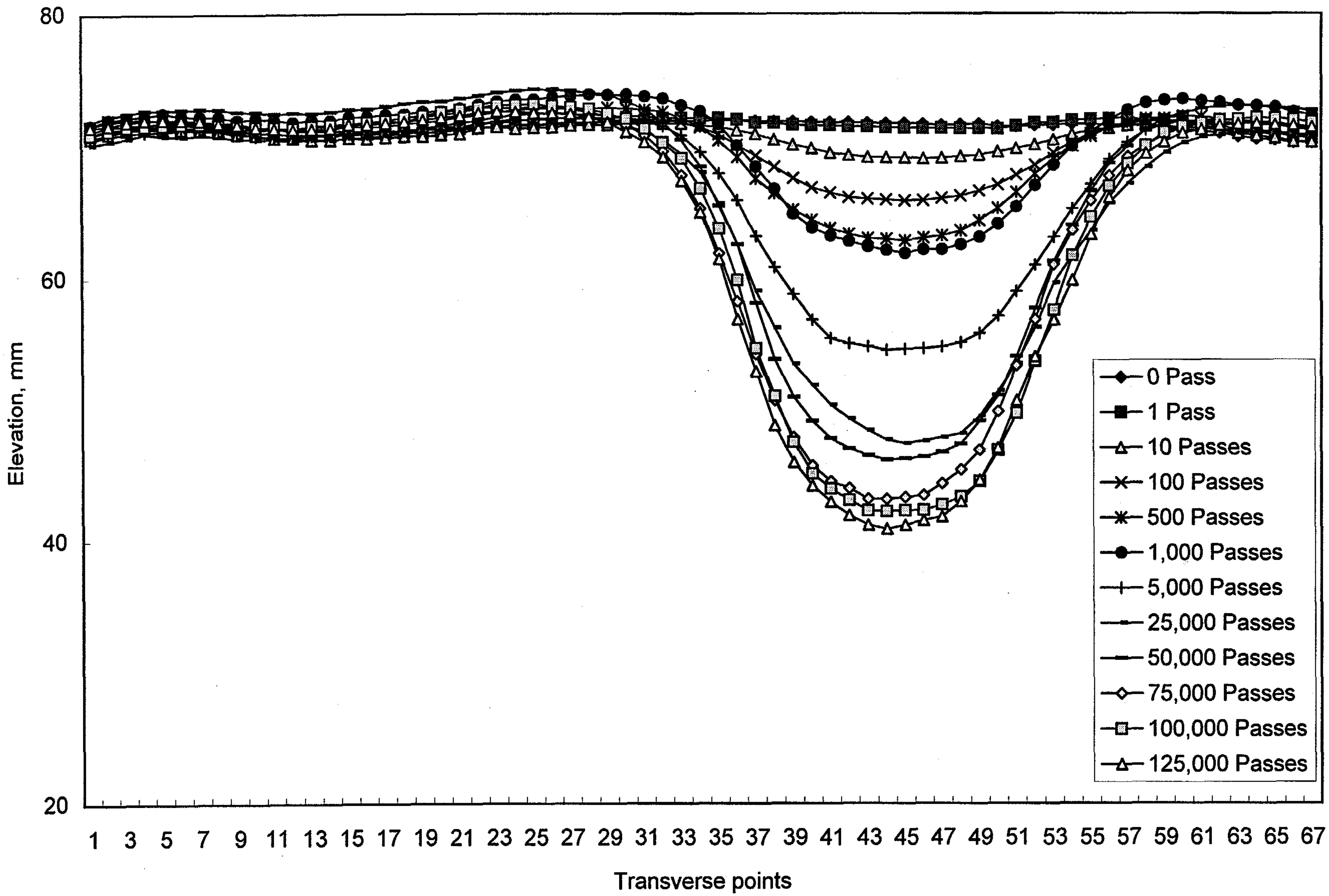

Figure 77. Transverse profiles for lane 7, site 1, Styrelf (PG 88) surface mixture at 70 °C.

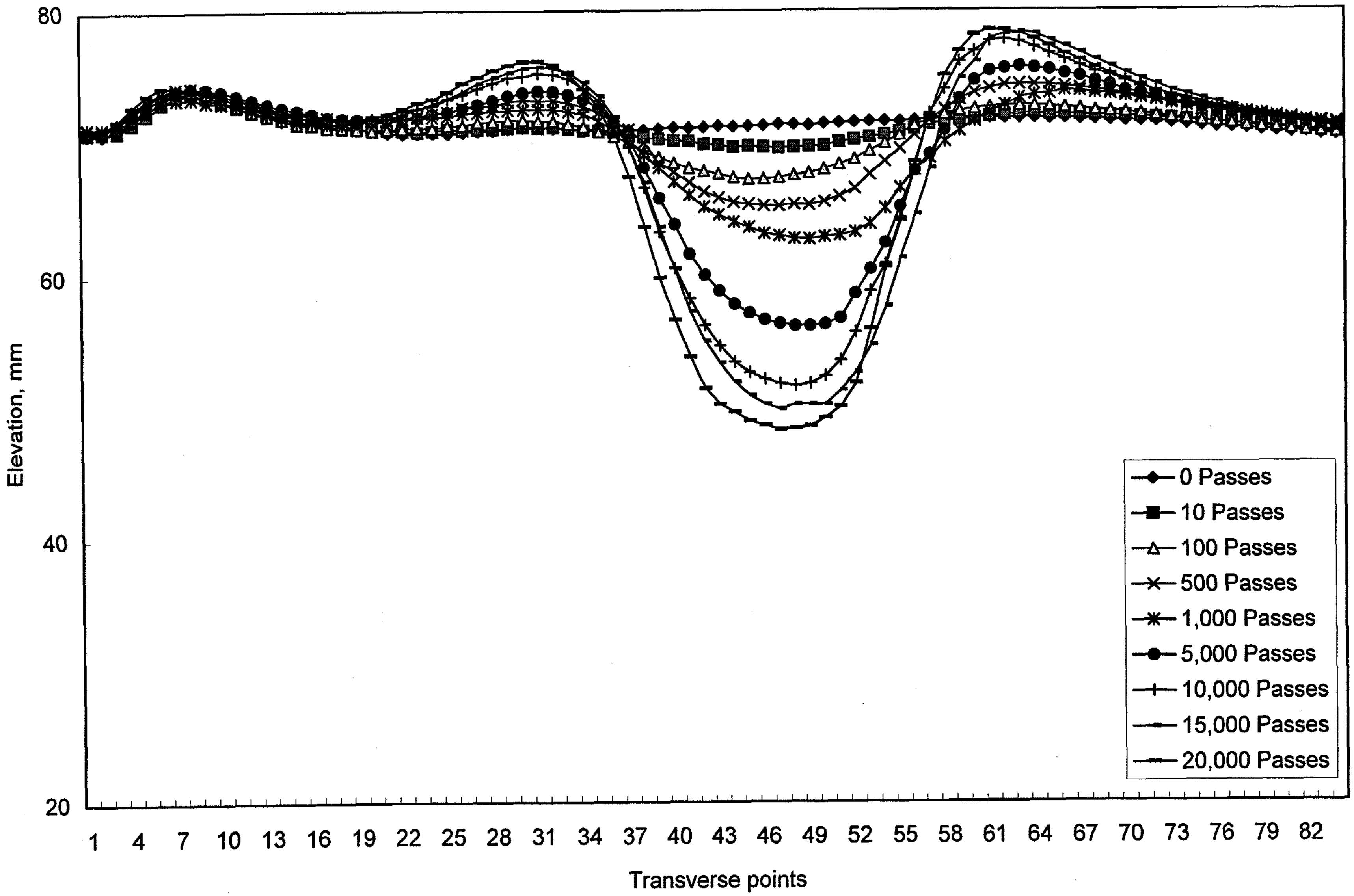

Figure 78. Transverse profiles for lane 10, site 4, AC-20 (PG 70) surface mixture at 58 °C.

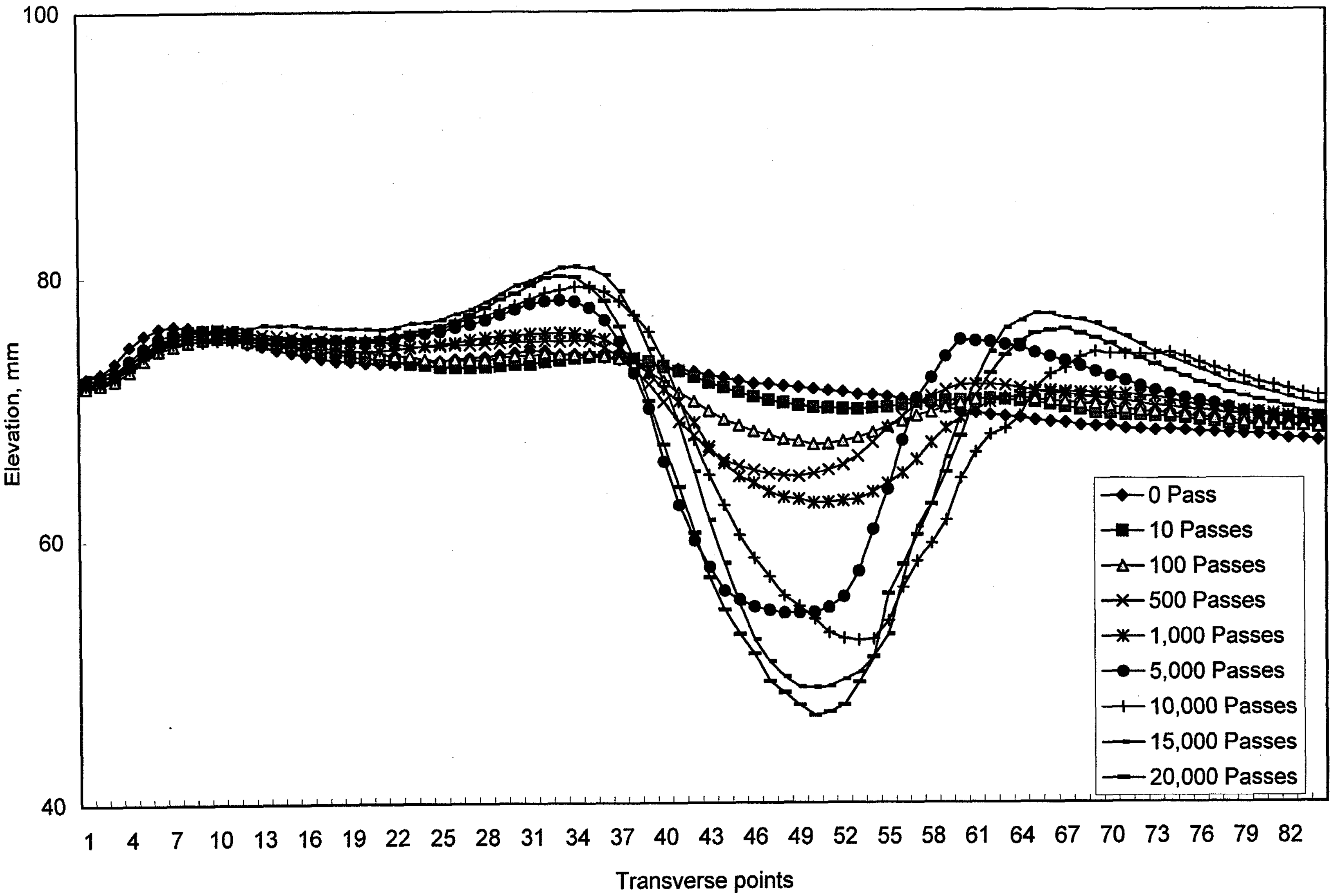

Figure 79. Transverse profiles for lane 10, site 3, AC-20 (PG 70) surface mixture at 58 °C.

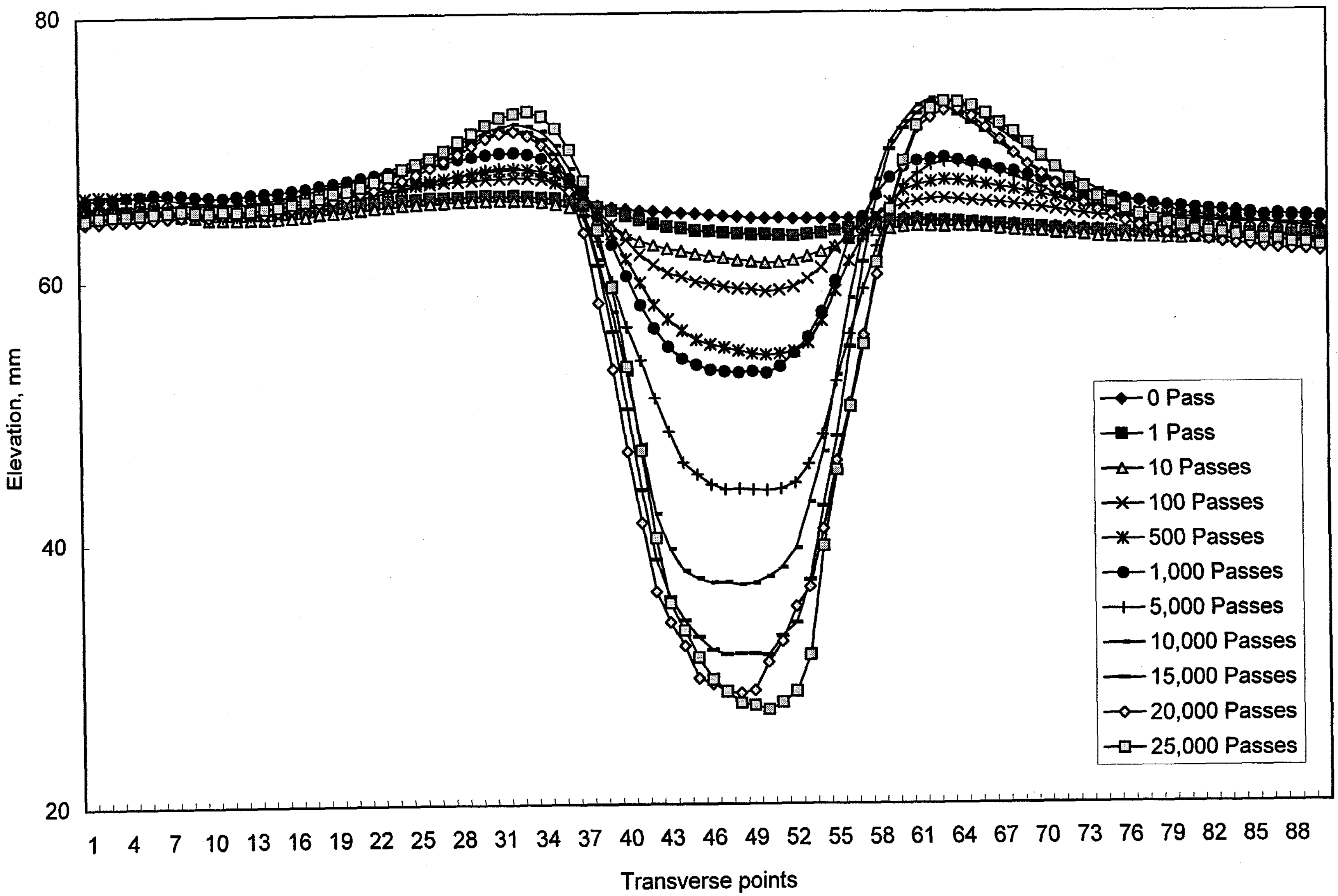

Figure 80. Transverse profiles for lane 5, site 1, AC-10 (PG 65) surface mixture at 52 °C.

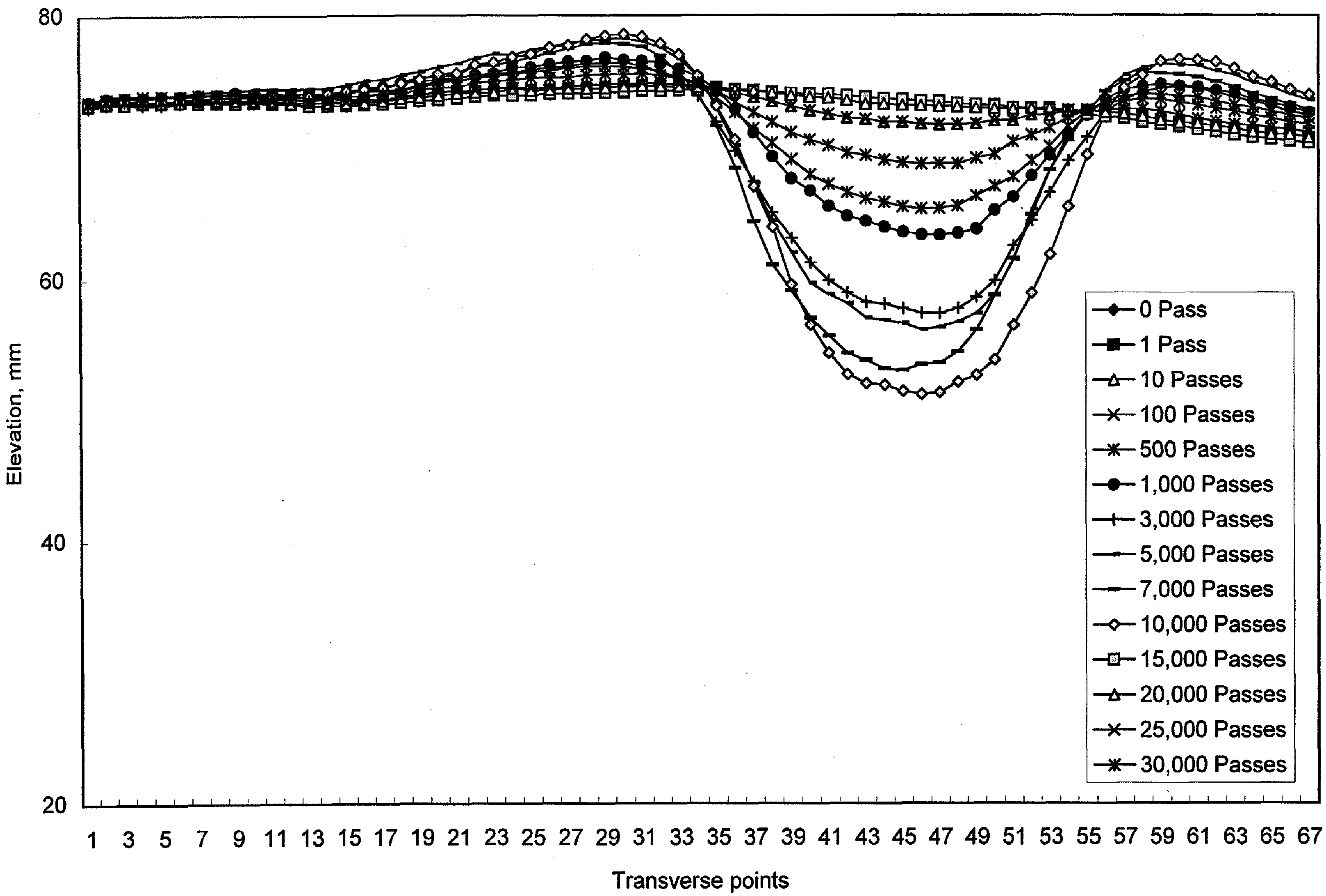

Figure 81. Transverse profiles for lane 11, site 1, AC-5 (PG 59) base mixture at 58 °C.

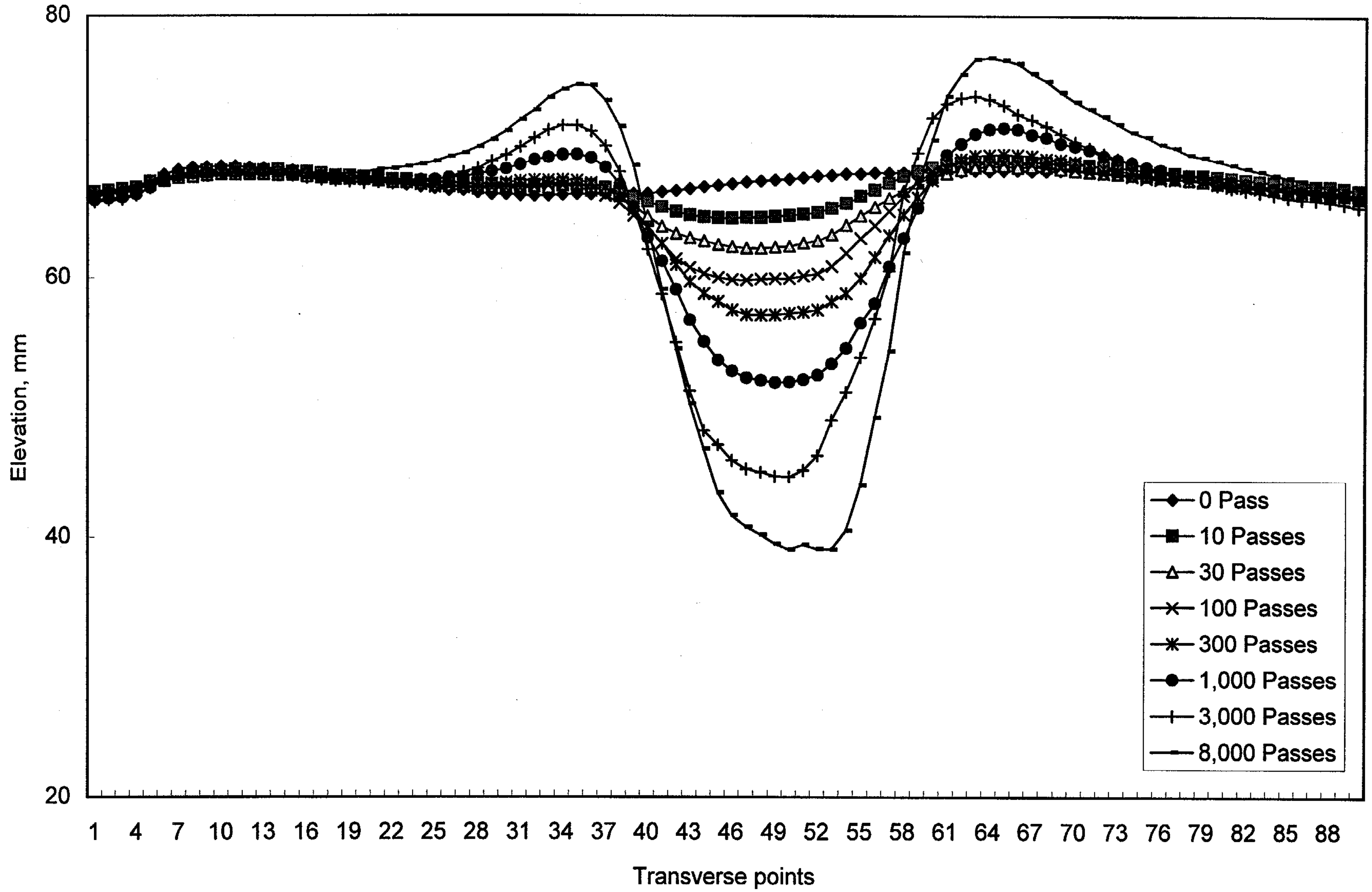

Figure 82. Transverse profiles for lane 6, site 2, AC-20 (PG 70) surface mixture at 64 °C.

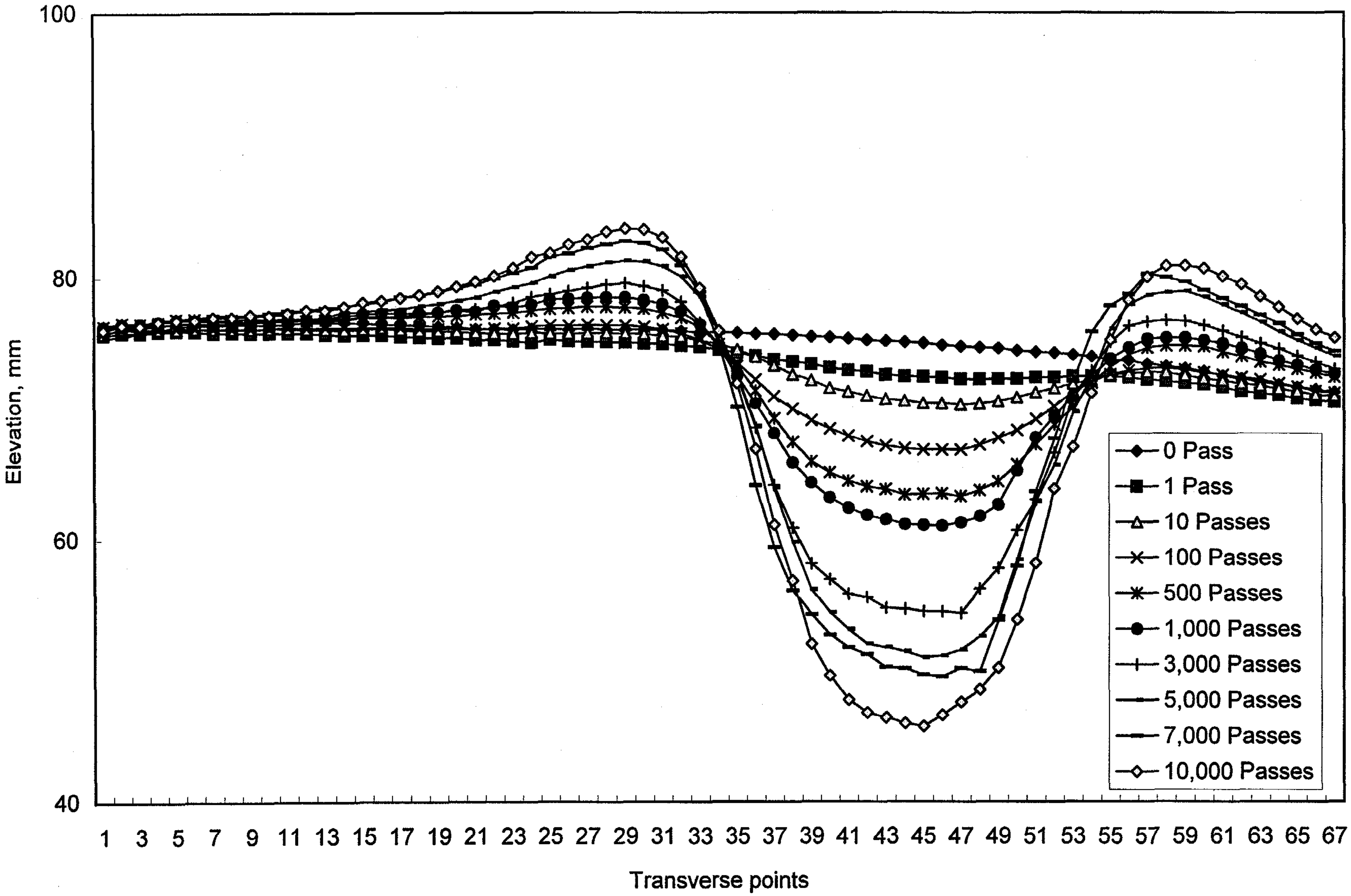

Figure 83. Transverse profiles for lane 10, site 1, AC-20 (PG 70) surface mixture at 58 °C.

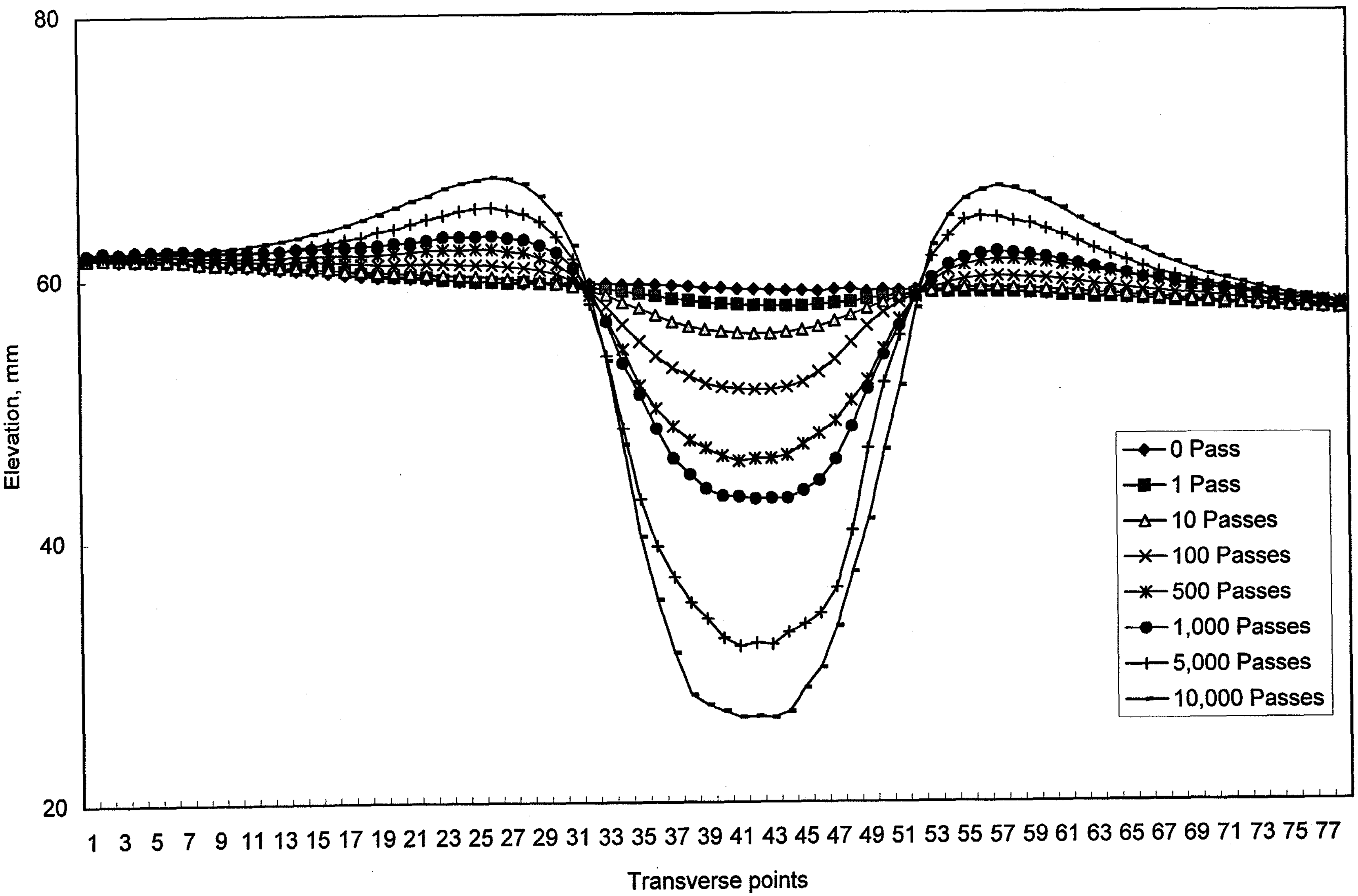

Figure 84. Transverse profiles for lane 10, site 2, AC-20 (PG 70) surface mixture at 58 °C.

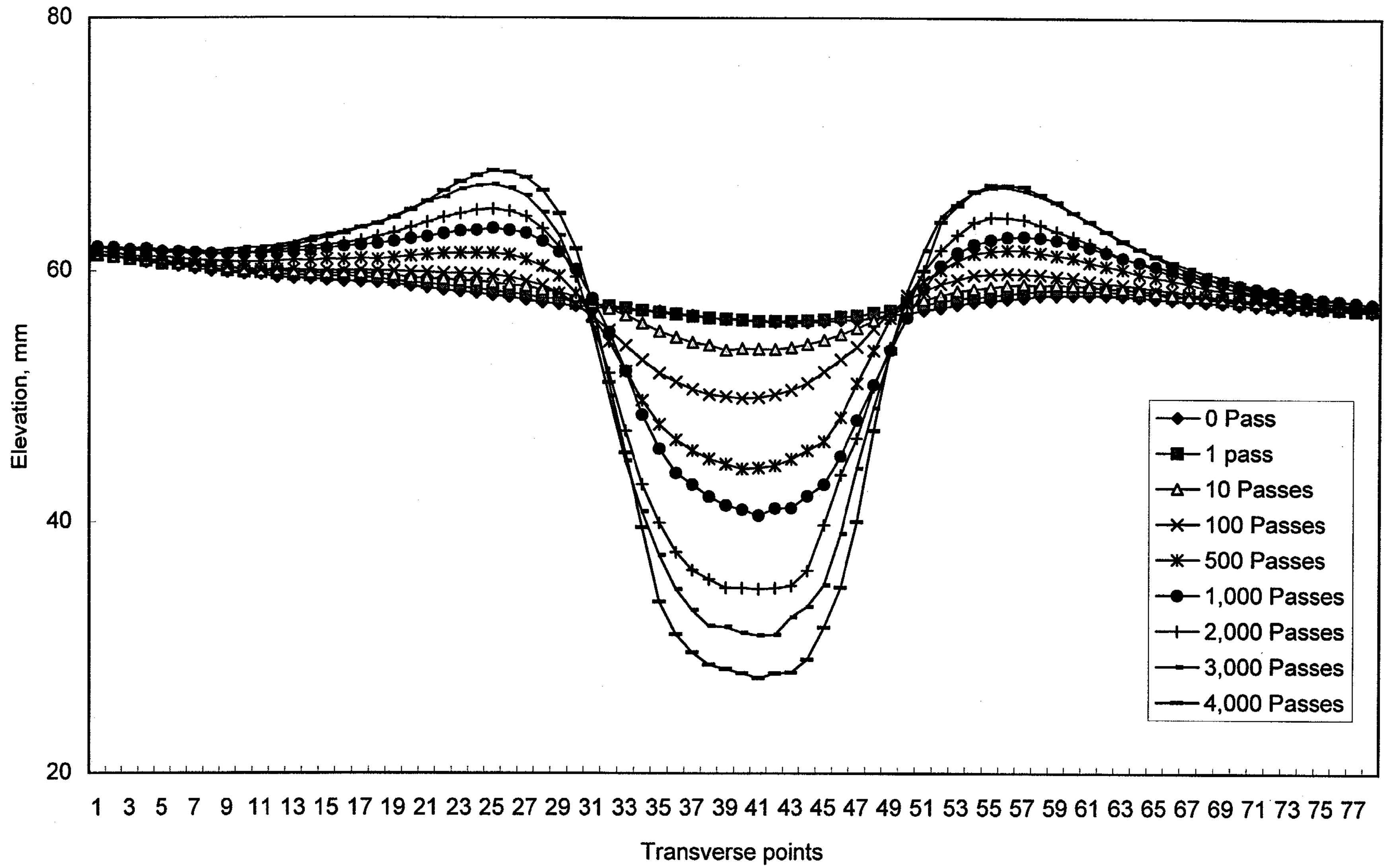

Figure 85. Transverse profiles for lane 5, site 2, AC-10 (PG 65) surface mixture at 58 °C.

Table 120. ALF wheel passes at failure based on the downward only total rut depth and the peak-to-valley total rut depth.

Lane & Site	Binder	Binder PG Grade	Test Temp °C	ALF Wheel Passes and Ranking at a 20-mm Downward Only Total Rut Depth		ALF Wheel Passes and Ranking at a 20-mm Peak-to-Valley Total Rut Depth	
L8 S2	Novophalt	77	58	39,600	1	55,260	1
L8 S1	Novophalt	77	70	30,840	2	27,420	2
L7 S2	Styrelf	88	58	23,160	3	16,660	3
L5 S4	AC-10	65	46	14,650	4	9,390	5
L7 S3	Styrelf	88	76	11,160	5	8,430	6
L7 S1	Styrelf	88	70	10,650	6	11,030	4
L10 S4	AC-20	70	58	7,930	7	4,880	7
L10 S3	AC-20	70	58	6,210	8	3,800	9
L5 S1	AC-10	65	52	6,070	9	1,910	10
L11 S1	AC-5 Base	59	58	5,900	10	4,090	8
L6 S2	AC-20	70	64	2,410	11	1,210	12
L10 S1	AC-20	70	58	1,860	12	1,510	11
L10 S2	AC-20	70	58	1,710	13	966	13
L5 S2	AC-10	65	58	1,160	14	544	14

Table 121. ALF wheel passes at failure based on the downward only rut depth and the peak-to-valley rut depth in the asphalt pavement layer alone.

Lane & Site	Binder	Binder PG Grade	Test Temp °C	ALF Wheel Passes and Ranking at a 20-mm Downward Only Rut Depth in the Asphalt Pavement Layer		ALF Wheel Passes and Ranking at a 20-mm Peak-to-Valley Rut Depth in the Asphalt Pavement Layer	
L8 S2	Novophalt	77	58	6,000,000	1	>9,000,000	1
L8 S1	Novophalt	77	70	340,000	2	268,000	3
L7 S3	Styrelf	88	76	236,000	3	528.000	2
L7 S2	Styrelf	88	58	220,000	4	225,000	4
L7 S1	Styrelf	88	70	98,300	5	113,000	5
L5 S4	AC-10	65	46	82,920	6	43,560	6
L5 S1	AC-10	65	52	21,720	7	3,780	10
L11 S1	AC-5 Base	59	58	15,000	8	9,950	7
L10 S4	AC-20	70	58	13,180	9	7,430	8
L10 S3	AC-20	70	58	12,720	10	6,560	9
L6 S2	AC-20	70	64	7,000	11	2,490	11
L10 S1	AC-20	70	58	2,740	12	1,950	12
L10 S2	AC-20	70	58	2,720	13	1,030	13
L5 S2	AC-10	65	58	1,900	14	800	14

Table 122. ALF wheel passes at failure for the Novophalt and Styrelf surface mixtures.

Lane & Site	Binder	Binder PG Grade	Test Temp °C	Downward Only Total Rut Depth		Peak-to-Valley Total Rut Depth	
L8 S1	Novophalt	77	70	30,840	1	27,420	1
L7 S1	Styrelf	88	70	10,650	2	11,030	2
L8 S2	Novophalt	77	58	39,600	1	55,260	1
L7 S2	Styrelf	88	58	23,160	2	16,660	2
				Downward Only Rut Depth in the Asphalt Pavement Layer		Peak-to-Valley Rut Depth in the Asphalt Pavement Layer	
L8 S1	Novophalt	77	70	340,000	1	268,000	1
L7 S1	Styrelf	88	70	98,300	2	113,000	2
L8 S2	Novophalt	77	58	6,000,000	1	>9,000,000	1
L7 S2	Styrelf	88	58	220,000	2	225,000	2

APPENDIX D: COMPARISON OF THE PERCENT PERMANENT STRAINS FROM VARIOUS TESTS

1. Test Data

Table 123 shows the average percent permanent strains provided by two asphalt binders based on binder, mixture, and pavement tests. Table 124 shows how the strains were calculated for the pavement tests. The permanent deformation measured at the 200th cycle of loading was divided by the asphalt pavement layer thickness of 200 mm to obtain the permanent strain at the 200th cycle of loading. The total strain at the 200th cycle of loading was not measured during the ALF pavement tests. It was calculated using the elastic equation $\epsilon_{total} = \sigma/E$ where σ is the stress applied by the ALF (load divided by area of loading) and E is the dynamic modulus of the mixture measured in the laboratory using an unconfined repeated load compression test. Table 125 show how the strains were calculated for the repeated load compression test. Table 126 shows a comparison of the average total strains.

Table 123. Percent permanent strain per cycle of loading at 58 °C.[1]

Asphalt Binder Grade	Binder Tests—Performed in the Linear Viscoelastic Range		ALF Pavement Test at 200th Wheel Pass (Estimated)	Repeated Load Compression Test at the 200th Cycle of Loading[3]
	Standardized DSR Test at 2 to 10 rad/s, sinδ x 100	Repeated Load DSR Test Using an Applied Stress of 500 Pa[2]		
PG 59 (AC-5)	99 %	97.0 %	2.9 %	2.0 %
PG 77 (Novophalt)	95 %	83.5 %	0.6 %	0.6 %

[1]Permanent strain x 100 ÷ total strain.

[2]The load duration was 1.0 s with a 9.0-s rest period, which allowed for the recovery of the time-dependant elastic strains.

[3]The load duration was 0.1 s with a 0.9-s rest period, which allowed for the recovery of the time-dependant elastic strains.

Table 124. Data from the ALF pavement tests at the 200th wheel pass.

Asphalt Binder Grade	Permanent Def, PD, (mm)	Permanent Strain, ϵ_p = PD/200 mm (mm/mm)	Stress Applied by the ALF, σ, (MPa)	Dynamic Modulus,[1] E, (MPa)	Total Strain $\epsilon_{total} = \sigma/E$ (mm/mm)	Percent Permanent Strain, $\epsilon_p(100)/\epsilon_{total}$
PG 59 AC-5	0.0225	0.0001125	0.690	176	0.00392	2.9
PG 77 Novophalt	0.0020	0.000010	0.690	427	0.00162	0.6

[1]Using a 0.1-s total load duration (the maximum load occurs at 0.05 s). The ALF load duration is greater than 0.1 s. It was estimated to be 0.4 s. However, the repeated load compression tests were only performed using a 0.1-s load duration.

Table 125. Data from the repeated load compression tests at the 200th cycle of loading.

Asphalt Binder Grade	Permanent Strain, (mm/mm)	Total Strain (mm/mm)	Percent Permanent Strain
PG 59 AC-5	0.000016	0.00080	2.0
PG 77 Novophalt	0.0000022	0.00034	0.6

Table 126. Comparison of the total strains in the tests (mm/mm).

Asphalt Binder Grade	Repeated Load DSR Test Using an Applied Stress of 500 Pa	ALF Pavement Test at 200th Wheel Pass	Repeated Load Compression Test at the 200th Cycle of Loading
PG 59 AC-5	1.64	0.00392	0.00080
PG 77 Novophalt	0.12	0.00162	0.00034

2. Comment

As expected, the average total strain and the average percent permanent strain are much higher greater for the DSR. The Superpave binder specification assumes that the ranking provided by the DSR for a set of asphalt binders does not change when the binders are added to a given aggregate gradation at the same volume. However, because of the large differences in the total strain and percent permanent strain, any interaction between the effects of the binders and the aggregate may lead to discrepancies in the rankings provided by binder, mixture, and pavement tests.

APPENDIX E: MASTIC TESTS ON ALF MATERIALS

IN-HOUSE FHWA TECHNICAL MEMORANDUM
by

Kevin D. Stuart, FHWA
Susan Needham, SaLUT
Pedro Romero, SaLUT
Naga Shashidhar, SaLUT

Asphalt Team
Office of Infrastructure R&D
Turner-Fairbank Highway Research Center
6300 Georgetown Pike
McLean, VA 22101-2296
TEL: (202) 493-3073
FAX: (202) 493-3161
August 23, 1999

Subject: PRELIMINARY MASTIC TEST RESULTS ON ALF MATERIALS

Superpave uses the parameter G*/sinδ to grade asphalt binders according to high-temperature rutting resistance. G*/sinδ is measured using a dynamic shear rheometer (DSR). Rutting resistance should increase with an increase in G*/sinδ. Pavements tested for rutting resistance by the Accelerated Loading Facility (ALF) provided a discrepancy for the two modified binders used in the pavements, namely Novophalt and Styrelf. Novophalt had a G*/sinδ that was significantly higher than for Styrelf at temperatures of 58, 70, and 76 °C, but the pavement with Novophalt had a significantly higher resistance to rutting at these temperatures. The following binder properties provided the same discrepancy: G*, δ, sinδ, tanδ, zero shear viscosity, absolute viscosity, δ using RTFO/PAV residues, cumulative permanent strain after four cycles of repeated loading, and the G*/sinδ's of binders recovered from pavement cores after failure. The use of DSR angular frequencies ranging from 2.0 to 100.0 rad/s was not beneficial. Thus, it was decided to test mastics.

The G*/sinδ's of eight mastics were measured using the DSR. The mastics consisted of the AC-10, AC-20, Novophalt, and Styrelf (PG 58-28, 64-22, 76-22, and 82-22) binders used in the ALF pavements and two fine-sized materials: (1) No. 10 diabase aggregate passing the 75-μm sieve, and (2) a blend of 82-percent No. 10 diabase aggregate with 18-percent hydrated lime. These two materials are defined as "fillers" in this memorandum. The second filler is more representative of the filler in the mixtures being tested by the ALF, whose composition is given in table 127. The pavement performances provided by the four binders, from least to most resistant to rutting, was AC-10, AC-20, Styrelf, and Novophalt. This was based on ALF pavement performance at 58 °C using a single aggregate gradation and a single binder content.

Testing mastics that duplicate the actual mastics in the pavements tested by the ALF would be difficult because there may be variations in the following parameters from location to location within a given lane and from lane to lane: (1) the volume of the mastic, (2) the volume concentrations of the aggregate and binder that constitute the mastic, and (3) the gradation of the aggregate within the mastic. Furthermore, mastics cannot be prepared in the laboratory using fillers extracted from cores because a high percentage of the aggregate particles passing the 75-μm sieve will agglomerate in the super-centrifuge used to recover this material. Therefore, the dispersion of the extracted aggregate particles in laboratory prepared mastics may not be the same as in the pavements. The standardized extraction procedures also use paper filters which trap a small portion of the aggregate.

Aggregate samples passing the 75-μm sieve obtained by washing fully graded laboratory-batched aggregate samples also agglomerate upon drying. Therefore, either the fraction passing the 75-μm sieve has to be removed by an air system, or the dust has to be obtained by dry sieving. Dry sieving often leaves a significant portion of the finest aggregate particles clinging to the larger aggregate sizes, which means that the gradation of the minus 75-μm material may not be correct.

The two fillers used in this study were chosen as follows. Samples of the No. 10 diabase aggregate passing the 75-μm sieve were removed from samples of the stockpiled No. 10 diabase aggregate by both wet and dry sieving. Figure 86 shows that the gradations were similar. Therefore, it was decided to obtain subsequent samples by dry sieving. Agglomerates obtained by wet sieving were dispersed by the Horiba™ particle size analyzer used to measure the gradations.

The gradations of the No. 68 ands No. 10 diabase aggregates passing the 75-μm sieve were slightly different. However, if the No. 68 diabase aggregate were to be included in the mastic, its effect on the overall gradation would be minor. It constituted only 9.9 percent of the total filler by mass. Both the No. 10 and No. 68 stockpiled aggregates were produced by the same aggregate crusher at the same quarry. Therefore, the No. 68 diabase aggregate was eliminated in order to reduce the amount of work involved in the experiment. The natural sand was not included because it was less than 5 percent of the filler. These materials can be included in future tests if necessary.

The concentration of the diabase filler in the mastic was 26.8 percent by volume, while the concentration of the diabase filler with hydrated lime was 27.8 percent. The volume concentrations were slightly different because the filler to asphalt blend was fixed based on mass and the specific gravities of the diabase material and hydrated lime were different. The filler to asphalt blend by mass was 5.1 kg to 4.85 kg. Note that table 127 shows a value of 5.531 kg passing the 75-μm sieve. The composition of the filler to be used in the laboratory tests had to be determined using the gradations and blend percentages of the stockpiled materials. The gradation provided by these stockpiles had 5.531-percent material passing the 75-μm sieve by mass. Extractions performed on pavement samples provided an average of 5.1-percent aggregate passing the 75-μm sieve. Therefore, the latter percentage was used when formulating the mastics.

Each binder and mastic was tested using a minimum of three replicates. Four replicates were used for the Novophalt and Styrelf mastics because of low repeatability. Tests on the mastics with Novophalt and Styrelf were also repeated using four new samples to check reproducibility. All tests were performed on unaged binders and mastics.

Tables 128 and 129 provides the $G^*/\sin\delta$'s and $\sin\delta$'s of the binders and mastics at 58 °C and the standard DSR frequency of 10.0 rad/s. Ninety-five-percent confidence limits ($\pm 2\sigma_{(n-1)}$) are included. Tables 130 and 131 provide the data at 58 °C and the ALF associated frequency of 2.51 rad/s. Statistical analyses of the data using *t*-tests at a 95-percent confidence level provide the following conclusions:

- The mastic consisting of Novophalt and diabase had a lower $G^*/\sin\delta$ than the mastic consisting of Styrelf and diabase based on the first set of tests, but a higher $G^*/\sin\delta$ based on the second set of tests.

- Both the first and second set of tests show that the mastic consisting of Novophalt, diabase, and hydrated lime had a higher $G^*/\sin\delta$ than the mastic consisting of Styrelf, diabase, and hydrated lime. The ranking provided by the four mastics using diabase and hydrated lime matched ALF pavement rutting performance.

- The hydrated lime significantly increased $G^*/\sin\delta$ even though the additional filler by volume was only 1 percent (26.8 vs. 27.8 percent). The increase using Novophalt was extremely high. A reason for this needs to be determined.

- The second set of tests on the Novophalt mastics provided significantly higher $G^*/\sin\delta$'s compared with the first set of tests. Therefore, the $G^*/\sin\delta$'s of the Novophalt mastics were not reproducible.

- DSR frequencies of 10.0 and 2.51 rad/s provided the same conclusions.

- The $\sin\delta$'s, which are the decimal percentage of the total strain that is permanent, were all relatively high. They ranged from 0.738 to 0.998. (Note: The inverse of the Superpave rutting parameter $\sin\delta/G^*$ is equal to the maximum shear strain from a constant applied maximum stress times the sine of the angle ($\sin\delta/G^* = \gamma_{max}\sin\delta$). Although $\sin\delta$ is the decimal percentage of γ_{max} that is permanent, γ_{max} can vary from binder to binder.)

Table 127. Composition of the filler in the ALF pavements.

Material	Decimal Fraction of Material Passing the 75-μm Sieve[1]		Blend for Stockpiled Materials Per 100-kg Mass		Composition of Minus 75-μm Material by Mass, kg	Composition of Minus 75-μm Material on a Percentage Basis
No. 68 Diabase	0.009	x	61	=	0.549	9.9
No. 10 Diabase	0.125	x	30	=	3.750	67.8
Natural Sand	0.029	x	8	=	0.232	4.2
Hydrated Lime	1.000	x	1	=	1.000	18.1
			100		5.531	100.0

[1]For example, if 1.0-percent material passed the 75-μm sieve, then the decimal fraction is $1.0 \div 100 = 0.01$.

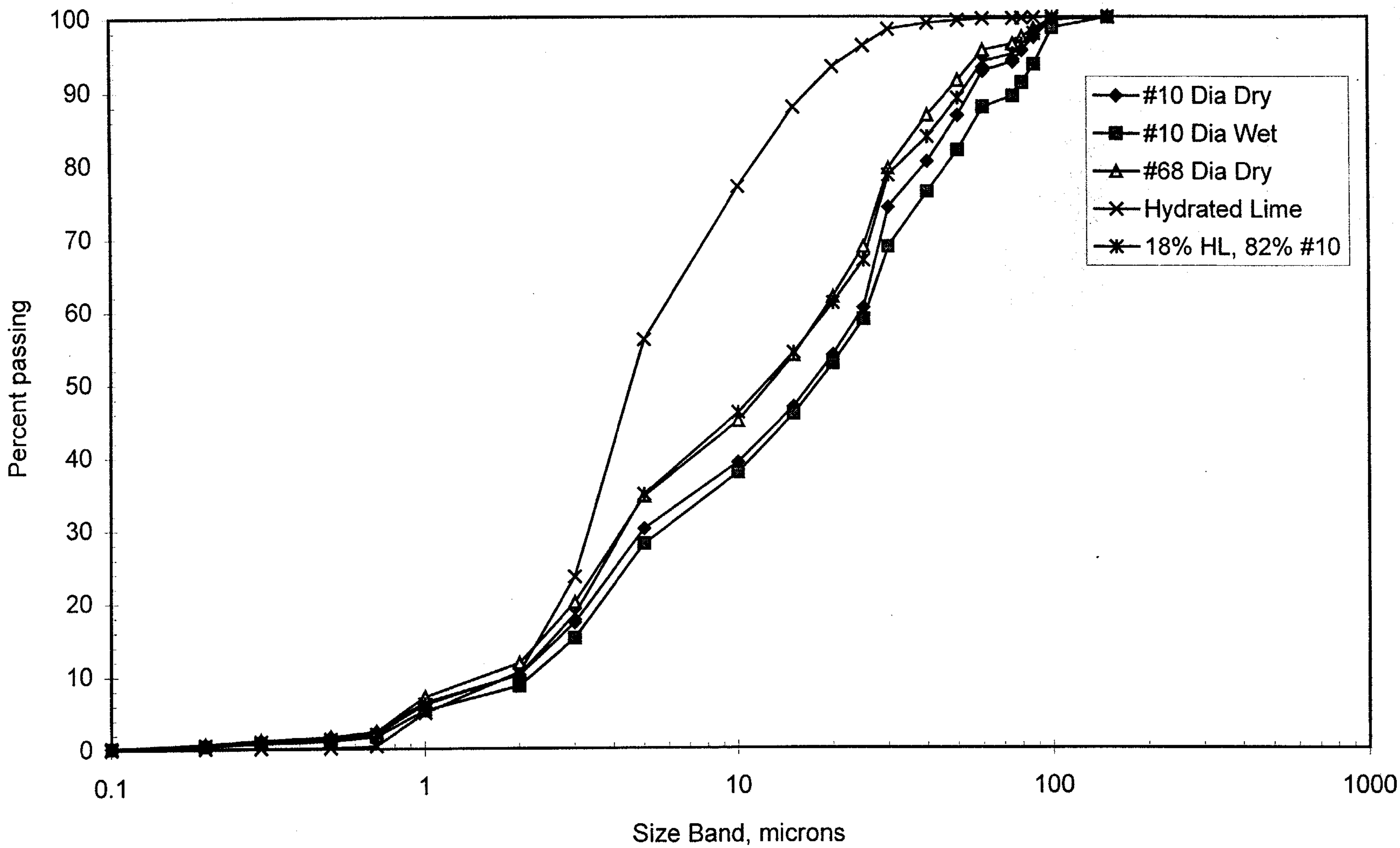

Figure 86. Gradations of the ALF aggregates and hydrated lime below 100 microns.

Table 128. G*/sinδ's of the unaged materials at 10.0 rad/s and 58 °C with 95-percent confidence limits ($\pm 2\sigma_{(n-1)}$).

Asphalt Binder	Continuous High-Temp Performance Grade (PG)	Percent Filler by Volume	G*/sinδ at 10.0 rad/s and 58 °C (Pa) (First Test)	G*/sinδ at 10.0 rad/s and 58 °C (Pa) (Second Test)
Asphalt Binder Test Results				
AC-10	65	0	2 030 ± 460	
AC-20	70	0	4 780 ± 210	
Styrelf	88	0	17 450 ± 1 020	
Novophalt	77	0	13 870 ± 1 450	
Asphalt Binder with Diabase Filler Test Results				
AC-10	65	26.8	7 080 ± 540	
AC-20	70	26.8	11 750 ± 570	
Styrelf	88	26.8	56 300 ± 7 100	53 800 ± 5 900
Novophalt	77	26.8	44 100 ± 2 800	62 300[1] ± 2 300
Asphalt Binder with Diabase Filler and Hydrated Lime Test Results				
AC-10	65	27.8	7 750 ± 345	
AC-20	70	27.8	19 240 ± 3 670	
Styrelf	88	27.8	82 700 ±10 500	75 900 ±11 200
Novophalt	77	27.8	141 000 ±54 100	196 400[1] ± 9 900

[1]One outlier removed.

Table 129. Sine of the phase angle (sinδ) at 10.0 rad/s and 58 °C.

Asphalt Binder	Continuous High-Temp Performance Grade (PG)	Percent Filler by Volume	Sinδ at 10.0 rad/s and 58 °C (First Test)	Sinδ at 10.0 rad/s and 58 °C (Second Test)
Asphalt Binder Test Results				
AC-10	65	0	0.995	
AC-20	70	0	0.990	
Styrelf	88	0	0.865	0.865
Novophalt	77	0	0.942	0.957
Asphalt Binder with Diabase Filler Test Results				
AC-10	65	26.8	0.993	
AC-20	70	26.8	0.991	
Styrelf	88	26.8	0.854	0.852
Novophalt	77	26.8	0.930	0.847
Asphalt Binder with Diabase Filler and Hydrated Lime Test Results				
AC-10	65	27.8	0.994	
AC-20	70	27.8	0.988	
Styrelf	88	27.8	0.838	0.841
Novophalt	77	27.8	0.872	0.790

Table 130. G*/sinδ's of the unaged materials at 2.51 rad/s and 58 °C with 95-percent confidence limits ($\pm 2\sigma_{(n-1)}$).

Asphalt Binder	Continuous High-Temp Performance Grade (PG)	Percent Filler by Volume	G*/sinδ at 2.51 rad/s and 58 °C (Pa) (First Test)	G*/sinδ at 2.51 rad/s and 58 °C (Pa) (Second Test)
Asphalt Binder Test Results				
AC-10	65	0	543 ± 126	
AC-20	70	0	1 320 ± 60	
Styrelf	88	0	7 000 ± 430	
Novophalt	77	0	4 260 ± 30	
Asphalt Binder with Diabase Filler Test Results				
AC-10	65	26.8	1 940 ± 150	
AC-20	70	26.8	3 250 ± 150	
Styrelf	88	26.8	23 300 ± 3 000	22 200 ± 2 500
Novophalt	77	26.8	16 400 ± 3 500	27 900[1] ± 3 500
Asphalt Binder with Diabase Filler and Hydrated Lime Test Results				
AC-10	65	27.8	2 110 ± 93	
AC-20	70	27.8	5 390 ± 1 040	
Styrelf	88	27.8	34 900 ± 4 700	32 200 ± 4 900
Novophalt	77	27.8	60 500 ±36 800	104 200[1] ± 8 200

[1]One outlier removed.

Table 131. Sine of the phase angle (sinδ) at 2.51 rad/s and 58 °C.

Asphalt Binder	Continuous High-Temp Performance Grade (PG)	Percent Filler by Volume	Sinδ at 2.51 rad/s and 58 °C (First Test)	Sinδ at 2.51 rad/s and 58 °C (Second Test)
Asphalt Binder Test Results				
AC-10	65	0	0.998	
AC-20	70	0	0.996	
Styrelf	88	0	0.866	
Novophalt	77	0	0.945	
Asphalt Binder with Diabase Filler Test Results				
AC-10	65	26.8	0.997	
AC-20	70	26.8	0.996	
Styrelf	88	26.8	0.850	0.849
Novophalt	77	26.8	0.929	0.808
Asphalt Binder with Diabase Filler and Hydrated Lime Test Results				
AC-10	65	27.8	0.998	
AC-20	70	27.8	0.995	
Styrelf	88	27.8	0.838	0.835
Novophalt	77	27.8	0.864	0.738